Electrochemical enzyme-based biosensor array for monitoring of organic acids and ethanol in biogas processes

Dissertation
zur
Erlangung des Doktorgrades
der Naturwissenschaften
(Dr. rer. nat.)

dem

Fachbereich Pharmazie der

Philipps-Universität Marburg

vorgelegt von

Johanna Pilas

aus **Mohrungen**

Marburg/Lahn **2020**

Gutachter: **Prof. Dr. Michael J. Schöning**

Gutachter: **Prof. Dr. Michael Keusgen**

Eingereicht am **10.02.2020**

Tag der mündlichen Prüfung am **23.03.2020**

Hochschulkennziffer: 1180

ERKLÄRUNG

Ich versichere, dass ich meine Dissertation

„Electrochemical enzyme-based biosensor array for monitoring of organic acids and ethanol in biogas processes“

selbständig und ohne unerlaubte Hilfe angefertigt und mich dabei keiner anderen als der von mir ausdrücklich bezeichneten Quellen bedient habe. Alle vollständig oder sinngemäß übernommenen Zitate sind als solche gekennzeichnet.

Die Dissertation wurde in der jetzigen oder ähnlichen Form noch bei keiner Hochschule eingereicht und hat noch keinen sonstigen Prüfungszwecken gedient.

Marburg, den 10.02.2020

Johanna Pilas

Abstract

In light of steadily increasing energy demand and irreversible exhaustion of fossil fuels, further expansion of renewable energy sources is continually gaining importance. Utilization of biomass, as a widely available energy carrier, is capable of providing great contribution to sustainable energy supply. The efficient production of biogas, however, calls for an improved biomass supply chain. Economic operation of biogas plants depends in particular on reliable process monitoring. Often, process disturbances are accompanied by fluctuations in the concentration profile of some intermediates produced during the anaerobic fermentation process. Nowadays, the focus has mainly been set on volatile fatty acids (such as acetate and propionate) as an indicator for imbalanced process conditions and only little account has been taken to the relevance of other organic acids and alcohols, like lactate, formate and ethanol.

In this work, an electrochemical enzyme-based biosensor array for simultaneous determination of D-lactate, L-lactate, formate and ethanol is developed. The amperometric sensing principle is based on two enzymes in each case: an analyte-specific NAD^+-dependent dehydrogenase combined with a diaphorase from *Clostridium kluyveri*. The latter converts its substrate $Fe(CN)_6^{3-}$ to $Fe(CN)_6^{4-}$, which generates a concentration-dependent current by oxidation at an polarized electrode. Enzymes were immobilized by chemical cross-linking with glutaraldehyde on platinum thin-film electrodes. The optimization of the biosensor performance has been investigated in regard to enzyme loading, glutaraldehyde concentration, cofactor concentration (NAD^+ and $Fe(CN)_6^{3-}$), pH value and temperature. The potential for repeated and long-term application has been proven by evaluation of operational and storage stability. Typically, enzyme-based biosensors are characterized by a high specificity due to the remarkable properties of enzymes as biological recognition element. Measurements in real samples, however, are prone to interfering effects by other electroactive species in the sample solution. The specificity of the biosensing system is determined in response to various interfering compounds and results reveal no cross-talk effects during simultaneous measurement of the four different analytes of interest. Successful practical performance for rapid and on-site analysis, has been demonstrated by quantification of D-lactate, L-lactate, formate and ethanol in various feedstocks (maize- and sugar cane silage) and spiked fermentation samples from three industrial biogas plants. Good correlation is obtained for results determined by the biosensor array in comparison to conventional commercial analytical methods applied (photometry and gas chromatography). In contrast to these techniques, the biosensor array offers the advantages of facile on-site application with a portable measurement set-up, rapid analysis time by simultaneous operation and application in untreated samples. The measuring system has also been applied for long-term monitoring of a lab-scale biogas reactor ($0.01\,m^3$) for a period of two months. Regular analysis of alcohol- and organic acid levels provides a beneficial supplementation

to standard monitoring parameters, like biogas production, methane yield, pH and temperature. This additional information can help to identify changes in the microbial methane formation and potentially indicate upcoming imbalances at an early stage.

For improved practical implementation of the developed biosensor array, the required cofactors have been co-immobilized on the sensor surface of screen-printed carbon electrodes. Modification with graphene oxide enables the establishment of a reagent-free biosensing system. Such biosensors can be manufactured economically by thick-film technology and used as disposable test strips for simplified on-site monitoring of several key intermediates in the biogas fermentation medium.

Contents

Abbreviations

ADH	alcohol dehydrogenase
ADP	adenosine 5'-diphosphate
AFM	atomic force microscopy
AK	acetate kinase
ASPA	aspartate ammonia-lyase
BD	below limit of detection
BP	biogas plant
BSA	bovine serum albumin
CA	cellulose acetate
CE	counter electrode
CS	citrate synthase
CV	cyclic voltammetry
DH	dehydrogenase
DIA	diaphorase
D-LDH	D-lactate dehydrogenase
EC	enzyme commission number
EEG	Renewable Energy Sources Act (German: Erneuerbare-Energien-Gesetz)
FAD	flavin adenine dinucleotide
FDH	formate dehydrogenase
FH	fumarate hydratase
FOS/TAC	volatile organic acids/total anorganic carbonate
GA	glutaraldehyde
GC	gas chromatography
GO	graphene oxide

HCF(II)	hexacyanoferrate(II)
HCF(III)	hexacyanoferrate(III)
HPLC	high-performance liquid chromatography
HRP	peroxidase from horseradish
iR drop	ohmic potential drop
IUPAC	International Union of Pure and Applied Chemistry
LAB	lactate acid bacteria
L-LDH	L-lactate dehydrogenase
LoC	lab-on-a-chip
LOD	limit of detection
MDH	malate dehydrogenase
MWCNT	multiwalled carbon nanotube
NAD^+	nicotinamide-adenine dinucleotide, oxidized
NADH	nicotinamide-adenine dinucleotide, reduced
OA	organic acid
PCB	printed circuit board
PCS	poly(carbamoyl)sulfonate
PCT	propionate CoA-transferase
PK	pyruvate kinase
PNIPAAm	poly(N-isopropylacrylamide)
POx	pyruvate oxidase
PVA	polyvinyl alcohol
RE	reference electrode
RMS	root-mean-square
SAM	self-assembled monolayer
SCAOx	short-chain acyl-CoA oxidase
SCE	saturated calomel electrode
SEM	scanning electron microscopy

SHE	standard hydrogen electrode
SHL	salicylate hydroxylase
SPCE	screen-printed carbon electrode
VFA	volatile fatty acid
WE	working electrode

1 Introduction

1.1 Biogas - energy from renewable resources

Economic and social development are considered to be inevitable related to adequate energy access and supply. Concerning the worldwide increasing energy demand and the associated harmful environmental impact, extensive changes in the global energy sector are required [1]. At present, most of the produced energy originates from fossil fuels, like oil, coal and gas. In Germany, e.g., the combustion of these energy systems is responsible for more than 80% of CO_2 emission [2], which drives among other things the ongoing process of global warming. The Renewable Energy Sources Act (EEG, German for "Erneuerbare-Energien-Gesetz") was adopted in 2000 by the German government, in order to reduce greenhouse gas emissions and encourage the generation of renewable electricity [3, 4]. Figure 1.1 shows the changes in the share of different energetic sources from 1990 compared to 2018. Currently, fossil fuels still account the largest percentage in the primary energy consumption, with predominant portion of mineral oil (33.8%). Most significant change in the last decades, however, relates to the steady increase of energy derived from sustainable resources such as water, waste, solar, wind and biomass.

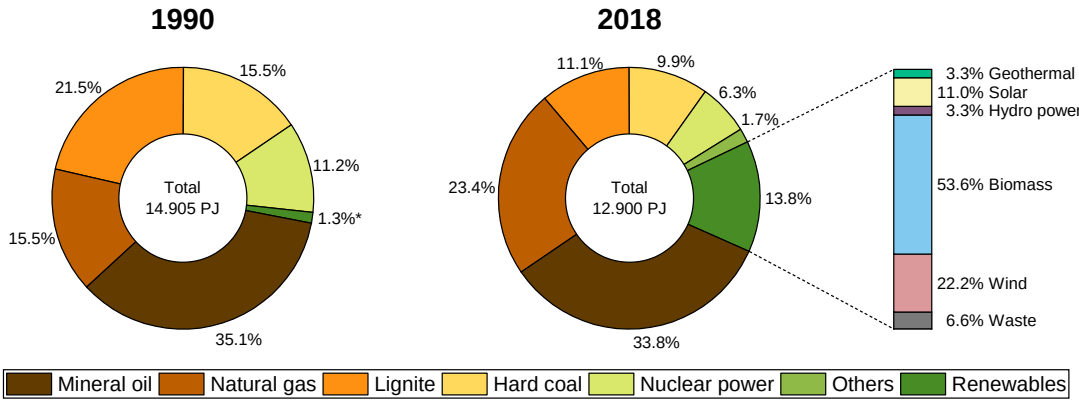

Fig. 1.1: Share of energy sources in primary energy consumption in Germany in 1990 and 2018 (* until 1999 share of Renewables was summarized with Others) [5, 6].

As illustrated in Fig. 1.1, biomass represents with 53.6% the largest group of utilized renewable energy carriers. It can be used in a versatile manner for the production of electricity, heat and vehicle fuel. The organic material is typically transformed to biogas by microbial degradation under anaerobic conditions [7]. The produced biogas is a combustible gaseous mixture, which essentially consists of 50–75% methane (CH_4), 25–45% carbon dioxide (CO_2) and 2–7% water (H_2O), with minor quantities of impurities, like nitrogen (N_2), oxygen (O_2), hydrogen (H_2) and hydrogen sulphide

(H_2S) [8]. Currently, more than 9,400 biogas plants are installed in Germany, which constitutes around 62% in Europe [9, 10]. This leading position in the biogas industry is mainly attributable to promotion as part of EEG [11]. In contrast to other renewable energy systems (such as wind or solar power), the main advantage of biogas is its versatility. Anaerobic digestion can basically be performed with any organic matter in small- and large-scale fermentation processes. Thereby, biogas quality and methane yield are affected by applied feedstock (type, composition) and process conditions [7, 12]. Nowadays, mainly energetic crops (48.9%) and animal excrements (44.5%) are utilized for the operation of biogas plants. Only less than 7% are exclusively fed with waste from municipal, industrial or agricultural sources [13]. Present developments, however, demand for more economical and sustainable use of organic matter due to environmental concerns and competing with food crops for land [14]. The majority of agricultural area in Germany is used for cultivation of animal feedstuff (58%) and foodstuff (26%), though 13% are claimed by energetic crops and 3% by industrial crops and wasteland [13].

Biogas technology provides an important contribution for managing the future requirements on the growing energy supply. For an enhanced utilization of biomass, however, further improvements of the feedstock supply, digestion process and plant design are indispensable [15]. In particular, application of unconventional feedstocks is a challenging task, which requires reliable, fast and on-line analytical techniques and measuring systems for stable process operation.

1.2 Fundamentals of anaerobic digestion

The anaerobic digestion of organic material is a complex biological process, which relies on the syntrophic interaction of a multitude of microorganisms [16]. In the absence of oxygen, the decomposition leads to methane formation basically in four fundamental steps: hydrolysis, acetogenesis, acidogenesis and methanogenesis. Figure 1.2 shows a schematic illustration of this process. Most biogas plants are designed as single-stage systems, where all four phases of microbial degradation occur simultaneously in one reactor. Lower investment costs and simple processing are the main advantages of this fermentation procedure [17]. Each of these four stages is characterized by different optimal environmental conditions required for the involved microorganisms. Therefore, in two- or multi-phase reactors the hydrolysis is performed in a separate tank, in order to adjust pH value and temperature to preferred optima for hydrolyzing bacteria for improved degradation kinetics and methane yields [18, 19].

The first step of anaerobic digestion is the **hydrolysis** of insoluble complex polymers, like carbohydrates, proteins and lipids to smaller units by strictly anaerob (*Clostridia*, *Bacteroides*, *Bifidobacteria*) or facultative anaerob microorganisms (*Streptococcus*, *Enterobacteriaceae*) [7]. These bacteria initiate the cleavage by excretion of hydrolytic enzymes, like cellulase, cellobiase, xylanase, amylase, lipase and protease [20]. The resulting mono- and oligomers (sugars, amino acids and fatty acids) can then be utilized by hydrolytic and acidogenic bacteria. The rate of degradation depends mainly on the composition of the applied feedstock. Substrates with a high content of (hemi)cellulose or fats are hydrolyzed rather slowly within several days, whereas carbohydrate-rich

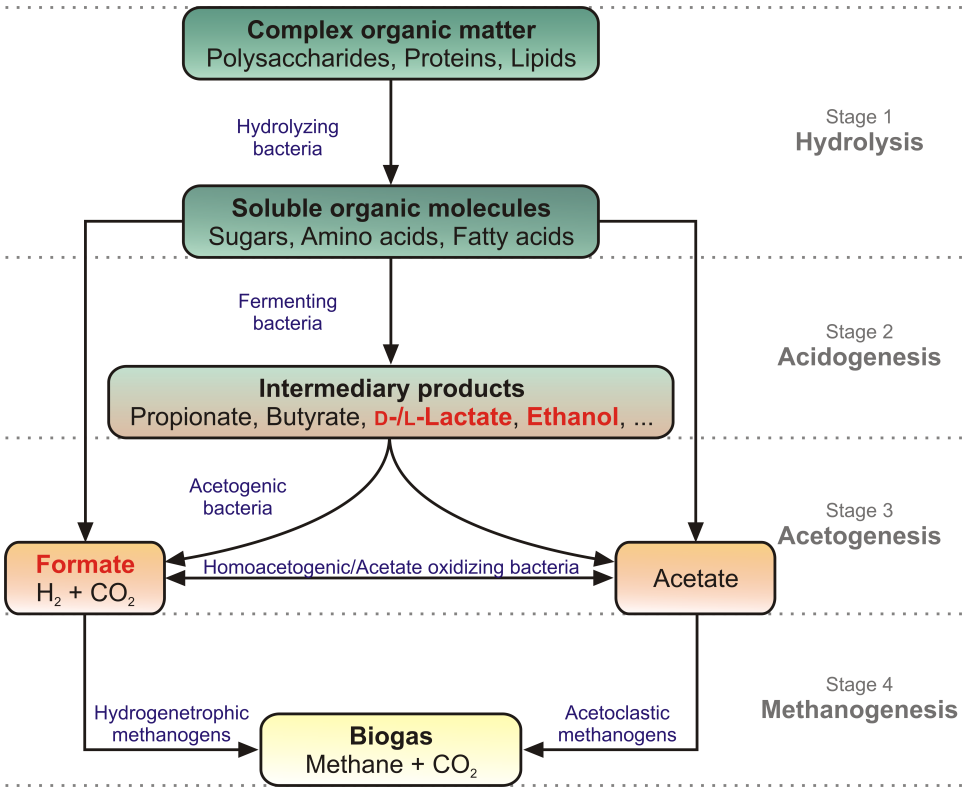

Fig. 1.2: Schematic diagram of methane formation by anaerobic digestion of organic material (adapted from [25]). The intermediates highlighted in red represent the analytes of the developed biosensor array of the present thesis.

substrates decompose within a few hours [21]. Thus, hydrolysis can become the rate-limiting step [22]. Application of various pre-treatment processes (including physical, chemical, and biological methods) can accelerate essential degradation of such complex substrates [23, 24].

Some of the remaining molecules produced throughout hydrolysis are still too big for utilization by other microorganisms. These components are further broken down by various fermentation reactions in the following **acidogenesis** to volatile fatty acids such as acetate, propionate, butyrate (VFAs), other organic acids (lactate, formate, succinate), alcohols, NH_3, CO_2 and H_2 [25–27]. The methanogenic products acetate, CO_2 and H_2 can be directly used for the formation of methane and CO_2. Fermentative bacteria are usually obligate anaerobes in genera such as *Lactobacillus*, *Clostridium*, *Eubacterium* and *Bacteroides* [16]. The acidogenesis phase is considered to be the fastest reaction in the anaerobic digestion process, due to the relatively fast generation times of the corresponding bacteria (depending on the substrate around 5 to 36 h) [28]. In contrast, for the acetogenesis and methanogenesis phases much longer generation times are reported in the range of 84-131 h and 15-85 h, respectively [29, 30]. The different growing kinetics can lead, especially for easily biodegradable compounds, to an accumulation of organic acids and subsequent acidification of the fermentation medium [20]. Further information about the impact of organic acids on the overall process

stability and strategies for monitoring of these compounds are provided in Sec. 1.4.1 and 1.4.3.

In the following **acetogenesis**, the VFAs and alcohols are oxidized to the methanogenic substrates acetate, CO_2 and H_2. This secondary fermentation step is performed by obligate H_2-producing acetogenic bacteria, which are sensitive to high levels of H_2 partial pressure. The released H_2 can be rapidly consumed by syntrophic association with H_2-consuming methanogens [26]. This inter-species electron transfer uses electron carriers, like H_2 and formate, to maintain conditions of low H_2 partial pressure [31, 32].

The final stage is the **methanogenesis**, where the intermediate products are converted into methane and CO_2. Basically, the methane can be synthesized by three different pathways from formate, H_2 and CO_2 (hydrogenotrophic), acetate (acetoclastic) and methylated compounds (methylotrophic) [33]. Approximately 70% of methane are produced via the acetoclastic pathway from acetate and around 30% by hydrogenotrophic reduction of CO_2 [34]. Methanogens are a relative diverse group of archaea, which require a lower redox potential and slightly higher pH value (6.8 to 7.5) than most of the other microorganisms involved in the anaerobic digestion [7].

1.3 Ensiling of energy crops

Most biogas plants in Germany are operated with energetic crops. Maize silage hereby represents with 69% the dominant feedstock, following grass silage (14%) and other plant materials, like grain and sugar beets [13]. Due to its advantageous characteristics (low nutrient demand, high water-use efficiency and high digestibility) and the obtained high methane yields, maize is the most resource-efficient plant for anaerobic digestion [35]. The organic material can be utilized all-season by preservation through acidic fermentation. This ensiling process enables storage over prolonged periods and feeding of biogas plants with substrate of defined composition [36, 37].

Basically, four different phases during ensiling are distinguished [38]. In the initial aerobic phase the remaining O_2 in the silo tank is consumed. The main fermentation phase is characterized by conversion of water-soluble carbohydrates to organic acids, mainly by lactate acid bacteria (LAB) via homo-, hetero-, or mixed acid fermentation. Under anaerobic conditions homofermentative LAB produce the main product lactate through the Embden-Meyerhof-Parnas pathway. The phosphoketolase pathway is used by heterofermentative LAB, which form equimolar amounts of lactate, ethanol, acetate and CO_2 [37, 39]. Mixed acid fermentation leads to the formation of lactate, ethanol, formate and acetate, depending on the environmental conditions [40]. The pH decreases to values around 4.0, due to excessive production of organic acids. At this stage, the high acid tolerance of LAB provides an competitive advantage over other undesirable microorganisms, whose growth is inhibited by the acidic conditions. The fermentation reaches a stable phase until the final feed-out period, where the silage is exposed to air for transportation or feeding. This stage may become critical, when aerobic microorganisms proliferate and thereby spoil the silage [41, 42]. Generally, good silage preservation has been reported for feedstocks with low moisture content, high accessible carbohydrates and low buffering capacity [43].

1.4 Monitoring of biogas plants

The broad spectrum of biomass materials, that can be used for biogas production by anaerobic digestion, provides a high degree of flexibility and versatility to the renewable energy sector. This remarkable potential, however, is still not fully utilized, since many biogas plants are operated in non-optimal conditions and below their rated capacity [44]. Currently, various research- and industrial activities are working on enhanced methane yields and economic operation with technological [45–47] and biological approaches [48, 49]. The successful application of all these different strategies relies in the end on an efficient monitoring system, which enables stable process conditions and early detection of emerging deterioration.

1.4.1 Process disturbances during methane formation

The stability of the anaerobic digestion process is mainly determined by the dynamics of the microbial community and their metabolic activity. Monitoring and control of the biogas plant are for this reason essential for efficient biogas formation. As presented in Fig. 1.3, the overall process stability is sensitive to changes in the operational conditions (e.g., temperature, stirring) and the composition of the applied feedstock. Severe process imbalances can lead to inhibited biogas production and imminent process failure, when appropriate counteractions are not initiated.

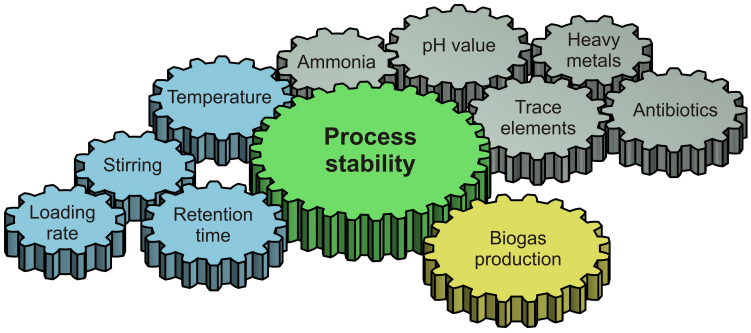

Fig. 1.3: Factors affecting the stability of the anaerobic digestion process and the overall biogas production.

Maintaining optimal environmental conditions is of crucial relevance for stable and successful operation of biogas plants. Especially, the temperature has a significant impact on the growth rate and metabolic activity of the different microorganisms involved in the complex fermentation process. Due to different preferences of the various microbial classes in growth temperature, biogas plants can be operated in a wide range of temperatures at psychrophilic (10–25 °C), mesophilic (25–45 °C) or thermophilic (50–58 °C) conditions. The latter is generally associated with higher degradation rates and increased biogas formation [50]. However, the thermophilic methanogens are more sensitive to temperature fluctuations than acidogenic and acetogenic bacteria, which implies a larger degree of imbalance and greater risk for process inhibition [7, 51]. Most biogas plants are thus operated in the mesophilic temperature region.

Likewise to different optimal temperature regions, the various groups of microbes also have specific preferences for the pH value. In a stable fermentation system the acid production and its degradation to CH_4 are typically balanced procedures. Thereby, biogas is formed within a quite narrow pH range (pH 6.5–8.5), with an optimum condition between pH 7.0 and 8.0 [7]. Methanogenic archea are severely inhibited below a pH of 6.2 or higher than 8.5 [52], whereas fermentative bacteria are tolerant to a wider pH interval (pH 4.0–8.0). The buffer capacity of the digester medium (mainly controlled by hydrogen carbonate and ammonium) generally permits stable pH conditions, which are shifted only in case of serious imbalances by uncontrolled accumulation of organic acids and VFAs [53]. Due to delayed reaction of the pH value to changes within the complex degradation system, this parameter is not particularly suitable for early indication of upcoming process disturbances.

The feeding rate of the applied feedstock is another important aspect affecting the process stability. Imbalances in the methane formation can arise from unstable feeding, organic or hydraulic overloading [54]. Varying organic loading rates typically lead only to fluctuations in the methane yield and thus, to decreased productivity of the biogas plant. In contrast, organic overloads occur when the input of organic material exceeds the overall degradation capacity of the microbes in the biogas plant [55]. This condition leads to insufficient degradation of the organic matter to VFAs and their accumulation in the fermentation system. This can also happen, if the hydraulic retention time is too short and microorganisms with a longer reproduction time are washed out. In both cases, the increasing VFA concentration results in an acidification of the medium and a drop in the pH value, when the buffer capacity is surpassed. The change in the VFA profile can serve as a first indicator for beginning disruptions in the biogas process [56].

The competitive advantage of biogas compared to other renewable resources is the potential application of biomass from different origin (e.g., energy crops, livestock manure or industrial waste). However, the composition of the applied substrates merits also special attention. Feedstock primarily from animal wastes (such as cattle- and pig slurry), for example, is typically characterized by high nitrogen contents. Anaerobic decomposition of such protein-rich substrates and other nitrogenous compounds results in an increasing release of ammonia (NH_3), mainly by metabolization of amino acids through the Stickland reaction. In aqueous solution ammonia is present in two principal forms, the un-ionized free NH_3 and the ammonium ion (NH_4^+). Elevated concentrations of NH_3 are known for inhibition of the degradation process directly by impairing the activity of methane-synthesizing enzymes or indirectly by causing toxic proton imbalances and intracellular pH changes within methanogens [57]. The dissociation equilibrium of NH_3 and thus, the grade of inhibition, depends predominantly on the environmental conditions. Increasing pH and temperature shift the equilibrium to the formation of NH_3. Recovery from NH_3 inhibition can be accomplished by different strategies, such as lowering the pH, reducing the feedstock input or chemical precipitation [58, 59].

Besides inhibitors that are formed during the decomposition process (e.g., VFA, NH_3), some harmful compounds can also be present in the feedstock itself and enter in this way the digester. Detrimental effects on the microbial activity may originate from introduced antibiotics, disinfects, solvents, herbicides, salts or heavy metals [53]. Contamination with antibiotics applies in particular to substrates based on farm manure and animal fats,

although the inhibitory action of specific antibiotics varies greatly [60]. Trace levels of cations of salts (Na^+, K^+, Mg^{2+}, Ca^{2+}, Al^{3+}) and heavy metal ions (Zn^{2+}, Pb^{2+}, Ni^{2+}, Cd^{2+}, Cu^{2+}, Cr^{6+}) generally have a stimulating effect on the biogas production, due to their essential role for activation and function of many enzymes and cofactors. Excessive concentrations, however, have an inhibitory or toxic influence on microbial growth by disrupting enzymatic functions and structures [61]. Heavy metals are not biodegradable and only harmful in their soluble form. Therefore, strategies for attenuation of this toxic potential include precipitation, sorption and chelation by organic and inorganic ligands [62].

For the growth and activity of the diverse microbial consortia not only balanced levels of heavy metal ions and cations of salts are essential, but also the availability of specific micronutrients (e.g., Fe, Ni, Co, Mo, Se and W) is of crucial importance. Especially, a deficiency of Fe, Ni and Co can cause decreasing methane yields, as these trace elements are essential enzyme cofactors in the methane formation pathway [63]. Sufficient supply is normally ensured in biogas plants fed with complex substrate material, however, mono-digestion of energy crops is more prone to limitations [64]. Supplementation with trace elements should be performed carefully, since overdosage can become inhibitory and exceeding concentrations of micronutrients in the digestate limit its subsequent utilization as organic fertilizer [54].

1.4.2 State of the art of basic process monitoring

The stability of the biological methane formation is affected by a broad range of parameters and thus, becomes susceptible to inevitable risks of process disturbances. Severely imbalanced systems result in diminished methane production entailing not insubstantial financial loss for the plant operator. Efficient control and monitoring of biogas plants represent hereby, the challenging task for detection of process instabilities at an early stage. The applied measuring systems should ideally identify the source of malfunction to enable timely initiation of appropriate countermeasures for recovery and stabilization of the process. As illustrated in Fig. 1.4, the key for reliable evaluation of the process performance, however, is not a single state indicator, but rather knowledge about a variety of physical, chemical and microbiological parameters [65]. Some of these are easily measurable and available for on-line or daily monitoring (such as biogas production rate, pH value or temperature), while others require sampling and extensive analysis with

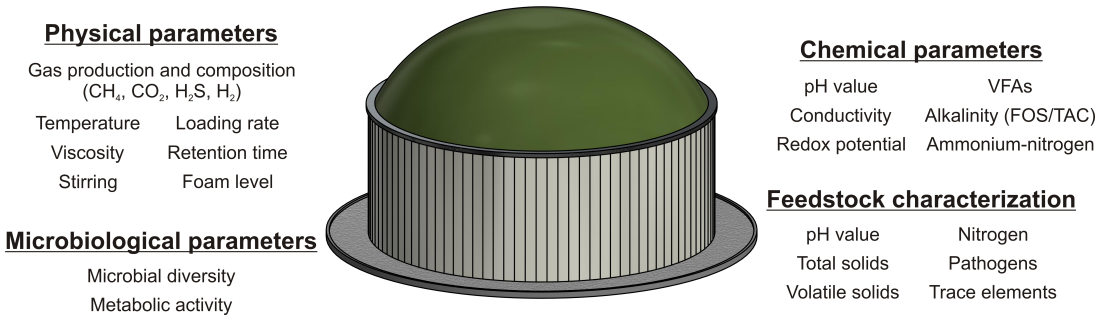

Fig. 1.4: Overwiew of parameters used for monitoring of biogas plants (adapted from [52, 54].

sophisticated instruments (e.g., VFAs, NH_4^+-N, microbial diversity) [66, 67]. Additional costs and time consumption are the downside of the latter, which limit their regular application to longer intervals on a weekly or monthly basis. The standard monitoring of biogas plants typically includes analysis of biogas production and its composition, process temperature, pH value and alkalinity of the digester medium.

For determination of the biogas production rate various measuring devices are applicable, which enable continuous recording. The instruments are based on either volumetric or direct mass-flow measurement. Most commonly vortex flow meters are installed [68]. The monitoring of the gas composition is typically performed with on-line measuring systems, but for smaller biogas plants also portable instruments are available. Thereby, CH_4 and CO_2 are measured by infrared- or thermal conductivity sensors. The amount of H_2S, H_2 and O_2 is analyzed with electrochemical sensors, for the latter paramagnetic sensors can be applied as well [53, 54]. Electrochemical sensors are generally subject to some sort of drift and require for this reason regular cleaning, calibration or replacement.

As described earlier in Sec. 1.4.1, maintenance of a constant temperature in the digester is essential for a stable fermentation process. The recommended tolerable daily variations range from <1 °C for thermophilic to 2–3 °C for mesophilic conditions [54]. The anaerobic digestion usually generates hardly any thermal energy, thus insulation and heating of the digester are required for sufficient temperature control [17]. Different types of measuring instruments can be applied for the monitoring, including resistance thermometer, thermo-elements and thermistors [69]. The choice of an appropriate sensing technology depends on the design of the biogas plant and the desired temperature region. Different positions within the reactor should be used for installation of the sensors, in order to identify inhomogeneous mixing and dead zones [53]. The on-line measurement of the process temperature is also of important relevance for reliable evaluation of other temperature-dependent parameters such as pH value, NH_4^+-N content and conductivity.

Monitoring and control of the pH value is essential for all bioprocesses due to the significant impact on the activity of enzymatic and bacterial reactions. Although this parameter reacts rather slow to changes in the microbial network and concomitant process disturbances, the analysis is typically performed on a regular basis. Conventional pH-glass electrodes are used for measurement of the pH value in the liquid phase. On-line application of such probes in digesters with a high total solid content is challenging, due to rapid electrode fouling and requirement of regular cleaning and calibration [70]. Most often measurements are therefore performed off-line, despite lower accuracy as a result of the required sampling- and storing procedure [54].

For improved evaluation of the process performance, the alkalinity ratio (FOS/TAC) is determined, which relates the contents of volatile organic acids (FOS) and total anorganic carbonate (TAC). The first term represents the acid concentration, providing information about accumulation of VFAs. The amount of TAC reflects the buffer capacity of the fermentation medium and thus, the ability to cope with moderate acid accumulation without a significant decrease in the pH value. The FOS/TAC is determined off-line by a low-cost and fast two-point titration measurement. Each biogas plant is characterized by a unique ideal ratio, so that absolute values for stable process operation are not comparable or transferable [71]. Application of this technique is limited to fermentation samples with a pH value up to 5.0 [72].

1.4.3 Impact of organic acids and alcohols on process stability

Basic process monitoring is an important assignment for operating biogas plants, but generally not sufficient for fast indication of process disturbances. For this reason, extensive research has focused on the identification of parameters, which are more sensitive to changes in the anaerobic digestion process [73–75]. The monitoring of several organic intermediates has thereby proved to be a promising approach for evaluation of the process stability, too. Uncontrolled accumulation of VFAs results eventually in acidification of the digester medium and a decrease in the pH level. Inhibition of methanogenesis and increasing risk of a total reactor failure are the consequences. The VFA concentration has thus been widely considered as a state indicator for anaerobic digestion processes. In this regard, various studies have aimed to identify key intermediates for indication of upcoming process disturbances such as acetate [75], propionate [76] or butyrate [77] (see Fig. 1.5). The obtained results, however, demonstrated that it is rather impossible to define generally applicable absolute concentrations or thresholds for a specific analyte, due to the complex nature of the fermentation process and the microbial ability to adapt to changing environmental conditions.

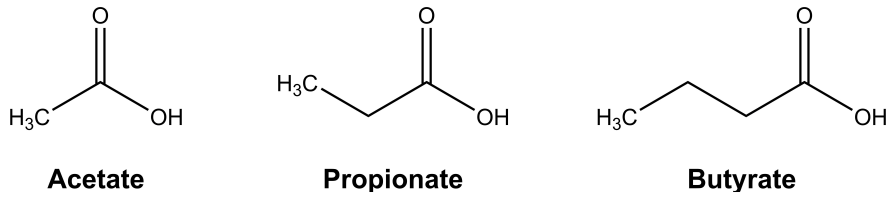

Fig. 1.5: Volatile fatty acids used for monitoring of anaerobic digestion processes.

For quantification of total VFA concentration various titration methods have been described [78, 79]. This value, however, often overestimates the actual acid concentration [80]. Measurement of individual VFAs can be accomplished by separating chromatographic methods, like high-performance liquid chromatography (HPLC) [81, 82], gas chromatography (GC) [83, 84] or headspace GC [85, 86]. Some of these techniques have been integrated in on-line monitoring systems for the analysis in the gas phase [87, 88]. Alternative approaches based on mid-infrared or near-infrared spectroscopy are also limited to VFA detection in the gaseous atmosphere [89, 90]. More precise process monitoring in the liquid phase generally requires laborious manual sampling. Fast sample handling, immediate cooling and defined storage conditions are important steps for reliable results [91]. For the measurement of VFAs in liquid samples only few biosensors have been reported in literature. Microbial electrochemical biosensors, for example, utilize electroactive biofilms as living recognition element that oxidize organic substrates, like acetate in a single-chamber compartment [92]. Thereby, the substrate concentration is measured as electric current generated by cellular respiration. Biosensors based on dual-chamber microbial fuel cells consist of an anodic (where e^- are produced by microbial oxidation) and a cathodic chamber separated by an ion exchange membrane [93, 94]. However, such biosensors are often limited by their substrate specificity. More specific determination of acetate and propionate has been realized with enzyme-based biosensors [95–97]. Further information about the mode of operation of

electrochemical biosensors is provided in Ch. 2.

In the field of monitoring anaerobic digestion processes, most research has focused on the influence of VFAs on the process stability. As illustrated in Fig. 1.2, further intermediates are also of central relevance for successful methane formation and merit consideration. This applies in particular to the analytes shown in Fig. 1.6: formate, both stereoisomers of lactate (D-lactate, L-lactate), and ethanol. These substances are more over essential end-products formed during ensiling of energy crops [98] (see Sec. 1.3). Since changes in the feedstock (in regard to quality and composition) can severely inhibit the overall anaerobic digestion process, regular characterization of the applied feedstock is as important as basic process monitoring, as presented in Fig. 1.4 [99].

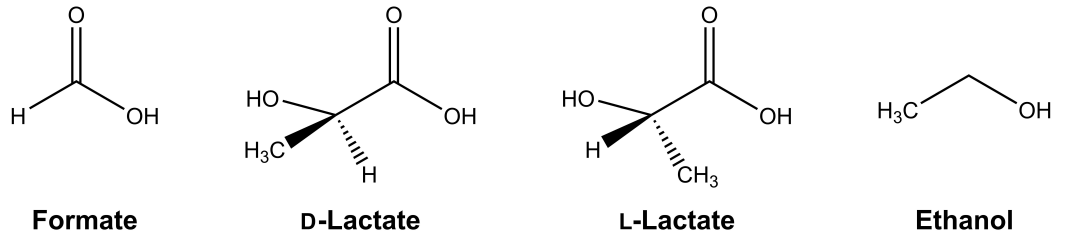

Fig. 1.6: Intermediates of the anaerobic degradation process used in the present thesis for evaluation of biogas processes.

Methane formation from methanogenic substrates (H_2, CO_2, **formate** and acetate) depends on direct interspecies electron transfer between acetogenic bacteria and methanogenic archaea within their syntrophic relationship [100]. Thereby, the syntrophic oxidation of acetate is severely affected by the concentrations of both H_2 and formate [101]. These two compounds function as essential electron carriers in methanogenic biomass degradation [102]. Generally, low H_2 partial pressure levels are preferred for methanogenesis, since high levels stimulate propionate and butyrate accumulation.

The intermediate **lactate** is produced mainly by LAB from the genera *Bacillus*, *Clostridium*, *Lactobacillus*, *Pediococcus* and *Streptococcus* [103]. It functions as a precursor that is primary oxidized to acetate and propionate during acetogenesis [104, 105]. As described earlier, accumulation of these intermediates is associated with disturbances in the microbial methane production. Lactate levels typically accumulate only on short-term in case of sudden increase of readily degradable substrates, like glucose, before energetically favorable consumption by other bacteria [106]. Changing organic loading rates with glucose as a sole carbon source, for example, resulted in coordinated reorganization of bacterial and archaeal populations [107]. Excess glucose was thereafter consumed rapidly, accompanied by accumulation of lactate, formate and ethanol. These intermediates were characteristic for deteriorated reactor performance. When the feedstock supply was changed again to a lower level, VFA (butyrate and propionate) concentration increased by depletion of lactate, formate and ethanol. The significant role of lactate on biogas production was also demonstrated by increased total biogas yield (up to 45%), when lactate-rich maize silage was used in comparison to lactate-devoid fresh maize [108]. For efficient utilization of high lactate content,

microbial communities depend on appropriate adaption (preferably in starter inocula). Otherwise, high concentrations of lactate can deteriorate the methane formation by accumulation of propionate [109].

Enhanced biogas formation can be achieved by imposed mixed lactate-ethanol fermentation in a two-phase reactor [110]. Direction of microbial degradation process towards **ethanol** and lactate production was used in the first reactor. These substrates were then directly available to the methanogenic bacteria in a second stage reactor, which improves methanogenesis. Similarly, fermenters pulsed daily with ethanol (50 to 100 mM) showed an increased methane production [111]. For adjustment of fluctuating energy demands, this effect can also be applied on a short-term basis, where methane increase occurs within 2 h [112].

Determination of ethanol, formate, D-lactate and L-lactate in fermentation samples is typically conducted, similarly to VFAs, by GC [114] or HPLC [113, 115]. These techniques, however, are rather laborious and require expensive instrumentation operated by trained personnel. The application of simplified and portable measuring devices for rapid analyte quantification would be therefore desirable. In this regard, electrochemical biosensors might provide a suitable option. Various enzymes-based biosensors are reported for specific detection of formate [116, 117], lactate [118, 119] and ethanol [120, 121]. However, biosensors for simultaneous analysis of several intermediates are rather rare, though, for practical and economic reasons integration of multiple bio-sensing electrodes within an array is more than reasonable.

1.5 Aim and outline of the work

The aim of this work is the development of an electrochemical biosensor system for the detection of different analytes, which could be used for characterization of the feedstock and stability of biogas processes. The intermediates ethanol, formate, D-lactate and L-lactate were chosen as promising state indicators for evaluation of the overall process stability due to their significant role during anaerobic degradation of organic material. Compared to state of the art techniques currently employed for the control of biogas plants, the intended monitoring system should especially provide advantages in terms of ease of use, miniaturization, portable instrumentation and rapid analysis. In this regard, the following objectives have been defined:

- selection of a suitable electrochemical enzyme-based detection principle for simultaneous quantification of D-lactate, L-lactate, ethanol and formate,
- selection of an appropriate strategy for immobilization of enzymes on the transducer surface of the sensor chip,
- optimization and characterization of the biosensor performance with regard to the envisaged monitoring of biogas processes and feedstocks,
- design and construction of a mobile hand-held device for on-site operation,
- operation under real conditions in complex samples, including evaluation of a suitable procedure for sample preparation,

- demonstration of the practical applicability by long-term monitoring of a biogas process and comparison with conventional analytical techniques,
- improvement of the biosensor array by development of a reagent-free biosensing system.

After a brief introduction to the basic principles of amperometric biosensors and enzymes as biological recognition elements in **Ch. 2**, the following **Chs. 3 to 7** refer to peer-reviewed publications that have been released in the course of this work.

The proof of concept for simultaneous measurement of different analytes with an enzyme-based biosensor is presented in **Ch. 3**. Thereby, an amperometric bi-enzymatic detection principle is introduced, which relies on NAD^+-dependent dehydrogenases in combination with a diaphorase from *Clostridium kluyveri* immobilized on platinum thin-film electrodes. This system has been used for the first time to realize a multi-parameter biosensor, which enables the rapid quantification of three compounds, namely formate, D-lactate and L-lactate.

In the following, this sensor concept has been further improved by integration of an additional ethanol-sensing electrode. In this way, a biosensor for concurrent determination of overall four analytes was realized. Application of different enzymes within one biosensing system requires evaluation of the best surrounding conditions to guarantee highest possible biocatalytic activity. The optimization and characterization of the performance for each individual biosensor are content of **Ch. 4**. The immobilization and measurement conditions were optimized in regard to enzyme loading, cross-linker concentration, temperature and buffer solution (pH and cofactor concentration). Subsequently, the performance of the biosensor array was characterized by the linear working range, sensitivity, lower detection limit, response time and working stability. Additionally, successful application of the elaborated amperometric detection system has been demonstrated with other NAD^+-dependent dehydrogenases for the construction of a biosensor array for malate, fumarate and aspartate by D.L. Röhlen.

An essential requirement for convenient, practical application of the developed biosensor was the integration within a portable measurement set-up. For this reason, the three-electrode arrangement was revised by integration of the formerly external counter electrode on the platinum biosensor chip. In this context, also a novel three-dimensional (3D)-printed measurement cell has been constructed. **Chapter 5** deals with the fabrication process of the thin-film electrodes and the mobile hand-held device. The chip production by thin-film technology is rather expensive, thus repeated and long-term use of such biosensors is desirable. After characterization of the operational stability (**Ch. 4**), the optimal storage conditions were also tested. Integration of the biosensor array within an microfluidic system has been conducted in collaboration with L. Breuer, who developed light-addressable hydrogel valves acting as actuators. In this way, a proof of concept of a lab-on-a-chip system has been established.

The application of biosensors in real samples is susceptible to interferences from other electroactive species and matrix effects. For this reason, correct sample preparation constitutes a critical aspect in the usage of biosensors. The effect of different potential interfering substances on the sensor response is discussed in **Ch. 6**. This work has been conducted in collaboration with D.L. Röhlen, who developed a biosensor for acetate and

propionate based on the amperometric detection of H_2O_2. Both biosensors have been used for the long-term monitoring of a lab-scale biogas reactor in order to demonstrate the potential for early detection of process disturbances.

So far, the detection principle required the addition of both cofactors (NAD^+ and $Fe(CN)_6^{3-}$) to the measurement solution. The immobilization of all necessary components on the electrode surface was therefore highly desirable. **Chapter 7** shows the transfer of the sensor concept to carbon-based screen-printed electrodes, modified with graphene oxide, for fabrication of reagentless and disposable biosensors.

In **Ch. 8**, a brief summary and discussion of the obtained results are presented, including possible future applications, potential improvements and challenges.

References

[1] Dincer, I. (1998) Energy and environmental impacts: Present and future perspectives. *Energy Sources* 20:427–423, doi:10.1080/00908319808970070.

[2] Juhrich, K. (2016) CO_2 emission factors for fossil fuels. *Climate Change 28/2016, Umweltbundesamt.*

[3] Bechberger, M.; Reiche, D. (2004) Renewable energy policy in Germany: Pioneering and exemplary regulations. *Energy Sustain. Dev.* 8:47–57, doi:10.1016/S0973-0826(08)60390-7.

[4] Frondel, M.; Ritter, N.; Schmidt, M.C.; Vance, M. (2010) Economic impacts from the promotion of renewable energy technologies: The German experience. *Energy Policy* 38:4048–4056, doi:10.1016/j.enpol.2010.03.029.

[5] Ziesing, H.-J. (2019) Energieverbrauch in Deutschland im Jahr 2018. Berlin: *Arbeitsgemeinschaft Energiebilanzen e.V.*.

[6] Arbeitsgemeinschaft Energiebilanzen e.V. (2019) Auswertungstabellen zur Energiebilanz Deutschland. Daten für die Jahre von 1990 bis 2018.

[7] Weiland, P. (2010) Biogas production: Current state and perspectives. *Appl. Microbiol. Biotechnol.* 85:849–860, doi:10.1007/s00253-009-2246-7.

[8] Edelmann, W. (2001) Biogas Production and Usage. In: Kaltschmitt, M.; Hartmann, H. (Eds.) Energy from Biomass: Basic Principles, Technologies and Processes. Leipzig: *Springer*.

[9] Torrijos, M. (2016) State of development of biogas production in Europe. *Procedia Environ. Sci.* 35:881–889, doi:10.1016/j.proenv.2016.07.043.

[10] Fachverband Biogas (2019) Anzahl der Biogasanlagen in Deutschland in den Jahren 1992 bis 2019. Retrieved October 18, 2019, from: `https://de.statista.com/statistik/daten/studie/167671/umfrage/anzahl-der-biogasanlagen-in-deutschland-seit-1992`.

[11] Rensberg, N.; Hennig, C.; Naumann, K.; Billig, E.; Sauter. P.; Daniel-Gromke, J.; Krautz, A.; Weiser, C.; Reinhold, G.; Graf, T. (2012) Monitoring zur Wirkung

des Erneuerbare-Energien-Gesetz (EEG) auf die Entwicklung der Stromerzeugung aus Biomasse (FZK: 03MAP138). *Endbericht zur EEG-Periode 2009 bis 2011.*

[12] Al Seadi, T.; Rutz, D.; Janssen, R.; Drosg, B. (2013) Biomass Resources for Biogas Production. In: Wellinger, A; Murphy, J.; Baxter, D. (Eds.) The Biogas Handbook: Science, Production and Applications. Oxford: *Woodhead Publishing*, doi:10.1533/9780857097415.1.19.

[13] Fachagentur Nachwachsende Rohstoffe e.V. (FNR) (2019) Basisdaten Bioenergie Deutschland 2019, Gülzow: *FNR.*

[14] Poeschl, M.; Ward, S.; Owende, P. (2010) Prospects for expanded utilization of biogas in Germany. *Renew. Sust. Energ. Rev.* 14:1782–1797, doi:10.1016/j.rser.2010.04.010.

[15] Scarlat, N.; Dallemand, J.-F.; Fahl, F. (2018) Biogas: Developments and perspectives in Europe. *Renew. Energy* 129:457–472, doi:10.1016/j.renene.2018.03.006.

[16] Klass, D.L. (1984) Methane from anaerobic fermentation. *Science* 223(4640):1021–1028, doi:10.1126/science.223.4640.1021.

[17] Bachmann, N. (2013) Design and Engineering of Biogas Plants. In: Wellinger, A; Murphy, J.; Baxter, D. (Eds.) The Biogas Handbook: Science, Production and Applications. Oxford: *Woodhead Publishing*, doi:10.1533/9780857097415.2.191.

[18] Pohland, F.G.; Ghosh, S. (1971) Developments in anaerobic stabilization of organic wastes – the two phase concept. *Environ. Lett.* 1(4):255–266, doi:10.1080/00139307109434990.

[19] Demirel, B.; Yenigün, O. (2002) Two-phase anaerobic digestion processes: A review. *J. Chem. Technol. Biotechnol.* 77:743–755, doi:10.1002/jctb.630.

[20] Merlin Christy, P.; Gopinath, L.R.; Divya, D. (2014) A review on anaerobic decomposition and enhancement of biogas production through enzymes and microorganisms. *Renew. Sust. Energ. Rev.* 34:167–173, doi:10.1016/j.rser.2014.03.010.

[21] Schnürer, A.; Jarvis, Å. (2010) Microbiological handbook for biogas plants. *Swedish Gas Centre Report* 207:1–142.

[22] Noike, T.; Endo, G.; Chang, J. E.; Yaguchi, J.; Matsumoto, J. (1985) Characteristics of carbohydrate degradation and the rate-limiting step in anaerobic digestion. *Biotechnol. Bioeng.* 27:1482–1489, doi:10.1002/bit.260271013.

[23] Ariunbaatar, J.; Panico, A.; Esposito, G.; Pirozzi, F.; Lens, P.N.L. (2014) Pretreatment methods to enhance anaerobic digestion of organic solid waste. *Appl. Energy* 123:143–156, doi:10.1016/j.apenergy.2014.02.035.

[24] Lee, B.; Park, J.-G.; Shin, W.-B.; Kim, B.-S.; Byun, B.; Jun, B.-S. (2019) Maximizing biogas production by pretreatment and by optimizing the mixture ratio of co-digestion with organic wastes. *Environ. Eng. Res.* 24(4):662–669, doi:10.4491/eer.2018.375.

[25] Gujer, W.; Zehnder, A.J.B. (1983) Conversion processes in anaerobic digestion.

Water Sci. Technol. 15:127–167, doi:10.2166/wst.1983.0164.

[26] Schink, B. (1997) Energetics of syntrophic cooperation in methanogenic degradation. *Microbiol. Mol. Biol. Rev.* 61(2):262–280.

[27] Zhou, M.; Yan, B.; Wong, J.W.C.; Zhang, Y. (2018) Enhanced volatile fatty acids production from anaerobic fermentation of food waste: A mini-review focusing on acidogenic metabolic pathways. *Bioresour. Technol.* 248:68–78, doi:10.1016/j.biortech.2017.06.121.

[28] Mosey, F.E.; Fernandes, X.A. (1989) Patterns of hydrogen in biogas from the anaerobic digestion of milk-sugars. *Wat. Sci. Tech.* 21:187–196, doi:10.2166/wst.1989.0222.

[29] Deublein, D.; Steinhauser, A. (2008) Biogas from Waste and Renewable Resources: An Introduction. Weinheim: *Wiley-VCH*.

[30] Ziemiński, K.; Frąc, M. (2012) Methane fermentation process as anaerobic digestion of biomass: Transformations, stages and microorganisms. *Afr. J. Biotechnol.* 11(18):4127–4139, doi:10.5897/AJBX11.054.

[31] Thiele, J.H.; Zeikus, J.G. (1988) Control of interspecies electron flow during anaerobic digestion: Significance of formate transfer versus hydrogen transfer during syntrophic methanogenesis in flocs. *Appl. Environ. Microbiol.* 54:20–29.

[32] Baek, G.; Kim, J.; Kim, J.; Lee, C. (2018) Role and potential of direct interspecies electron transfer in anaerobic digestion. *Energies* 11:107, doi:10.3390/en11010107.

[33] Ferry, J.G. (2010) The chemical biology of methanogenesis. *Planet. Space Sci.* 58:1775–1783, doi:10.1016/j.pss.2010.08.014.

[34] Anderson, K.; Sallis, P.; Uyanik, S. (2003) Anaerobic treatment processes. In: Mara, D.; Horan, N. (Eds.) Handbook of Water and Wastewater Microbiology. London: *Academic Press*, doi:10.1016/B978-012470100-7/50025-X.

[35] Herrmann, A. (2013) Biogas production from maize: Current state, challenges, and prospects. 2. Agronomic and environmental aspects. *Bioenerg. Res.* 6:372–387, doi:Herrmann.2013.

[36] Weiland, P. (2003) Production and energetic use of biogas from energy crops and wastes in Germany. *Appl. Microbiol. Biotechnol.* 109:263–274, doi:10.1385/ABAB:109:1-3:263.

[37] Herrmann, C.; Heiermann, M.; Idler, C. (2011) Effects of ensiling, silage additives and storage period on methane formation of biogas crops. *Bioresour. Technol.* 102:5153–5161, doi:10.1016/j.biortech.2011.01.012.

[38] Pahlow, G.; Muck, R.E.; Driehuis, F.; Oude Elferink, S.J.W.H.; Spoelstra, S.F. (2003) Microbiology of Ensiling. In: Buxton, D.R.; Muck, R.E.; Harrison, Joseph H. (Eds.) Silage Science and Technology. Madison: *American Society of Agronomy*, doi:10.2134/agronmonogr42.c2.

[39] Whittenbury, R.; McDonald, P.; Bryan-Jones, D.G. (1967) A short review of some

biochemical and microbiological aspects of ensilage. *J. Sci. Food Agric.* 18:441–444, doi:10.1002/jsfa.2740181001.

[40] Hofvendahl, K.; Hahn–Hägerdal, B. (2000) Factors affecting the fermentative lactic acid production from renewable resources. *Enzyme Microb. Technol.* 26:87–107, doi:10.1016/S0141-0229(99)00155-6.

[41] Herrmann, C.; Idler, C.; Heiermann, M. (2015) Improving aerobic stability and biogas production of maize silage using silage additives. *Bioresour. Technol.* 197:393–403, doi:10.1016/j.biortech.2015.08.114.

[42] Borreani, G.; Tabacco, E.; Schmidt, R.J.; Holmes, B.J.; Muck, R.E. (2018) Silage review: Factors affecting dry matter and quality losses in silages. *J. Dairy Sci.* 101:3952–3979, doi:10.3168/jds.2017-13837.

[43] Teixeira Franco, R.; Buffière, P.; Bayard, R. (2016) Ensiling for biogas production: Critical parameters. A review. *Biomass Bioenergy* 94:94–104, doi:10.1016/j.biombioe.2016.08.014.

[44] Ward, A.J.; Hobbs, P.J.; Holliman, P.J.; Jones, D.L. (2008) Optimisation of the anaerobic digestion of agricultural resources. *Bioresour. Technol.* 99:7928–7940, doi:10.1016/j.biortech.2008.02.044.

[45] Walla, C.; Schneeberger, W. (2008) The optimal size for biogas plants. *Biomass Bioenergy* 32(6):551–557, doi:10.1016/j.biombioe.2007.11.009.

[46] Balussou, D.; Heffels, T.; McKenna, R.; Möst, D.; Fichtner, W. (2014) An evaluation of optimal biogas plant configurations in Germany. *Waste Biomass. Valor.* 5:743–758, doi:10.1007/s12649-013-9284-1.

[47] Achinas, S.; Achinas, V.; Euverink, G.J.W. (2017) A technological overview of biogas production from biowaste. *Engineering* 3:299–307, doi:10.1016/J.ENG.2017.03.002.

[48] Bagi, Z.; Acs, N.; Bálint, B.; Horváth, L.; Dobó, K.; Perei, K.R.; Rákhely, G.; Kovács, K.L. (2007) Biotechnological intensification of biogas production. *Appl. Microbiol. Biotechnol.* 76:473–482, doi:10.1007/s00253-007-1009-6.

[49] Vervaerena, H.; Hostyn, K.; Ghekiere, G.; Willems, B. (2010) Biological ensilage additives as pretreatment for maize to increase the biogas production. *Renew. Energy* 35:2089–2093, doi:10.1016/j.renene.2010.02.010.

[50] Lin, Q.; Vrieze, J.D.; Li, J. Li, X. (2016) Temperature affects microbial abundance, activity and interactions in anaerobic digestion. *Bioresour. Technol.* 209:228–236, doi:10.1016/j.biortech.2016.02.132.

[51] Gerardi, M.H. (2003) The Microbiology of Anaerobic Digesters. Hoboken, New Jersey: *John Wiley & Sons, Inc*, doi:10.1002/0471468967.

[52] Switzenbaum, M.S.; Giraldo-Gomez, E.; Hickey, R.F. (1990) Monitoring of the anaerobic methane fermentation process. *Enzyme Microb. Technol.* 12:722–730, doi:10.1016/0141-0229(90)90142-D.

[53] Fachagentur Nachwachsende Rohstoffe e.V. (2012) Guide to biogas: From production to use. Gülzow-Prüzen: *FNR*.

[54] Drosg, B. (2013) Process monitoring in biogas plants. In: Frost, P.; Baxter, D. (Eds.) Task 37: Energy from Biogas. Hillsborough, Petten: *IEA Bioenergy*.

[55] Holm-Nielsen, J.B.; Oleskowicz-Popiel, P. (2013) Process Control in Biogas Plants. In: Wellinger, A; Murphy, J.; Baxter, D. (Eds.) The Biogas Handbook: Science, Production and Applications. Oxford: *Woodhead Publishing*, doi:10.1533/9780857097415.2.228.

[56] Wijekoon, K.C.; Visvanathan, C.; Abeynayaka, A. (2011) Effect of organic loading rate on VFA production, organic matter removal and microbial activity of a two-stage thermophilic anaerobic membrane bioreactor. *Bioresour. Technol.* 102:5353–5360, doi:10.1016/j.biortech.2010.12.081.

[57] Calli, B.; Mertoglu, B.; Inanc, B.; Yenigun, O. (2005) Effects of high free ammonia concentrations on the performances of anaerobic bioreactors. *Process Biochem.* 40:1285–1292, doi:10.1016/j.procbio.2004.05.008.

[58] Yenigün, O; Demirel, B. (2013) Ammonia inhibition in anaerobic digestion: A review. *Process Biochem.* 48:901–911, doi:10.1016/j.procbio.2013.04.012.

[59] Krakat, N.; Demirel, B.; Anjum, R.; Dietz, D. (2017) Methods of ammonia removal in anaerobic digestion: A review. *Wat. Sci. Tech.* 76(8):1925–1938, doi:10.2166/wst.2017.406.

[60] Mitchell, S.M.; Ullman, J.L.; Teel, A.L.; Watts, R.J.; Frear, C. (2013) The effects of the antibiotics ampicillin, florfenicol, sulfamethazine, and tylosin on biogas production and their degradation efficiency during anaerobic digestion. *Bioresour. Technol.* 149:244–252, doi:10.1016/j.biortech.2013.09.048.

[61] Hickey, R.F.; Vanderwielen, J.; Switzenbaum, M.S. (1989) The effect of heavy metals on methane production and hydrogen and carbon monoxide levels during batch anaerobic sludge digestion. *Water Res.* 23(2):207–218, doi:10.1016/0043-1354(89)90045-6.

[62] Chen, Y.; Cheng, J.J.; Creamer, K.S. (2008) Inhibition of anaerobic digestion process: A review. *Bioresour. Technol.* 99:4044–4064, doi:10.1016/j.biortech.2007.01.057.

[63] Theuerl, S.; Klang, J.; Prochnow, A. (2019) Process disturbances in agricultural biogas production – causes, mechanisms and effects on the biogas microbiome: A review. *Energies* 12:365, doi:10.3390/en12030365.

[64] Demirel, B.; Scherer, P. (2011) Trace element requirements of agricultural biogas digesters during biological conversion of renewable biomass to methane. *Biomass Bioenergy* 35:992–998, doi:10.1016/j.biombioe.2010.12.022.

[65] Liebetrau, J.; Pfeiffer, D.; Thrän, D. (2015) Messmethodensammlung Biogas: Methoden zur Bestimmung von analytischen und prozessbeschreibenden Parametern im Biogasbereich. Schriftenreihe des Förderprogramms „Energetische

Biomassenutzung“, Vol. 7. Leipzig: *DBFZ*.

[66] VDI-Gesellschaft Energie und Umwelt (2011) VDI-Richtlinien: Gütekriterien für Biogasanlagen (VDI 4631). Berlin: *Beuth Verlag GmbH*.

[67] Scholwin, F.; Liebetrau, J.; Edelmann, W.; Ritzkowski, M.; Körner, I. (2009) Biogaserzeugung und -nutzung. In: Kaltschmitt, M.; Hartmann, H.; Hofbauer, H. (Eds.) Energie aus Biomasse: Grundlagen, Techniken und Verfahren. Berlin, Heidelberg: *Springer*, doi:10.1007/978-3-540-85095-3_16.

[68] Effenberger, M.; Aschmann, V.; Herb, C.; Helm, M.; Müller, J.S. (2012) Empfehlungen für die messtechnische Ausstattung landwirtschaftlicher Biogasanlagen. In: ALB Bayern e.V. (Ed.) Biogas Forum Bayern Nr.IV – 07/2012.

[69] Ghanavati, H. (2018) Biogas Production Systems: Operation, Process Control, and Troubleshooting. In: Tabatabaei, M.; Ghanavati, H. (Eds.) Biogas: Fundamentals, Process, and Operation. Cham: *Springer*, doi:10.1007/978-3-319-77335-3_8.

[70] Wolf, C.; Gaida, D.; Bongards, M. (2014) Online-measurement systems for agricultural and industrial AD plants – a review and practice test. *Kompendium der Forschungsgemeinschaft: 2012-2014*.

[71] Voß, E.; Weichgrebe, D.; Rosenwinkel, K. (2009) FOS/TAC – deduction, methods, application and significance. *Internationale Wissenschaftskonferenz „Biogas Science 2009 – science meets practice”*, LfL-Bayern, 2–4. 12.09, Erding.

[72] Strach, K.; Zechendorf, M.D. (2015) Bestimmung des FOS-Wertes (nach Kapp) und des FOS/TAC-Wertes (nach FAL). In: Liebetrau, J.; Pfeiffer, D.; Thrän, D. (Eds.) Messmethodensammlung Biogas: Methoden zur Bestimmung von analytischen und prozessbeschreibenden Parametern im Biogasbereich. Schriftenreihe des Förderprogramms „Energetische Biomassenutzung“, Vol. 7. Leipzig: *DBFZ*.

[73] Archer, D.B.; Hilton, M.G.; Adams, P.; Wiecko, H. (1986) Hydrogen as a process control index in a pilot scale anaerobic digester. *Biotechnol. Lett.* 8:197–202, doi:10.1007/BF01029380

[74] Nakakubo, R.; Møller, H.B.; Nielsen, A.M.; Matsuda, J. (2008) Ammonia inhibition of methanogenesis and identification of process indicators during anaerobic digestion. *Environ. Eng. Sci.* 25:1487–1496, doi:10.1089/ees.2007.0282.

[75] Boe, K.; Batstone, D.J.; Steyer, J.-P.; Angelidaki, I. (2010) State indicators for monitoring the anaerobic digestion process. *Water Res.* 44:5973–5980, doi:10.1016/j.watres.2010.07.043.

[76] Nielsen, H.B.; Uellendahl, H.; Ahring, B.K. (2007) Regulation and optimization of the biogas process: Propionate as a key parameter. *Biomass Bioenergy* 31:820–830, doi:10.1016/j.biombioe.2007.04.004.

[77] Ahring, B.K.; Sandberg, M.; Angelidaki, I. (1995) Volatile fatty acids as indicators of process imbalance in anaerobic digestors. *Appl. Microbiol. Biotechnol.* 43:559–565, doi:10.1007/BF00218466.

[78] Feitkenhauer, H.; von Sachs, J.; Meyer, U. (2002) On-line titration of volatile fatty

acids for the process control of anaerobic digestion plants. *Water Res.* 36:212–218, doi:10.1016/S0043-1354(01)00189-0.

[79] Sun, H.; Guo, J.; Wu, S.; Liu, F.; Dong, R. (2017) Development and validation of a simplified titration method for monitoring volatile fatty acids in anaerobic digestion. *Waste Manage.* 67:43–50, doi:10.1016/j.wasman.2017.05.015.

[80] Lützhøft, H.-C.H.; Boe, K.; Fang, C.; Angelidaki, I. (2014) Comparison of VFA titration procedures used for monitoring the biogas process. *Water Res.* 54:262–272, doi:0.1016/j.watres.2014.02.001.

[81] Schiffels, J.; Baumann, M.E.M.; Selmer, T. (2011) Facile analysis of short-chain fatty acids as 4-nitrophenyl esters in complex anaerobic fermentation samples by high performance liquid chromatography. *J. Chromatogr. A* 1218:5848–5851, doi:10.1016/j.chroma.2011.06.093.

[82] Canale, A.; Valente, M.E.; Ciotti, A. (1984) Determination of volatile carboxylic acids (C_1–C_{5i}) and lactic acid in aqueous acid extracts of silage by high performance liquid chromatography. *J. Sci. Food Agric.* 35:1178–1182, doi:10.1002/jsfa.2740351106.

[83] Diamantis, V.; Melidis, P.; Aivasidis, A. (2006) Continuous determination of volatile products in anaerobic fermenters by on-line capillary gas chromatography. *Anal. Chim. Acta* 573-574:189–194, doi:10.1016/j.aca.2006.05.036.

[84] Ghidotti, M.; Fabbri, D.; Torri, C.; Piccinini, S. (2018) Determination of volatile fatty acids in digestate by solvent extraction with dimethyl carbonate and gas chromatography-mass spectrometry. *Anal. Chim. Acta* 1034:92–101, doi:10.1016/j.aca.2018.06.082.

[85] Cruwys, J.A; Dinsdale, R.M.; Hawkes, F.R.; Hawkes, D.L. (2002) Development of a static headspace gas chromatographic procedure for the routine analysis of volatile fatty acids in wastewaters. *J. Chromatogr. A* 945:195–209, doi:10.1016/S0021-9673(01)01514-X.

[86] Boe, K.; Batstone, D.J.; Angelidaki, I. (2005) Online headspace chromatographic method for measuring VFA in biogas reactor. *Water Sci. Technol.* 52:473–478, doi:10.2166/wst.2005.0555.

[87] Pind, P.F.; Angelidaki, I.; Ahring, B.K. (2003) A new VFA sensor technique for anaerobic reactor systems. *Biotechnol. Bioeng.* 82:54–61, doi:10.1002/bit.10537.

[88] Boe, K.; Batstone, D.J.; Angelidaki, I. (2007) An innovative online VFA monitoring system for the anerobic process, based on headspace gas chromatography. *Biotechnol. Bioeng.* 96(4):712–721, doi:10.1002/bit.21131.

[89] Falk, H.M.; Reichling, P.; Andersen, C.; Benz, R. (2015) Online monitoring of concentration and dynamics of volatile fatty acids in anaerobic digestion processes with mid-infrared spectroscopy. *Bioprocess. Biosyst. Eng.* 38:237–249, doi:10.1007/s00449-014-1263-9.

[90] Stockl, A.; Lichti, F. (2018) Near-infrared spectroscopy (NIRS) for a real

time monitoring of the biogas process. *Bioresour. Technol.* 247:1249–1252, doi:10.1016/j.biortech.2017.09.173.

[91] Wagner, A.O.; Markt, R.; Puempel, T.; Illmer, P.; Insam, H.; Ebner, C. (2016) Sample preparation, preservation, and storage for volatile fatty acid quantification in biogas plants. *Eng. Life Sci.* 00:1–8, doi:10.1002/elsc.201600095.

[92] Kretzschmar, J.; Koch, C.; Liebetrau, J.; Mertig, M.; Harnisch, F. (2017) Electroactive biofilms as sensor for volatile fatty acids: Cross sensitivity, response dynamics, latency and stability. *Sens. Actuators B Chem.* 241:466–472, doi:10.1016/j.snb.2016.10.097.

[93] Kaur, A.; Kim, J.R.; Michie, I.; Dinsdale, R.M.; Guwy, A. J.; Premier, G.C. (2013) Microbial fuel cell type biosensor for specific volatile fatty acids using acclimated bacterial communities. *Biosens. Bioelectron.* 47:50–55, doi:10.1016/j.bios.2013.02.033.

[94] Jin, X.; Li, X.; Zhao, N.; Angelidaki, I.; Zhang, Y. (2017) Bio-electrolytic sensor for rapid monitoring of volatile fatty acids in anaerobic digestion process. *Water Res.* 111:74–80, doi:10.1016/j.watres.2016.12.045.

[95] Mizutani, F.; Sawaguchi, T.; Yabuki, S.; Iljima, S. (2001) Amperometric determination of acetic acid with a trienzyme/poly(dimethylsiloxane)-bilayer-based sensor. *Anal. Sci.* 73:5738–5742, doi:10.1021/ac010622i.

[96] Mieliauskiene, R.; Nistor, M.; Laurinavicius, V.; Csöregi, E. (2006) Amperometric determination of acetate with a tri-enzyme based sensor. *Sens. Actuators B Chem.* 113:671–676, doi:10.1016/j.snb.2005.07.016.

[97] Sode, K.; Tsugawa, W.; Aoyagi, M.; Rajashekhara, E.; Watanabe, K. (2008) Propionate sensor using coenzyme-A transferase and acyl-CoA oxidase. *Protein Peptide Lett.* 15:779–781, doi:10.2174/092986608785203737.

[98] Daniel, J.L.P.; Weiß, K.; Custódio, L.; Neto, A.S.; Santos, M.C.; Zopollatto, M.; Nussio, L.G. (2013) Occurrence of volatile organic compounds in sugarcane silages. *Anim. Feed Sci. Technol.* 185:101–105, doi:10.1016/j.anifeedsci.2013.06.011.

[99] Wu, D.; Li, L.; Zhao, X.; Peng, Y.; Yang, P.; Pen, X. (2019) Anaerobic digestion: A review on process monitoring. *Renewable Sustainable Energy Rev.* 22(1):1–12, doi:10.1016/j.rser.2018.12.039.

[100] Crable, B.R.; Plugge, C.M.; McInerney, M.J.; Stams, A.J.M. (2011) Formate formation and formate conversion in biological fuels production. *Enzyme Res.* 2011:1–8, doi:10.4061/2011/532536.

[101] Hattori, S.; Luo, H.; Shoun, H.; Kamagata, Y. (2001) Involvement of formate as an interspecies electron carrier in a syntrophic acetate-oxidizing anaerobic microorganism in coculture with methanogens. *J. Biosci. Bioeng.* 91:294–298, doi:10.1263/jbb.91.294.

[102] Montag, D.; Schink, B. (2016) Biogas process parameters – energetics and kinetics of secondary fermentations in methanogenic biomass degradation. *Appl. Microbiol.*

Biotechnol. 100:1019–1026, doi:10.1007/s00253-015-7069-0.

[103] Bohn, J.; Yüksel-Dadak, A.; Dröge, S.; König, H. (2017) Isolation of lactic acid-forming bacteria from biogas plants. *J. Biotechnol.* 244:4–15, doi:10.1016/j.jbiotec.2016.12.015.

[104] Cibis, K.G.; Gneipel, A.; König, H. (2016) Isolation of acetic, propionic and butyric acid-forming bacteria from biogas plants. *J. Biotechnol.* 220:51–63, doi:10.1016/j.jbiotec.2016.01.008.

[105] Detman, A.; Mielecki, D.; Pleśniak, Ł.; Bucha, M.; Janiga, M.; Matyasik, I.; Chojnacka, A.; Jędrysek, M.-O.; Błaszczyk, M.K.; Sikora, A. (2018) Methane-yielding microbial communities processing lactate-rich substrates: A piece of the anaerobic digestion puzzle. *Biotechnol. Biofuels* 11:116, doi:10.1186/s13068-018-1106-z.

[106] Costello, D.J.; Greenfield, P.F.; Lee, P.L. (1991) Dynamic modelling of a single-stage high-rate anaerobic reactor – I. Model derivation. *Water Res.* 25:847–858, doi:10.1016/0043-1354(91)90166-N.

[107] Hori, T.; Haruta, S.; Sasaki, D.; Hanajima, D.; Ueno, Y.; Ogata, A.; Ishii, M.; Igarashi, Y. (2015) Reorganization of the bacterial and archaeal populations associated with organic loading conditions in a thermophilic anaerobic digester. *J. Biosci. Bioeng.* 119:337–344, doi:10.1016/j.jbiosc.2014.09.003.

[108] Satpathy, P.; Steinigeweg, S.; Siefert, E.; Cypionka, H. (2017) Effect of lactate and starter inoculum on biogas production from fresh maize and maize silage. *Adv. Microbiol.* 7:358–376, doi:10.4236/aim.2017.75030.

[109] Zhang, B.; Cai, W.; He, P. (2007) Influence of lactic acid on the two-phase anaerobic digestion of kitchen wastes. *J. Environ. Sci.* 19:244–249, doi:10.1016/S1001-0742(07)60040-0.

[110] Pipyn, P.; Verstraete, W. (1981) Lactate and ethanol as intermediates in two-phase anaerobic digestion. *Biotechnol. Bioeng.* 23:1145–1154, doi:10.1002/bit.260230521.

[111] Refai, S.; Wassmann, K.; van Helmont, S.; Berger, S.; Deppenmeier, U. (2014) Increase of methane formation by ethanol addition during continuous fermentation of biogas sludge. *J. Ind. Microbiol. Biotechnol.* 41:1763–1772, doi:10.1007/s10295-014-1524-2.

[112] Refai, S.; Wassmann, K.; Deppenmeier, U. (2014) Short-term effect of acetate and ethanol on methane formation in biogas sludge. *Appl. Microbiol. Biotechnol.* 98:7271–7280, doi:10.1007/s00253-014-5820-6.

[113] Gey, M. (1988) Characterization of biotechnological processes and products using high-performance liquid chromatography (HPLC): I. Separations of carbohydrates, organic acids and lipids. *Acta Biotechnol.* 8:197–205, doi:10.1002/abio.370080216.

[114] Playne, M.J. (1985) Determination of ethanol, volatile fatty acids, lactic and succinic acids in fermentation liquids by gas chromatography. *J. Sci. Food Agric.* 35:638–644, doi:10.1002/jsfa.2740360803.

[115] Doyon, G.; Gaudreau, G.; St-Gelais, D.; Beaulieu, Y.; Randall, C.J. (1991) Simultaneous HPLC determination of organic acids, sugars and alcohols. *Can. Inst. Sci. Technol. J.* 24:87–94, doi:10.1016/S0315-5463(91)70025-4.

[116] Tzang, C.H.; Yuan, R.; Yang, M. (2001) Voltammetric biosensors for the determination of formate and glucose-6-phosphate based on the measurement of dehydrogenase-generated NADH and NADPH. *Biosens. Bioelectron.* 16:211–219, doi:10.1016/S0956-5663(00)00143-3.

[117] Mak, K.K.W.; Wollenberger, U.; Scheller, F.W.; Renneberg, R. (2003) An amperometric bi-enzyme sensor for determination of formate using cofactor regeneration. *Biosens. Bioelectron.* 18:1095–1100, doi:10.1016/S0956-5663(02)00245-2.

[118] Rassaei, L.; Olthuis, W.; Tsujimura, S.; Sudhölter, E.J.R.; van den Berg, A. (2014) Lactate biosensors: Current status and outlook. *Anal. Bioanal. Chem.* 406:123–137, doi:10.1007/s00216-013-7307-1.

[119] Rathee, K.; Dhull, V.; Dhull, R.; Singh, S. (2016) Biosensors based on electrochemical lactate detection: A comprehensive review. *Biochem. Biophys. Rep.* 5:35–54, doi:10.1016/j.bbrep.2015.11.010.

[120] Azevedo, A.M.; Prazeres, D.M.F.; Cabral, J.M.S.; Fonseca, L.P. (2005) Ethanol biosensors based on alcohol oxidase. *Biosens. Bioelectron.* 21:235–247, doi:10.1016/j.bios.2004.09.030.

[121] Thungon, P.D.; Kakoti, A.; Ngashangva, L.; Goswami, P. (2017) Advances in developing rapid, reliable and portable detection systems for alcohol. *Biosens. Bioelectron.* 97:83–99, doi:10.1016/j.bios.2017.05.041.

2 Theory

2.1 Analytical electrochemistry

Electroanalysis is a section of analytical chemistry, concerned with the interaction of electrical and chemical phenomena occurring at the electrode/solution interface. Various concentration-dependent electrical quantities, like current, potential, charge, conductance or resistance, are the basis for numerous electroanalytical techniques. For the measurement of reactions at the electrode/electrolyte interface these may be classified in static methods without current flow (potentiometry) and dynamic methods with current flow (voltammetry, amperometry and coulometry) [1]. The following sections provide fundamentals of the applied measurement principles that have been used in this work for the characterization of amperometric enzyme-based biosensors.

2.1.1 Electrode processes

Chemical and biochemical redox reactions are characterized by the transfer of electrons between two species. Such a process can generally be described by the following Eq. 2.1:

$$\mathrm{Ox} + n\mathrm{e}^- \rightleftharpoons \mathrm{Red} \tag{2.1}$$

where Ox is the oxidized species, Red the reduced form and n is the number of electrons e^- exchanged between these two. In case of electrochemical reactions, the electron flow takes place at the interface between a solid electrode and a liquid electrolyte. This arrangement forms with a second electrode the so-called electrochemical cell, which is classified in galvanic (if they generate electrical energy) and electrolytic cells (when they consume electricity to initiate chemical reactions). The electrochemical conversion occurring in these cells comprises three consecutive steps: transport of the analyte from the solution to the electrode surface, heterogeneous electron transfer and transport of the released product to the bulk solution. Thereby, the mass transport can occur by migration, convection or diffusion [2]. In the presence of an additional conductive salt (at concentrations ca. 100 times greater than the amount of the electroactive species), the migratory effect of the analyte ions becomes negligible [3]. Convection is the movement by mechanical (such as stirring, vibrating, rotating) or hydrodynamic forces (thermal or density gradients), which can be avoided in quiescent solutions. Under these conditions, the mass-transport is only limited to the diffusive mode. Diffusion processes are controlled by concentration gradients, where molecules move from a region of high concentration to a region of low concentration in order to minimize the concentration differences. Under the assumption of steady state, the transport of a species across a

concentration gradient is expressed by Eq. 2.2, also known as Fick's first law of diffusion:

$$J = -D\frac{\partial \mathrm{c}}{\partial \mathrm{x}} \tag{2.2}$$

This equation states a proportional relationship between the flux J and the change in the concentration c with respect to the distance x from an electrode, depending on the diffusion coefficient D. In case of non-stationary conditions, the concentration differs not only in position but also in time [4]. This connection is described by Fick's second law of diffusion (Eq. 2.3):

$$\frac{\partial \mathrm{c}}{\partial \mathrm{t}} = D\frac{\partial^2 \mathrm{c}}{\partial \mathrm{x}^2} \tag{2.3}$$

For initiation of the oxidation- or reduction process, respectively, application of an electrode potential with correct polarity and sufficient magnitude is required. The Nernst equation (Eq. 2.4) relates this electrode potential E for reversible electrode systems (Eq. 2.1) to the activities (often approximated by concentrations) of the oxidized [Ox] and reduced species [Red] [5]:

$$E = E^0 + \frac{RT}{nF} ln \frac{[\mathrm{Ox}]}{[\mathrm{Red}]} \tag{2.4}$$

Here, E_0 is the standard potential, R is the ideal gas constant, T is the temperature, n is the number of transferred electrons and F is the Faraday constant.

2.1.2 Voltammetry

Voltammetric techniques belong to the dynamic electrochemical methods by measuring the current in response to a varying potential applied to an electrode in the presence of electroactive species. In comparison to amperometric analyses, where a constant potential is applied, the obtained current-voltage curves offer both qualitative and quantitative information about the kinetic and thermodynamic details of electrochemical processes. Thereby, various forms for potential excitation are available, including linear sweeps, (differential) pulses, sine waves and triangular scans [6].

The simplest experimental set-up consists of a reference electrode (RE) and a working electrode (WE), where the heterogeneous electron transfer takes place. In this two-electrode arrangement the RE completes the circuit and the potential is measured across the complete electrochemical cell. The RE should ideally be non-polarizable and provide a stable potential over time [7]. However, the current flow between the WE and the RE is accompanied by a potential drop (iR drop) due to the cell resistance, influenced by the electrolyte conductivity, magnitude of current and the distance between the two electrodes. The stability of the applied potential may suffer from this iR drop, which may be compensated by increasing the solution conductivity or decreasing the WE surface [8]. For this reason, most commonly a three-electrode configuration is utilized in electrochemistry, where the current is passed between the WE and an additional counter electrode (CE). This electrode is often made of Pt, with a substantially larger area (advisable 10 times) than the WE [9]. Popular electrode types used as RE include the silver/silver-chloride electrode (Ag/AgCl), saturated calomel electrode (SCE) and

standard hydrogen electrode (SHE) [10]. The WE can be composed of a wide range of inert materials, such as metals (particularly Au and Pt), carbon and conducting polymers. The choice of an adequate material depends mainly on its accessible potential window, which should cover the required working potential of the analyte of interest [11]. Improved interaction with the electroactive species can be achieved, for example, by chemical modification of the WE with e.g., self-assembled monolayers (SAMs), polymer coatings, functional groups or nanomaterials [7, 12].

The most widely used method is the cyclic voltammetry (CV), which is characterized by application of a linear sweeping voltage between the WE and RE. Thereby, the potential is scanned between two limits: beginning at the start potential E_{start} to the switching potential E_{end} and then, the scan direction is reversed to the initial value. As depicted in Fig. 2.1a the applied potential versus the time follows a triangular waveform. Measurements are generally performed in quiescent solutions with a constant rate of voltage change over the time (typically in the range of 10–100 $\mathrm{mV\,s^{-1}}$) [13]. In this way, the reactivity of an electrochemical system can be evaluated over a wide range of potentials within one single sweep.

Figure 2.1b shows the typical cyclic voltammogram of a reversible redox couple (such as $\mathrm{Fe(CN)_6}^{3-}/\mathrm{Fe(CN)_6}^{4-}$) and in Fig. 2.1c the corresponding change in the analyte concentration near the electrode surface is illustrated. For an oxidation, the cycle starts

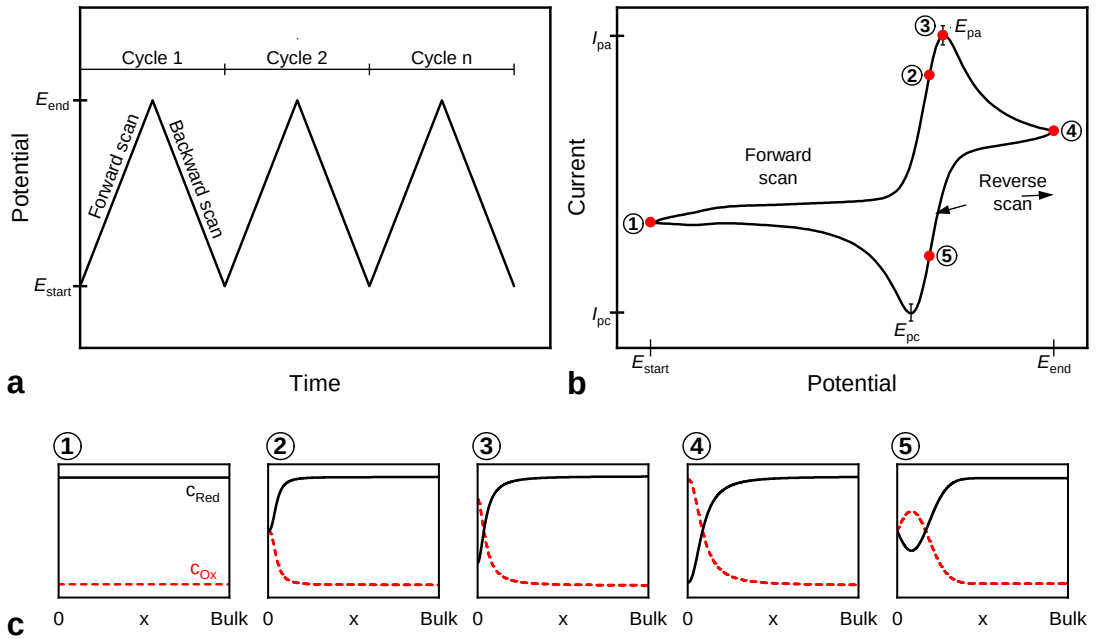

Fig. 2.1: Triangular potential waveform scanned between fixed potentials (E_{start} and E_{end}) during cyclic voltammetry for n cycle(s) **(a)** and typical cyclic voltammogram for a reversible reaction, where I_{pc} and I_{pa} represent the cathodic and anodic peak current, respectively, at the anodic peak potential E_{pa}, and cathodic peak potential E_{pc} **(b)**. Concentration profiles of reduced $\mathrm{c_{Red}}$ (black solid line) and oxidized species $\mathrm{c_{Ox}}$ (red dashed line) of a reversible redox couple as a function of the distance x from the electrode surface at various points throughout the scan (①-⑤) **(c)** (adapted from [11, 14]).

from an electrode potential where no electrochemical reactions take place. Under the assumption that only the reduced form is present (Figs. 2.1b,c ①), no current is flowing. As the applied potential is scanned towards more positive values, the concentration of the reduced species at the electrode surface changes over time in accordance to the Nernst equation (Eq. 2.4). Thereby, the oxidation of the analyte leads to an initial increase of the current. This current depends on the transport of the substrate to the electrode, which occurs only by diffusion. In contrast to amperometric measurements, the solution is not stirred and the reduced analyte is steadily depleted near the electrode surface (corresponds to position ② in Figs. 2.1b,c). The thickness of the diffusion layer is not constant and continues to grow throughout the scan. This slows down the mass-transport and the current reaches a maximum anodic peak (I_{pa}), when the analyte concentration equals zero (Figs. 2.1b,c ③). In the following, the diffusion-controlled process is slower than the electrode reaction and thus, the current decays with $\sqrt{t}$ as described by the Cottrell Eq. 2.8. The direction of the potential scan is reversed, when the switching potential is reached (at position ④ in Figs.2.1b,c). During the backwards scan, the accumulated oxidized molecules are reduced (Figs. 2.1b,c ⑤). The generated current shows basically the same curve as in the forward scan, but in the opposite direction with a maximum cathodic peak (I_{pc}). The peak current depends not only on the concentration of the species and the diffusional properties, but also on the applied scan rate, which defines how fast the potential range is scanned. A mathematical description of the peak current I_p for a reversible redox system (at 25 °C) is given by the Randles-Ševčík equation (Eq. 2.5) [11, 15, 16]:

$$I_p = (2.69 \times 10^5) n^{3/2} A c D^{1/2} v^{1/2} \tag{2.5}$$

where n is the number of electrons transferred in the redox event, A the electrode surface area, c the bulk concentration of the electroactive species, D the diffusion coefficient and v the applied scan rate. The linear relationship between the obtained current and the square root of the scan rate provides information about the diffusion coefficient and the stoichiometry of the redox reaction. The formal potential of the redox couple is located between E_{pa} and E_{pc}. In this way, the working potential of a redox-active species can be estimated from CV experiments. The peak-to-peak separation ΔE_p is another important parameter, which is defined for reversible electrochemical reactions as following Eq. 2.6:

$$\Delta E_p = E_{pa} - E_{pc} = \frac{59}{n} mV \tag{2.6}$$

Here, the position of the anodic and cathodic peak potentials is theoretically independent of the scan rate. In practical applications, however, generally higher peak separations are achieved than the ideal theoretical value of 59/n mV due to uncompensated solution resistance and preparation of the WE [9]. This results in a slow electron transfer kinetic characterized by increasing ΔE_p with increasing scan rate. The peak-to-peak separation, and thus, the electron transfer, can be improved by cleaning the surface of the WE with different pretreatment procedures [17].

2.1.3 Amperometry

Amperometric measurements are based on the recording of current generated by oxidation/reduction of an electroactive species at a controlled fixed potential applied to a WE. Typically, the measurement set-up consists of a three-electrode arrangement as also used in voltammetry. The most simple, but widely performed technique relies on stepping of the applied potential to a constant value and monitoring of the resulting current as a function of time. Thereby, the obtained current obeys Faraday's laws (hence, also termed Faradaic current I_f) and is proportional to the electric charge Q passed through the electrode. According to Eq. 2.2, at steady-state conditions this current depends on the bulk analyte concentration c_0 (Eq. 2.7):

$$I = \frac{d\mathrm{Q}}{d\mathrm{t}} = -nFAD\frac{c_0}{\delta} \tag{2.7}$$

Here, n is the number of transferred electrons, F is the Faraday constant, A is the electrode area, D the diffusion coefficient and δ the diffusion layer thickness. This thickness corresponds to the distance from the electrode where the analyte concentration is different to the bulk concentration c_0. In Fig. 2.2, the difference in the layer thickness in stirred and quiescent solutions is shown. Under steady-state conditions, the diffusion layer thickness is constant, whereas in non-stirred solutions the layer is growing with time [18]. This time-dependent behavior follows Eq. 2.3.

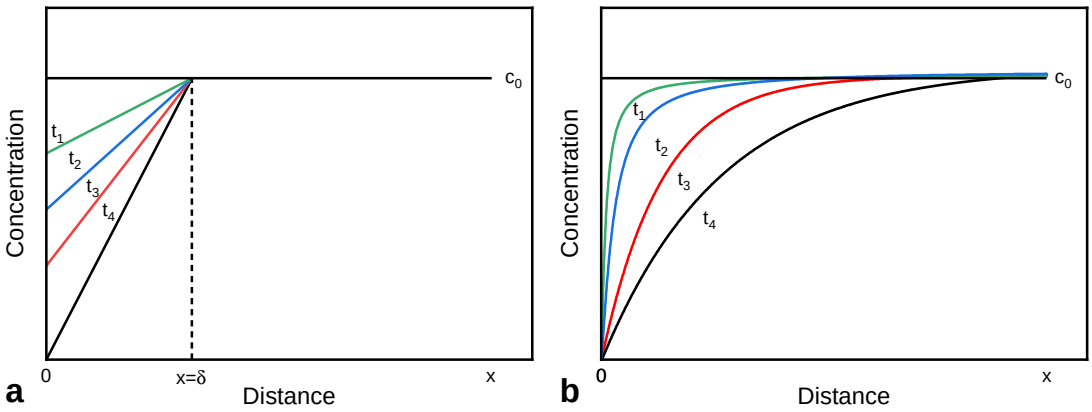

Fig. 2.2: Concentration gradients and temporal change ($0<t_1<t_2<t_3<t_4$) of the diffusion layer thickness δ at the electrode surface (x=0) in stirred **(a)** and quiescent solutions **(b)**, c_0 represents the bulk concentration (adapted from [1, 13]).

For diffusion-controlled processes at planar electrodes, the change in the Faradaic current I_f with respect to time t is given by the Cottrell equation (Eq. 2.8) [9, 19]:

$$I_f(t) = \frac{nFAc\sqrt{D}}{\sqrt{\pi t}} \tag{2.8}$$

with n is the number of electrons, F the Faraday constant, A the area of the electrode, c the concentration and D the diffusion coefficient of the analyte. Figure 2.3a illustrates a potential ramp applied in a chronoamperometric experiment and the resulting change

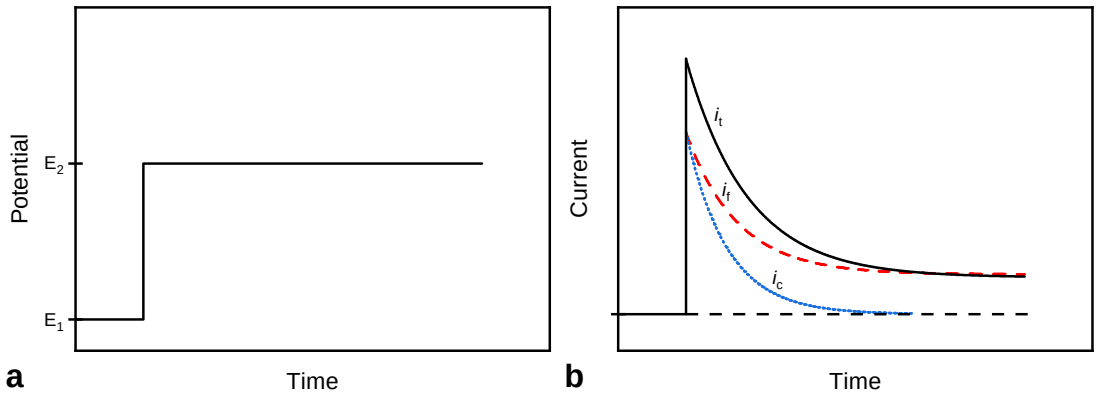

Fig. 2.3: Potential ramp applied in chronoamperometry from a value E_1 without electrochemical reaction to a potential E_2 where the analyte is electroactive **(a)** and corresponding total current i_t (black solid line) response due to changes in the applied with portion of capacitive i_c (blue dotted line) and Faradaic current i_f (red dashed line) **(b)** (adapted from [21]).

in the current response is depicted in Fig. 2.3b. The potential is stepped from a value E_1 where no Faradaic current i_f occurs to a potential E_2 sufficient for electrochemical conversion of the analyte. In accordance to Eq. 2.8, the Faradaic current is not constant but decays with $t^{-1/2}$ (Fig. 2.3b). The total, overall obtained signal i_t in the measurement, however, is characterized by the contribution of an additional current, the so-called capacitive or charging current i_c, of non-Faradaic source. This portion is not generated by chemical reactions but by unwanted physical side-effects. When a potential is applied to an electrode immersed into a solution, ions migrate toward and away from the electrode to compensate the charge developed at the electrode surface until reaching zero charge [20]. Accumulation of ions in front of the electrode surface leads to the formation of a structured electrode-solution interface, called electrical double layer, with capacitive characteristics. Since, the capacitive current decays exponentially with a faster rate (with a time constant consisting of an uncompensated resistance and a double-layer capacitance) than the Faradaic current, it becomes neglectable after a certain period (depends on electrolyte properties, electrode size and material) [21].

Application of a potential ramp is often performed in chronoamperometry for determination of the diffusion coefficient, which typically ranges in aqueous solutions from 10^{-5} to $10^{-6}\,\mathrm{cm^2\,s^{-1}}$ [11]. The redox couple $Fe(CN)_6^{4-}/Fe(CN)_6^{3-}$ is a popular model system in electrochemistry with a diffusion coefficient at 25 °C in 0.1 M of 6.5×10^{-6} and $7.6 \times 10^{-6}\,\mathrm{cm^2\,s^{-1}}$, respectively [9].

2.2 Electrochemical enzyme-based biosensors

Biosensors have become indispensable analytical tools in a wide field of applications ranging from biomedcial diagnostics [22, 23], industrial process control [24], environmental analysis [25, 26], agricultural monitoring [27] to food safety assessment [28, 29]. According to the definition proposed by the International Union of Pure and Applied Chemistry (IUPAC), a biosensor is a self-contained integrated device for selective quantification of

an analyte using a biological recognition element [30]. Characteristic is the integration of the receptor within or in close proximity to the transduction system. The interaction of the analyte of interest with the biological component generates chemical or physical alterations, which are converted by the transducer into a detectable electrical signal. In comparison to conventional analytical techniques, biosensors offer main advantages of minimal sample preparation, ease of operation and rapid analysis time. Due to these properties, they are attractive for the construction of portable and cost-efficient sensing devices. They are classified either by the type of biological signaling mechanism or the mode of physicochemical transduction. The selective response to a particular analyte can be realized with different organic materials such as enzymes, cells, microorganisms, nucleic acids or antibodies. Based on the applied transducer, biosensors are distinguished in six different categories: electrochemical, electrical, optical, thermal, mass-sensitive and magnetic. The basis for the electrochemical detection is the measurement of changes in the current or charge (amperometric or coulometric), potential (potentiometric), field-effect or conductivity (conductometric, impedimetric). Among the variety of possible combinations, electrochemical enzyme-based biosensors are by far the most commonly used. Especially, enzymatic amperometric biosensors for the point-of-care monitoring of blood glucose levels in diabetic patients are the most successful commercial product on the global market [31]. In most cases glucose oxidases or glucose dehydrogenases are utilized. These enzymes belong to the large class of oxidoreductases that catalyze biological oxidation/reduction and they are often used for the development of biosensors [32]. The remarkable characteristics of enzymes, including their high selectivity and specificity, are ideal prerequisites for the electrochemical detection in complex matrices [33]. Important parameters for evaluation of the biosensor performance include the sensitivity, linear working range, lower detection limit, response time, repeatabiliy and life-time.

2.2.1 Enzyme kinetics

Various aspects have to be considered for evaluation of the suitability of an enzyme as biological receptor molecule in biosensing devices. On the one hand, the catalytic activity is an important criterion, since it mainly determines the biosensor sensitivity. On the other hand, substrate specificity and the operational and storage stability are further key parameters, which influence the overall performance. Given the economic constraints associated with biosensor design, cost-efficient enzyme isolation and purification are also crucial for successful commercial application. The significance of each of these factors depends finally on the desired technical requirements of the biosensor. In this regard, knowledge about the fundamentals of enzyme kinetics is essential. Enzymes are efficient catalysts for biochemical reactions by lowering the activation energy. The principle of this pathway with one substrate involved is shown by Eq. 2.9:

$$\mathrm{E} + \mathrm{S} \underset{k_{-1}}{\overset{k_1}{\rightleftharpoons}} \mathrm{ES} \xrightarrow{k_2} \mathrm{E} + \mathrm{P} \tag{2.9}$$

The mechanism is characterized by reversible binding of the substrate S to the enzyme E and formation of an intermediate complex ES with the rate constant k_1. The complex falls apart in the reverse reaction with k_{-1} to E and S. Subsequently, the substrate is

converted and the complex dissociates into the product P and the free enzyme (with rate constant k_2). The complex can also break down back into substrate and enzyme. In 1924, the researchers Briggs and Haldane assumed a steady-state condition, in which the concentration of the complex [ES] remains constant due to equal rate constants for formation and dissociation (see Eq. 2.10) [34].

$$\frac{d[\mathrm{ES}]}{dt} = k_1[\mathrm{E}][\mathrm{S}] - (k_{-1} + k_2)[\mathrm{ES}] = 0 \tag{2.10}$$

Assuming the amount of enzyme [E] does not change during the reaction, the rate of product formation v is described as a function of the substrate concentration [S] by the so-called Michaelis-Menten equation (Eq. 2.11) shown below [35]. Two important parameters derive from this mathematical model: the Michaelis-Menten constant K_m and the maximum rate achieved by the system v_max.

$$v = \frac{d[\mathrm{P}]}{dt} = \frac{v_{max} \cdot [\mathrm{S}]}{K_m + [\mathrm{S}]} \tag{2.11}$$

As depicted in Fig. 2.4, the kinetic of enzyme-catalyzed reactions is characterized by a saturation behavior. At high substrate concentrations, almost all active sites of the enzyme are occupied. For this stage, the reaction rate depends only on the enzyme concentration and approaches asymptotically v_max. The term K_m corresponds to the substrate concentration at which the reaction rate is half of v_max. This value is an intrinsic parameter, which indicates the substrate affinity of an enzyme under fixed environmental conditions (pH, temperature, etc.). Typical values for K_m cover a broad range from 10^{-1} to 10^{-7} M, due to the multitudinous amount of biologically active enzymes in nature with different functions. A linear relationship between [S] and reaction rate is observed for low substrate concentrations ($[\mathrm{S}] \ll K_\mathrm{m}$). This analytically useful region enables determination of the enzymatic activity, which is defined as the amount of the enzyme that catalyzes the conversion of one micromole of substrate per minute under defined conditions [36]. Typically, spectrophotometric assays are performed for

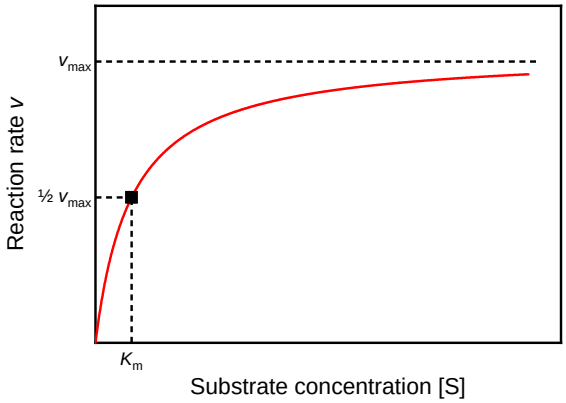

Fig. 2.4: Relationship between reaction rate v and substrate concentration [S] of an enzyme-catalyzed reaction following the Michaelis-Menten kinetic, characterized by the Michaelis-Menten constant K_m and the maximal reaction rate v_max (adapted from [37]).

determination of the enzymatic activity. As described earlier, the catalytic properties are influenced by various operational parameters, thus, precise control of the experimental conditions is of great importance [37]. Enzyme electrodes follow essentially also the Michaelis-Menten kinetic, however, it has to be taken into account that the kinetic of immobilized enzymes is different to free enzymes in solution. The chemical and physical properties of the molecule are subject to alterations due to the immobilization process, mainly caused by steric hindrance, changes in the three-dimensional structure or altered diffusion characteristics.

2.2.2 Enzyme immobilization

The immobilization of the biological recognition element is a crucial step in the design process of biosensors. Especially, the fixation of enzymes becomes challenging due to altered catalytic characteristics of the immobilized protein in comparison to the free form in solution [38]. This effect can mainly be attributed to changes in the three-dimensional conformation and diffusion constraints [39]. Different strategies have been developed in order to maintain the enzymatic activity, which primarily determines the overall biosensor performance. Further important parameters affected by the applied immobilization procedure include the response time, operational and storage stability, selectivity and reproducibility [40]. Based on physical or chemical binding properties, five principle methods are classified: adsorption, encapsulation, entrapment, covalent binding and cross-linking [41, 42] (Fig. 2.5). Each of these approaches is characterized by specific advantages and limitations. Therefore, selection of the most suitable technique requires consideration of these with regard to the intended enzyme, transducer principle and final application.

Non-covalent **adsorption** represents the simplest method for physical immobilization of enzymes. The molecules are attached on support materials or directly on the transducer surface through non-specific, weak bondings (ionic or electrostatic interactions, hydrogen bonds and van der Waals forces). A wide range of organic and inorganic materials can be used as carriers [43]. Thereby, especially nanomaterials in form of nanoparticles and nanostructured films are popular for the modification of electrode surfaces [44]. The adsorptive immobilization requires usually no additional chemicals, so that the native structure of the biocatalyst is not disrupted and high enzymatic activities can be retained. However, non-specific binding of other proteins and poor operational

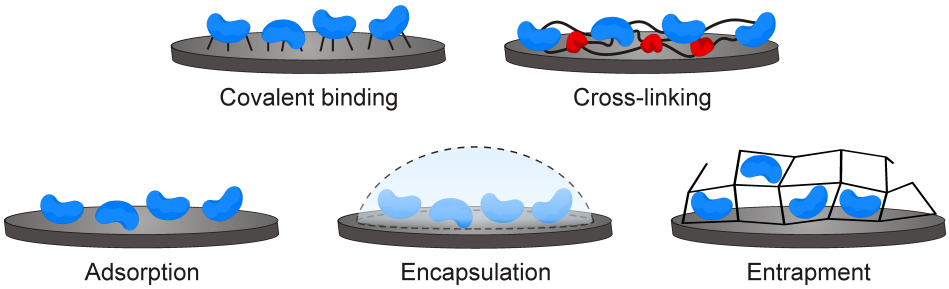

Fig. 2.5: Schematic illustration of different methods used for immobilization of enzymes (blue) onto electrode surfaces, optionally with additional inert proteins (red) (adapted from [11, 45]).

stability are major drawbacks of this technique. The interactions between the enzyme and surface are sensitive to changes in the environment (pH value, temperature and ionic strength), leading to desorption and enzyme leaching. Anyhow, this attribute can be used strategically for reversible immobilization of enzymes. The pH-induced adsorption and desorption of glucose oxidase and urease on hydroxyapatite were, e.g. described for the development of a reusable flow-injection biosensor for calorimetric detection of glucose and urea [46].

Physical enclosure of enzymes in a confined space is achieved by **encapsulation** with membranes or **entrapment** in three-dimensional matrices. The first enzyme-based biosensor for potentiometric detection of glucose was reported in 1962 by Clark and Lyons. This device was based on physically immobilized glucose oxidase trapped between cuprophane membranes [47]. Typically, semipermeable membranes (made of e.g., cellulose acetate or nafion) are employed, which also enable exclusion of interfering substances, such as ascorbic acid and uric acid [48]. Immobilization by this approach is very gentle, however, high diffusion barriers can limit the biosensor performance in terms of response time. Another option for irreversible fixation of enzymes is the entrapment within networks, like electropolymerized films [49], photopolymers [45], sol-gels [50], polysaccharides [51] or carbon pastes [52]. There is no direct chemical interaction between the enzyme and matrix material, so that the enzyme structure is barely affected and high catalytic activities can be retained. In this regard, especially electrochemical polymerization of conductive polymers, such as polypyrrol, polyaniline and polythiophene, is an attractive approach for simple and controlled immobilization in mild conditions [53]. Precise formation of the polymer film on the electrode surface with controlled thickness and thus, defined amount of biomolecules, results in reproducible sensor characteristics. Another advantage is the simultaneous deposition of several enzymes and additional substances within the growing polymer network. However, the requirement of high enzyme loadings and monomer concentrations for the polymerization process and potential enzyme leakage can in some cases restrict the application of this technique [54]. Successful combination of encapsulation and entrapment was described for the development of an reagentless amperometric D-lactate biosensor [55]. In a first step, the mediator $Fe(CN)_6^{3-}$ was immobilized within an electropolymerized film of polypyrrol on a platinum electrode. The enzymes (D-lactate dehydrogenase and diaphorase) and the modified cofactor (NAD-dextran) were afterwards entrapped with a semipermeable membrane on top of the polymer structure. This biosensor exhibited good performance in terms of sensitivity and response time, but further improvement of the linear range and lower detection limit was necessary.

Chemical immobilization by covalent binding or cross-linking leads generally to irreversible attachment of the biomolecules [56]. In case of **covalent binding**, this is realized by formation of strong bonds between functional groups on the surface of the enzyme and chemically activated groups present on the surface of the support. The functional groups often involved in these interactions belong to the amino acid side chains of lysine and argine (amino group), aspartate and glutamate (carboxyl group), serine and threonine (hydroxyl group) and cysteine (sulfhydryl group) [57]. Conformational alterations in the molecular structure and as a consequence, the loss in catalytic activity, are the major drawbacks of this technique. For this reason, coupling reactions should

only be performed with functional groups, which are not located in the active site of the biocatalyst. The vast amount of available organic and inorganic carrier materials and selection of appropriate binding mechanisms [58], make this technique rather laborious and time-consuming. However, in comparison to physical immobilization, the binding is more stable and thus, resistant to a broad range of operational conditions [13].

Immobilization of enzymes by **cross-linking** with bi- or multifunctional reagents is another popular approach for the development of biosensors [45]. The most commonly used agent is glutaraldehyde, which reacts with free amino groups of lysine residues and cross-links the enzymes with each other within an insoluble gel. Similar to covalent binding, the intermolecular fixation may lead to high loss in enzyme activity. Application of inert, lysine-rich auxiliary proteins, like bovine serum albumin (BSA) or gelatin, prevents excessive cross-linking of the target enzyme [59]. Although the simplicity of this procedure seems advantageous, high reproducibility is still a challenging aspect due to the complexity in the chemistry of glutaraldehyde in aqueous solutions [60].

2.2.3 Electrochemical NADH detection

Nicotinamide adenine dinucleotide (NAD) is an important cofactor involved in a wide range of cellular reactions, like glycolysis, oxidative phosphorylation, and citric acid cycle [61]. The main function is the transfer of two electrons and one proton (H^+) from the reduced form (NAD^+) to the oxidized form (NADH). This mechanism is the basis for dehydrogenase-catalyzed reactions. With more than 300 dehydrogenases, this subclass of enzymes represents an attractive approach for the construction of diverse biosensors [62]. Thereby, the released NADH can be used for electrochemical quantification of the corresponding substrate concentration. The redox potential of the couple NAD^+/NADH depends, according to the Nernst equation Eq. 2.4, on the ratio of these two, as well as on the pH and the solvent. In aqueous solutions (pH 7) at 30 °C the redox potential is $-0.318\,\mathrm{V}$ *vs.* SHE [63]. However, for direct oxidation of NADH at bare electrodes an activation energy with high overpotential (in the range of $1.1\,\mathrm{V}$ *vs.* Ag/AgCl for C and $1.3\,\mathrm{V}$ *vs.* Ag/AgCl for Pt electrodes) is required. Application of such high potentials is accompanied by oxidation of other interfering electroactive species and electrode fouling as NAD^+ dimers accumulate on the electrode surface. There are basically two strategies in order to diminish the required working potential: One approach relies on a consecutive enzymatic reaction, in which the NADH gets regenerated, for example, by a diaphorase [64, 65], salicylate hydroxylase [66, 67] or NADH oxidase [68, 69]. The amperometric detection is then realized by direct oxidation of $Fe(CN)_6{}^{4-}$, O_2 and H_2O_2, respectively. Integration of an electron transfer mediator into the reaction system comprises the other strategy [70]. A variety of compounds has been identified for the mediated oxidation of NADH such as metal complexes, quinones, fluorenones, phenazines, and phenoxazines [71, 72].

As described earlier (Sec. 2.2.2), immobilization of the biological recognition element is of crucial relevance for the overall biosensor performance. This becomes even more challenging for dehydrogenase-based biosensors. In contrast to oxidases with cofactors tightly bound at the active site of the enzyme, dehydrogenases depend on the availability of soluble NAD^+ and in addition on a mediator, second enzyme and/or substrate. The

coimmobilization of the expensive cofactor and the other compounds is expedient for economical and practical reasons. Various techniques have been used for the design of reagentless biosensors, for example, by entrapment behind membranes [73, 74], binding to functionalized SAMs [75] or immobilization within carbon pastes [76, 77], sol-gels [78] and electropolymerized films [55].

2.3 Electrode fabrication

The wide application range of electrochemical biosensors has promoted the demand for novel sensor architectures along with economic production processes. For *in vivo* utilization of biosensing systems miniaturized electrode geometries are required [79]. The technological advances also focused on the development of multielectrode arrays. The integration of several electrodes within one single chip offers the potential of increased analytical information [80]. All amperometric biosensors rely primarily on an appropriate conductive material as WE, that provides an efficient electron transfer [81]. The biosensor fabrication can generally be accomplished by either thin-film or thick-film technology. In this work, in-house manufactured platinum thin-film electrodes (Ch. 3 to Ch. 6) and commercial screen-printed carbon electrodes (Ch. 7) have been used for the construction of amperometric enzyme-based biosensor arrays.

2.3.1 Thin-film technology

The microfabrication of electrochemical transducers stems from standard manufacturing processes applied in the semiconductor industry. In general, the production proceeds in five basic steps: oxidation, thin-film deposition, photolithography, etching and bonding. Depending on the electrode design and structure, these steps are applied several times optionally in varying order. Thin films are deposited on a substrate by two common techniques: chemical (plasma-enhanced, low pressure) and physical vapor deposition [sputtering, (electron-beam) evaporation]. The typical film thickness achieved by both processes ranges from tens of nanometers up to a few micrometers [82]. Common materials utilized for metallization of the electrode surface of electrochemical biosensors include noble metals, like Pt, Au, Ag and Ir. Typically, an additional layer of Si_3N_4, Ti, Ta or Cr is deposited for improved adhesion to the substrate [83]. In this regard, Si wafers represent a well established substrate material for microelectronics. The Si surface is first passivated with a thin layer of SiO_2 by thermal dry (in atmospheric O_2) or wet oxidation (H_2O vapor) at temperatures from 800 to 1200 °C [84]. Photolithography is conducted for pattering of the desired electrode geometries, such as single electrodes, microelectrode arrays or interdigitated electrodes. For this purpose, the wafer is covered by spin-coating with a UV-sensitive photoresist and afterwards, selectively exposed to UV-light through a proper mask. The radiation provokes chemical reactions and thus, the solubility of the resist material increases in the exposed (positive resist) or unexposed regions (negative resist). Removal of the soluble parts is carried out with a developer. In the following, chemical agents are used for an etching step in order to transfer the pattern to the underlying material that is not protected by the remaining photoresist. In case the photoresist masking is unsuitable for an etching process, alternatively the so-

called lift-off technique can be applied. This process is characterized by direct thin-film deposition (often noble metals, like Pt and Ir) on the developed photoresist. The desired thin-film pattern is lifted by dissolving the photoresist in an appropriate solvent. After separation of the individual chips from the wafer, electrical connections are realized by thermosonic or ultrasonic bonding using Al, Au or Cu wires. Encapsulation of bond pads and bond wires is required for protection and electrical isolation from aqueous samples [5].

These process steps enable precise fabrication of biosensor chips with high reproducibility and flexibility in the electrode design at a micrometer dimensional accuracy. However, due to high investment- and operation costs, this technology is generally only economic at larger production numbers for re-usable sensors.

2.3.2 Thick-film technology

The thick-film technology is an additive fabrication process that uses sequential deposition of conductive, resistive and insulating films on substrate materials for patterning specific sensor designs. Different layers are mainly applied by screen-printing processes and in comparison to the thin-film technique, much thicker films are obtained (typically between 20 to 100 µm) [85]. This fabrication method is particularly utilized for the construction of electrochemical biosensors in widespread applications for environmental, clinical, pharmaceutical and industrial analyses [86, 87]. Hereby, screen-printed test strips for glucose detection constitute by far the greatest share [31]. The fabrication follows basically three steps: placement of an ink onto a screen or stencil with open areas that define the electrode pattern, pulling a flexible squeegee across the mask for homogeneous distribution of the ink and finally, drying and curing of the printed structure at temperatures from 300 to 1200 °C [88]. This additive process is repeated several times with different inks, so that in a simple manner whole electrochemical electrode systems, consisting of RE, WE and CE, can be realized on one substrate. The overall sensor performance depends on the ink and applied printing conditions (pressure, temperature etc.), which influence the structure quality in terms of mean thickness, thickness uniformity, fine line resolution and voids. Different commercial conductive and dielectric pastes are available, on the basis of fine powders, solvents and polymeric binders. For specific applications, modification with a variety of additives allows improvement of the printing process, dispersion- and adhesion characteristics. Conductive films often include noble metals, such as Au, Pt and Pd, or non-metallic considerably less expensive materials, like C. Electronic tracks are mostly made with Ag. Depending on the intended application and requirements, the structures can be printed on solid ceramics (AlO_2, AlN, glass, quartz) or more flexible substrates, like plastic foils or paper.

The main advantages of the thick-film technology are the simple fabrication procedure and comparatively low material and investment costs. These features are ideal for the mass production of disposable, single-use biosensors, though the electrode geometries are restricted to a line width of around 100 µm in comparison to thin-film technology with small micrometer dimension electrodes [83, 89].

References

[1] Buchberger, W. (1998) Elektrochemische Analyseverfahren: Grundlagen, Instrumentation, Anwendungen. Berlin, Heidelberg: *Spektrum Akademischer Verlag.*

[2] Oldham, K.B.; Zoski, C.G. (1986) Mass Transport to Electrodes. In: Bamford, C.H.; Compton, R.G. (Eds.) Electrode Kinetics: Principles and Methodology. Comprehensive Chemical Kinetics, Vol. 26. Amsterdam, New York: *Elsevier* 88:309–352, doi:10.1016/S0069-8040(08)70026-8.

[3] Ciobanu, M.; Wilburn, J.P.; Krim, M.L.; Cliffel, D.E. (2007) Fundamentals. In: Zoski, C.G. (Ed.) Handbook of Electrochemistry. Amsterdam: *Elsevier*, doi:10.1016/B978-044451958-0.50002-1.

[4] Eddowes, M.J. (1990) Theoretical Methods For Analysing Biosensor Performance. In: Cass, A.E.G. (Ed.) Biosensors: A Practical Approach. Oxford: *IRL Press.*

[5] Buerk, D.G. (2014) Biosensors: Theory and Applications. Boca Raton: *CRC Press*, doi:10.1201/9781498710770.

[6] Denuault, G.; Sosna, M.; Williams, K.J. (2007) Classical Experiments. In: Zoski, C.G. (Ed.) Handbook of Electrochemistry. Amsterdam: *Elsevier*, doi:10.1016/B978-044451958-0.50024-0.

[7] Scholz, F. (2010) Electroanalytical Methods: Guide to Experiments and Applications. Berlin, Heidelberg: *Springer-Verlag*, doi:10.1007/978-3-642-02915-8.

[8] Britz, D. (1978) iR elimination in electrochemical cells. *J. Electroanal. Chem.* 88:309–352, doi:10.1016/S0022-0728(78)80122-3.

[9] Bard, A.J.; Faulkner, L.R. (2001) Electrochemical Methods: Fundamentals and Applications. Hoboken (NJ): *Wiley-VCH.*

[10] Shinwari, M.W.; Zhitomirsky, D.; Deen, I.A.; Selvaganapathy, P.R.; Deen, M.J.; Landheer, D. (2010) Microfabricated reference electrodes and their biosensing applications. *Sensors* 10:1679–1715, doi:10.3390/s100301679.

[11] Wang, J. (2006) Analytical Electrochemistry. New York: *Wiley-VCH*, doi:10.1002/0471790303.

[12] Bartlett, P.N. (1990) Modified electrode surface in amperometric biosensors. *Med. Biol. Eng. Comput.* 28:B10–B17, doi:10.1007/bf02442675.

[13] Cammann, K. (2001) Instrumentelle Analytische Chemie: Verfahren, Anwendungen und Qualitätssicherung. Berlin, Heidelberg: *Spektrum Akademischer Verlag.*

[14] Compton, R. G.; Banks, C.E. (2011) Understanding Voltammetry. London: *Imperial College Press*, doi:10.1142/p726.

[15] Randles, J.E.B. (1948) A cathode ray polarograph. Part II: The current-voltage curves. *Trans. Faraday Soc.* 44:327–338 , doi:10.1039/TF9484400327.

[16] Ševčík, A. (1948) Oscillographic polarography with periodical triangular voltage. *Collect. Czechoslov. Chem. Commun.* 13:349–377, doi:10.1135/cccc19480349.

[17] Fischer, L.M.; Tenje, M.; Heiskanen, A.R.; Masuda, N.; Castillo, J.; Bentien, A.; Émneus, J.; Jakobsen, M.H.; Boisen, A. (2009) Gold cleaning methods for electrochemical detection applications. *Microelectron. Eng.* 86:1282–1285, doi:10.1016/j.mee.2008.11.045.

[18] Scholz, F. (2015) Voltammetric techniques of analysis: The essentials. *ChemTexts* 1:17, doi:10.1007/s40828-015-0016-y.

[19] Cottrell, F.G. (1903) Der Reststrom bei galvanischer Polarisation, betrachtet als ein Diffusionsproblem. *Z. Phys. Chem.* 42:385–431, doi:10.1515/zpch-1903-4229.

[20] Cazes, J. (2004) Ewing's Analytical Instrumentation Handbook. Boca Raton: *CRC Press*.

[21] Hall, E.A.H (1990) Biosensoren. Berlin: *Springer*, doi:10.1007/978-3-642-78660-0.

[22] Wang, J. (1999) Amperometric biosensors for clinical and therapeutic drug monitoring: A review. *J. Pharm. Biomed. Anal.* 19:47–53, doi:10.1016/S0731-7085(98)00056-9.

[23] Rocchitta, G.; Spanu, A.; Babudieri, S.; Latte, G.; Madeddu, G.; Galleri, G.; Nuvoli, S.; Bagella, P.; Demartis, M.I.; Fiore, V.; Manetti, R.; Serra, P.A. (2016) Enzyme biosensors for biomedical applications: Strategies for safeguarding analytical performances in biological fluids. *Sensors* 16:780, doi:10.3390/s16060780.

[24] Scheper, T. (1992) Biosensors for process monitoring. *J. Ind. Microbiol.* 9:163–172, doi:10.1007/BF01569620.

[25] Rodriguez-Mozaz, S.; Lopez de Alda, M.J.; Barceló, D. (2006) Biosensors as useful tools for environmental analysis and monitoring. *Anal. Bioanal. Chem.* 386:1025–1041, doi:10.1007/s00216-006-0574-3.

[26] Justino, C.I.L.; Duarte, A.C.; Rocha-Santos, T.A.P. (2017) Recent progress in biosensors for environmental monitoring: A review. *Sensors* 17:2918, doi:10.3390/s17122918.

[27] Tothill, I.E. (2001) Biosensors developments and potential applications in the agricultural diagnosis sector. *Comput. Electron. Agric.* 30:205–218, doi:10.1016/S0168-1699(00)00165-4.

[28] Prodromidis, Mamas I.; Karayannis, Miltiades I. (2002) Enzyme based amperometric biosensors for food analysis. *Electroanal.* 14:241–264, doi:10.1002/1521-4109(200202)14:4%3C241::AID-ELAN241%3E3.0.CO;2-P.

[29] Rotariu, L.; Lagarde, F.; Jaffrezic-Renault, N.; Bala, C. (2016) Electrochemical biosensors for fast detection of food contaminants – trends and perspective. *Trends Anal. Chem.* 79:80–87, doi:10.1016/j.trac.2015.12.017.

[30] Thévenot, D.R.; Toth, K.; Durst, R.A.; Wilson, G.S. (2001) Electrochemical biosensors: Recommended definitions and classification. *Biosens. Bioelectron.* 16:121–131, doi:10.1016/S0956-5663(01)00115-4.

[31] Newman, J.D.; Turner, A.P.F (2005) Home blood glucose biosensors: A commercial

perspective. *Biosens. Bioelectron.* 20:2435–2453, doi:10.1016/j.bios.2004.11.012.

[32] May, S.W. (1999) Applications of oxidoreductases. *Curr. Opin. Biotechnol.* 10:370–375, doi:10.1016/S0958-1669(99)80067-6.

[33] Leca-Bouvier, B.D.; Blum L.J. (2010) Enzyme for biosensing applications. In: Zourob M. (Ed.) Recognition Receptors in Biosensors. New York: *Springer*, doi:10.1007/978-1-4419-0919-0_4.

[34] Briggs, G.E.; Haldane, J.B.S. (1925) A note on the kinetics of enzyme action. *Biochem. J.* 19:338–339, doi:10.1042/bj0190338.

[35] Michaelis, L.; Menten, M.L. (1913) Die Kinetik der Invertinwirkung. *Biochem. Z.* 49:333–369.

[36] Labuda, J.; Bowater, R.P.; Fojta, M.; Gauglitz, G.; Glatz, Z.; Hapala, I.; Havliš, J.; Kilár, F.; Kilar, A.; Malinovská, L.; Sirén, H.M.M.; Skládal, P.; Torta, F.; Valachovič, M.; Wimmerová, M.; Zdráhal, Z.; Hibbert, D.B. (2018) Terminology of bioanalytical methods (IUPAC Recommendations 2018). *Pure Appl. Chem* 90(7):1121–1198, doi:10.1515/pac-2016-1120.

[37] Bisswanger, H. (2014) Enzyme assays. *Perspect. Sci.* 1:41–56, doi:10.1016/j.pisc.2014.02.005.

[38] Worsfeld, P.J. (1995) Classification and chemical characteristics of immobilized enzymes. *Pure Appl. Chem* 67(4):597–600, doi:10.1351/pac199567040597.

[39] Goldstein, L.; Manecke, G. (1976) The chemistry of enzyme immobilization. *Appl. Biochem. Bioeng.* 1:23–126, doi:10.1016/B978-0-12-041101-6.50008-X.

[40] Vasylieva, N.; Marinesco S. (2012) Enzyme Immobilization on Microelectrode Biosensors. In: Marinesco, S.; Dale, N. (Eds.) Microelectrode Biosensors. Neuromethods, Vol. 80. New Jersey: *Humana Press*, doi:10.1007/978-1-62703-370-1_53.

[41] Scouten, W.H.; Luong, J.H.T.; Brown, R.S. (1995) Enzyme or protein immobilization techniques for applications in biosensor design. *Trends Biotechnol.* 13(5):178–185, doi:10.1016/S0167-7799(00)88935-0.

[42] Mulchandani, A. (1998) Principles of Enzyme Biosensors. In: Mulchandani, A.; Rogers, K.R. (Eds.) Enzyme and Microbial Biosensors: Techniques and Protocols. Methods in Biotechnology, Vol. 6. New Jersey: *Humana Press*, doi:10.1385/0-89603-410-0:3.

[43] Jesionowski, T.; Zdarta, J.; Krajewska, B. (2014) Enzyme immobilization by adsorption: A review. *Adsorption* 20(5-6):801–821, doi:10.1007/s10450-014-9623-y.

[44] Bhakta, S.A.; Evans, E.; Benavidez, T.E.; Garcia, C.D. (2015) Protein adsorption onto nanomaterials for the development of biosensors and analytical devices: A review. *Anal. Chim. Acta* 872:7–25, doi:10.1007/s10450-014-9623-y.

[45] Sassolas, A.; Blum, L.J.; Leca-Bouvier, B.D. (2012) Immobilization strategies to develop enzymatic biosensors. *Biotechnol. Adv.* 30:489–511, doi:10.1016/j.biotechadv.2011.09.003.

[46] Salman, S.; Soundararajan, S.; Safina, G.; Satoh, I.; Danielsson, B. (2008) Hydroxyapatite as a novel reversible in situ adsorption matrix for enzyme thermistor-based FIA. *Talanta* 77(2):490–493, doi:10.1016/j.talanta.2008.04.003.

[47] Clark, L.C.; Lyons, C. (1962) Electrode systems for continuous monitoring in cardiovasculas surgery. *Ann. N.Y. Acad. Sci.* 102:29–45, doi:10.1111/j.1749-6632.1962.tb13623.x.

[48] Kulkarni, T.; Slaughter, G. (2016) Application of semipermeable membranes in glucose biosensing. *Membranes* 6(4):55, doi:10.3390/membranes6040055.

[49] Bartlett, P. N.; Cooper, J. M. (1993) A review of the immobilization of enzymes in electropolymerized films. *J. Electroanal. Chem.* 362(1-2):1–12, doi:10.1016/0022-0728(93)80001-X.

[50] Pierre, A.C. (2004) The sol-gel encapsulation of enzymes. *Biocatal. Biotransform.* 22(3):145–170, doi:10.1080/10242420412331283314.

[51] Suginta, W.; Khunkaewla, P.; Schulte, A. (2013) Electrochemical biosensor applications of polysaccharides chitin and chitosan. *Chem. Rev.* 113:5458–5479, doi:10.1021/cr300325r.

[52] Švancara, I.; Vytřas, K.; Kalcher, K.; Walcarius, A.; Wang, J. (2009) Carbon paste electrodes in facts, numbers, and notes: A review on the occasion of the 50-years jubilee of carbon paste in electrochemistry and electroanalysis. *Electroanal.* 21:7–28, doi:10.1002/elan.200804340.

[53] Ahuja, T.; Mir, I.A.; Kumar, D.; Rajesh. (2007) Biomolecular immobilization on conducting polymers for biosensing applications. *Biomaterials* 28(5):791–805, doi:10.1016/j.biomaterials.2006.09.046.

[54] Cosnier, S. (2003) Biosensors based on electropolymerized films: New trends. *Anal. Bioanal. Chem.* 377:507–520, doi:10.1007/s00216-003-2131-7.

[55] Gros, P.; Comtat, M. (2004) A bioelectrochemical polypyrrole-containing $Fe(CN)_6^{3-}$ interface for the design of a NAD-dependent reagentless biosensor. *Biosens. Bioelectron.* 20(2):204–210, doi:10.1016/j.bios.2004.02.023.

[56] Brena, B.; González-Pombo, P.; Batista-Viera, F. (2013) Immobilization of Enzymes: A Literature Survey. In: Guisan, J. (Ed.) Immobilization of Enzymes and Cells. Methods in Molecular Biology, Vol. 1051. New Jersey: *Humana Press*, doi:10.1007/978-1-62703-550-7_2.

[57] Srere, P.A.; Uyeda, K. (1976) Functional groups on enzymes suitable for binding to matrices. *Meth. Enzymol.* 44:11–19, doi:10.1016/S0076-6879(76)44004-1.

[58] Novick S.J., Rozzell J.D. (2005) Immobilization of Enzymes by Covalent Attachment. In: Barredo J.L. (Ed.) Microbial Enzymes and Biotransformations. Methods in Biotechnology, Vol. 17. Totowa: *Humana Press*, doi:10.1385/1-59259-846-3:247.

[59] Broun, G.; Thomas, D.; Gellf, G.; Domurado, D.; Berjonneau, A.M.; Guillon, C. (1973) New methods for binding enzyme molecules into a water-insoluble matrix: Properties after insolubilization. *Biotechnol. Bioeng.* XV:359–375,

doi:10.1002/bit.260150211.

[60] Walt, D.R.; Agayn, V.I. (1994) The chemistry of enzyme and protein immobilization with glutaraldehyde. *Trends Anal. Chem.* 13(10):425–430, doi:10.1016/0165-9936(94)85023-2.

[61] Berg, J.M.; Tymoczko, J.L.; Stryer, L. (2013) Stryer Biochemie. Berlin, Heidelberg: *Springer Spektrum*, doi:10.1007/978-3-8274-2989-6.

[62] Katakis, I.; Domínguez, E. (1997) Catalytic electrooxidation of NADH for dehydrogenase amperometric biosensors. *Microchim. Acta* 126:11–32, doi:10.1007/BF01242656.

[63] Dawson, R.M.C.; Elliott, D.C. (2002) Data for Biochemical Research. Oxford: *Clarendon Press*.

[64] Durliat, H.; Causserand, C.; Comtat, M. (1990) Bienzyme amperometric lactate-specific electrode. *Anal. Chim. Acta* 231:309–311, doi:10.1016/S0003-2670(00)86432-6.

[65] Antiochia, R.; Cass, A.E.G.; Palleschi, G. (1997) Purification and sensor applications of an oxygen insensitive, thermophilic diaphorase. *Anal. Chim. Acta* 345:17–28, doi:10.1016/S0003-2670(96)00618-6.

[66] Kwan, R.C.H.; Hon, P.Y.T.; Mak, W.C.; Law, L.Y.; Hu, J.; Renneberg, R. (2006) Biosensor for rapid determination of 3-hydroxybutyrate using bi-enzyme system. *Biosens. Bioelectron.* 21:1101–1106, doi:10.1016/j.bios.2005.04.005.

[67] Cui, Y.; Barford, J.P.; Renneberg, R. (2006) Amperometric determination of phosphoglucomutase activity with a bienzyme screen-printed biosensor. *Anal. Biochem.* 354:162–164, doi:10.1016/j.ab.2006.03.045.

[68] Leca, B.; Marty, J.-L. (1997) Reagentless ethanol sensor based on a NAD-dependent dehydrogenase. *Biosens. Bioelectron.* 12(11):1083–1088, doi:10.1016/S0956-5663(97)00075-4.

[69] Serban, S.; El Murr, N. (2006) Redox-flexible NADH oxidase biosensor: A platform for various dehydrogenase bioassays and biosensors. *Electrochim. Acta* 51(24):5143–5149, doi:10.1016/j.electacta.2006.03.052.

[70] Lobo, M.J.; Miranda, A.J.; Tuñón, P. (1997) Amperometric biosensors based on NAD(P)-dependent dehydrogenase enzymes. *Electroanal.* 9(3):191–202, doi:10.1002/elan.1140090302.

[71] Gorton, L.; Dominguez, E. (2002) Electrocatalytic oxidation of NAD(P)/H at mediator-modified electrodes. *Rev. Mol. Biotechnol.* 82:371–392, doi:10.1016/S1389-0352(01)00053-8.

[72] Kochius, S.; Magnusson, A.O.; Hollmann, F.; Schrader, J.; Holtmann, D. (2012) Immobilized redox mediators for electrochemical $NAD(P)^+$ regeneration. *Appl. Microbiol. Biotechnol.* 93:2251–2264, doi:10.1007/s00253-012-3900-z.

[73] Miyamoto, S.; Murakami, T.; Saito, A.; Kimura, J. (1991) Development of an

amperometric alcohol sensor based on immobilized alcohol dehydrogenase and entrapped NAD^+. *Biosens. Bioelectron.* 6:563–567, doi:10.1016/0956-5663(91)80020-X.

[74] Sprules, S.D.; Hart, J.P.; Wring, S.A.; Pittson, R. (1995) A reagentless, disposable biosensor for lactic acid based on a screen-printed carbon electrode containing Meldola's Blue and coated with lactate dehydrogenase, NAD^+ and cellulose acetate. *Anal. Chim. Acta* 304:17–24, doi:10.1016/0003-2670(94)00565-4.

[75] Willner, I.; Riklin, A. (1994) Electrical communication between electrodes and $NAD(P)^+$-dependent enzymes using pyrroloquinolinequinone-enzyme electrodes in a self-assembled monolayer configuration: Design of a new class of amperometric biosensors. *Anal. Chem.* 66:1535–1539, doi:10.1021/ac00081a028.

[76] Weiss, D.J.; Dorris, M.; Loh, A.; Peterson, L. (2007) Dehydrogenase based reagentless biosensor for monitoring phenylketonuria. *Biosens. Bioelectron.* 22:2436–2441, doi:10.1016/j.bios.2006.09.001.

[77] Fernández, J.J; López, J.R.; Correig, X.; Katakis, I. (1998) Reagentless carbon paste phosphate biosensors: Preliminary studies. *Sens. Actuators B Chem.* 47:13–20, doi:10.1016/S0925-4005(98)00003-3.

[78] Prieto-Simón, B.; Fàbregas, E. (2004) Comparative study of electron mediators used in the electrochemical oxidation of NADH. *Biosens. Bioelectron.* 19:1131–1138, doi:10.1016/j.bios.2003.10.010.

[79] Spichiger-Keller, U.E. (1998) Chemical Sensors and Biosensors for Medical and Biological Applications. Weinheim: *Wiley-VCH*, doi:10.1002/9783527612284.

[80] Diamond, D. (1993) Progress in sensor array research. *Electroanal.* 5:795–802, doi:10.1002/elan.1140050913.

[81] Grieshaber, D.; MacKenzie, R.; Vörös, J.; Reimhult, E. (2008) Electrochemical biosensors – sensor principles and architectures. *Sensors* 8:1400–1458, doi:10.3390/s80314000.

[82] Hierlemann, A.; Brand, O.; Hagleitner, C.; Baltes, H. (2003) Microfabrication techniques for chemical/biosensors. *Proc. IEEE* 91(6):839–863, doi:10.1109/JPROC.2003.813583.

[83] Fiaccabrino, G.C.; Koudelka-Hep, M. (1998) Thin-film microfabrication of electrochemical transducers. *Electroanal.* 10(4):217–222, doi:10.1002/(SICI)1521-4109(199804)10:4<217::AID-ELAN217>3.0.CO;2-W.

[84] Li, C.M.; Dong, H.; Zhou, Q.; Goh, K.H. (2008) Biochips – Fundamentals and Applications. In: Zhang, X.; Ju, H.; Wang, J. (Eds.) Electrochemical Sensors, Biosensors and their Biomedical Applications. Amsterdam: *Academic Press*, doi:10.1016/B978-012373738-0.50013-1.

[85] Metters, J.P.; Kadara, R.O.; Banks, C.E. (2011) New directions in screen printed electroanalytical sensors: An overview of recent developments. *Analyst* 136:1067–1076, doi:10.1039/c0an00894j.

[86] Hart, J.P.; Crew, A.; Crouch, E.; Honeychurch, K.C.; Pemberton, R.M. (2004) Some recent designs and developments of screen-printed carbon electrochemical sensors/biosensors for biomedical, environmental, and industrial analyses. *Anal. Lett.* 37(5):789–830, doi:10.1081/AL-120030682.

[87] Hughes, G.; Westmacott, K.; Honeychurch, K.C.; Crew, A.; Pemberton, R.M.; Hart, J.P. (2016) Recent advances in the fabrication and application of screen-printed electrochemical (bio)sensors based on carbon materials for biomedical, agri-food and environmental analyses. *Biosensors* 6(4):50, doi:10.3390/bios6040050.

[88] Galán-Vidal, C.A.; Muñoz, J.; Domínguez, C.; Alegret, S. (1995) Chemical sensors, biosensors and thick-film technology. *Trends Anal. Chem.* 15(5):225–231, doi:10.1016/0165-9936(95)91375-3.

[89] Leppävuori, S.; Väänänen, J.; Lahti, M.; Remes, J.; Uusimäki, A. (1994) A novel thick-film technique, gravure offset printing, for the realization of fine-line sensor structures. *Sens. Actuators A Phys.* 42:593–596, doi:10.1016/0924-4247(94)80060-X.

3 Development of a multi-parameter sensor chip for the simultaneous detection of organic compounds in biogas processes

Physica Status Solidi A (2015), 212(6):1306–1312

J. Pilas[1], H. Iken[1], T. Selmer[1], M. Keusgen[2] and M.J. Schöning[1,3]

[1] Institute of Nano- and Biotechnologies (INB), FH Aachen, Jülich, Germany
[2] Institute of Pharmaceutical Chemistry, Philipps-Universität Marburg, Marburg, Germany
[3] Peter Grünberg Institute (PGI-8), Forschungszentrum Jülich, Jülich, Germany

Submitted: 12-09-2014; Accepted: 03-10-2015; Published: 03-27-2015

https://doi.org/10.1002/pssa.201431894

Keywords: β-nicotinamide adenine dinucleotide, biogases, biosensors, enzymes, formate, lactate

Abstract

An enzyme-based multi-parameter biosensor is developed for monitoring the concentration of formate, D-lactate and L-lactate in biological samples. The sensor is based on the specific dehydrogenation by an oxidised β-nicotinamide adenine dinucleotide (NAD^+)-dependent dehydrogenase (formate dehydrogenase, D-lactic dehydrogenase and L-lactic dehydrogenase, respectively) in combination with a diaphorase from *Clostridium kluyveri* (EC 1.8.1.4). The enzymes are immobilized on a platinum working electrode by cross-linking with glutaraldehyde (GA). The principle of the determination scheme in case of L-lactate is as follows: L-lactic dehydrogenase (L-LDH) converts L-lactate into pyruvate by reaction with NAD^+. In the presence of $Fe(CN)_6{}^{3-}$, the resulting reduced β-nicotinamide adenine dinucleotide (NADH) is then regenerated enzymatically by diaphorase. The electrochemical detection is based on the current generated by oxidation of $Fe(CN)_6{}^{4-}$ at an applied potential of +0.3 V *vs.* a Ag/AgCl reference electrode. The biosensor will be electrochemically characterized in terms of linear working range and sensitivity. Additionally, the successful practical application of the sensor is demonstrated in an extract from maize silage.

3.1 Introduction

The production of biogas through anaerobic digestion of energy crops or organic matter is an attractive approach as an alternative to fossil fuels. During the process, organic biopolymers are hydrolyzed and fermented by a multitude of microorganisms to intermediates, which in the end are converted to methane, carbon dioxide and H_2O by methanogens [1]. However, stable operation conditions of the sensitive process depend on a balanced relationship between the involved microbial groups [2].

Process imbalances, amongst others, are characterized by a drop in pH and the accumulation of volatile fatty acids such as acetate and propionate, accompanied with fluctuations in gas composition and production [3]. Due to the complexity of the process it is difficult to determine one specific parameter, which reflects the state of a biogas plant. Therefore, the development of reliable tools for the monitoring of several key parameters is of huge importance for an efficient conversion of biomass to energy. In this regard, the increase of intermediates, like lactate, formate and alcohols might provide an attractive approach for the early detection of undesired conditions that might lead to total process failures.

Lactate is chiral and has two optical isomers: namely D- and L-lactate. The most abundant enantiomer in the human body is L-lactate. Whereas, the isomer D-lactate is only produced by bacteria and acts as a major metabolic end product of microbial carbohydrate fermentation [4]. In general, both of the lactate enantiomers are metabolized to acetate, a main substrate for the methanogenic bacteria. For this reason, it is important to monitor not only the L-lactate level in biogas processes, but both of the enantiomers. Specific differentiation between the two isoforms is achieved by dehydrogenases that use oxidized β-nicotinamide adenine dinucleotide (NAD^+). The oxidation of D- and L-lactate to pyruvate is catalyzed by D- and L-lactic dehydrogenase (D-LDH, L-LDH), respectively. These enzymatic reactions require the cofactor NAD^+,

which is converted to the reduced form of β-nicotinamide adenine dinucleotide (NADH). By the production of NADH a mechanism for the amperometric detection is provided. However, direct electrochemical oxidation of NADH is restricted to several drawbacks [5–7]. The regeneration of NADH occurs at an applied potential of ca. 0.7 V and ca. 1.0 V *vs.* saturated calomel electrode (SCE) for platinum and gold electrodes, respectively. High overpotentials limit the sensitivity and promote interferences from other electroactive species present in real samples [8]. An accelerated oxidation of NADH to NAD^+ has been achieved enzymatically by coupling with NADH oxidase (Enzyme Comission (EC) Number 1.6.99.3) [9, 10] and diaphorase (EC 1.8.1.4) [11, 12]. NADH oxidase regenerates NADH by using O_2 as an electron acceptor and production of H_2O_2. In the present work, the NADH detection is realized by a diaphorase-catalyzed reaction with $Fe(CN)_6^{3-}$ as developed by Comtat *et al.* [13] and Durliat *et al.* [14].

The schematic of the sensor principle, exemplarily shown for the detection of L-lactate, is presented in Fig. 3.1. In the presence of an electron acceptor, like $Fe(CN)_6^{3-}$, the oxidation of NADH to NAD^+ is catalyzed by the enzyme diaphorase. Thereby, the electron acceptor is reduced to $Fe(CN)_6^{4-}$. The amperometric detection is based on the anodic oxidation of $Fe(CN)_6^{4-}$, which results in a generated current. This general approach can be applied with any NAD^+-dependent dehydrogenase.

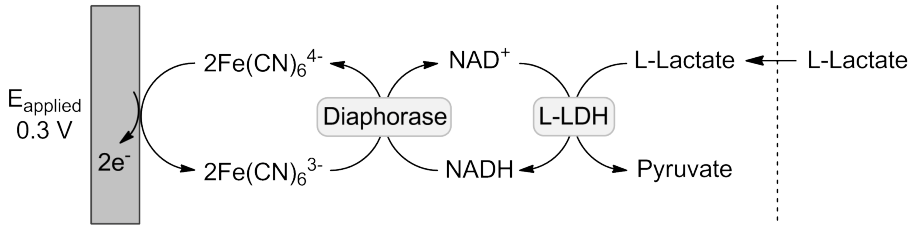

Fig. 3.1: Schematic illustration of the principle for the detection of L-lactate (L-LDH, L-lactic dehydrogenase). The same principle is used for the analysis of D-lactate and formate by the application of D-lactic dehydrogenase and formate dehydrogenase, respectively.

In this work, we present for the first time an amperometric enzyme-based multiparameter biosensor array for the simultaneous detection of formate, D- and L-lactate. The biosensor chip has been fabricated by means of thin-film technology. The practical application of the developed sensor array was demonstrated by the detection of D- and L-lactate in an extract from maize silage.

3.2 Material and methods

3.2.1 Materials

Formate dehydrogenase (FDH) (EC 1.2.1.2, from *Candida boidinii*), L-lactic dehydrogenase (L-LDH) (EC 1.1.1.27, from *Bacillus stearothermophilus*), D-lactic dehydrogenase (D-LDH) (EC 1.1.1.28 from *Lactobacillus leichmanii*), and diaphorase (EC 1.8.1.4, from *Clostridium kluyveri*) were obtained from Sigma-Aldrich Co. (St. Louis, MO, USA). Bovine serum albumin (BSA), glutaraldehyde solution (GA) (25 %), glycerol, iron(III) nitrate nonahydrate, KCl, KH_2PO_4, K_2HPO_4, β-nicotinamide adenine dinucleotide

hydrate (NAD^+), sodium formate, sodium D-lactate, sodium L-lactate, potassium $Fe(CN)_6^{4-}$, and $Fe(CN)_6^{3-}$ were also purchased from Sigma-Aldrich.

3.2.2 Sensor fabrication

The developed multi-parameter sensor combines up to five working electrodes for the individual detection of various substrates on one single chip. In Fig. 3.2, the sensor layout of the fabricated array in thin-film technology is shown. The sensor chip was processed by photolithographic techniques from a p-type silicon (Si) wafer (resistivity >1000 Ω cm, orientation <100>). A 500 nm thin layer of SiO_2 was grown by thermal wet oxidation at 1000 °C for 30 min. Spin-coating at 4000 rpm for 60 s was used for the deposition of the photoresist (AZ5214E, MicroChemicals GmbH, Ulm, Germany). Afterwards, the photoresist film was exposed and developed. 20 nm titanium and 200 nm platinum were patterned by electron beam evaporation and lift-off technique. The resulting circular platinum working electrodes had a diameter of 2 mm. The wafer was diced, then chips were mounted into printed circuit boards and wire-bonded with an ultrasonic wedge bonder. Bond wires and circuit paths were encapsulated with silicone. More detailed information about sensor fabrication is given in [15–17].

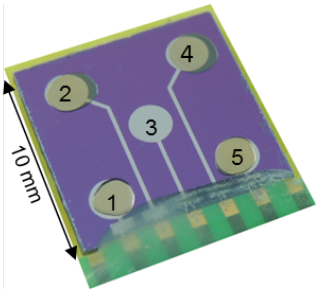

Fig. 3.2: Biosensor chip with five individual working electrodes (WE) with different enzyme membranes: (1) BSA as control, (2) L-lactic dehydrogenase and diaphorase, (3) blank WE, (4) D-lactic dehydrogenase and diaphorase, and (5) formate dehydrogenase and diaphorase.

3.2.3 Enzyme immobilization

Prior to enzyme immobilization, the platinum electrodes were cleaned with acetone, 2-propanol and deionized H_2O under sonication for 10 min each. The individual enzyme membranes were constructed by cross-linking with GA. In each case, 2.8 µL of an enzyme solution (containing diaphorase and the specific dehydrogenase dissolved in 0.1 M phosphate buffer, pH 7.4) were mixed with 1.4 µL BSA (10 vol%). Immobilisation of enzymes with GA leads to severe conformational changes. Therefore, the lysine-rich protein BSA, which exhibits no catalytic activity, was used as an inert protein to decrease the loss of enzyme activity [18, 19]. Then, 2.8 µL of GA (2.5 vol%) in 10% glycerol were added. Glycerol in the immobilisation mixture acts as an emollient, which supports an even spreading of the enzymes on the membrane surface. Finally, 1.5 µL of the enzyme/BSA/GA solution were applied to the electrode surface by drop-coating resulting in an enzyme loading of 1 unit/electrode of diaphorase and 0.75 units/electrode

of dehydrogenase (D-LDH, L-LDH and FDH, respectively). Afterwards, the sensors were dried for 4 h at ambient temperature to promote evaporation of water and finally, stored at 4 °C until required. The modified electrodes were thoroughly rinsed with 0.1 M phosphate buffer (pH 7.4) to remove excess-free enzymes from the surface before use. A membrane on which only BSA was immobilized served as a control. For this purpose, 1.5 µL of an immobilization mixture (4.2 µL BSA (10 vol%) mixed with 2.8 µL GA) were deposited on the electrode surface.

3.2.4 Measurement setup and amperometric detection

The electrochemical response of the enzyme-modified electrodes was measured with a conventional three-electrode system. An external platinum electrode with a diameter of 7.5 mm served as a counter electrode. In order to oxidize the $Fe(CN)_6^{4-}$, which is the final product of the bi-enzymatic reaction, a constant potential of +0.3 V *vs.* Ag/AgCl reference electrode (Model 6.0726.107, Methrom) was applied to the on-chip platinum working electrodes (diameter 2 mm). Therefore, the electrodes were connected to a potentiostat (PalmSens with a multichannel multiplexer, Palm Instruments BV).

The buffer contained 5 mM $Fe(CN)_6^{3-}$ and 2 mM NAD^+ dissolved in 20 mL 0.1 M phosphate buffer (pH 7.4). Agitation of the solution was performed with a magnetic stirrer. Prior amperometric detection, the sensors were incubated for 10 min in the buffer solution to allow diffusion of NAD^+ and $Fe(CN)_6^{3-}$ into the enzyme membranes. The calibration curves were adjusted by titration of stock solutions of sodium formate, sodium D- and L-lactate.

3.2.5 Cyclic voltammetry

The required potential for the oxidation of $Fe(CN)_6^{4-}$ was investigated by cyclic voltammetry in a three-electrode system. Cyclic voltammograms were recorded from -0.1 to +0.6 V *vs.* Ag/AgCl reference electrode in a 0.1 M KCl solution (pH 7.4) as the supporting electrolyte. The scan rate was varied from 50 to 500 $mV\,s^{-1}$.

3.2.6 Extract from maize silage

An extract from maize silage was prepared by using 100 mL of deionized H_2O as the extracting solvent for 10 g of maize silage. The mixture was agitated by a magnetic stir bar at ambient temperature for 30 min and afterwards filtered. The obtained extract was clarified by protein precipitation using $Fe(CN)_6^{4-}$ and $ZnSO_4 \cdot 3\,H_2O$ as described by Carrez [20]. These reagents form a soluble complex of $Zn_2[Fe(CN)_6]$, which leads to the precipitation of proteins and fats. By the addition of 1 M NaOH the pH was adjusted to 7.4 and excess Zn^{2+} ions were removed. Subsequently, the sample was diluted with deionized H_2O to a final dilution of 1:2 and centrifuged. The clear supernatant was used for the amperometric detection of formate, D- and L-lactate. After the purification process, the extract was tested for residual amounts of $Fe(CN)_6^{4-}$ by addition of iron(III) nitrate nonahydrate. In the presence of iron(III) ions, $Fe(CN)_6^{4-}$ oxidizes immediately to the dark blue pigment $Fe_4[Fe(CN)_6]_3$ (also known as Prussian Blue). The described

clarification procedure was performed in order to obtain a clear and neutral sample solution.

The extract was also assayed using a commercially available kit for the determination of D- and L-lactate following the manufacturer's instructions (Megazyme International Ireland Co., Ireland).

3.3 Results and discussion

3.3.1 Cyclic voltammetry

Cyclic voltammetry was used for the determination of the oxidation potential of $Fe(CN)_6^{4-}$ together with the developed biosensor chip. In accordance to the applied potential the oxidation of $Fe(CN)_6^{4-}$ or the reduction of $Fe(CN)_6^{3-}$ can occur. As shown in Eq. 3.1 the transfer of an electron results in a current response.

$$Fe(CN)_6^{4-} \leftrightarrow Fe(CN)_6^{3-} + e^- \tag{3.1}$$

The corresponding cyclic voltammograms are presented in Fig. 3.3a. As the electrode is scanned towards a more positive potential, the electrode becomes a sufficiently strong oxidant to oxidize the $Fe(CN)_6^{4-}$ to $Fe(CN)_6^{3-}$ and the anodic current increases. When the applied potential further raises, the concentration of $Fe(CN)_6^{4-}$ at the electrode surface decreases. The curve reaches a peak maximum at a potential of about +0.3 V; at this point almost no more $Fe(CN)_6^{4-}$ is available for oxidation. Because of the depletion of $Fe(CN)_6^{4-}$, the current decays and the electrode surface is surrounded by $Fe(CN)_6^{3-}$. At the switching potential of +0.6 V, the scan is reversed back to the starting potential. During the reverse scan the reduction of the electroactive species occurs. With decreasing potential, $Fe(CN)_6^{3-}$ is reduced to $Fe(CN)_6^{4-}$ and the current reaches a peak at approximately +0.13 V before returning to the starting potential. The similar shape of the oxidation and the reduction peak suggest a reversible reaction system [21, 22]. By increasing the scan rate the peak current raises. As presented in Fig. 3.3b, the peak currents of the voltammograms are linearly proportional to the square root of the scan rate, indicating a fast electron transfer on the fabricated working electrode, which is limited by the diffusion of the analyte to the electrode surface [23].

Based on the obtained results, in the following experiments a working potential of +0.3 V was chosen for the detection of $Fe(CN)_6^{4-}$.

3.3.2 Characterization of the biosensor performance

The performance of the multi-parameter biosensor chip for the determination of formate, D- and L-lactate was characterized in terms of sensitivity and linear detection range. For this reason, stock solutions of the corresponding substrate were added successively to the buffer solution in a concentration range from 0.02 to 20 mM. The sensor signal was recorded for approximately 3 min. After the calibration, the sensor was washed with buffer solution and reused for further measurements.

Figure 3.4a shows exemplarily the current-time curve of the D-lactate electrode obtained by the successive addition of various concentrations of D-lactate. It can be

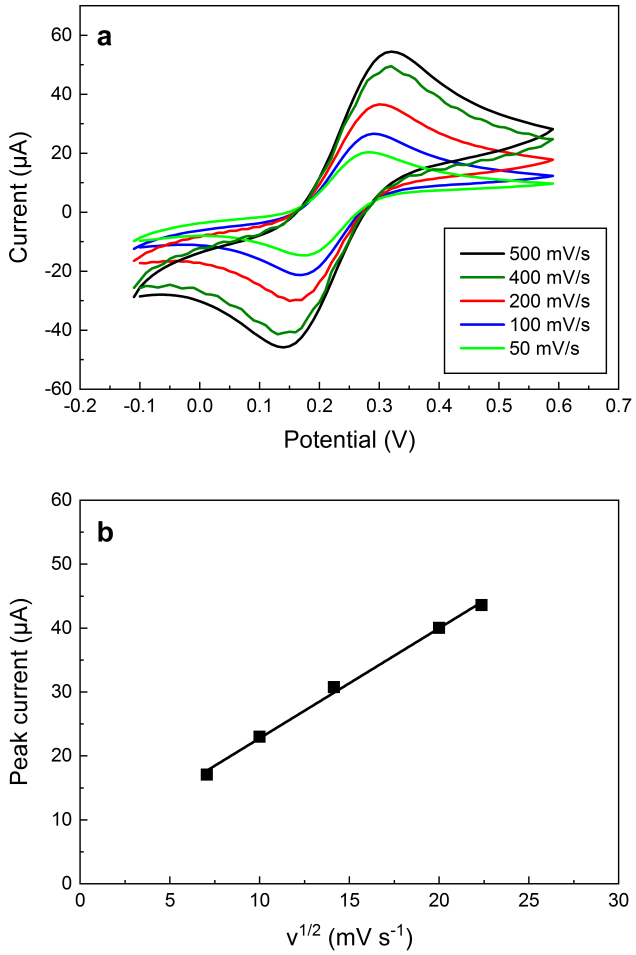

Fig. 3.3: Cyclic voltammograms of 5 mM $Fe(CN)_6^{4-}$ in 0.1 M KCl (pH 7.4) at various scan rates: 50, 100, 200, 400, and 500 mV s^{-1} **(a)**. Variation of the peak current I_p *vs.* the square root of the scan rate **(b)**.

seen that the current increased after the addition of D-lactate due to the oxidation of $Fe(CN)_6^{4-}$, which is the product of the enzymatic reaction by D-LDH and diaphorase. The sensor showed a rapid responds towards D-lactate (attaining 95% of the steady state current within ~4 s). Thereby, the response time of the sensor signal was independent of the substrate concentration.

In Fig. 3.4b, the calibration curve of the current response to the substrate concentration is presented. The linear calibration curves for the D- and L-lactate electrodes are depicted in Fig. 3.5a and for the formate sensor in Fig. 3.5b. Both of the lactate sensors showed a quite similar linear relationship between current response and substrate concentration in the range of 0.1–1 mM. Within this range, the sensitivity was 0.55 µA mM^{-1} (R = 0.996) for the L-lactate sensor and 0.42 µA mM^{-1} (R = 0.997) for the D-lactate sensor. For higher substrate concentrations, a saturation of both of the sensors was achieved, due to saturated enzymes. In this condition, the sensor signal reaches a plateau and is no longer dependent upon the substrate concentration.

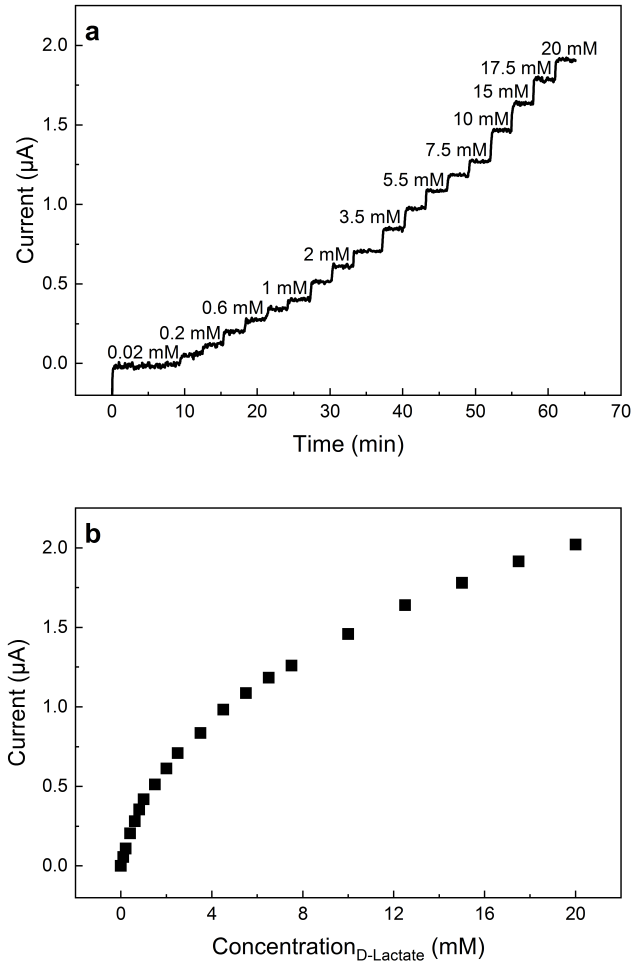

Fig. 3.4: Steady-state current response of the D-lactate electrode (0.75 U D-LDH, 1.0 U diaphorase) to successive increments of D-lactate concentration in 0.1 M) phosphate buffer at an applied potential of +0.3 V *vs.* Ag/AgCl **(a)**. Corresponding calibration curve of the current response on the D-lactate concentration **(b)**.

Similar linear detection ranges have been reported for D-lactate biosensors using D-LDH in combination with NADH oxidase (0.04–1.5 mM) [12] or screen-printed electrodes with D-LDH, NAD^+ and Meldola's Blue (0.1–1.0 mM) [24]. These findings indicate that the developed biosensor chip provides a useful system for the detection of D-lactate. In addition, this biosensor array allows the simultaneous measurement of L-lactate and formate with similar performance.

The formate sensor showed a broader linear detection range in comparison to the both lactate sensors. A linear relationship between the current increase and the formate concentration was obtained up to a concentration of 2 mM with a lower detection limit of about 0.02 mM. The sensor showed a sensitivity of 2.46 µA mM^{-1} ($R = 0.998$). A different bi-enzymatic approach for the formate detection was used by the co-immobilization of FDH with salicylate hydroxylase and NAD^+ in front of a Clark electrode [25]. This amperometric sensor achieved a linear working range of 0.001–0.3 mM and a lower

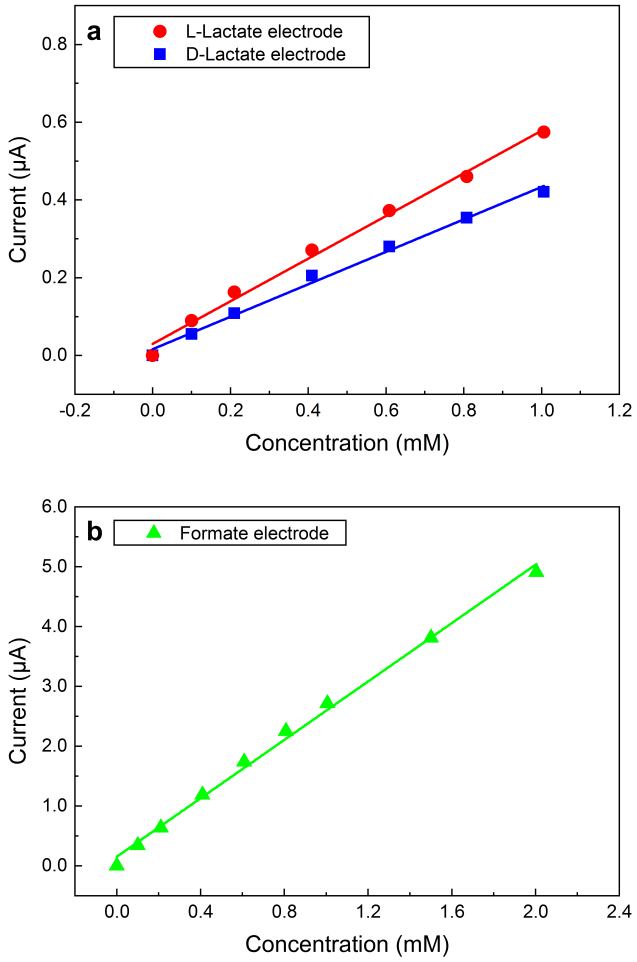

Fig. 3.5: Linear calibration curves for the diaphorase-based sensors by using different dehydrogenases L-LDH **(a)** and D-LDHH and FDH **(b)**.

detection limit of 1.98×10^{-7} M. A further enzyme-based methodology was described by using FDH with an electropolymerized 3,4-dihydroxybenzaldehyde membrane. This biosensor showed a linear detection range from 0.07 to 1.1 mM [26]. In comparison to these two reported formate sensors, the proposed multi-parameter biosensor chip enables similar results concerning the linear detection range. However, in both reported systems, the FDH loading on the electrodes was higher; namely 0.8 units [25] and 6 units [26] compared to 0.75 units on the multi-parameter biosensor chip. The higher FDH loadings might explain the better lower detection limit of these biosensors. Therefore, the enzyme membrane of the proposed biosensor chip requires optimization in order to improve the detection limit.

In Tab. 3.1, the characteristics of each substrate-specific sensor are summarized. The enzyme membranes of these three sensors were prepared by the same immobilization procedure, though, the sensitivity is different. Compared to both lactate sensors, the FDH-based sensor exhibits a higher sensitivity. In this regard, the sensor performance is especially influenced by the enzyme activity on the electrode surface. Due to its

Tab. 3.1: Electrochemical characteristics of the multi-parameter biosensor chip.

Substrate	Linear detection range (mM)	Sensitivity ($\mu A\,mM^{-1}$)
D-Lactate	0.1-1	0.42
L-Lactate	0.1-1	0.55
Formate	0.04-2	2.46

simplicity and versatility the immobilization of enzymes with GA has been a popular technique in the design of biosensors [18, 27]. Thereby, the concentration of GA, buffer composition, pH and additives such as BSA have a significant effect on the enzyme activity. It might be possible that the used dehydrogenases (D-LDH, L-LDH and FDH) react differently to the applied immobilization procedure and that the enzyme activity of FDH is less impaired by the use of GA. For this enzyme, even an increased activity was observed after the immobilization with GA [28].

3.3.3 Simultaneous measurement of organic compounds

As mentioned above the amperometric detection of the different organic compounds is based on the oxidation of $Fe(CN)_6^{4-}$. Simultaneous measurements were performed in order to investigate if the electrodes only showed current response when the corresponding substrate was available. In Fig. 3.6, the current response of the three sensors, which were arranged on one chip, to the successive addition of D-lactate, L-lactate and formate is depicted. By the time L-lactate was added to the buffer solution, only the current signal of the sensor with immobilized L-LDH and diaphorase increased; neither the D-lactate nor the formate sensor showed a current response. This behavior was also the case after the addition of D-lactate and formate, respectively. The current of all sensors only increased when the corresponding substrate was available in the buffer solution.

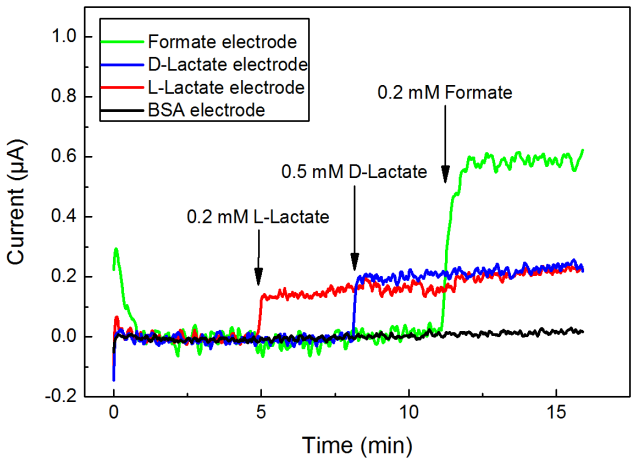

Fig. 3.6: Measurement curves for simultaneous determination of D-lactate, L-lactate, and formate by means of the biosensor chip.

3.3.4 Determination of substrate concentrations in real samples

In order to demonstrate the practical applicability of the multi-parameter biosensor chip, the response of the sensor in an extract from maize silage was investigated. Measurements were conducted within the linear working range by appropriate dilution of the extract. Based on the obtained current response the concentration of D- and L-lactate was calculated by use of the calibration curves depicted in Fig. 3.5a. The results obtained with the proposed biosensor were compared with those obtained with a commercial kit. As presented in Tab. 3.2, the concentrations determined with the developed biosensor are in good agreement with those obtained with the reference method. Thereby, the capability of the biosensor for the reliable measurement of D- and L-lactate is shown. In comparison to commercially available kits, the proposed biosensor provides the advantages of rapid, simultaneous and multiple applications as well as reusability.

In the analyzed extract, D- and L-lactate are present in almost equal proportions. This observation underlines the importance to determine both of the isoforms. In comparison to the lactate concentration the level of formate is noticeably lower. Since, in maize silage predominately lactic acid bacteria are present, the higher proportion of lactate seems reasonable [29].

Tab. 3.2: Comparison of results obtained for D- and L-lactate in an extract of maize silage by different methods. The formate concentration was not detected (n.d.) with the photometric kit.

Substrate	Multi-parameter biosensor (mM)	Photometric kit (mM)
D-Lactate	7.26±0.53	7.12±0.17
L-Lactate	6.35±0.39	6.29±0.11
Formate	1.23±0.07	n.d.

3.4 Conclusion and outlook

In the present work, we have demonstrated the development and characterization of a new multi-parameter biosensor for the measurement of three different substrates based on a dehydrogenase/diaphorase-catalyzed reaction. The amperometric sensor array enables the simultaneous determination of formate, D- and L-lactate. We have successfully applied the sensor array to the quantification of these compounds in an extract of maize silage for the first time. However, for practical applications the performance of the sensor array requires further improvement. An optimization of the enzyme membrane and the working conditions (buffer composition, NAD^+ and $Fe(CN)_6^{3-}$ concentration) might enhance the sensitivity and improve the lower detection limit. Further important parameters are the storage and operational stability of the multi-parameter biosensor, which will be characterized and optimized in the future.

An advantage of the present system is that it can also be extended with different NAD^+-dependent dehydrogenases. Thus, further organic compounds, which are important for

the monitoring of biogas-related parameters, can be controlled. The combination of different parameters allows an improved understanding of the operation conditions, in order to react readily to minor changes and to avoid establishment of an unstable process. Therefore, future work aims for the implementation of all required electrodes onto one sensor chip, which enables the development of a reliable tool for on-site monitoring of organic compounds in biogas processes. In this regard, the integration of both a miniaturized reference [30] and counter electrode onto the sensor chip is envisaged.

Acknowledgements

The authors thank the German Federal Ministry of Food and Agriculture (BMEL) and the "Fachagentur Nachwachsende Rohstoffe e.V." (FNR) for financial support of the project (FKZ: 22006613).

References

[1] Weiland, P. (2010) Biogas production: Current state and perspectives. *Appl. Microbiol. Biotechnol.* 85:849–860, doi:10.1007/s00253-009-2246-7.

[2] Switzenbaum, M.S.; Giraldo-Gomez, E.; Hickey, R.F. (1990) Monitoring of the anaerobic methane fermentation process. *Enzyme Microb. Technol.* 12:722–730, doi:10.1016/0141-0229(90)90142-D.

[3] Nielsen, H.B.; Uellendahl, H.; Ahring, B.K. (2007) Regulation and optimization of the biogas process: Propionate as a key parameter. *Biomass Bioenergy* 31:820–830, doi:10.1016/j.biombioe.2007.04.004.

[4] Kandler, O. (1983) Carbohydrate metabolism in lactic acid bacteria. *A. Van. Leeuw.* 49:209–224, doi:10.1007/BF00399499.

[5] Lobo, M.J.; Miranda, A.J.; Tuñón, P. (1997) Amperometric biosensors based on NAD(P)-dependent dehydrogenase enzymes. *Electroanal.* 9(3):191–202, doi:10.1002/elan.1140090302.

[6] Prodromidis, M.I.; Karayannis, M.I. (2002) Enzyme based amperometric biosensors for food analysis. *Electroanal.* 14(4):241–261, doi:10.1002/1521-4109(200202)14:4<241::AID-ELAN241>3.0.CO;2-P.

[7] Radoi, A.; Compagnone, D. (2009) Recent advances in NADH electrochemical sensing design. *Bioelectrochemistry* 76(1-2):126–137, doi:10.1016/j.bioelechem.2009.06.008.

[8] Katakis, I.; Domínguez, E. (1997) Catalytic electrooxidation of NADH for dehydrogenase amperometric biosensors. *Microchim. Acta* 126(1-2):11–32, doi:10.1007/BF01242656.

[9] Serban, S.; El Murr, N. (2006) Redox-flexible NADH oxidase biosensor: A platform for various dehydrogenase bioassays and biosensors. *Electrochim. Acta* 51:5143–5149, doi:10.1016/j.electacta.2006.03.052.

[10] Ghica, M.E.; Pauliukaite, R.; Marchand, N.; Devic, E.; Brett, C.M.A. (2007) An improved biosensor for acetaldehyde determination using a bienzymatic strategy at poly(neutral red) modified carbon film electrodes. *Anal. Chim. Acta* 591:80–86, doi:10.1016/j.aca.2007.03.047.

[11] Noguer, T.; Marty, J.L. (1995) An amperometric bienzyme electrode for acetaldehyde detection. *Enzyme Microb. Technol.* 17:453–456, doi:10.1016/0141-0229(94)00068-3.

[12] Montagné, M.; Erdmann, H.; Comtat, M.; Marty, J.-L. (1995) Comparison of the performances of two bi-enzymatic sensors for the detection of D-lactate. *Sens. Actuators B Chem.* 27:440–443, doi:10.1016/0925-4005(94)01636-V.

[13] Comtat, M.; Galy, M.; Goulas, P.; Souppe, J. (1988) Amperometric bienzyme electrode for L-carnitine. *Anal. Chim. Acta* 208:295–300, doi:10.1016/S0003-2670(00)80759-X.

[14] Durliat, H.; Causserand, C.; Comtat, M. (1990) Bienzyme amperometric lactate-specific electrode. *Anal. Chim. Acta* 231:309–311, doi:10.1016/S0003-2670(00)86432-6.

[15] Leinhos, M.; Schusser, S.; Bachmann, B.; Bäcker, M.; Poghossian, A.; Schöning, M.J. (2014) Micromachined multi-parameter sensor chip for the control of polymer-degradation medium. *Phys. Status Sol. A* 211(6):1346–1351, doi:10.1002/pssa.201330364.

[16] Iken, H.; Ahlborn, K.; Gerlach, F.; Vonau, W.; Zander, W.; Schubert, J.; Schöning, M.J. (2013) Development of redox glasses and subsequent processing by means of pulsed laser deposition for realizing silicon-based thin-film sensors. *Electrochim. Acta* 113:762–767, doi:10.1016/j.electacta.2013.08.092.

[17] Spelthahn, H.; Kirsanov, D.; Legin, A.; Osterrath, T.; Schubert, J.; Zander, W.; Schöning, M.J. (2012) Development of a thin-film sensor array for analytical monitoring of heavy metals in aqueous solutions. *Phys. Status Sol. A* 209:885–891, doi:10.1002/pssa.201100733.

[18] Migneault, I.; Dartiguenave, C.; Bertrand, M.J.; Waldron, K.C. (2004) Glutaraldehyde: Behavior in aqueous solution, reaction with proteins, and application to enzyme crosslinking. *BioTechniques* 37(5):790–802, doi:10.2144/04375RV01.

[19] Broun, G.B. (1976) Chemically aggregated enzymes. *Meth. Enzymol.* 44:263–280, doi:10.1016/S0076-6879(76)44022-3.

[20] Carrez, M.C. (1908) Le ferrocyanure de potassium et l'acétate de zinc comme agents de défécation des urines. *Ann. Chim. Anal.* 13(286):97–101.

[21] Wang, J. (2001) Analytical Electrochemistry. New York: *Wiley-VCH.*

[22] Nicholson, R.S. (1965) Theory and application of cyclic voltammetry for measurement of electrode reaction kinetics. *Anal. Chem.* 37:1351–1355, doi:10.1021/ac60230a016.

[23] Bard, A.J.; Faulkner, L.R. (2001) Electrochemical Methods: Fundamentals and

Applications. New York: *Wiley-VCH.*

[24] Avramescu, A.; Noguer, T.; Magearu, V. Marty, J.-L. (2001) Chronoamperometric determination of D-lactate using screen-printed enzyme electrodes. *Anal. Chim. Acta* 433(1):81–88, doi:10.1016/S0003-2670(00)01386-6.

[25] Mak, K.K.W.; Wollenberger, U.; Scheller, F.W.; Renneberg, R. (2003) An amperometric bi-enzyme sensor for determination of formate using cofactor regeneration. *Biosens. Bioelectron.* 18(9):1095–1100, doi:10.1016/S0956-5663(02)00245-2.

[26] Hung Tzang, C.; Yuan, R.; Yang, M. (2001) Voltammetric biosensors for the determination of formate and glucose-6-phosphate based on the measurement of dehydrogenase-generated NADH and NADPH. *Biosens. Bioelectron.* 16(3):211–219, doi:10.1016/S0956-5663(00)00143-3.

[27] Sassolas, A., Blum, L.J., Leca-Bouvier, B.D. (2012) Immobilization strategies to develop enzymatic biosensors. *Biotechnol. Adv.* 30:489–511, doi:10.1016/j.biotechadv.2011.09.003.

[28] Kim, M.H.; Park, S.; Kim, Y.H.; Won, K.; Lee, S.H. (2013) Immobilization of formate dehydrogenase from *Candida boidinii* through cross-linked enzyme aggregates. *J. Mol. Catal. B: Enzym.* 97:209–214, doi:10.1016/j.molcatb.2013.08.020.

[29] Meeske, R.; Basson, H.M. (1998) The effect of a lactic acid bacterial inoculant on maize silage. *Anim. Feed Sci. Technol.* 70(3):239–247, doi:10.1016/S0377-8401(97)00066-7.

[30] Simonis, A.; Lüth, H.; Wang, J.; Schöning, M.J. (2004) New concepts of miniaturised reference electrodes in silicon technology for potentiometric sensor systems. *Sens. Actuators B Chem.* 103:429–435, doi:10.1016/j.snb.2004.04.072.

4 Optimization of an amperometric biosensor array for simultaneous measurement of ethanol, formate, D- and L-lactate

Electrochimica Acta (2017), 251:256-262

J. Pilas[1,2], Y. Yazici[1], T. Selmer[1], M. Keusgen[2] and M.J. Schöning[1,3]

[1] Institute of Nano- and Biotechnologies (INB), FH Aachen, Jülich, Germany
[2] Institute of Pharmaceutical Chemistry, Philipps-Universität Marburg, Marburg, Germany
[3] Peter Grünberg Institute (PGI-8), Forschungszentrum Jülich, Jülich, Germany

Submitted: 05-17-2017; Accepted: 07-20-2017; Published: 09-01-2017

https://doi.org/10.1016/j.electacta.2017.07.119

Keywords: dehydrogenase, diaphorase, enzymatic biosensor, simultaneous determination

Abstract

The immobilization of NAD^+-dependent dehydrogenases, in combination with a diaphorase, enables the facile development of multiparametric sensing devices. In this work, an amperometric biosensor array for simultaneous determination of ethanol, formate, D- and L-lactate is presented. Enzyme immobilization on platinum thin-film electrodes was realized by chemical cross-linking with glutaraldehyde. The optimization of the sensor performance was investigated with regard to enzyme loading, glutaraldehyde concentration, pH, cofactor concentration and temperature. Under optimal working conditions (potassium phosphate buffer with pH 7.5, 2.5 mM NAD^+, 2.0 mM $Fe(CN)_6^{3-}$, 25 °C and 0.4% glutaraldehyde) the linear working range and sensitivity of the four sensor elements was improved. Simultaneous and cross-talk free measurements of four different metabolic parameters were performed successfully. The reliable analytical performance of the biosensor array was demonstrated by application in a clarified sample of inoculum sludge. Thereby, a promising approach for on-site monitoring of fermentation processes is provided.

4.1 Introduction

In the course of ongoing and rapid development of novel biosensing technologies, the construction of multiparametric biosensors has become the next logical step for fast determination of several analytes [1]. Such devices for simultaneous measurement of various species are of great interest for the application in biotechnological [2], biomedical [3, 4], environmental [5] and industrial fields [6]. In this context, the monitoring of parameters such as ethanol, lactate and formate is, for example, important for the control of fermentation processes. The determination of ethanol is also relevant in clinical analysis of human body fluids. Lactate, as a key metabolite, is important in metabolism and serves, for example, as freshness indicator in the food processing industry [7]. Formate is also an important intermediate in aerobic and anaerobic fermentation processes. Currently, conventional methods for analyses of these compounds are performed by spectrophotometry, gas chromatography and high-performance liquid chromatography [8, 9]. These techniques are expensive, laborious, time-consuming and often require extensive sample pre-treatment. In this regard, enzyme-based biosensors are an attractive alternative. Due to their versatility, they fulfill the requirements for multi-analyte detection by rapid, sensitive and selective monitoring features.

Amperometric enzyme-based biosensors rely often on the catalytic activity of an oxidase or dehydrogenase. However, most of the devices reported in literature, that are capable of simultaneous measurement, operate with oxidases. A potential drawback in using oxidases for biosensor development, is the low specifity of these enzymes and their cross-talk tendencies. Therefore, application of dehydrogenases in biosensor arrays seems feasible, despite the requirement of the cofactor NAD^+. More than 250 NAD^+-dependent dehydrogenases are known [10] and thus, a huge potential for the development of further biosensors is provided. Numerous examples of dehydrogenase-based sensors for detection of ethanol [11], formate [12], D-lactate [13] and L-lactate [14] have been recently described. However, reports on integration of multiple dehydrogenases into

a single sensing device are rare. Miertuš *et al.* have used solid binding matrices for the development of two multi-biosensors for simultaneous amperometric detection of glucose, fructose and ethanol with one of the systems, and L-lactate, L-malate and sulfite with the other [15]. The enzyme electrodes were modified with both oxidases and dehydrogenases, according to the analyte and the associated detection principle.

Recently, we have reported on the development of an amperometric multi-parameter sensor chip for simultaneous detection of formate, D- and L-lactate in biogas processes [16]. The detection principle is based on a two-enzyme system, consisting of a dehydrogenase and a diaphorase [17]. In a first step, the substrate (formate, D- and L-lactate, respectively) is converted to a product (CO_2 or pyruvate), as presented in reaction (Eq. 4.1). This reaction is catalyzed by a specific dehydrogenase (formate dehydrogenase, D- and L-lactate dehydrogenase, respectively). Thereby, the cofactor NAD^+ is reduced to NADH.

$$\text{Substrate} + \text{NAD}^+ \xrightarrow{\text{Dehydrogenase}} \text{Product} + \text{NADH} \tag{4.1}$$

In a second enzymatic reaction, the released NADH is regenerated by a diaphorase and the reduction of the cofactor $Fe(CN)_6{}^{3-}$ to $Fe(CN)_6{}^{4-}$ (Eq. 4.2).

$$\text{Fe(CN)}_6{}^{3-} + \text{NADH} \xrightarrow{\text{Diaphorase}} \text{Fe(CN)}_6{}^{4-} + \text{NAD}^+ \tag{4.2}$$

Amperometric detection of the substrate concentration is realized by anodic oxidation of $Fe(CN)_6{}^{4-}$ at +0.3 V *vs.* Ag/AgCl according to the following reaction (Eq. 4.3).

$$\text{Fe(CN)}_6{}^{4-} \xrightarrow{\text{Oxidation}} \text{Fe(CN)}_6{}^{3-} + \text{e}^- \tag{4.3}$$

The focus of the present study is the improvement of a multi-parametric biosensor array for simultaneous determination of ethanol, formate, D- and L-lactate using various specific dehydrogenases. The performance of the biosensor array was optimized with regard to enzyme loading, concentration of cross-linking agent, pH, cofactor concentration and temperature. Compatibility of four different sensing elements, integrated within one biosensor array, was investigated by parallel amperometric measurement.

4.2 Experimental

4.2.1 Chemicals and reagents

Alcohol dehydrogenase EC 1.1.1.1 from *Saccharomyces cerevisiae* (ADH, 310 U mg^{-1}), diaphorase EC 1.8.1.4 (also known as dihydrolipoyl dehydrogenase) from *Clostridium kluyveri* (DIA, 51 U mg^{-1}), D-lactate dehydrogenase EC 1.1.1.28 from *Lactobacillus leichmanii* (D-LDH, 213 U mg^{-1}) and L-lactate dehydrogenase EC 1.1.1.27 from *Bacillus stearothermophilus* (L-LDH, 174.5 U mg^{-1}) were obtained from Sigma-Aldrich. Formate dehydrogenase EC 1.2.1.2 from *Candida boidinii* (FDH, 0.49 U mg^{-1}) was purchased from Roche Diagnostics GmbH. Bovine serum albumin (BSA), glutaraldehyde solution (25%), glycerol, $Fe(CN)_6{}^{3-}$, sodium D-lactate and ethanol standard solution were supplied by Sigma-Aldrich, too. Sodium formate, sodium L-lactate and β-nicotinamide adenine dinucleotide (NAD^+) were from AppliChem GmbH. The buffer components K_2HPO_4,

KH_2PO_4, Tris, HCl and H_2SO_4 were bought from Roth. Ethanol, formate, D- and L-lactate assay kits used for comparative purposes were purchased from Megazyme International Ireland.

Stock solutions of ADH, FDH, D-LDH and L-LDH were prepared in 100 mM potassium phosphate buffer (pH 7.5). The DIA solution contained additionally 0.5 mM flavin adenine dinucleotide (FAD). In order to fabricate sensors with reproducible enzyme loadings, the activity of the different enzyme solutions was determined photometrically (Ultrospec 2100 pro, Amersham Biosciences). For this reason, the dehydrogenase activity of ADH, FDH, D-LDH and L-LDH was measured by monitoring the NADH production at 340 nm [18, 19]. The DIA activity was evaluated by following the decrease in NADH absorbance, using $Fe(CN)_6^{3-}$ as substrate [20]. The indicated enzyme loadings (activity in Units per electrode) refer to 1.5 µL of immobilization mixture applied to each electrode.

4.2.2 Sensor preparation

The biosensor array chips ($10 \times 10\,mm^2$), each consisting of five platinum thin-film working electrodes, were fabricated from a p-Si wafer by photolithographic techniques. Fig. 4.1 shows an image of the multi-parameter biosensor with different enzyme membranes immobilized on each working electrode. Detailed description of the fabrication process was provided earlier [16]. In this work, the sensor chips were additionally modified by spin-coating a 20 µm passivation layer of SU-8 photo resist (SU-8 25, micro resist technology GmbH) [21]. Prior enzyme immobilization, the biosensor surface was electrochemically pretreated in 0.5 M H_2SO_4 by applying an anodic current of +2.0 V *vs.* Ag/AgCl for 2 min. Afterwards, potential cycling between −0.2 V and +1.4 V at a scan rate of $100\,mV\,s^{-1}$ was performed until reproducible voltammograms were obtained [22].

The various enzyme membranes of the biosensor array were constructed by chemical cross-linking using glutaraldehyde 4 vol% (prepared with 10 vol% glycerol). Thereby, enzyme solutions with defined activity of the particular dehydrogenase and DIA (total volume 4 µL were mixed with 0.5 µL BSA 24%. Finally, 1.5 µL of glutaraldehyde were added and mixed carefully. For adjustment of enzyme loading or glutaraldehyde concentration in the immobilization matrix, solutions were diluted appropriately. For simultaneous measurements an additional blank electrode without catalytic activity was utilized. In this case, 4.5 µL BSA 1.3% were mixed with 1.5 µL glutaraldehyde (1.2 vol%). In each case, the electrode surface was modified by drop-coating 1.5 µL of a

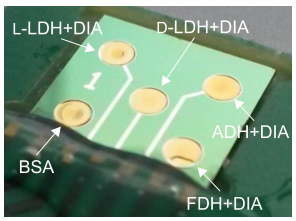

Fig. 4.1: Multi-parameter biosensor chip (10×10 mm^2) with five working electrodes, each modified by immobilization of different enzymes (L-LDH+DIA, D-LDH+DIA, ADH+DIA and FDH+DIA). One electrode without enzymatic activity (only BSA) is serving as a reference.

particular immobilization mixture. The electrodes were dried overnight and stored at 4 °C when not in use.

4.2.3 Apparatus and measurement

Amperometric measurements and cyclic voltammetry were executed by using a potentiostat (PalmSens, Palm Instruments BV) in combination with an eight-channel multiplexer (MUX8, Palm Instruments BV). Experiments were performed in a three-electrode setup, consisting of a platinum counter electrode (diameter 7.5 mm), a double junction Ag/AgCl reference electrode (Metrohm, 3 M KCl) and a biosensor array chip with five platinum working electrodes (diameter each 2 mm). The measurement cell was equipped with a magnetic stir bar (200 rpm) and a working potential of +300 mV *vs.* Ag/AgCl was applied to the working electrodes [16]. Optimization of the working conditions was carried out in 12 mL potassium phosphate buffer (100 mM, pH 7.5) with various concentrations of $Fe(CN)_6^{3-}$ (0.1–6.0 mM), NAD^+ (0.1–4.0 mM) and glutaraldehyde (0.2–1.0%), in the presence of 1.0 mM of each analyte. For investigation of the effect of the temperature on the sensor signal, the temperature was varied in the range of 15 to 50 °C. The pH value of the measurement solution was optimized by using 100 mM potassium phosphate buffer (pH 6.0–8.0) and 100 mM Tris-HCl buffer (pH 8.0–10.0), respectively. For practical reasons, the effect of the enzyme loading on the sensor response was analyzed for each analyte separately. Calibration curves for the characterization of the optimized sensor performance were generated by successive addition of various volumes of a multi-component stock solution with a concentration of 40 mM of each analyte.

The sensor signal was defined as the change in current response. Thereby, the signal was normalized to the maximum obtained average current change, presented as relative sensor signal. All experiments were performed in three replicates and error bars indicate the standard deviations.

4.2.4 Application to real samples

An inoculum sludge for a biogas fermentation process was used to evaluate the biosensor performance in real samples. Details about preparation of the sample were provided elsewhere [16]. As a reference method an established commercial enzymatic kit for photometric determination of ethanol, formate, D- and L-lactate was used, following the manufacturer‘s instructions. For both measurement techniques samples were diluted accordingly with distilled water to enable analysis in the linear detection range.

4.3 Results and discussion

4.3.1 Optimization of enzyme loading

In a first step, experiments were carried out in order to investigate the effect of different enzyme loadings on the sensor signal. For this reason, a series of biosensors were prepared with various loadings of dehydrogenase and DIA, maintaining constant temperature, buffer composition and glutaraldehyde concentration. The enzyme amount of the

formate sensor was not yet optimized. In this case, the broader variation of enzyme ratio was impractical because of the low specific activity of the FDH. Viscous enzyme solutions used for the immobilization, resulted in fast cross-linking reactions and thereby, the formation of homogeneous enzyme membranes was hindered. Therefore, for further experiments with the formate electrode an ideal enzyme loading of 1.5 U FDH and 1.0 U DIA was selected.

Figure 4.2 shows the influence of various enzyme ratios on the sensor response of the D-lactate, L-lactate and ethanol sensor. For each instance, the dehydrogenase loading was varied and a particular constant amount of DIA was used (Fig. 4.2a-c). The results show that the signal of all three sensors increased with increasing dehydrogenase concentration. However, in each case the sensor signal reached a plateau. Maximum sensor response was obtained with 0.5 U D-LDH, 0.75 U L-LDH and 7.5 U ADH, respectively. Afterwards, these dehydrogenase loadings were used and kept constant, while varying the DIA loading in the range from 0.5 to 3.0 U per membrane (Fig. 4.2d-f). Similarly, the signal response increased with increasing DIA amount. Reaching a saturation of the relative sensor, at some point an increasement of the DIA loading did not improve the sensor reponse significantly. Enzyme loadings of 0.5 U D-LDH/2.5 U DIA, 0.75 U L-LDH/3.0 U DIA and 7.5 U ADH/2.0 U DIA were sufficient for maximum sensor performance and used for further experiments. These enzyme mixtures correspond to a *dehydrogenase/DIA* ratio of 0.2, 0.25 and 3.75 for D-lactate, L-lactate and ethanol, respectively. The requirement of a higher dehydrogenase loading

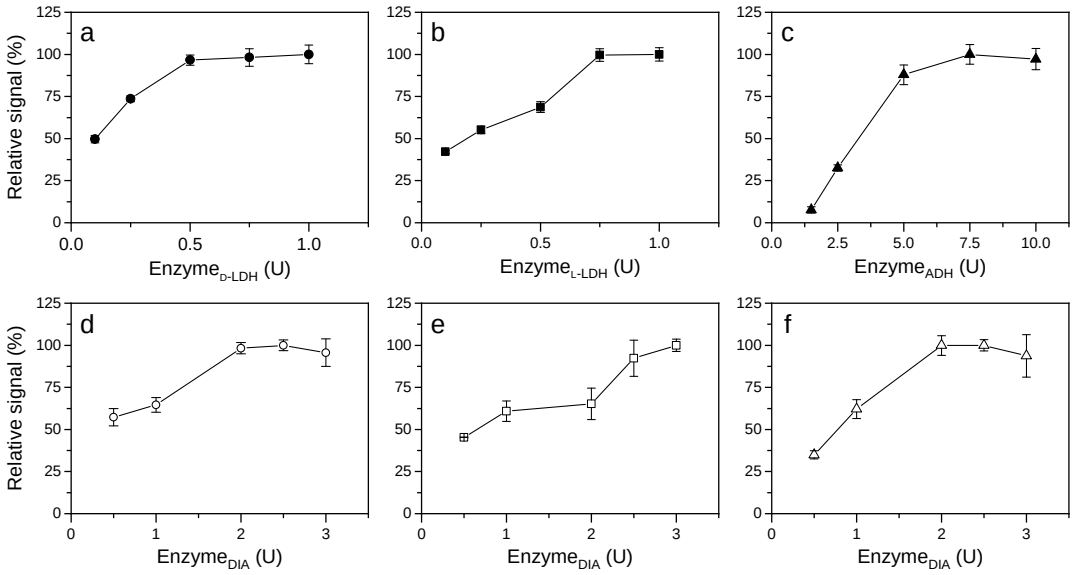

Fig. 4.2: Effect of enzyme loadings on the sensor response of the D-lactate, L-lactate and ethanol sensor. Closed symbols represent variation of dehydrogenase loading at constant diaphorase loading (**a:** 2.5 U DIA ●, **b:** 3.0 U DIA ■, **c:** 2.0 U DIA ▲) and open symbols represent variation of diaphorase loading at constant dehydrogenase amount (**d:** 0.5 U D-LDH ❍, **e:** 0.75 U L-LDH ❑, **f:** 7.5 U ADH △). Experiment carried out in 100 mM potassium phosphate buffer (pH 7.5, 2.0 mM $Fe(CN)_6^{3-}$, 2.5 mM NAD^+, 1.0 mM of each analyte) at 25 °C with 0.4% glutaraldehyde in the enzyme membrane.

on the ethanol electrode might be caused by a lower immobilization efficiency or changes in the conformational structure of ADH after glutaraldehyde treatment [23, 24]. Similar observations were made by immobilization of ADH on gold electrodes. Thereby, best sensor response was obtained at 0.5% glutaraldehyde, whereas at concentrations of 2.0 and 5.0% no sensor signal was recorded [25].

4.3.2 Optimization of glutaraldehyde concentration

Chemical cross-linking of enzymes with glutaraldehyde has been a popular technique, due to its simplicity and versatility [26]. However, the harsh treatment might inhibit the catalytic activity and thus, also the biosensor performance. The relationship of the glutaraldehyde concentration on the sensor signal of the ethanol, D- and L-lactate sensor is depicted in Fig. 4.3. Maximum sensor response was obtained at

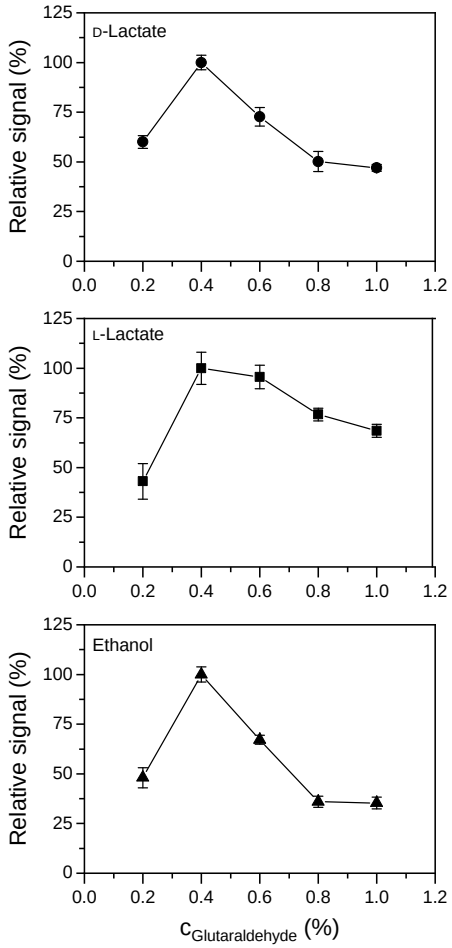

Fig. 4.3: Influence of glutaraldehyde concentration on sensor signal of the D-lactate, L-lactate and ethanol electrode. Experiments carried out in 100 mM phosphate buffer (pH 7.5, 2.0 mM $Fe(CN)_6^{3-}$, 2.5 mM NAD^+ and 1.0 mM of each analyte) at 25 °C with an enzyme loading of 0.5 U D-LDH/2.5 U DIA ●, 0.75 U L-LDH/3.0 U DIA ■ and 7.5 U ADH/2.0 U DIA ▲.

0.4% glutaraldehyde. At higher concentrations all of the three sensors showed a similar trend; with increasing concentration of the cross-linking agent the sensor signal decreased. However, the performance of the ethanol sensor was more affected by higher glutaraldehyde concentrations than the L-lactate sensor. For 1% glutaraldehyde the ethanol sensor exhibited 35% of the maximum signal, whereas the L-lactate sensor worked with 68%. These findings indicate that ADH is more susceptible to the immobilization with the cross-linking agent glutaraldehyde [23]. As mentioned before, this might explain the higher ADH loading (7.5 U) in comparison to both lactate sensors (0.5 U and 0.75 U for D- and L-lactate, respectively). Lower concentrations of glutaraldehyde (0.2%) were not sufficient for stable enzyme immobilization (data not shown). Membranes prepared with this amount of glutaraldehyde were characterized by a lower sensor response and a shorter life-time. Overall, for the presented immobilization conditions an optimal concentration of 0.4% glutaraldehyde for enzyme cross-linking was selected for further experiments with each sensor.

4.3.3 Optimization of buffer solution

The working conditions were also optimized in regard to pH and cofactor loadings. As presented in Fig. 4.4, for investigation of optimal pH value, the biosensor array was studied in potassium phosphate buffer (pH 6–8) and Tris-HCl buffer (pH 8–10). Both of the lactate sensors exhibited maximum signal response at pH 7.5. This optimum pH

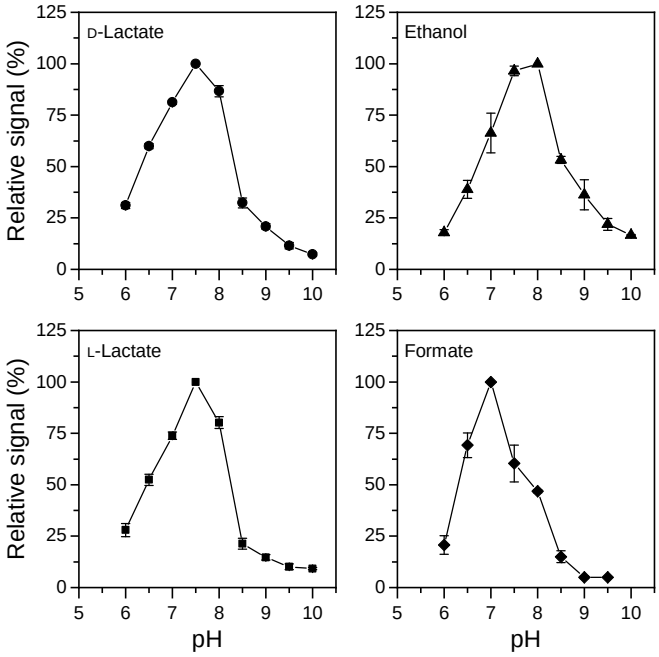

Fig. 4.4: Influence of pH on the sensor response of the D-lactate, L-lactate, ethanol and formate electrode. Experiments carried out at 25 °C in 2.0 mM, 2.5 mM NAD^+ and 1.0 mM of each analyte and with an enzyme loading of 0.5 U D-LDH/2.5 U DIA ●, 0.75 U L-LDH/3.0 U DIA ■, 7.5 U ADH/2.0 U DIA ▲, 0.75 U U FDH/1.0 U U DIA ◆.

is in agreement with values reported for lactate biosensors [20, 27]. For the ethanol and formate sensor the highest signal was obtained at pH 8.0 and 7.0, respectively. Similar values were reported in the literature [12, 28]. Simultaneous measurements for all four analytes were therefore performed at pH 7.5, representing a compromise between the requirement of the four different sensor elements.

The influence of the cofactor concentration on the sensor response is exemplarily shown for the D-lactate sensor in Fig. 4.5. Cofactor loading of NAD^+ was varied from 0.1 to 4.0 mM with a constant $Fe(CN)_6^{3-}$ concentration of 2.0 mM. The amperometric response increased with increasing amount of NAD^+, reaching a plateau for 2.5 mM. Higher concentrations did not further improve the sensor signal. Similarly, the effect of the $Fe(CN)_6^{3-}$ loading was evaluated by varying the concentration from 0.1 to 6.0 mM at constant 2.5 mM NAD^+ (Fig. 4.5b). The sensor signal increased with increasing $Fe(CN)_6^{3-}$ concentration up to 2.0 mM, above this value no further change in the current response was observed due to saturation of the sensor. For subsequent experiments an optimal cofactor loading of 2.5 mM NAD^+ and 2.0 mM $Fe(CN)_6^{3-}$ was chosen.

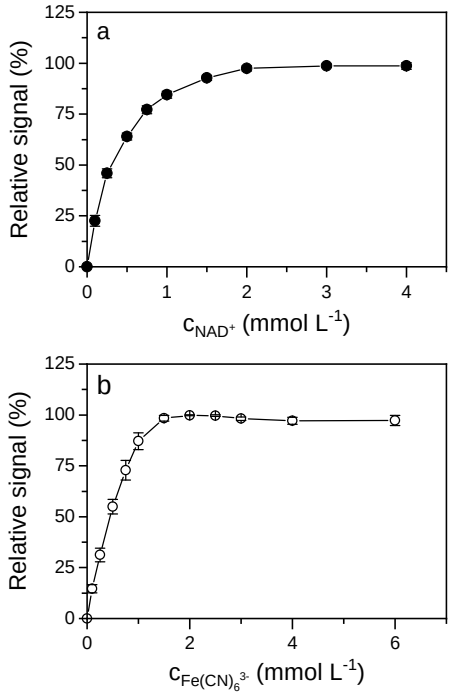

Fig. 4.5: Determination of optimal cofactor loadings of NAD^+ **(a)** and $Fe(CN)_6^{3-}$ **(b)** for the D-lactate sensor. Experiment carried out in potassium phosphate buffer (100 mM, pH 7.5) at 25 °C in the presence of 1.0 mM D-lactate with an enzyme loading of 0.5 U D-LDH/2.5 U DIA, immobilized with 0.4% glutaraldehyde.

4.3.4 Effect of temperature

The catalytic activity of enzymes mainly depends on the temperature, therefore, also the effect of the temperature on the sensor response was investigated. Experiments

were carried out from 15 to 50 °C under optimized conditions (Fig. 4.6). The highest amperometric response was obtained at 30 °C for the D-lactate, ethanol and formate sensor. Similar optimal temperatures were reported for various dehydrogenase-based biosensors [29, 30]. For higher temperatures the signal of both the D-lactate and formate sensor decreased rapidly. The response of the ethanol sensor was less impaired by higher temperatures. This was also the case for the L-lactate sensor, showing highest response at temperatures around 45 °C. The high optimum temperature of L-LDH seems reasonable, since this recombinantly expressed enzyme was primary isolated from the thermophil microorganism *Bacillus stearothermophilus*. Nevertheless, a temperature of 25 °C was used for further experiments, due to the improved operational stability.

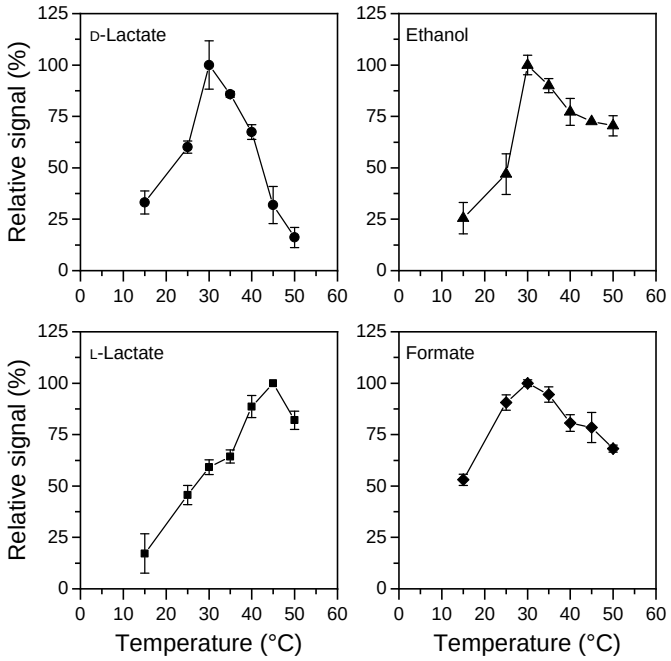

Fig. 4.6: Effect of temperature on the sensor response of the D-lactate, L-lactate, ethanol and formate electrode. Experiments carried out in 100 mM potassium phosphate buffer (pH 7.5, 2.0 mM $Fe(CN)_6^{3-}$, 2.5 mM NAD^+ and 1.0 mM of each analyte) with an enzyme loading of 0.5 U D-LDH/2.5 U DIA ●, 0.75 U L-LDH/3.0 U DIA ■, 7.5 U ADH/2.0 U DIA ▲, 0.75 U FDH/1.0 U DIA ◆ and 0.4% glutaraldehyde.

4.3.5 Characterization of the sensor performance

The characteristics of the individual sensor elements are summarized in Tab. 4.1. A linear relationship between analyte concentration and current response was obtained in the range of 0.004 to 2.5 mM for D-lactate, 0.002 to 2.0 mM for L-lactate, 0.002 to 1.5 mM for ethanol and 0.02 up to 3.0 mM for formate. Thereby, a sensitivity in the range of 20.5 to 37.2 $\mu A\,mM^{-1}\,cm^{-2}$, depending on the analyte, was achieved. The applied optimization procedure resulted in a broader linear detection range, as well as an increased sensitivity. In the first approach of the biosensor array, a linear detection

Tab. 4.1: Characteristics of the optimized biosensor array. Calibration conducted simultaneously at 25 °C in 100 mM potassium phosphate buffer (pH 7.5, 2.0 mM $Fe(CN)_6^{3-}$, 2.5 mM NAD^+).

	D-Lactate	L-Lactate	Ethanol	Formate
Linear range (mM)	0.004–2.5	0.002–2.0	0.002–1.5	0.02–3.0
Sensitivity ($\mu A\,mM^{-1}\,cm^{-2}$)	28.4 ± 0.9	37.2 ± 2.0	35.7 ± 1.1	20.5 ± 0.5
Limit of detection (S/N=3) (µM)	0.9	0.7	0.7	1.3
Response time τ_{95} (s)	∼45	∼35	∼38	∼85
Working stability* (%)	80	75	72	54

* remaining signal after 15 subsequent measurements

range from 0.1 to 1.0 mM with a sensitivity of 13.4 and 17.5 $\mu A\,mM^{-1}\,cm^{-2}$ for the D- and L-lactate sensor, respectively, was reported [16]. After optimization of the enzyme loading, glutaraldehyde concentration, pH, cofactor loading and temperature, the sensors exhibited more twice as high sensitivity, while covering a broader linear range. Furthermore, the sensor array was extended by integration of an additional ethanol sensor. The response time to reach 95% of the steady-state current, varied for the different analytes from 35 to 85 s. These values correspond to typical time ranges reported for enzyme-based biosensors [14, 31]. Generally, differences in the response time are mainly attributable to diverse diffusion conditions of each analyte-specific enzyme membrane. The different enzyme loadings on each of these membranes influence the membrane thickness and permeability and thus, the diffusion properties. In this regard, the longest response time displayed by the formate sensing electrode (85 s) might be explained by the low specific activity of FDH. In this case, a high protein loading was required to establish the desired enzyme loading, resulting in a rather thick and dense membrane. The formate sensor also showed the lowest working stability, remaining 54% signal response after 15 subsequent measurements (Tab. 4.1). The stability of the formate electrode could be improved by application of a more gentle immobilization procedure compared to the rather harsh treatment with glutaraldehyde.

4.3.6 Evaluation of the sensor performance

The modification of the biosensor array with different sensing elements enables simultaneous determination of four analytes by the same detection principle. Thereby, an attractive approach for facile and rapid monitoring is presented by the proposed biosensor array. In Fig. 4.7, an example of a multi-parametric measurement is shown, realized by successive addition of stock solutions of D-lactate, L-lactate, ethanol and formate. In case of the analyte D-lactate, only for the electrode with an D-LDH/DIA membrane, a change in the current response was observed. Neither the BSA blank electrode, nor the three other electrodes showed a significant increase in the sensor signal. After stepwise addition of the other analytes (L-lactate, ethanol and formate, respectively), for each instance only the corresponding electrode with the specific immobilized dehydrogenase reacted with change in the current reponse. These results indicate that no cross-talk existed between the different electrodes. The potential for simultaneous measurement is demonstrated by subsequent addition of a multi-component stock solution. In this

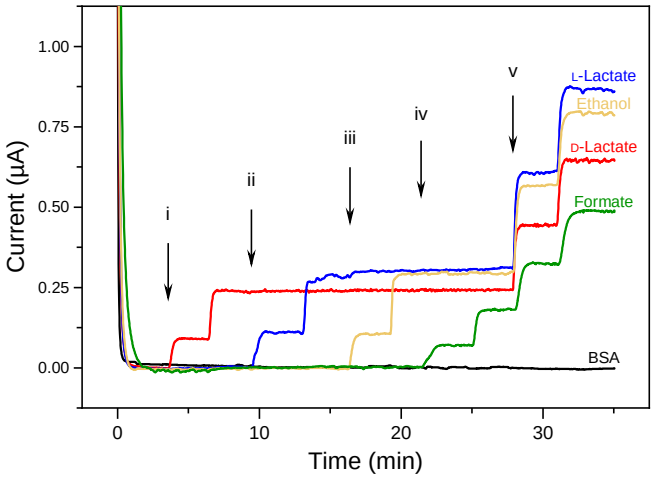

Fig. 4.7: Simultaneous measurement with the multi-parameter biosensor array operated in potassium phosphate buffer (100 mM, pH 7.5, 2.5 mM NAD^+, 2.0 mM $Fe(CN)_6^{3-}$). Cross-talk free response of each electrode is demonstrated by successive addition of single-analyte stock solutions. Arrows indicate point of insertion of (i) D-lactate, (ii) L-lactate, (iii) ethanol, (iv) formate (each 0.1 and 0.25 mM, respectively) and (v) multi-component stock solution (0.5 and 0.75 mM for each analyte). A membrane with immobilized BSA served as a reference.

case, all of the electrodes, except for the reference membrane with BSA, respond in an increase of the current signal. In comparison to a previously reported biosensor array [16], an additional ethanol sensor was integrated into this biosensor array. The applied extension distinctly improved the potential application of the biosensor for multi-analyte detection in fermentation-related processes. The proposed biosensor system was used for preliminary experiments for determination of ethanol, formate, D-lactate and L-lactate in

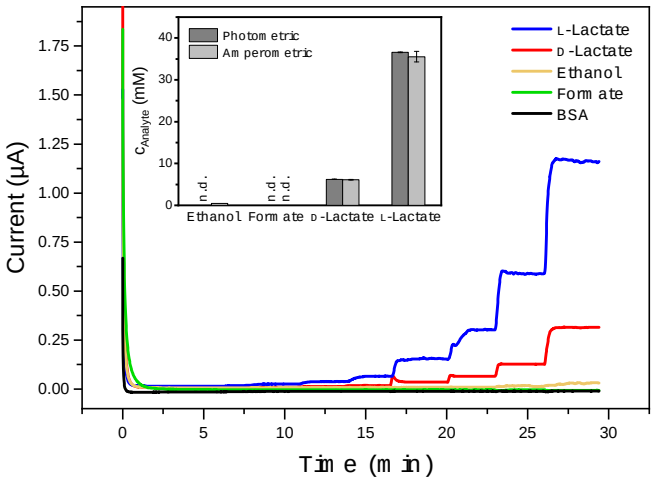

Fig. 4.8: Application of the multi-parametric biosensor array for simultaneous determination of ethanol, formate, D- and L-lactate in an clarified inoculum sample. Inset: Comparison of results obtained by amperometric and photometric detection (n.d.: not detectable).

a clarified inoculum sample (used as a starter culture for biogas plants). Figure 4.8 shows exemplarily a simultaneous measurement with the biosensor array by successive addition of a real sample. The constant signal of the BSA reference proves that the proposed sensor system is free from sample effects. Concentrations of ethanol and formate in the sample solution were probably below the lower detection limit of both techniques applied and therefore, could not be detected. Overall, results obtained by amperometric detection are in good agreement with the photometric reference measurement (inset of Fig. 4.8), supporting the potential of the biosensor array for simple and reliable analysis of different analytes. In comparison to the applied photometric reference measurement, the biosensor array enables also a reusable, faster and less laborious measurement system due to the simultaneous mode of operation.

4.4 Conclusion

The development of an amperometric biosensor array for simultaneous measurement of four analytes has been demonstrated. The sensor performance was optimized in terms of the enzyme loading, cross-linking procedure, pH, cofactor concentration and temperature. Thereby, the linear working range and sensitivity for detection of ethanol, formate, D- and L-lactate were improved. Rapid, cross-talk free and simultaneous analysis of these compounds was successfully realized.

In the future, measurements in real samples of fermentative processes are to be performed, where the proposed multi-parameter biosensor device can be applied for the on-site monitoring of key parameters in fermentation plants.

Acknowledgements

This work was supported by the German Federal Ministry of Food and Agriculture (BMEL) and the Agency of Renewable Resources (FNR) [grant number 22006613]. The authors gratefully thank H. Iken for fabrication of platinum sensors and K. Mariano for technical support.

References

[1] Misiakos, K.; Kakabakos, S.E. (2002) International workshop on multi-analyte biosensing devices, 13–14 April, 2000. *Biosens. Bioelectron.* 17(4):vii–viii, doi:10.1016/S0956-5663(01)00299-8.

[2] Bäcker, M.; Delle, L.; Poghossian, A; Biselli, M; Zang, W.; Wagner, P.; Schöning, M.J. (2011) Electrochemical sensor array for bioprocess monitoring. *Electrochim. Acta* 56:9673–9678, doi:10.1016/j.electacta.2011.04.030.

[3] Rocchitta, G.; Spanu, A.; Babudieri, S.; Latte, G.; Madeddu, G.; Galleri, G.; Nuvoli, S.; Bagella, P.; Demartis, M.I.; Fiore, V.; Manetti, R.; Serra, P.A. (2016) Enzyme biosensors for biomedical applications: Strategies for safeguarding analytical performances in biological fluids. *Sensors* 16(6):1–21, doi:10.3390/s16060780.

[4] Zhang, X.; Ju, H.; Wang, J. (2008) Electrochemical sensors, biosensors and their biomedical applications. Amsterdam: *Academic Press*.

[5] Rodriguez-Mozaz, S.; Lopez de Alda, M.J.; Marco, M.-P.; Barcelo, D. (2005) Biosensors for environmental monitoring: A global perspective. *Talanta* 65(2):291–297, doi:10.1016/j.talanta.2004.07.006.

[6] Prodromidis, Mamas I.; Karayannis, Miltiades I. (2002) Enzyme based amperometric biosensors for food analysis. *Electroanal.* 14:241–264, doi:10.1002/1521-4109(200202)14:4%3C241::AID-ELAN241%3E3.0.CO;2-P

[7] Rassaei, L.; Olthuis, W.; Tsujimura, S.; Sudhölter, E.J.R.; van den Berg, A. (2014) Lactate biosensors: Current status and outlook. *Anal. Bioanal. Chem.* 406:123–137, doi:10.1007/s00216-013-7307-1.

[8] Lai, B.; Plan, M.; Hodson, M.; Krömer, J. (2016) Simultaneous determination of sugars, carboxylates, alcohols and aldehydes from fermentations by high performance liquid chromatography. *Fermentation* 2(1):6, doi:10.3390/fermentation2010006.

[9] Doyon, G.; Gaudreau, G.; St-Gelais, D.; Beaulieu, Y.; Randall, C.J. (1991) Simultaneous HPLC determination of organic acids, sugars and alcohols. *Can. Inst. Sci. Technol. J.* 24:87–94, doi:10.1016/S0315-5463(91)70025-4.

[10] Wijayawardhana, C.A.; Halsall, H.B.; Heineman, W.R. (2002) Electrochemical Immunoassay. In: Bard, A.J. (Ed.) Encyclopedia of Electrochemistry. Weinheim: *Wiley-VCH*, doi:10.1002/9783527610426.bard090005.

[11] Santos, A.S.; Pereira, A.C.; Durán, N.; Kubota, L.T. (2006) Amperometric biosensor for ethanol based on co-immobilization of alcohol dehydrogenase and Meldola's Blue on multi-wall carbon nanotube. *Electrochim. Acta* 5(1):215–220, doi:10.1016/j.electacta.2006.04.060.

[12] Mak, K.K.W.; Wollenberger, U.; Scheller, F.W.; Renneberg, R. (2003) An amperometric bi-enzyme sensor for determination of formate using cofactor regeneration. *Biosens. Bioelectron.* 18:1095–1100, doi:10.1016/S0956-5663(02)00245-2.

[13] Avramescu, A.; Noguer, T.; Magearu, V. Marty, J.-L. (2001) Chronoamperometric determination of D-lactate using screen-printed enzyme electrodes. *Anal. Chim. Acta* 433(1):81–88, doi:10.1016/S0003-2670(00)01386-6.

[14] Rathee, K.; Dhull, V.; Dhull, R.; Singh, S. (2016) Biosensors based on electrochemical lactate detection: A comprehensive review. *Biochem. Biophys. Rep.* 5:35–54, doi:10.1016/j.bbrep.2015.11.010.

[15] Miertuš, S.; Katrlík, Ja.; Pizzariello, A.; Stred'anský, M.; Švitel, J.; Švorc, J. (1998) Amperometric biosensors based on solid binding matrices applied in food quality monitoring. *Biosens. Bioelectron.* 13:911–923, doi:10.1016/S0956-5663(98)00063-3.

[16] Pilas, J.; Iken, H.; Selmer, T.; Schöning, M.J. (2015) Development of a multiparameter sensor chip for the simultaneous detection of organic compounds in biogas processes. *Phys. Status Sol. A* 212:1306–1312, doi:10.1002/pssa.201431894.

[17] Comtat, M.; Galy, M.; Goulas, P.; Souppe, J. (1988) Amperometric bien-

zyme electrode for L-carnitine. *Anal. Chim. Acta* 208:295–300, doi:10.1016/S0003-2670(00)80759-X.

[18] Walker, J.R.L. (1992) Spectrophotometric determination of enzyme activity: Alcohol dehydrogenase (ADH). *Biochem. Educ.* 20(1):42–43, doi:10.1016/0307-4412(92)90021-D.

[19] Höpner, T.; Knappe, J. (1970) Formate Dehydrogenase. In: Bergmeyer, H.-U. (Ed.) Methods of Enzymatic Analysis. New York: *Academic Press.*

[20] Antiochia, R.; Cass, A.E.G.; Palleschi, G. (1997) Purification and sensor applications of an oxygen insensitive, thermophilic diaphorase. *Anal. Chim. Acta* 345:17–28, doi:10.1016/S0003-2670(96)00618-6.

[21] Kirchner, P.; Reisert, S.; Pütz, P.; Keusgen, M.; Schöning, M.J. (2012) Characterisation of polymeric materials as passivation layer for calorimetric H_2O_2 gas sensors. *Phys. Status Sol. A* 209(5):859–863, doi:10.1002/pssa.201100773.

[22] Swain, G.M. (2007) Solid Electrode Materials: Pretreatment and Activation. In: Zoski, C.G. (Ed.) Handbook of Electrochemistry. Amsterdam: *Elsevier*, doi:10.1016/B978-044451958-0.50006-9.

[23] Barry, S.; Griffin, T.; Johnson, D.B. (1978) Yeast alcohol dehydrogenase immobilized on sepharose derivatives by non-specific adsorption followed by cross-linkage with glutaraldehyde. *Int. J. Biochem.* 9:289–292, doi:10.1016/0020-711X(78)90012-5.

[24] Mateo, C.; Palomo, J.M.; van Langen, L.M.; van Rantwijk, F.; Sheldon, R.A. (2004) A new, mild cross-linking methodology to prepare cross-linked enzyme aggregates. *Biotechnol. Bioeng.* 86:273–276, doi:10.1002/bit.20033.

[25] Miyamoto, S.; Murakami, T.; Saito, A.; Kimura, J. (1991) Development of an amperometric alcohol sensor based on immobilized alcohol dehydrogenase and entrapped NAD^+. *Biosens. Bioelectron.* 6:563–567, doi:10.1016/0956-5663(91)80020-X.

[26] Migneault, I.; Dartiguenave, C.; Bertrand, M.J.; Waldron, K.C. (2004) Glutaraldehyde: Behavior in aqueous solution, reaction with proteins, and application to enzyme crosslinking. *BioTechniques* 37(5):790–802, doi:10.2144/04375RV01.

[27] Kwan, R.C.H.; Hon, P.Y.T.; Mak, K.K.W.; Renneberg, R. (2004) Amperometric determination of lactate with novel trienzyme/poly(carbamoyl) sulfonate hydrogel-based sensor. *Biosens. Bioelectron.* 19:1745–1752, doi:10.1016/j.bios.2004.01.008.

[28] Tsai, Y.C.; Huang, J.D.; Chiu, C.C. (2007) Amperometric ethanol biosensor based on poly(vinyl alcohol)-multiwalled carbon nanotube-alcohol dehydrogenase biocomposite. *Biosens. Bioelectron.* 22:3051–3056, doi:10.1016/j.bios.2007.01.005.

[29] Montagné, M.; Erdmann, H.; Comtat, M.; Marty, J.-L.(1995) Comparison of the performances of two bi-enzymatic sensors for the detection of D-lactate. *Sens. Actuators B Chem.* 26-27:440–443, doi:10.1016/0925-4005(94)01636-V.

[30] Samphao, A.; Kunpatee, K.; Prayoonpokarach, S.; Wittayakun, J.; Švorc, L.; Stankovic, D.M.; Zagar, K.; Ceh, M.; Kalcher, K. (2015) An ethanol biosensor based

on simple immobilization of alcohol dehydrogenase on Fe_3O_4@Au nanoparticles. *Electroanal.* 27:2829–2837, doi:10.1002/elan.201500315.

[31] Lobo, M.J.; Miranda, A.J.; Tuñón, P. (1997) Amperometric biosensors based on NAD(P)-dependent dehydrogenase enzymes. *Electroanal.* 9(3):191–202, doi:10.1002/elan.1140090302.

4.5 Supplementary information

After successful application and optimization of the DIA-based detection principle for the simultaneous measurement of ethanol, formate, D- and L-lactate, this approach has been further evaluated with a different NAD^+-dependent dehydrogenase. In this regard, three biosensors have been developed for the amperometric detection of L-malate, fumarate and L-aspartate. The results were published in the journal *Appl. Biochem. Biotechnol.*[1] and the contribution to this publication comprised the technical support in the amperometric measurement procedure, sensor preparation and immobilization of enzymes.

Figure 4.9 shows the detection principle of the three electrochemical biosensors, which are all based on a malate-specific dehydrogenase from porcine heart (MDH, EC 1.1.1.37) combined with a DIA. Stepwise expansion of the malate-sensing platform with the enzymes fumarate hydratase from porcine heart (FH, EC 4.2.1.2) and aspartate ammonia-lyase from *Escherichia coli* (ASPA, EC 4.3.1.1), resulted in multi-enzyme reaction cascades for the measurement of fumarate and aspartate.

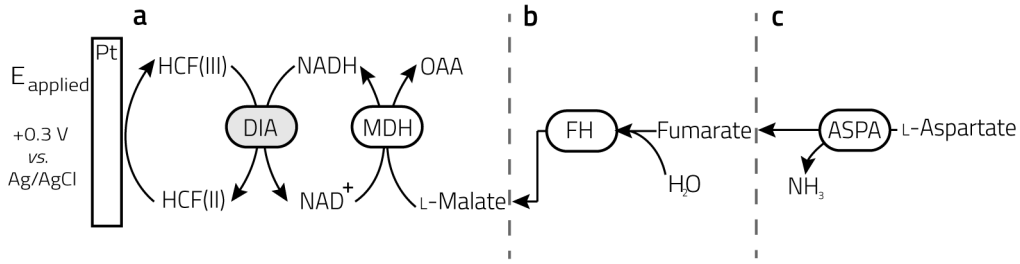

Fig. 4.9: Detection principle for the three amperometric biosensors. Illustration of the enzymatic reactions used for the electrochemical detection of L-malate **(a)**, fumarate **(b)**, and L-aspartate **(c)**. Aspartate ammonia-lyase (ASPA) catalyzes the deamination of L-aspartate into fumarate and NH_3. Hydration of the former to malate is catalyzed by fumarate hydratase (FH). The released malate is oxidized to oxaloacetate (OAA) by a malate dehydrogenase (MDH) using reduction of NAD^+ to NADH. Diaphorase (DIA) regenerates NAD^+ by reduction of $Fe(CN)_6^{3-}$ [HCF(III), hexacyanoferrate(III)] to $Fe(CN)_6^{4-}$ [HCF(II), hexacyanoferrate(II)] (reprinted with permission from D.L. Röhlen *et al.*[1] (Copyright 2017, Springer Nature)).

Similarly to the optimization procedure described in Ch. 4, the optimal measurement conditions were defined by adjustment of the cofactor concentrations (NAD^+, $Fe(CN)_6^{3-}$), buffer pH, and immobilization procedure in terms of the applied GA concentration. The optimized sensor performances were characterized by a linear working range between 1 to 10 mM for the aspartate sensor and up to 3 mM for the L-malate and fumarate electrodes, respectively. Thereby, sensitivities of 0.7, 0.4 and 0.09 µA mM^{-1} were obtained for the L-malate, fumarate and L-aspartate biosensors, respectively. The corresponding linear calibration curves are depicted in Fig. 4.10. These findings demonstrated the versatility of the amperometric detection system, which can easily be employed with other NAD^+-dependent dehydrogenases. Thereby, a powerful

[1] Röhlen, D.L.; **Pilas, J.**; Schöning, M.J.; Selmer, T. (2017) Development of an amperometric biosensor platform for the combined determination of L-malic, fumaric, and L-aspartic acid. *Appl. Biochem. Biotechnol.* 183:566–581, doi:10.1007/s12010-017-2578-1.

tool for the development of biosensors is provided, that are applicable for a wide range of substrates.

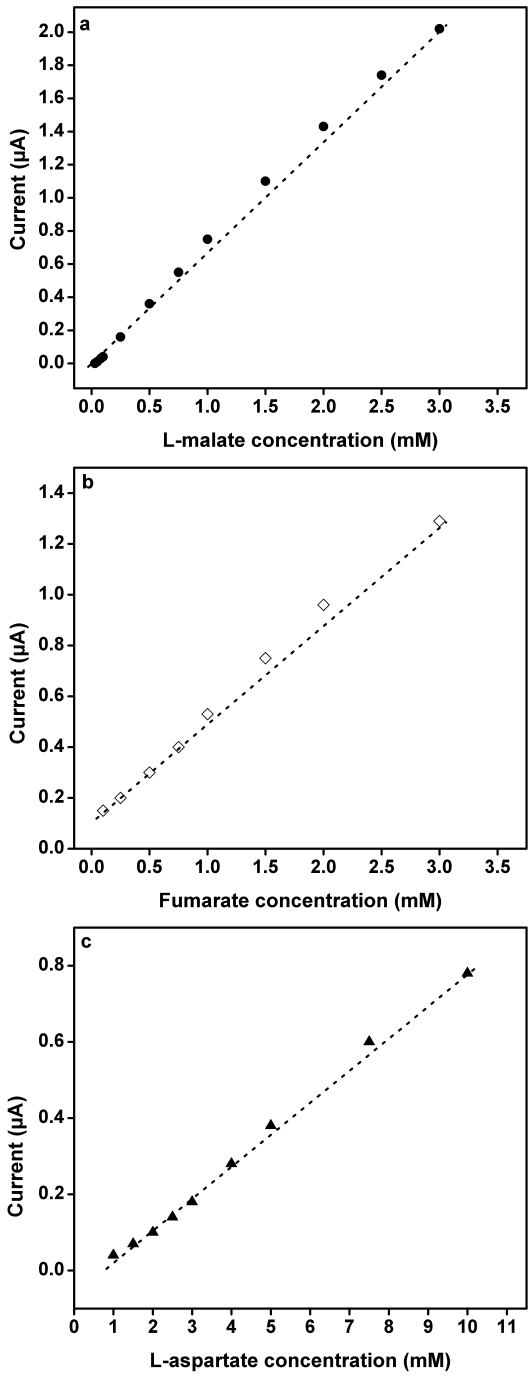

Fig. 4.10: Linear calibration curves of the three biosensors for the detection of L-malate **(a)**, fumarate **(b)**, and L-aspartate **(c)** (reprinted with permission from D.L. Röhlen *et al.*[1] (Copyright 2017, Springer Nature)).

5 Application of a portable multi-analyte biosensor for organic acid determination in silage

Sensors (2018), 18(5):1470, 1–12

J. Pilas[1,2], Y. Yazici[1], T. Selmer[1], M. Keusgen[2] and M.J. Schöning[1,3]

[1] Institute of Nano- and Biotechnologies (INB), FH Aachen, Jülich, Germany
[2] Institute of Pharmaceutical Chemistry, Philipps-Universität Marburg, Marburg, Germany
[3] Institute of Complex Systems 8 (ICS-8), Forschungszentrum Jülich, Jülich, Germany

Submitted: 03-01-2018; Accepted: 05-03-2018; Published: 05-08-2018

https://doi.org/10.3390/s18051470

Keywords: biosensor, ethanol, formate, D-/L-lactate, multi-analyte, silage

Abstract

Multi-analyte biosensors may offer the opportunity to perform cost-effective and rapid analysis with reduced sample volume, as compared to electrochemical biosensing of each analyte individually. This work describes the development of an enzyme-based biosensor system for multi-parametric determination of four different organic acids. The biosensor array comprises five working electrodes for simultaneous sensing of ethanol, formate, D-lactate, and L-lactate, and an integrated counter electrode. Storage stability of the biosensor was evaluated under different conditions (stored at +4 °C in buffer solution and dry at −21 °C, +4 °C, and room temperature) over a period of 140 days. After repeated and regular application, the individual sensing electrodes exhibited the best stability when stored at −21 °C. Furthermore, measurements in silage samples (maize- and sugarcane silage) were conducted with the portable biosensor system. Comparison with a conventional photometric technique demonstrated successful employment for rapid monitoring of complex media.

5.1 Introduction

Ethanol, formate, and lactate, existing in two isoforms (D- and L-lactate) are biological components with remarkable relevance in the clinical, food, environmental, and bioprocess industries. For medical surveillance, the levels of L-lactate and ethanol in human fluids (blood, serum, saliva, sweat, etc.) are of great interest, particularly in sports medicine [1] and for the evaluation of pathological conditions [2, 3]. In mammalian cells, predominantly L-lactate is present, whereas D-lactate is mainly produced by microorganisms as an important intermediate or end-product in various metabolic pathways. Since ethanol as well as D- and L-lactate play a significant role in the alcohol, lactic, and malolactic fermentation processes, they serve as a valuable indicator for monitoring the freshness and quality of food products and beverages [4, 5]. Formate is another relevant metabolite in many aerobic and anaerobic bacteria, with central significance in the methanogenic cascade [6, 7]. In order to enable efficient operation of anaerobic digestors, feedstock with constant quality and composition are required. In this regard, silage preparation is an established method for preservation and storage of organic material. In anaerobic environments, different fermentation pathways occur, which are dominated by lactic acid-producing bacteria [8]. For successful control of ensiling or other fermentation processes, therefore, continuous monitoring of different intermediates (like ethanol, formate, D-lactate, and L-lactate) is mandatory. The most common analytical techniques for quantification of these analytes are high-performance liquid chromatography [9, 10], gas chromatography [11], and UV-VIS spectrophotometry. These methods generally possess high accuracy and sensitivity, but also may be associated with some potential drawbacks. For example, in some cases the expensive and advanced instruments require laborious sample pretreatment procedures for elimination of interfering substances and particles. These characteristics result in time-consuming and delayed analyses that are rather unsuited for real-time and on-site monitoring. In this regard, electrochemical biosensor arrays may provide an attractive and competitive alternative due to their selectivity and potential for miniaturization. Integration of

several analyte-specific electrodes within an array enables construction of portable hand-held devices for monitoring purposes [12, 13]. Although multitudinous electrochemical enzyme-based biosensors are described for detection of ethanol [14, 15], formate [16, 17], D-lactate, and L-lactate [18, 19] individually, so far only few efforts have been described for combined analysis of these or other substrates [5, 20, 21].

We have recently reported on the development and extensive optimization of different enzyme-based biosensor arrays for the parallel determination of several analytes [22, 23]. The combination of different dehydrogenases and a diaphorase, required for the amperometric detection principle and regeneration of the cofactor nicotinamide adenine dinucleotide (NAD) [24, 25], allowed construction of electrochemical multiparametric biosensors. The optimal working conditions and immobilization parameters were identified, resulting in improved sensor performance. There are several examples of economically successful biosensors [26], that are mostly designed as single-use and disposable devices, such as sensors for monitoring blood glucose levels of diabetic patients. From an operational point of view, however, reusable applicability is preferable, especially when costly biological materials are used as sensing elements. The stability of enzyme-based biosensors mainly depends on the activity of the employed proteins. For this reason, lot of research has been devoted to the immobilization procedure in order to extend the long-term applications [27, 28].

The main objective of this work was to evaluate the capability of a multi-analyte biosensor for multiple usage in complex media from fermentation processes. For this reason, the storage stability under different conditions was investigated. A potential application as a portable sensor system for simultaneous determination of ethanol, formate, D-lactate, and L-lactate was demonstrated in pretreated samples of silage.

5.2 Material and methods

5.2.1 Chemicals and reagents

The enzymes alcohol dehydrogenase (ADH, Enzyme Commission number (EC) 1.1.1.1, 310 $\mathrm{U\,mg^{-1}}$) from *Saccharomyces cerevisiae*, formate dehydrogenase (FDH, EC 1.2.1.2, 0.49 $\mathrm{U\,mg^{-1}}$) from *Candida boidinii*, L-lactate dehydrogenase (L-LDH, EC 1.1.1.27, 174.5 $\mathrm{U\,mg^{-1}}$) from *Bacillus stearothermophilus*, D-lactate dehydrogenase (D-LDH, EC 1.1.1.28, 213 $\mathrm{U\,mg^{-1}}$) from *Lactobacillus leichmanii*, and diaphorase (DIA, EC 1.8.1.4, 51 $\mathrm{U\,mg^{-1}}$) from *Clostridium kluyveri* were purchased from Sigma-Aldrich (St. Louis, MO, USA). Bovine serum albumin (BSA), glutaraldehyde solution (GA) (25% in H_2O, glycerol, potassium ferricyanide ($K_3[Fe(CN)_6]$), sodium D-lactate, and ethanol standard solution were also supplied by Sigma-Aldrich. Sodium formate, sodium L-lactate, and the cofactor nicotinamide adenine dinucleotide (NAD^+) were obtained from AppliChem (Darmstadt, Germany). Potassium phosphate buffer (K_2HPO_4, KH_2PO_4) and H_2SO_4 were from Carl Roth GmbH & Co. KG (Karlsruhe, Germany).

All reagents were of analytical grade and were prepared in deionized water. Enzymatic stock solutions (ADH, DIA, FDH, D-LDH and L-LDH, respectively) were prepared in 0.1 M potassium phosphate buffer (pH 7.5). The DIA solution was supplemented with 0.5 mM flavin adenine dinucleotide.

5.2.2 Sensor fabrication and design

For simultaneous amperometric detection of several substrates, the multi-analyte biosensor chip ($14 \times 14\,mm^2$) features five circular working electrodes (each Ø 2 mm) and a rectangular counter electrode ($40.5\,mm^2$). The schematic steps for thin-film fabrication of the biosensor are depicted in Fig. 5.1a [21]. Firstly, a 500-nm-thick layer of SiO_2 was grown onto a p-type silicon wafer (Ø 3 inch) by thermal wet oxidation at 1000 °C for 30 min. Deposition of photoresist AZ5214E (MicroChemicals GmbH, Ulm, Germany) was achieved by spin-coating at 4000 rpm for 30 s. A photolithographic step was used for patterning of the sensor layout by application of a custom-made mask and exposure of the photoresist film for 7.5 s at $8\,mW\,cm^{-2}$. The photoresist film was then developed using developer AZ 326 MIF (micro resist technology GmbH, Berlin, Germany). Afterwards, electron beam evaporation was used for the deposition of 20 nm of titanium (Ti) as an adhesion layer and a 200-nm-thick layer of platinum(Pt). The Pt/Ti electrodes were patterned through a lift-off process in dimethyl sulfoxide (DMSO) using ultrasonication. For passivation, an epoxy-based photoresist (SU-8 25, micro resist technology GmbH, Berlin, Germany) was spin-coated onto the wafer for 30 s at 1500 rpm, resulting in a 20-µm-thick layer [29, 30]. A soft-bake process was used (9 min at 95 °C) for evaporation of the solvent. Initial cross-linking of the photoresist was then realized by exposure for 25 s at a wavelength of 356 nm. Following, a post-exposure bake step was performed for 4 min at 95 °C. The counter electrode, working electrodes, and contact pads were re-opened by development of the photoresist with the developer mr-Dev 600 (micro resist technology GmbH, Berlin, Germany). Finally, the wafer was

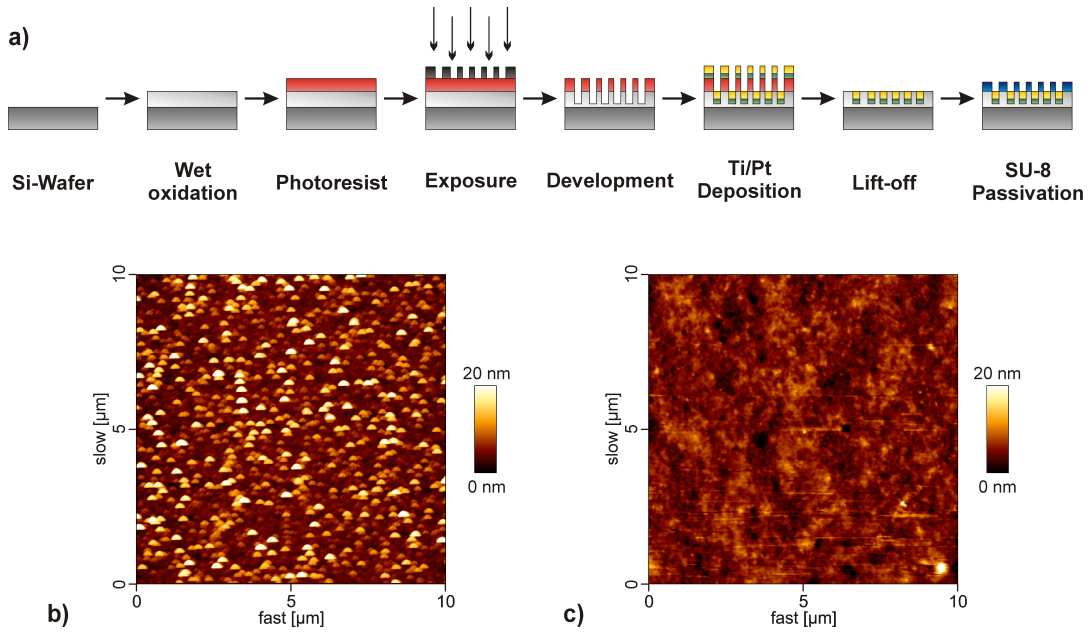

Fig. 5.1: Schematic process flow for fabrication of the silicon-based multi-analyte biosensor chip **(a)**. Atomic force microscopy images ($10 \times 10\,\mu m^2$) of the blank platinum electrode **(b)** and the sensor surface after immobilization of D-lactate dehydrogenase (D-LDH) and diaphorase (DIA) **(c)**.

diced into 16 single chips. Each chip was then cleaned and glued onto printed circuit boards and an electrical connection was established by ultrasonic wedge bonding with an AlSi bonding wire (Heraeus, Hanau, Germany). As presented in Fig. 5.1b,c, the sensor morphology was characterized by atomic force microscopy (BioMat Workstation, JPK Instruments, Berlin, Germany) in tapping mode. The roughness of the surface after enzyme immobilization was comparable to that of the blank platinum electrode (4.4 nm). The close-up view in Fig. 5.2 shows an image of the completed biosensor.

5.2.3 Sensor preparation and measurement set-up

The multi-analyte biosensor was constructed by modification of each working electrode with a different analyte-specific dehydrogenase. Prior the immobilization process, the platinum surface was cleaned electrochemically in 0.5 M H_2SO_4 [22, 31]. The enzymes were immobilized by chemical cross-linking with glutaraldehyde. This procedure was selected due to its simplicity and flexibility, which enables facile and low-cost immobilization of the different enzymes required for the biosensor array. Detailed description of the individual enzyme loading on each working electrode can be found elsewhere [22]. Briefly, for each working electrode an individual mixture was prepared, consisting of BSA, DIA, and the particular dehydrogenase (ADH, FDH, D-LDH, and L-LDH, respectively). Each solution was then carefully mixed with 2.4 vol% glutaraldehyde (with 10 vol% glycerol) and a volume of 1.5 µL was applied on the working electrode. One working electrode was functionalized only with the inert protein BSA, serving as a reference without catalytic activity. Passivation of the sensor chip with SU-8 promoted homogeneous distribution of the enzymatic solutions within the entire area of the working electrode. After drying overnight in the fridge, the enzyme membranes were stable and ready to use.

Electrochemical measurements were performed in a conventional three-electrode set-up with a three-dimensional (3D)-printed chip holder made of composite material (ZP 151, 3D Systems GmbH, Darmstadt, Germany). Figure 5.2 shows an exploded view of the custom-made measurement cell, which provides facile electrical connection of the biosensor and miniaturized Ag/AgCl reference electrode (Sensolytics GmbH, Bochum, Germany). Simultaneous measurement of five electrodes was realized by application of a compact potentiostat EmStat3 with an integrated 16-channel multiplexer MUX16 (PalmSens BV, Houten, The Netherlands). Thereby, the working electrodes are constantly polarized by sharing a common reference and on-chip integrated counter electrode. The applied working potential was set to +0.3 V *vs.* the Ag/AgCl reference electrode for anodic oxidation of enzymatically produced $K_4[Fe(CN)_6]$. Sensor calibration and sample analysis were performed at room temperature in 2.0 mL of measurement solution (0.1 M potassium phosphate buffer, pH 7.5, with 2.5 mM NAD^+ and 2.0 mM $K_3[Fe(CN)_6]$). For a fast and homogeneous distribution of the sample solution, a magnetic stir bar was used. These conditions represent the optimal working environment for the multi-analyte biosensor [22]. In comparison to a previously developed biosensor chip [22], the novel sensor design with the integrated counter electrode facilitates the miniaturization of the measurement set-up, resulting in reduced sample volume.

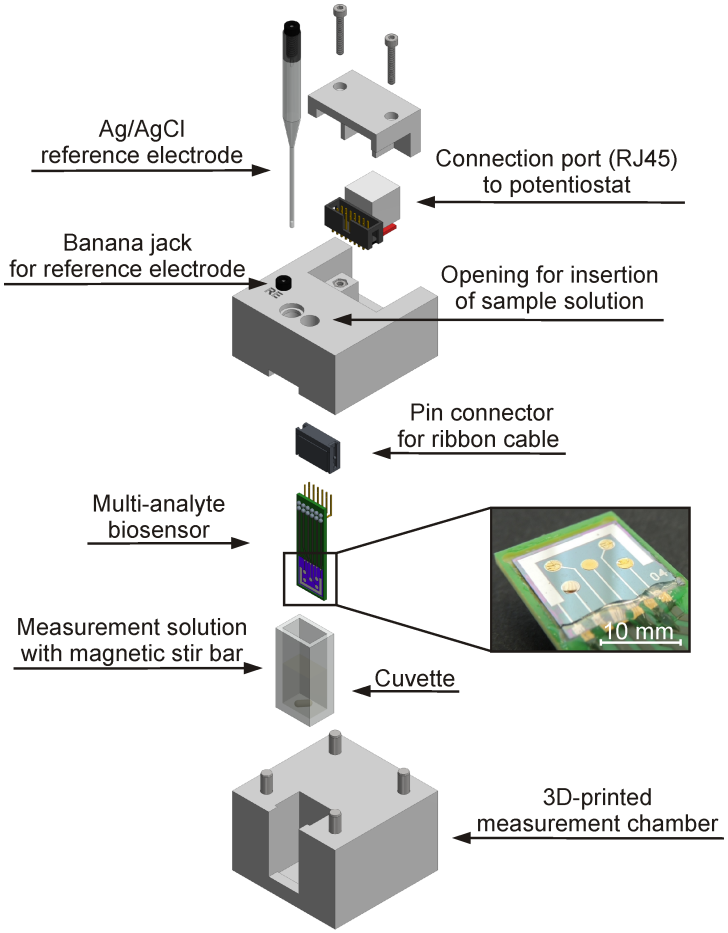

Fig. 5.2: Explosion drawing of the compact three-dimensional (3D)-printed measurement set-up ($60 \times 60 \times 70\,\mathrm{mm}^3$) for facile application of the multi-analyte biosensor. Close-up shows biosensor chip ($14 \times 14\,\mathrm{mm}^2$) with five working electrodes and an integrated counter electrode, incorporated into a printed circuit board, with immobilized enzyme membranes on the working electrodes.

5.2.4 Sample preparation and analysis

Samples of maize- and sugarcane silage were used for demonstration of applicability of the biosensor. Since liquid and clear sample solutions are required, especially for the reference measurement (photometric analysis), a pretreatment according to Carrez clarification was performed [24, 32]. For this reason, 10 g (wet weight) of feedstock were incubated in 100 mL of deionized water for 30 min. Then, 15 mL of this solution were mixed with 3 mL Carrez I (0.68 mM $K_4[Fe(CN)_6] \cdot 3\,H_2O$) and 3 mL Carrez II (2 mM $ZnCl_2$). After incubation for 5 min, the solution was neutralized by addition of 7.5 mL NaOH (0.4 mM) and 1.5 mL H_2O. This mixture was centrifuged for 20 min at 7500 rpm and the particle-free supernatant was used for further analysis.

Prior to sample analysis, a calibration of the biosensor was performed by successive addition of a multi-analyte stock solution (40 mM of each analyte) and recording of the

corresponding increase in current signal. The biosensor was then washed with potassium phosphate buffer (0.1 mM, pH 7.5) and used for determination of organic acids in real samples. Defined volumes of sample solution were added to the measurement solution in order to generate different dilutions. Based on the obtained calibration curves and the dilution factor of the sample, the concentration of each analyte was calculated (defined as weight of analyte per wet weight of silage). Reference analytics were performed with commercial photometric kits following the manufacturer's instructions (Megazyme International, Wicklow, Ireland).

5.3 Results and discussion

5.3.1 Simultaneous measurement procedure

Integration of several analyte-specific working electrodes that rely on the same detection principle within one biosensor chip facilitates the construction of multi-analyte systems. In this work, different NAD^+-dependent dehydrogenases were used for simultaneous determination of ethanol, formate, D-lactate, and L-lactate at the same applied working potential. Figure 5.3 shows the method of simultaneous operation for detection of different analytes. Multi-analyte assays in particular depend on appropriate substrate specificity in order to exclude potential interferences. The cross-talk free performance of the developed biosensor is demonstrated by successive addition of each analyte separately. It becomes obvious that only the corresponding electrode reacts with an increase in the current signal when the analyte is present in the measurement solution. Furthermore, the blank signal (BSA electrode) remains constant throughout the measurement. This sensor characteristic allows the simultaneous quantification of several analytes within a shorter analysis time compared to the single detection of each substrate.

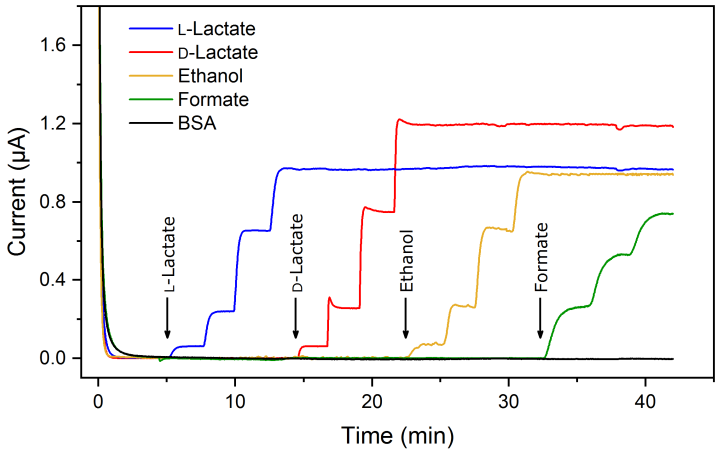

Fig. 5.3: Chronoamperometric current responses of the multi-analyte biosensor to successive addition of single analyte stock solutions (L-lactate, D-lactate, ethanol, and formate) in 100 mM potassium phosphate buffer (pH 7.5). A working electrode with immobilized bovine serum albumin (BSA) served as a blank signal.

5.3.2 Evaluation of storage stability

The storage stability of any biosensor is an important aspect when it comes to the requirement of long-term applications [27]. The decisive factor in this context is the immobilization of the biological component with ideally minimum enzyme leakage and denaturation. Stability of the multi-analyte biosensor was examined by storage under dry conditions at −21 °C, +4 °C, and room temperature, as well as immersion in buffer solution at +4 °C (0.1 mM potassium phosphate buffer, pH 7.5). The response to 1 mM of each analyte (ethanol, formate, D-lactate, and L-lactate, respectively) was investigated regularly for a period of 20 weeks. After each measurement the sensors were washed with phosphate buffer (0.1 M, pH 7.5) and stored under the particular conditions until further use. In Fig. 5.4a the results are exemplarily presented for the D-lactate-sensing electrode. During the first four weeks of storage, there was a sharp decline in the sensor response for all storing conditions tested. Subsequently, the signal decreased gradually and between weeks 7 and 20 the obtained current remained almost stable. The D-lactate electrode retained 53% of its initial signal after more than 4 months

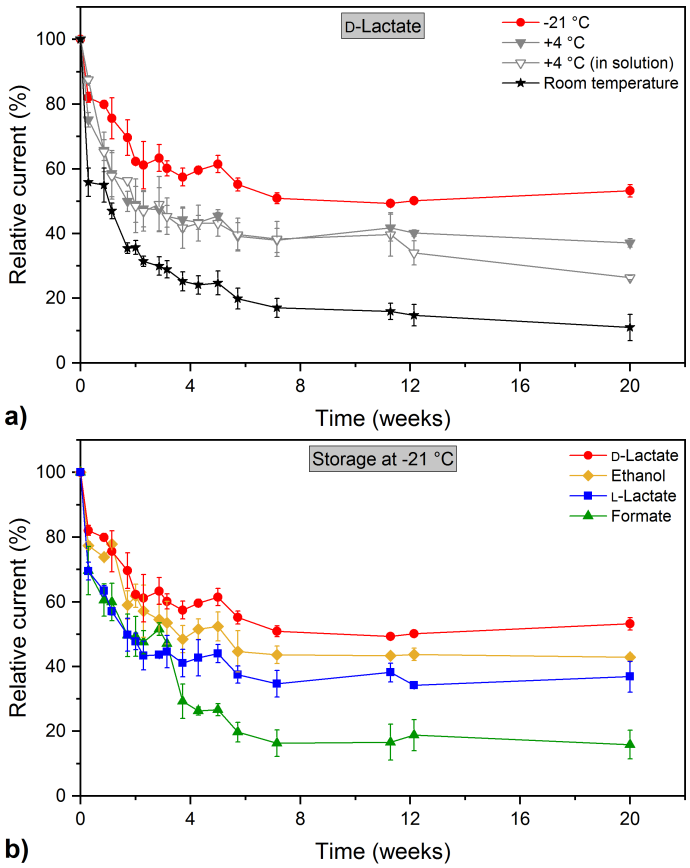

Fig. 5.4: (a) Relative current signal as a function of storage time of the D-lactate-sensing electrode in the presence of 1 mM D-lactate in different storage conditions (−21 °C, +4 °C, +4 °C in buffer solution and room temperature, respectively); **(b)** Storage stability of the multi-analyte biosensor stored in a freezer at −21 °C for a period of 20 weeks ($n = 3$ sensors).

of intermittent application when stored at −21 °C. Storage in the fridge at +4 °C resulted in 37% of original response (dry state) and 26% (in solution), respectively. At ambient temperatures the D-lactate electrode exhibited the greatest decrease in sensor response (11%), indicating that storing the sensor under this condition is not suitable for long-term applications.

The storage stability at −21 °C of the individual electrodes of the multi-analyte biosensor is depicted in Fig. 5.4b. Within the first 7 weeks the relative response of the different electrodes declined rapidly. Thereafter, the overall sensor performance did not change significantly. The biosensor showed good stability and maintained 43% and 37% of its initial response after 140 days for the ethanol and L-lactate electrode, respectively. The formate electrode was the least stable, characterized with 16% of original maximum obtained current at the end of investigation. Despite the repeated freezing and thawing, which is known to be harmful for enzyme stability [33, 34], storage at −21 °C proved to be best for preservation of the sensor stability. The L-lactate electrode was the only one which showed improved stability after storage at +4 °C in buffer solution (see Tab. 5.1). These findings may be associated with the applied L-LDH from *B. stearothermophilus*, which is probably less stable at freezing temperatures. An overview of different enzyme-based biosensors and the characteristics of their storage stability is summarized in Tab. 5.1. Hereby, stability is defined as storage time t_{L50} necessary for the initial sensor response to decrease by 50% [35]. In most of these studies the biosensors were stored at +4 °C in buffer solution and exhibited under this condition similar stability over several days or weeks in comparison to the multi-analyte biosensor stored at −21 °C. The stability of enzyme-based biosensors is particularly influenced by the applied procedure for immobilization of the biological component. More gentle immobilization treatments than cross-linking with glutaraldehyde can facilitate long-term storage for up to 5 months at room temperature [36].

Although the individual electrodes of the multi-analyte biosensor showed different characteristics in their storage stability, the overall capability of long-term and multiple usage was demonstrated successfully. For practical applications, however, a recalibration of the biosensor is mandatory due to steady decrease in sensor response.

Tab. 5.1: Comparison of the storage stability of various enzyme-based biosensors (d: day; m: month; SHL: salicylate hydroxylase; POx: pyruvate oxidase; PCS: poly(carbamoyl)sulfonate; PVA: polyvinyl alcohol; MWCNT: multiwalled carbon nanotube).

Analyte	Enzymes	Detection	Immobilization	Stability t_{L50}	Storage	Reference
D-Lactate	D-LDH	Toluidine blue O	Carbon paste	<30 d	4 °C	[37]
D-Lactate	D-LDH+DIA	$Fe(CN)_6^{4-}$	Entrapment	40 d	4 °C in buffer	[25]
D-Lactate	D-LDH+DIA	$Fe(CN)_6^{4-}$	Glutaraldehyde	50 d	−21 °C	This work
L-Lactate	L-LDH+SHL+POx	O_2 consumption	PCS hydrogel	11 d	4 °C in buffer	[38]
L-Lactate	L-LDH+DIA	$Fe(CN)_6^{4-}$	Graphite powder	>5 m	RT, sealed	[36]
L-Lactate	L-LDH+DIA	$Fe(CN)_6^{4-}$	Glutaraldehyde	40 d	4 °C in buffer	This work
L-Lactate	L-LDH+DIA	$Fe(CN)_6^{4-}$	Glutaraldehyde	14 d	−21 °C	This work
Ethanol	ADH	Toluidine blue O	Glutaraldehyde	20 d	4 °C in buffer	[39]
Ethanol	ADH	NADH	Glutaraldehyde	35 d	−20 °C	[40]
Ethanol	ADH	NADH	PVA–MWCNT	7 d	4 °C in buffer	[41]
Ethanol	ADH+DIA	$Fe(CN)_6^{4-}$	Glutaraldehyde	22 d	−21 °C	This work
Formate	FDH+SHL	O_2 consumption	PVA matrix	10 d	23 °C	[17]
Formate	FDH+DIA	$Fe(CN)_6^{4-}$	Glutaraldehyde	20 d	−21 °C	This work

5.3.3 Measurement of organic acids in silage

The developed multi-analyte biosensor system was used for determination of the organic acid concentration in two different silage samples, namely maize- and sugarcane. These energy crops are typical feedstocks used for biogas production from renewable resources [42, 43]. Since the methane yield during the fermentation process is mainly influenced by the composition of the applied substrate, systematic and regular characterization of the silage is of huge importance for an efficient conversion of organic material to biogas [44–46]. The amount of organic acids was also measured with a commercial reference technique. This method likewise is based on an enzymatic detection principle (spectrophotometric analysis of NADH increase at a wavelength of 340 nm). However, in this case each analyte has to be quantified separately, resulting in a more time-consuming and laborious analysis procedure. Table 5.2 and Fig. 5.5 illustrate the concentrations obtained by both analytical methods. The results demonstrate a good correlation ($R^2 = 0.998$) between the two techniques for all four analytes with an apparent recovery in the range of 93.7 to 109.3% [47]. Although sometimes values greater than 100% were obtained, overall the multi-analyte biosensor provides the advantage of facile and simultaneous determination of several analytes in complex media in comparison to the photometric analysis. The particular sensor characteristics of each electrode of the multi-analyte array have been extensively optimized in earlier studies [22]. Detection of formate and D-lactate was performed with a sensitivity of 20.5 and 28.4 $\mu A\,mM^{-1}\,cm^{-2}$, respectively. The ethanol and L-lactate electrodes were characterized by slightly higher sensitivities (35.7 and 37.2 $\mu A\,mM^{-1}\,cm^{-2}$, respectively). Based on a signal-to-noise ratio of 3, the limit of detection (LOD) for ethanol, L-lactate, and D-lactate was 0.7, 0.7, and 0.9 µM, respectively. The obtained values for the LOD for these three electrodes (ethanol, D-lactate, and L-lactate) were in a similar or better range in comparison to other enzyme-based biosensors reported for the detection of ethanol [14], D-lactate, and L-lactate [19]. These sensor characteristics enabled successful quantification of

Tab. 5.2: Determination of organic acids in silage samples using two different analytical techniques (BD: below the lower detection limit). The apparent recovery was defined as the observed value/reference value.

Sample	Analyte	Photometric kit ($g\,kg^{-1}$)	Multi-analyte biosensor ($g\,kg^{-1}$)	Apparent recovery (%)
Maize silage	D-Lactate	7.73 ± 0.06	7.83 ± 0.07	101.3
	L-Lactate	5.74 ± 0.03	5.54 ± 0.13	96.5
	Ethanol	6.96 ± 0.79	6.52 ± 0.06	93.7
	Formate	0.27 ± 0.03	0.30 ± 0.04	109.3
Sugarcane silage	D-Lactate	0.29 ± 0.05	0.30 ± 0.03	103.5
	L-Lactate	0.28 ± 0.01	0.25 ± 0.07	106.2
	Ethanol	9.20 ± 0.78	9.51 ± 0.36	103.3
	Formate	BD	BD	-

several organic acids in silage samples. However, no formate was detectable in the sugarcane silage, probably because the concentration of this acid was below the LOD of the corresponding formate electrode (LOD = 1.3 µM). In literature, various enzyme-based formate biosensors are described, which utilize a different detection principle. Electrocatalytic oxidation of NADH on a glassy carbon electrode, modified with 3,4-dihydroxybenzaldehyde and FDH, allowed formate sensing with a LOD of 50 µM [16]. A detection limit of 0.198 µM was realized by combination of FDH with a salicylate hydroxylase for monitoring the enzymatic oxygen consumption with a Clark electrode [17]. When it comes to the development of biosensors, consideration of the intended field of application and required sensor performances is also of great interest. For the analysis of the acid composition in silage samples, typically concentrations below the micromolar range are not of great importance, because they will not influence the biogas fermentation process. In this regard, the presented characteristics of the developed multi-analyte biosensor system meet the requirements for the desired application, and compared to single biosensors for individual analyte detection, the array configuration permits a faster analysis.

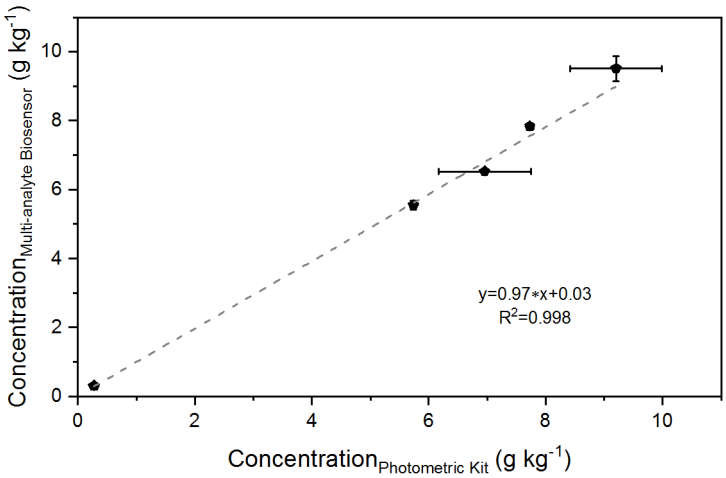

Fig. 5.5: Comparison between the organic acid concentrations (ethanol, formate, D-lactate, and L-lactate) obtained by the amperometric and photometric method.

5.4 Conclusions

Within this study, a multi-analyte biosensor system for the detection of four different organic acids is introduced. Simultaneous and cross-talk free measurements of ethanol, formate, D-lactate, and L-lactate were realized by immobilization of analyte-specific enzymes on each working electrode. The storage stability of the presented biosensor array was investigated at different storage conditions for a period of 20 weeks. For this reason, sensors were stored in buffer solution at +4 °C and dry at −21 °C, +4 °C, and room temperature, respectively. Storing at −21 °C proved to be the best storage option, although repeated freezing and thawing affected each sensor element differently. With almost 53% of the initial activity after 140 days of intermittent usage, the D-lactate

electrode exhibited the highest long-term stability. The formate electrode retained only 16% of its initial sensor signal.

Successful application of the biosensor for quantification of organic acids in complex media was demonstrated in silage samples (maize and sugarcane). Data obtained by amperometric measurements were in good agreement with a commercial reference technique. In comparison to conventional analytical methods, the described biosensor system offers the advantages of rapid and simultaneous detection, and capability for repeated application due to long-term stability. For particular requirements, the flexible system can be easily enhanced with additional electrodes for further analytes [23]. Future investigations will focus on application of the biosensor in different biological samples and evaluation of the compact and portable measurement device for long-term and on-site monitoring of fermentation processes. In this regard, the construction of a reagentless biosensor is planned through the coimmobilization of the cofactors NAD^+ and $K_3[Fe(CN)_6]$ for improved ease of use.

Acknowledgements

The research was supported by the German Federal Ministry of Food and Agriculture (BMEL) [grant number 22006613]. The authors thank H. Iken for fabrication of the sensor chips and J. Arreola for performing the atomic force microscopy measurements. We also acknowledge S. Jansen from the NOWUM-Energy Institute for providing the silage samples.

References

[1] Goodwin, M.L.; Harris, J.E.; Hernández, A.; Gladden, L.B. (2007) Blood lactate measurements and analysis during exercise: A guide for clinicians. *J. Diabetes Sci. Technol.* 1:558–569, doi:10.1177/193229680700100414.

[2] Wang, J. (1999) Amperometric biosensors for clinical and therapeutic drug monitoring: A review. *J. Pharm. Biomed. Anal.* 19:47–53, doi:10.1016/S0731-7085(98)00056-9.

[3] Schlatter, J.; Chiadmi, F.; Gandon, V.; Chariot, P. (2014) Simultaneous determination of methanol, acetaldehyde, acetone, and ethanol in human blood by gas chromatography with flame ionization detection. *Hum. Exp. Toxicol.* 33:74–80, doi:10.1177/0960327113482845.

[4] Shapiro, F.; Silanikove, N. (2010) Rapid and accurate determination of D- and L-lactate, lactose and galactose by enzymatic reactions coupled to formation of a fluorochromophore: Applications in food quality control. *Food Chem.* 119:829–833, doi:10.1016/j.foodchem.2009.07.029.

[5] Goriushkina, T.B.; Soldatkin, A.P.; Dzyadevych, S.V. (2009) Application of amperometric biosensors for analysis of ethanol, glucose, and lactate in wine. *J. Agric. Food. Chem.* 57:6528–6535, doi:10.1021/jf9009087.

[6] Crable, B.R.; Plugge, C.M.; McInerney, M.J.; Stams, A.J.M. (2011) Formate formation and formate conversion in biological fuels production. *Enzyme Res.* 2001:1–8, doi:10.4061/2011/532536.

[7] Lins, P.; Schwarzenauer, T.; Reitschuler, C.; Wagner, A.O.; Illmer, P. (2012) Methanogenic potential of formate in thermophilic anaerobic digestion. *Waste Manage. Res.* 30:1031–1040, doi:10.1177/0734242X12445655.

[8] Whittenbury, R.; McDonald, P.; Bryan-Jones, D.G. (1967) A short review of some biochemical and microbiological aspects of ensilage. *J. Sci. Food Agric.* 18:441–444, doi:10.1002/jsfa.2740181001.

[9] Doyon, G.; Gaudreau, G.; St-Gelais, D.; Beaulieu, Y.; Randall, C.J. (1991) Simultaneous HPLC determination of organic acids, sugars and alcohols. *Can. Inst. Sci. Technol. J.* 24:87–94, doi:10.1016/S0315-5463(91)70025-4.

[10] Gey, M. (1988) Characterization of biotechnological processes and products using high-performance liquid chromatography (HPLC): I. Separations of carbohydrates, organic acids and lipids. *Acta Biotechnol.* 8:197–205, doi:10.1002/abio.370080216.

[11] Playne, M.J. (1985) Determination of ethanol, volatile fatty acids, lactic and succinic acids in fermentation liquids by gas chromatography. *J. Sci. Food Agric.* 35:638–644, doi:10.1002/jsfa.2740360803.

[12] Diamond, D. (1993) Progress in sensor array research. *Electroanal.* 5:795–802, doi:10.1002/elan.1140050913.

[13] Stefan, R.I.; van Staden, J.F.; Aboul-Enein, H.Y. (1999) Electrochemical sensor arrays. *Crit. Rev. Anal. Chem.* 29:133–153, doi:10.1080/10408349891199293.

[14] Azevedo, A.M.; Prazeres, D.M.F.; Cabral, J.M.S.; Fonseca, L.P. (2005) Ethanol biosensors based on alcohol oxidase. *Biosens. Bioelectron.* 21:235–247, doi:10.1016/j.bios.2004.09.030.

[15] Prodromidis, M.I.; Karayannis, M.I. (2002) Enzyme based amperometric biosensors for food analysis. *Electroanal.* 14:241–261, doi:10.1002/1521-4109(200202)14:4<241::AID-ELAN241>3.0.CO;2-P.

[16] Tzang, C.H.; Yuan, R.; Yang, M. (2001) Voltammetric biosensors for the determination of formate and glucose-6-phosphate based on the measurement of dehydrogenase-generated NADH and NADPH. *Biosens. Bioelectron.* 16:211–219, doi:10.1016/S0956-5663(00)00143-3.

[17] Mak, K.K.W.; Wollenberger, U.; Scheller, F.W.; Renneberg, R. (2003) An amperometric bi-enzyme sensor for determination of formate using cofactor regeneration. *Biosens. Bioelectron.* 18:1095–1100, doi:10.1016/S0956-5663(02)00245-2.

[18] Rassaei, L.; Olthuis, W.; Tsujimura, S.; Sudhölter, E.J.R.; van den Berg, A. (2014) Lactate biosensors: Current status and outlook. *Anal. Bioanal. Chem.* 406:123–137, doi:10.1007/s00216-013-7307-1.

[19] Rathee, K.; Dhull, V.; Dhull, R.; Singh, S. (2016) Biosensors based on electrochemical lactate detection: A comprehensive review. *Biochem. Biophys. Rep.* 5:35–54,

doi:10.1016/j.bbrep.2015.11.010.

[20] Moser, I.; Jobst, G.; Urban, G.A. (2002) Biosensor arrays for simultaneous measurement of glucose, lactate, glutamate, and glutamine. *Biosens. Bioelectron.* 17:297–302, doi:10.1016/S0956-5663(01)00298-6.

[21] Bäcker, M.; Delle, L.; Poghossian, A.; Biselli, M.; Zang, W.; Wagner, P.; Schöning, M.J. (2011) Electrochemical sensor array for bioprocess monitoring. *Electrochim. Acta* 56:9673–9678, doi:10.1016/j.electacta.2011.04.030.

[22] Pilas, J.; Yazici, Y.; Selmer, T.; Keusgen, M.; Schöning, M.J. (2017) Optimization of an amperometric biosensor array for simultaneous measurement of ethanol, formate, D- and L-lactate. *Electrochim. Acta* 251:256–262, doi:10.1016/j.electacta.2017.07.119.

[23] Röhlen, D.L.; Pilas, J.; Schöning, M.J.; Selmer, T. (2017) Development of an amperometric biosensor platform for the combined determination of L-malic, fumaric, and L-aspartic acid. *Appl. Biochem. Biotechnol.* 183:566–581, doi:10.1007/s12010-017-2578-1.

[24] Pilas, J.; Iken, H.; Selmer, T.; Schöning, M.J. (2015) Development of a multiparameter sensor chip for the simultaneous detection of organic compounds in biogas processes. *Phys. Status Sol. A* 212:1306–1312, doi:10.1002/pssa.201431894.

[25] Montagné, M.; Erdmann, H.; Comtat, M.; Martya, J.L. (1995) Comparison of the performances of two bi-enzymatic sensors for the detection of D-lactate. *Sens. Actuators B Chem.* 27:440–443, doi:10.1016/0925-4005(94)01636-V.

[26] Bahadir, E.B.; Sezgintürk, M.K. (2015) Applications of commercial biosensors in clinical, food, environmental, and biothreat/biowarfare analyses. *Anal. Biochem.* 478:107–120, doi:10.1016/j.ab.2015.03.011.

[27] Gibson, T.D. (1999) Biosensors: The stability problem. *Analusis* 27:630–638, doi:10.1051/analusis:1999270630.

[28] D'Souza, S.F. (2001) Immobilization and stabilization of biomaterials for biosensor applications. *Appl. Biochem. Biotechnol.* 96:225–238, doi:10.1385/ABAB:96:1-3:225.

[29] Lorenz, H.; Despont, M.; Fahrni, N.; LaBianca, N.; Renaud, P.; Vettiger, P. (1997) SU-8: A low-cost negative resist for MEMS. *J. Micromech. Microeng.* 7:121–124, doi:10.1088/0960-1317/7/3/010.

[30] Kirchner, P.; Reisert, S.; Pütz, P.; Keusgen, M.; Schöning, M.J. (2012) Characterisation of polymeric materials as passivation layer for calorimetric H_2O_2 gas sensors. *Phys. Status Sol. A* 10:859–863, doi:10.1002/pssa.201100773.

[31] Swain, G.M. (2007) Solid Electrode Materials: Pretreatment and Activation. In: Zoski, C.G.A. (Ed.) Handbook of Electrochemistry. Amsterdam: *Elsevier*, doi:10.1016/B978-044451958-0.50006-9.

[32] Carrez, M.C. (1908) Le ferrocyanure de potassium et l'acétate de zinc comme agents de défécation des urines. *Ann. Chim. Anal.* 13:97–101.

[33] Cao, E.; Chen, Y.; Cui, Z.; Foster, P.R. (2003) Effect of freezing and thawing rates on denaturation of proteins in aqueous solutions. *Biotechnol. Bioeng.* 82:684–690, doi:10.1002/bit.10612.

[34] Nema, S.; Avis, K.E. (1993) Freeze-thaw studies of a model protein, lactate dehydrogenase, in the presence of cryoprotectants. *J. Parenter. Sci. Technol.* 47:76–83.

[35] Thévenot, D.R.; Toth, K.; Durst, R.A.; Wilson, G.S. (2001) Electrochemical biosensors: Recommended definitions and classification. *Biosens. Bioelectron.* 16:121–131, doi:10.1016/S0956-5663(01)00115-4.

[36] Katrlík, J.; Pizzariello, A.; Mastihuba, V.; Švorc, J.; Stred'anský, M.; Miertuš, S. (1999) Biosensors for L-malate and L-lactate based on solid binding matrix. *Anal. Chim. Acta* 379:193–200, doi:10.1016/S0003-2670(98)00610-2.

[37] Shu, H.C.; Mattiasson, B.; Persson, B.; Nagy, G.; Gorton, L.; Sahni, S.; Geng, L.; Boguslavsky, L.; Skotheim, T. (1995) Reagentless amperometric electrode based on carbon paste, chemically modified with D-lactate dehydrogenase, NAD^+, and mediator containing polymer for D-lactic acid analysis. I. Construction, composition, and characterization. *Biotechnol. Bioeng.* 46:270–279, doi:10.1002/bit.260460310.

[38] Kwan, R.C.H.; Hon, P.Y.T.; Mak, K.K.W.; Renneberg, R. (2004) Amperometric determination of lactate with novel trienzyme/poly(carbamoyl) sulfonate hydrogel-based sensor. *Biosens. Bioelectron.* 19:1745–1752, doi:10.1016/j.bios.2004.01.008.

[39] Alpat, S.; Telefoncu, A. (2010) Development of an alcohol dehydrogenase biosensor for ethanol determination with toluidine blue O covalently attached to a cellulose acetate modified electrode. *Sensors* 10:748–764, doi:10.3390/s100100748.

[40] Miyamoto, S.; Murakami, T.; Saito, A.; Kimura, J. (1991) Development of an amperometric alcohol sensor based on immobilized alcohol dehydrogenase and entrapped NAD^+. *Biosens. Bioelectron.* 6:563–567, doi:10.1016/0956-5663(91)80020-X.

[41] Tsai, Y.C.; Huang, J.D.; Chiu, C.C. (2007) Amperometric ethanol biosensor based on poly(vinyl alcohol)-multiwalled carbon nanotube-alcohol dehydrogenase biocomposite. *Biosens. Bioelectron.* 22:3051–3056, doi:10.1016/j.bios.2007.01.005.

[42] Zwart, K.B.; Langeveld, J.W.A.(2010) Biomass Refining and Conversion: Biogas. In: Langeveld, H.; Sanders, J.; Meeusen, M. (Eds.) The Biobased Economy: Biofuels, Materials and Chemicals in the Post-oil Era. London: Routledge, doi:10.4324/9781849774802.

[43] Herrmann, A.; Rath, J. (2012) Biogas production from maize: Current state, challenges, and prospects. 1. Methane yield potential. *Bioenerg. Res.* 5:1027–1049, doi:10.1007/s12155-012-9202-6.

[44] Janke, L.; Leite, A.; Nikolausz, M.; Schmidt, T.; Liebetrau, J.; Nelles, M.; Stinner, W. (2015) Biogas production from sugarcane waste: Assessment on kinetic challenges for process designing. *Int. J. Mol. Sci.* 16:20685–20703, doi:10.3390/ijms160920685.

[45] Herrmann, C.; Idler, C.; Heiermann, M. (2015) Improving aerobic stability and biogas production of maize silage using silage additives. *Bioresour. Technol.* 197:393–403, doi:10.1016/j.biortech.2015.08.114.

[46] Franco, R.T.; Buffière, P.; Bayard, R. (2016) Ensiling for biogas production: Critical parameters. A review. *Biomass Bioenergy* 94:94–104, doi:10.1016/j.biombioe.2016.08.014.

[47] Burns, D.T.; Danzer, K.; Townshend, A. (2002) Use of the term "recovery" and "apparent recovery" in analytical procedures (IUPAC Recommendations 2002). *Pure Appl. Chem.* 74:2201–2205, doi:10.1351/pac200274112201.

5.5 Supplementary information

The construction of the presented measurement cell and the integration of the counter electrode on the sensor chip were important steps in the development process of the amperometric multi-analyte biosensor. However, further development is required for the realization of an automated measurement process. In this regard, the advances in the field of lab-on-a-chip (LoC) systems and microfluidic devices are of great interest. The proper operation of such systems relies for example on actuators, which act as microvalves or pumps. In collaboration with L. Breuer, a proof of concept experiment has been conducted in order to realize such a LoC device. The obtained results were part of a publication in the journal *Sens. Actuators B Chem.*[1].

The proof of concept sensor platform is based on light-addressable hydrogels with incorporated graphene oxide (GO), that have been developed by L. Breuer, and an amperometric multi-analyte biosensor, which is the object of this thesis. The hydrogels were fabricated within microfluidic channels by *in situ* photopolymerization of poly(N-isopropylacrylamide) (PNIPAAm) modified with GO nanoparticles. The GO modification enables stimulation with light at a wavelength of 445 nm. Optothermal heating with a laser results in a significant volume alteration of the hydrogels, after exceeding the characteristic switching temperature. Thereby, the state of the hydrogels changes from swollen to collapsed. With this feature the hydrogel can be utilized as a valve in microfluidic channels, which are blocked in the swollen state and opened upon light illumination. Figure 5.6 shows a schematic of the applied measurement set-up, consisting of two microfluidic channels with responsive hydrogel valves located upstream to the multi-analyte biosensor. For practical reasons, the biosensor was only equipped with two L-lactate-sensitive electrodes.

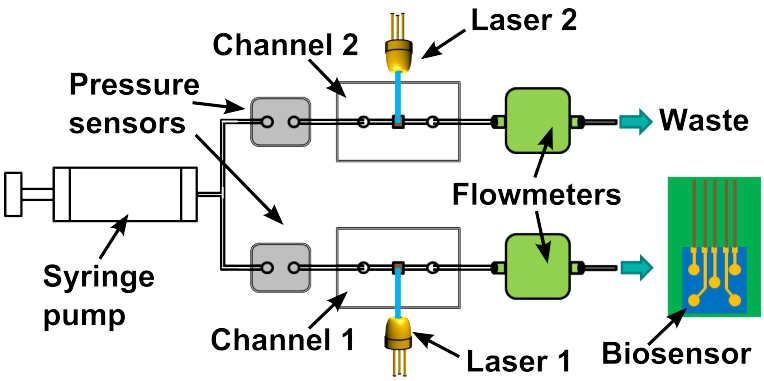

Fig. 5.6: Proof of concept sensor platform: Two light-addressable valves connected in parallel to control the supply of L-lactate to the amperometric biosensor (reprinted with permission from L. Breuer *et al.*[1] (Copyright 2019, Elsevier B.V.)).

The two valves were stimulated individually and alternately with a corresponding laser

[1]Breuer, L.; **Pilas, J.**; Guthmann, E.; Schöning, M.J.; Thoelen, R.; Wagner, T. (2019) Towards light-addressable flow control: Responsive hydrogels with incorporated graphene oxide as laser-driven actuator structures within microfluidic channels. *Sens. Actuators B Chem.* 288:579–585, doi:10.1016/j.snb.2019.02.086.

diode. Thereby, the flow path of an L-lactate solution through the microfluidic system was controlled. In Fig. 5.7, the corresponding current response of the two L-lactate electrodes is presented. The signal increased, when laser 1 was switched on (red area) and the channel was opened for the flow of the analyte solution. In times channel 1 was blocked (laser 2 on, yellow area) the signal reached a plateau due to constant L-lactate concentration presented to the sensor environment. These results demonstrate promising potential for the construction of an amperometric enzyme-based LoC with hydrogel actuators.

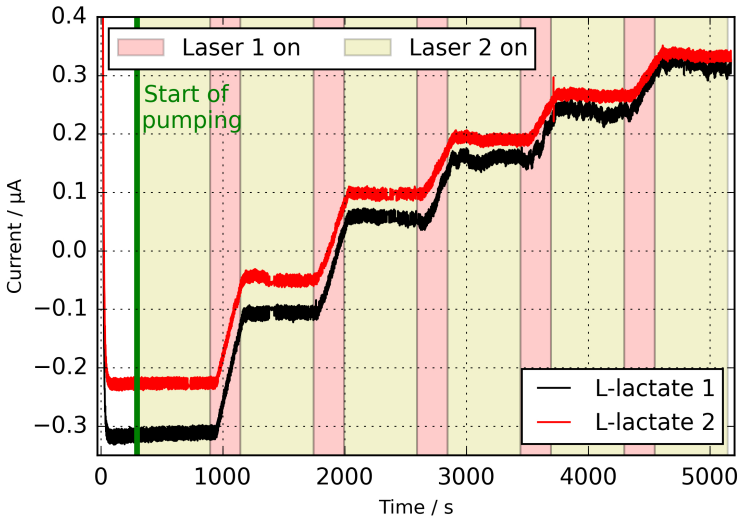

Fig. 5.7: Controlling the analyte supply of a biosensor: L-lactate is only pumped towards the biosensor while the corresponding valve in series is open (Laser 1, red area) so that the signal of both electrodes (L-lactate 1, L-lactate 2) increases. If the valve in parallel to the biosensor is open (Laser 2, yellow area), the signal saturates because there is no increase in L-lactate concentration at the sensor surface (reprinted with permission from L. Breuer *et al.*[1] (Copyright 2019, Elsevier B.V.)).

6 Toward a hybrid biosensor system for analysis of organic and volatile fatty acids in fermentation processes

Frontiers in Chemistry **(2018), 6:284, 1–11**

D.L. Röhlen[1*], **J. Pilas[1,2*]**, M. Dahmen[3], T. Selmer[1], M. Keusgen[2] and M.J. Schöning[1,4]

[1] Institute of Nano- and Biotechnologies (INB), FH Aachen, Jülich, Germany
[2] Institute of Pharmaceutical Chemistry, Philipps-Universität Marburg, Marburg, Germany
[3] Institute NOWUM-Energy, FH Aachen, Jülich, Germany
[4] Institute of Complex Systems 8 (ICS-8), Forschungszentrum Jülich, Jülich, Germany
[*] These authors have contributed equally to this work.

Submitted: 03-28-2018; Accepted: 06-22-2018; Published: 07-17-2018

`https://doi.org/10.3389/fchem.2018.00284`
Keywords: multi-analyte biosensor, biogas, electrochemical detection, organic acids, volatile fatty acids

Abstract

Monitoring of organic acids (OA) and volatile fatty acids (VFA) is crucial for the control of anaerobic digestion. In case of unstable process conditions, an accumulation of these intermediates occurs. In the present work, two different enzyme-based biosensor arrays are combined and presented for facile electrochemical determination of several process-relevant analytes. Each biosensor utilizes a platinum sensor chip ($14 \times 14\,\mathrm{mm}^2$) with five individual working electrodes. The OA biosensor enables simultaneous measurement of ethanol, formate, D- and L-lactate, based on a bi-enzymatic detection principle. The second VFA biosensor provides an amperometric platform for quantification of acetate and propionate, mediated by oxidation of hydrogen peroxide. The cross-sensitivity of both biosensors towards potential interferents, typically present in fermentation samples, was investigated. The potential for practical application in complex media was successfully demonstrated in spiked sludge samples collected from three different biogas plants. Thereby, the results obtained by both of the biosensors were in good agreement to the applied reference measurements by photometry and gas chromatography, respectively. The proposed hybrid biosensor system was also used for long-term monitoring of a lab-scale biogas reactor ($0.01\,\mathrm{m}^3$) for a period of two months. In combination with typically monitored parameters, such as gas quality, pH and FOS/TAC (volatile organic acids/total anorganic carbonate), the amperometric measurements of OA and VFA concentration could enhance the understanding of ongoing fermentation processes.

6.1 Introduction

In light of the depletion of fossil fuels, the public interest of biogas production from renewable resources is steadily increasing. A particular advantage of anaerobic digestion is the ability for simultaneous utilization of industrial waste and thus, providing a promising approach for dealing with another problem of today's world [1, 2]. However, in order to realize the potential of the growing market, several technological and economic aspects need to be improved to ensure process stability and efficient methane (CH_4) production. Some of these important factors comprise appropriate biogas purification technologies, a suitable feedstock composition and ideal conditions inside the biogas reactor [3–5]. The latter is guaranteed by continuous monitoring of various physical and biochemical parameters indicating system stability (pH, alkalinity, gas quality, FOS/TAC [volatile organic acids/total anorganic carbonate)]. Process imbalances are thereby reflected by acidification of the reactor due to accumulation of volatile fatty acids (e.g., acetate, propionate, butyrate) and organic acids, like lactate, formate and alcohols [6–9]. Hitherto, estimation of the acid composition is conventionally carried out by gas chromatography [10], spectroscopy [11, 12] or HPLC (high-performance liquid chromatography) [13, 14]. Common disadvantages of these methods are elaborate sample pre-treatment and high costs per analysis, since these are usually executed by external service laboratories. Obviously, the main drawback is the inevitable time delay between sampling and availability of the results, making immediate intervention impossible and therefore represent an element of uncertainty for the plant operators. For these reasons, the acid content is typically only analyzed once or twice per month.

In order to overcome this problem, biosensors have been developed as reliable tools for fast and accurate analysis of several compounds.

Much attention has been paid to the development of lactate and ethanol biosensors, due to their diverse applications in food industry and healthcare [15, 16]. Apart from that, several studies imply an association between these intermediates and process stability of the biogas reactor [17, 18]. For this reason, the development and optimization of an organic acid (OA) biosensor, comprising enzymes for the specific detection of D/L-lactate, formate and ethanol was a subject of earlier studies [19]. In contrast, only a limited number of volatile fatty acid (VFA) biosensors have been described in the literature up to now. The detection of these analytes was accomplished with microbial fuel cells [20], microbial electrolysis cells [21] or dissolved oxygen probes with an immobilized biofilm [22]. On-line shock sensors, based on microbial fuel cells were also reported in the literature [23]. Specific determination of individual substrates, e.g., propionate and acetate, was realized using enzyme-based sensors [24–26].

In the presented approach, the above mentioned OA biosensor is combined with a new established system for concurrent detection of acetate and propionate. Figure 6.1a shows the enzymatic principle of the OA biosensor for parallel determination of ethanol, formate, D- and L-lactate. In each case, a specific dehydrogenase (DH) is used, which oxidizes its corresponding substrate to acetaldehyde, CO_2 and pyruvate, respectively. In these reactions, reduction of the cofactor NAD^+ to NADH is catalyzed. Then, diaphorase (DIA) regenerates the released NADH by reducing the electron acceptor $Fe(CN)_6^{3-}$ to $Fe(CN)_6^{4-}$. At an applied working potential of +0.3 V *vs.* Ag/AgCl, $Fe(CN)_6^{4-}$ is re-oxidized at the platinum working electrode and the generated current is proportional over a certain linear range to the particular substrate concentration. This method facilitates integration of several analyte-sensing electrodes within one biosensor array. On the contrary, the VFA biosensor works with a different principle for amperometric quantification of acetate and propionate. The working potential is set to +0.6 V *vs.* Ag/AgCl for anodic oxidation of H_2O_2. This compound is produced in both enzymatic reactions. For this reason, propionate CoA-transferase (PCT) and short-chain acyl-CoA oxidase (SCAOx) are immobilized on the working electrode for electrochemical sensing of propionate (Fig. 6.1b). As illustrated in Fig. 6.1c, acetate is indirectly determined by application of acetate kinase (AK), pyruvate kinase (PK) and pyruvate oxidase (POx).

In this work, we present for the first time a modular system for the combined amperometric detection of the OA formate, D/L-lactate and ethanol and for the VFA acetate and propionate. Each biosensor utilizes a different enzyme-based detection principle and thereby, simultaneous determination of four and two analytes was realized. The cross-sensitivity and sensor performance in spiked samples of fermentation broth were investigated. Practical application of both biosensors was demonstrated by long-term monitoring of the OA and VFA concentration in a lab-scale biogas reactor. The proposed hybrid biosensor system proved to be a promising device for rapid and facile quantification of several OA and VFAs in real samples. In this regard, the combination of various parameters enables an enhanced understanding of the process conditions within a biogas reactor and thus facilitates an efficient CH_4 production.

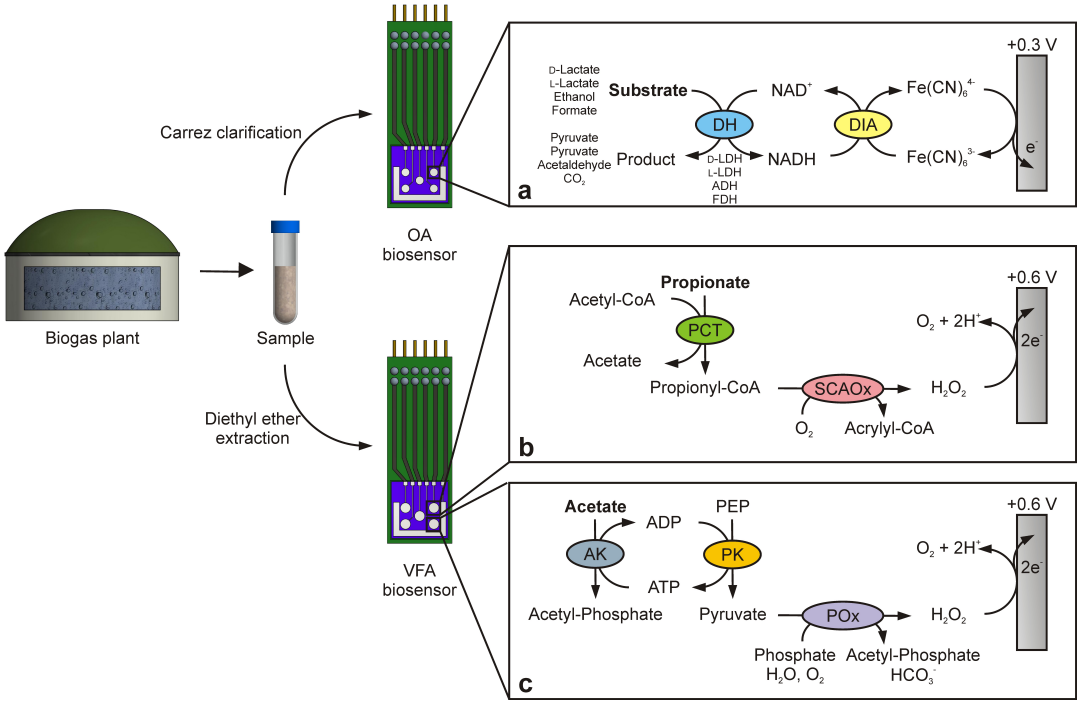

Fig. 6.1: Amperometric detection principles of the organic acid (OA) and volatile fatty acid (VFA) biosensor. A sample of fermentation broth is taken from a biogas plant and pretreated by either Carrez clarification or ether extraction. Determination of ethanol, formate, D- and L-lactate is then realized by using a bi-enzymatic system, consisting of a specific dehydrogenase (DH) and diaphorase (DIA) **(a)**. For simultaneous detection, on each working electrode DIA with a different DH is immobilized, namely D-lactate dehydrogenase (D-LDH), L-lactate dehydrogenase (L-LDH), alcohol dehydrogenase (ADH) and formate dehydrogenase (FDH), respectively. The product $Fe(CN)_6^{4-}$ is re-oxidized at an applied potential of +0.3 V *vs.* Ag/AgCl. The oxidation of H_2O_2 at a working potential of +0.6 V *vs.* Ag/AgCl is used for measurement of propionate **(b)** and acetate **(c)**. For propionate quantification, propionate CoA-transferase (PCT) and short-chain acyl-CoA oxidase (SCAOx) are used. Combination of acetate kinase (AK), pyruvate kinase (PK) and pyruvate oxidase (POx) enables amperometric detection of acetate.

6.2 Material and methods

6.2.1 Chemicals and reagents

For construction of the biosensors and realization of photometric assays, the following enzymes were used: Acetate kinase from *Escherichia coli* (AK, 150 U mg^{-1}), alcohol dehydrogenase from *Saccharomyces cerevisiae* (ADH, 310 U mg^{-1}), citrate synthase from porcine heart (CS, 100 U mg^{-1}), diaphorase from *Clostridium kluyveri* (DIA, 51 U mg^{-1}), formate dehydrogenase from *Candida boidinii* (FDH, 0.49 U mg^{-1}), D-lactate dehydrogenase from *Lactobacillus leichmanii* (D-LDH, 213 U mg^{-1}), L-lactate dehydrogenase from *Bacillus stearothermophilus* (L-LDH, 174.5 U mg^{-1}) and pyruvate kinase from rabbit muscle (PK, 1000 U mg^{-1}) were each obtained from Sigma-Aldrich

(St. Louis, MO, USA). Peroxidase from horseradish (HRP, 200 U mg^{-1}) and pyruvate oxidase from *Aerococcus viridans* (POx, 25 U mg^{-1}) were from Merck (Darmstadt, Germany).

Adenosine 5'-diphosphate sodium salt (ADP), bovine serum albumin (BSA), butyryl coenzyme A lithium salt, capronic acid, ethanol, ethylenediaminetetraacetic acid tetrasodium salt dihydrate (EDTA), flavin adenine dinucleotide disodium salt (FAD), glutaraldehyde solution (GA) (25% in H_2O, glycerol, sodium D-lactate, potassium ferricyanide ($K_3[Fe(CN)_6]$), potassium ferrocyanide ($K_3[Fe(CN)_6 \cdot 3\,H_2O]$), propionyl coenzyme A lithium salt, sodium propionate, sodium pyruvate, thiamine pyrophosphate (TPP), Triton X-100, valeric acid and $ZnCl_2$ were also supplied by Sigma-Aldrich. Adenosine 5'-triphosphate disodium salt (ATP), (2,2'-azino-bis(3-ethylbenzothiazoline-6-sulphonic acid) diammonium salt (ABTS), acetyl coenzyme A trilithium salt, sodium formate, sodium L-lactate, nicotinamide adenine dinucleotide (NAD^+), oxaloacetic acid and phospho(enol)pyruvic acid monopotassium salt (PEP) were purchased from AppliChem (Darmstadt, Germany). Diethyl ether, 5,5'-dithiobis-(2-nitrobenzoic acid), potassium phosphate buffer (K_2HPO_4, KH_2PO_4), Tris-(hydroxymethyl)-aminomethane, H_2SO_4, $MgCl_2$ and NaOH were from Carl Roth GmbH & Co. KG (Karlsruhe, Germany). Dithiothreitol (DTT), sodium phosphate buffer (Na_2HPO_4, NaH_2PO_4), sodium acetate and sodium butyrate were acquired from Merck (Darmstadt, Germany). d-Desthiobiotin was provided by IBA (Göttingen, Germany).

6.2.2 Cloning

The propionate-sensing system is composed of two recombinantly produced enzymes, a propionate CoA-transferase (PCT, EC 2.8.3.1) from *Clostridium propionicum* and a short-chain acyl-CoA oxidase (SCAOx, EC 1.3.3.6) derived from *Arabidopsis thaliana*. Fabrication of the propionate electrode involved cloning of the corresponding genes into designated expression vectors, biomass production and purification of the proteins.

Based on the published sequence [27], the SCAOx gene was codon-optimized for expression in *E. coli* and synthesized by Eurofins Genomics (Ebersberg, Germany). Moreover, internal restriction sites for *Esp*3I were removed. The resulting sequence was amplified by polymerase chain reaction (PCR) using two primers (SCAOx for 5'-AAGCTCTTCAATGGCGGTTCTGTCAAGCG-3' and SCAOx rev 5'-AAGCTCTTCACCCTTACAAACGAGAGCGGGTAGC-3') with incorporated *Lgu*I restriction sites (underlined). After analysis of the purified PCR product by chip electrophoresis (MCE-202 MultiNA; Shimadzu, Duisburg, Germany), the SCOAx gene was digested with *Lgu*I and cloned into a pENTRY vector (IBA, Göttingen, Germany). *E. coli* DH5α-competent cells were transformed with the resultant plasmid. Following sequence analysis (Eurofins Genomics, Ebersberg, Germany), the SCAOx gene cassette was subcloned into the *Esp*3I site of a StarGate Acceptor Vector (IBA, Göttingen, Germany), containing an N-terminal-fused Strep-tag. Expression plasmids harboring propionate CoA-transferase fused to an N-terminal Strep-tag, were synthesized as previously described [28].

6.2.3 Gene expression and protein purification

E. coli BL21(DE3) cells carrying the constructed plasmids were used for production of the recombinant proteins. Following pre-cultivation at 28 °C for approx. 15 h in 100 mL LB medium (Luria-Bertani) with 50 µg mL^{-1} carbenicillin, the culture was inoculated to 500 mL of the same medium. At optical density (OD_{578nm}) of 0.6–0.8, gene expression was initiated by treatment with 200 ng mL^{-1} AHT. Post induction, cells harboring recombinant SCAOx were incubated for 2 h at 28 °C and finally harvested by centrifugation. Cell pellets were washed once with 50 mL PBS [137 mM NaCl, 2.7 mM KCl, 10 mM Na_2HPO_4, 1.8 mM KH_2PO_4 (pH 7.4)] and afterwards stored at −80 °C until used for protein purification. PCT-containing *E. coli* cells were cultivated for 3 h at 28 °C post induction and washed with 50 mL TBS [50 mM Tris, 150 mM NaCl (pH 7.5)] prior storage.

Purification of SCAOx was accomplished by affinity chromatography with a Strep-Tactin Macroprep column (IBA GmbH, Göttingen, Germany) as outlined earlier [29]. Briefly, cell pellets were suspended in 100 mM sodium phosphate buffer (pH 7.5, supplemented with 150 mM NaCl and 10 µM FAD) and lysed by sonication. Next, cell debris was pelleted by ultracentrifugation and the clear supernatant was loaded onto the equilibrated column. Elution of the protein was effected by addition of 2.5 mM d-desthiobiotin in aforementioned buffer. Protein concentration and purity were verified by sodium dodecyl sulfate polyacrylamide gel electrophoresis (SDS-PAGE) and Bradford analysis. Purified protein fractions were concentrated by ultrafiltration and 10 vol% glycerol was added for storage at −20 °C. Similarly, recombinant PCT was purified using 100 mM Tris-HCl pH 8.0 (supplemented with 150 mM NaCl, 1.0 mM EDTA, 1.0 mM DTT) as resuspension buffer and additionally 2.5 mM d-desthiobiotin for subsequent elution. Prior enzyme immobilization, the storage buffer was exchanged with 100 mM sodium phosphate buffer pH 7.5, 1.0 mM DTT, 1.0 mM EDTA.

6.2.4 Enzyme activity measurements

Enzyme activities were determined spectrophotometrically at 25 °C in 1 mL reaction mixture using an Ultrospec 2100 pro spectrophotometer (Amersham Biosciences, UK).

Short-chain acyl-CoA oxidase activity was measured in a coupled assay with HRP according to [30]. The assay mixture included 100 mM sodium phosphate buffer (pH 7.4), supplemented with 0.05 mM FAD, 0.05 mM acyl-CoA, 2.0 mM ABTS and 5.0 U HRP. The reaction was started by addition of the enzyme and the increase in absorbance at 405 nm, due to oxidation of ABTS, was monitored. A molar extinction coefficient ε_{405nm} of 18.4 $mM^{-1}\,cm^{-1}$ was used for calculation of enzyme activities [31].

Propionate CoA-transferase activity was determined by detection of free CoA via a coupled citrate synthase-DTNB reaction [32]. The reaction mixture consisted of 100 mM sodium phosphate (pH 7.4), 0.05 mM propionyl-CoA, 20 mM sodium acetate, 1 mM DTNB (5,5'-dithiobis-(2-nitrobenzoic acid)) and 1 mM oxaloacetate and 3 U citrate synthase. The assay was initiated by addition of PCT and the change in absorbance was followed at 415 nm. Enzyme activities were calculated using a molar extinction coefficient ε_{415nm} of 14.14 $mM^{-1}\,cm^{-1}$.

6.2.5 Biosensor preparation

The multi-parameter biosensor chips ($14 \times 14\,mm^2$) were fabricated by thin-film technology [33]. Each biosensor array consists of five individual platinum working electrodes and an additional counter electrode (area $40.5\,mm^2$). The diameter of each working electrode of the OA biosensor was 2 mm, whereas the working electrodes of the VFA biosensor were slightly larger (Ø 2.5 mm) for immobilization of an increased volume of enzyme solution. Before the enzymes were immobilized onto the electrodes, the biosensor chips were cleaned by electrochemical treatment in 0.5 M H_2SO_4 until a stable signal was obtained (+2.0 V *vs.* Ag/AgCl for 2 min and subsequent cyclic voltammetry from −0.2 to +1.4 V *vs.* Ag/AgCl).

Enzymes were immobilized by chemical cross-linking with 0.4 vol% GA solution, supplemented with 10 vol% glycerol and 2% BSA. In case of the OA biosensor, each working electrode was endowed with a different DH (ADH, FDH, D-LDH and L-LDH, respectively) in combination with the DIA. Thereby, a volume of 1.5 µL of each enzyme mixture was applied on one of the working electrodes. The fifth working electrode served as a reference and was modified only with the inert protein BSA, which does not exhibit any catalytic activity. Details of exact enzyme loadings on the OA biosensor were given earlier [19].

For construction of the VFA biosensor, GA concentrations were adjusted to 0.24 vol% (propionate electrode) and 0.7 vol% (acetate electrode) each with 2% BSA. The propionate-specific electrode contained 0.032 U PCT and 0.057 U SCAOx embedded in the BSA-GA matrix. Acetate detection was accomplished by an enzyme layer consisting of 3 U POx, 6 U PK and 6 U AK. Each electrode was equipped with 3 µL of the corresponding enzyme mixture.

6.2.6 Experimental set-up and operation

All electrochemical experiments were conducted at room temperature in a three-electrode arrangement with a Ag/AgCl reference electrode (with KCl as inner electrolyte; Sensolytics, Bochum, Germany) and the biosensor, comprising the working electrode (each with five working electrodes per biosensor) and counter electrode. The set-up consisted of a custom-made measurement cell connected to a potentiostat with integrated multiplexer (EmStat3 and MUX 16, PalmSens BV, Houten, Netherlands) [33]. Figure 6.2 shows an image of the applied set-up. For operation of the OA biosensor, a working potential of +0.3 V *vs.* Ag/AgCl was applied for anodic oxidation of enzymatically produced $Fe(CN)_6^{4-}$. Standard reaction mixture contained 2.5 mM NAD^+ and 2 mM $Fe(CN)_6^{3-}$ dissolved in 100 mM potassium phosphate buffer (pH 7.5).

Detection of acetate and propionate with the VFA biosensor was realized at an applied potential of +0.6 V *vs.* Ag/AgCl for oxidizing H_2O_2. Measurements were carried out in 100 mM potassium phosphate buffer (pH 7.0), supplemented with 5 mM $MgCl_2$, 0.6 mM TPP, 0.02 mM FAD, 2 mM PEP, 1 mM ATP and 0.4 mM acetyl-CoA. Due to the rapid loss of enzyme activity, an additional 11.84 U PK and 2.5 U AK were added to the reaction mixture. For both biosensors, a volume of 2 mL of the corresponding measurement solution was used. Homogeneous distribution of the calibration and sample solution, respectively, was accomplished with a magnetic stirrer.

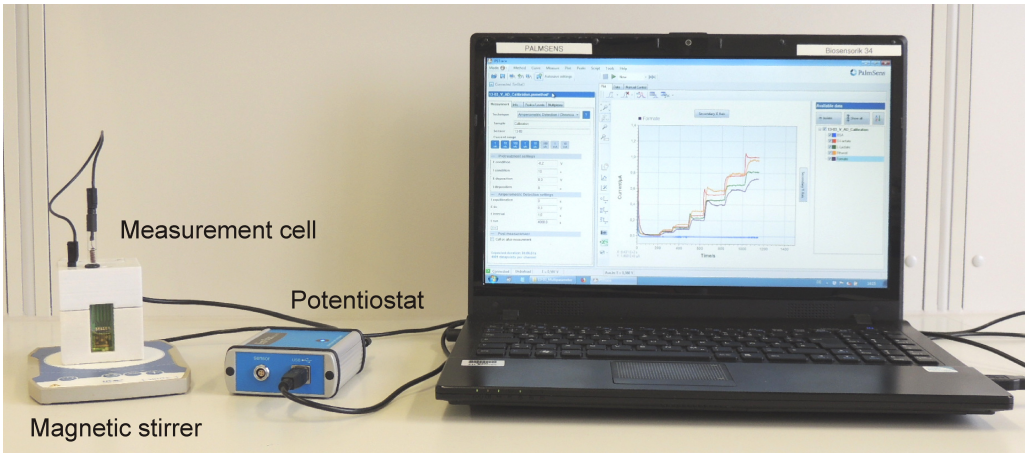

Fig. 6.2: Photograph of measurement set-up with biosensor and Ag/AgCl reference electrode connected to a potentiostat and software device.

6.2.7 Analysis of fermentation broth from biogas plants

Samples of fermentation broth (approximately 50 mL) were collected one-time from three industrial continuously operated biogas plants in Germany and regularly from a lab-scale biogas reactor. Fermentation sludge from the industrial plants was stored frozen at −21 °C until further measurements, whereas samples from biogas test reactor were analyzed immediately after sampling. For application of the OA and VFA biosensor, as well as analysis by reference techniques, samples were pretreated by two different procedures (see Fig. 6.1). On the one hand, samples for the OA biosensor were clarified by Carrez precipitation [34]. A volume of 10 mL of fermentation sludge was mixed carefully with 2 mL of 0.68 M $K_4[Fe(CN)_6] \cdot 3\,H_2O$ and subsequently, 2 mL of 2 M $ZnCl_2$ were added and agitated again. Following, precipitation was induced by addition of 5 mL of 0.4 M NaOH and the final volume was adjusted to 20 mL with deionized water. Insoluble compounds were then separated by centrifugation and the clear supernatant was used for further investigations. For comparative studies, the concentration of ethanol, formate, D- and L-lactate was as well determined with commercial photometric kits (Megazyme International, Wicklow, Ireland) following the manufacturers' instructions. On the other hand, a diethyl ether extraction method was adopted for analysis of acetate and propionate by the VFA biosensor [14]. Therefore, 300 µL of the fermentation broth were mixed with 0.2 g NaCl, 50 µL concentrated HCl and 800 µL diethyl ether. Samples were briefly centrifuged and the ether phase was diluted into 600 µL sodium phosphate buffer pH 7.0. The content of VFA was additionally quantified by a gas chromatograph (GC-2010, Shimadzu, Duisburg, Germany) equipped with a poly ethylene glycol column (FS-FFAP-CB-0.25, CS-Chromatographie Service GmbH, Langerwehe, Germany) and a flame ionization detector.

The OA and VFA biosensors were also applied for the long-term monitoring of a lab-scale biogas reactor (CSTR-10S, Bioprocess Control AB, Lund, Sweden) with 0.01 m^3 working volume, equipped with a wall jacket and an external water bath [ICC basic pro 9, IKA (Staufen, Germany)] for operation at constant temperature (40 °C). The

continuously operated reactor received a daily feeding of approximately 60 g of sugar cane silage. Analysis of the biogas composition (CH_4 and CO_2) was performed online by an infrared sensor system (BlueSens, Herten, Germany) on a daily basis. The pH and FOS/TAC were determined offline once per week. During a period of two months, digestate samples (50 mL) were taken once a week, purified as described above and subsequently used for electrochemical analysis.

Prior application of the biosensors in real samples, calibration curves were obtained by monitoring the increase in the current signal after successive addition of a stock solution with defined concentration (each consisting of all analytes). Real samples were analyzed by subsequent titration to the reaction buffer, resulting in different dilutions. Based on the sensitivities of the calibration curves, the concentration of each analyte was calculated for each dilution step.

6.3 Results and discussion

6.3.1 Sensor characteristics

The sensor performances were characterized in terms of sensitivity and linear detection range by successive addition of standard solutions with defined concentrations of each analyte. In Figs. 6.3a,b the calibration curves of the OA and VFA biosensor are presented. The individual electrodes exhibited a linear relationship between current increase and analyte concentration. Table 6.1 summarizes the results obtained for both biosensors. The four analyte sensing elements of the OA biosensor had a similar linear detection range with a sensitivity from 0.64 to 1.16 µA mM^{-1}. Substantially, the different electrodes of the VFA biosensor possessed a sensitivity of 0.27 and 2.11 µA mM^{-1} for acetate and propionate, respectively. In literature, a propionate biosensor based on the same detection principle was reported, hereby, the enzymes were immobilized within a polymer of poly(vinyl alcohol) with styrylpyridinium groups (PVA-SbQ) [26]. This biosensor displayed a linear detection range of 10–100 µM with a sensitivity of 1.7 µA mM^{-1} cm^{-2}. With a normalized sensitivity of 42.9 µA mM^{-1} cm^{-2} the propionate electrode of the VFA biosensor shows an almost 25 times higher sensitivity over a broader linear range.

Only few electrochemical enzyme-based acetate biosensors are mentioned in literature.

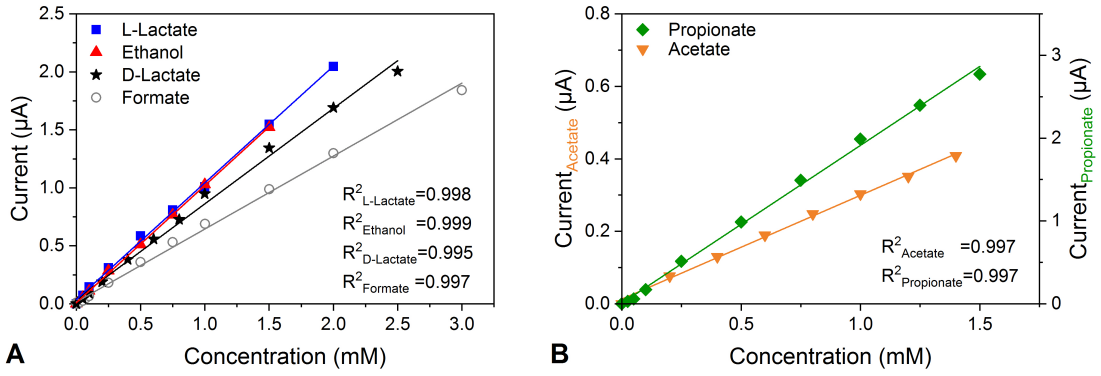

Fig. 6.3: Calibration curves of the organic acid **(a)** and the volatile fatty acid biosensor **(b)**.

Tab. 6.1: Sensor characteristics of the volatile fatty acid (VFA) and organic acid (OA) biosensor operated at an applied potential of +0.6 and +0.3 V *vs.* Ag/AgCl, respectively.

Biosensor	Analyte	Sensitivity ($\mu A\,mM^{-1}$)	Linear range (mM)
VFA	Propionate	2.11 ± 0.41	0–1.5
VFA	Acetate	0.27 ± 0.05	0–1.4
OA	D-Lactate	0.89 ± 0.03	0–2.5
OA	L-Lactate	1.16 ± 0.06	0–2.0
OA	Formate	0.64 ± 0.02	0–3.0
OA	Ethanol	1.12 ± 0.03	0–1.5

One of them was also a tri-enzyme system, consisting of AK, PK and POx, which were entrapped on the platinum electrode in a membrane of polydimethylsiloxane (PDMS) [24]. Measurements were performed at an applied potential of −0.4 V *vs.* Ag/AgCl for monitoring of the oxygen consumption. Under this condition, a linear correlation between current signal and acetate concentration was obtained in a narrow range of 5 µM to 0.5 mM compared to the VFA biosensor of the present study (0.2–1.4 mM).

6.3.2 Evaluation of interferences

Given the complex chemical composition of biogas sludges, interfering effects of different substances were investigated prior to application of the sensors in real samples. The examined compounds were selected according to the substrate spectrum of the employed enzymes and potential occurrence in the fermentation broth. In each measurement, the respective compound was added individually to the reaction buffer and substrate-related current changes were determined. All tests were conducted in triplicate. Table 6.2 summarizes the results of the influence of potential interferents on the sensor response of both biosensors. Obtained current responses were normalized against current signals monitored for the intended substrate.

The selectivity of the VFA biosensor was investigated by introduction of 0.5 mM substrate to the reaction mixture. Several different short-chain fatty acids were deployed for cross-sensitivity tests with the propionate-sensing electrode. Relevant current changes were solely observed for butyrate (28%), a natural substrate for PCT [32] and, in the activated form (butyryl-CoA), for SCAOx [27]. However, the combination of both enzymes strongly favors the enzymatic conversion of propionate (100%), which is consistent with data from the literature describing a propionate electrode and a photometric assay based on the same enzyme cascade [26, 35].

The concentration and specific ratio of volatile fatty acids in a biogas reactor is highly dependent on the feedstock and type of digestion. Although butyric acid is usually present in the biogas broth, and thus both substrates compete for the same catalytic binding site of the PCT, typical concentrations of this fatty acid are decisively lower compared to propionate [36]. Therefore, the usual ratio of the acids on the one hand and the affinity of the biosensor for the specific substrates on the other hand favor the detection of propionate in the fermentation broth. In addition, due to the

Tab. 6.2: Effect of potential interferents on the different electrodes of the volatile fatty acid (VFA) and organic acid (OA) biosensor. Change in the current signal was normalized to the current obtained for the intended substrate (-: not evaluated).

	VFA biosensor		OA biosensor				
Interferent	Acetate (%)	Propionate (%)	D-Lactate (%)	L-Lactate (%)	Formate (%)	Ethanol (%)	BSA blank (%)
Acetate	100	0	-	-	0	0	0
Propionate	6	100	-	-	0	0	0
D-Lactate	-	-	100	0	0	0	0
L-Lactate	-	-	0	100	0	0	0
Formate	3	-	0	0	100	0	0
Ethanol	0	-	0	0	0	100	0
Pyruvate	117	-	0	0	0	0	0
Malate	-	-	9	12	4	7	0
Butyrate	0	28	-	-	0	-	0
Valerate	-	1	-	-	-	-	0
Capronate	-	0	-	-	-	-	0
Glycerol	0	-	-	-	-	-	0
n-Propanol	-	-	-	-	-	61	0
n-Butanol	-	-	-	-	-	43	0
Methanol	-	-	-	-	0	0	0
Ascorbate	-	-	75	53	-	-	100
Cysteine	-	-	36	29	-	-	65
Urea	-	-	1	1	-	-	6

thermodynamic unfavorable conditions for propionate degradation, the short-chain fatty acid persists longer in the fermentation broth than other volatile fatty acids and is therefore regarded as a reliable indicator for process monitoring [6].

The acetate-sensing electrode was also subjected to interference study using potential AK substrates (propionate, formate, ethanol, butyrate, and glycerol) and pyruvate, the main substrate of POx. While no signal response was observed with ethanol, butyrate and glycerol, slight current increase was monitored for propionate (6%) and formate (3%). Interference with propionic acid was likewise reported by different acetate biosensors using AK [24, 37]. Nevertheless, our findings suggest a clear preference of AK for acetate over the other substrates tested. Apart from this, both substrates are naturally not present to the same extent and the propionate concentration is significantly lower as compared to acetate [9]. Cross-sensitivity with propionate thereby has rather little effect on the amperometric acetate detection. Not surprisingly, the acetate sensor showed the highest sensor response upon addition of pyruvate (117%). However, as intermediate of several metabolic pathways [38], pyruvate degrades rapidly and thus extracellular concentrations of the POx substrate are negligible compared to the acetate levels in the biogas medium. Previous studies on the accumulation of extracellular metabolites from *E. coli* under anaerobic conditions showed only minimal levels of pyruvic acid compared to the concentration of acetate and other acids [39, 40].

Evaluation of possible susceptibility of the OA biosensor to potential interferents was accomplished by observing the change in current signal after addition of several substrates (each 1 mM) to the measurement solution. Both lactate electrodes exhibited sensitivity towards ascorbate, cysteine and to some small extent to urea. All of these compounds are known reducing agents at the applied positive working potentials [41, 42]. For this

reason, an increase in the current signal was observed for the electrode covered with BSA. The ethanol electrode was also sensitive to other alcohols, namely n-propanol (61%) and n-butanol (43%). This interference is mainly caused by the broad substrate spectrum of the applied ADH from *S. cerevisiae* [43]. The substrate specificity of electrochemical ethanol biosensors is generally a great challenge, since detection principles based on the enzyme alcohol oxidase show this characteristic behavior, too [44].

Due to the substrate range of AK on the one hand and the PCT-catalyzed formation of acetate from acetyl-CoA on the other hand, potential cross-talk between the two VFA electrodes was investigated by successive addition of the analytes. As depicted in Fig. 6.4, only the corresponding electrode showed a current response upon introduction of the substrate. Similarly, no inadvertent interactions were observed for simultaneous determination of ethanol, formate, D- and L-lactate with the OA biosensor as described earlier [19].

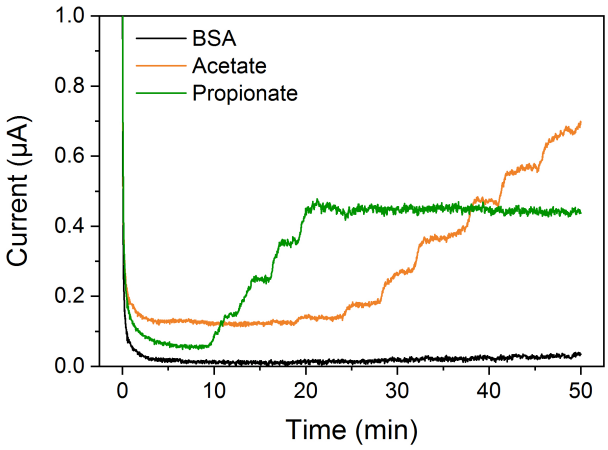

Fig. 6.4: Chronoamperometric measurement with the VFA biosensor in 100 mM potassium phosphate buffer (pH 7.0) with 5 mM $MgCl_2$, 0.6 mM TPP, 0.02 mM FAD, 2 mM PEP, 1 mM ATP and 0.4 mM acetyl-CoA, 11.8 U PK and 2.5 U AK. Cross-talk free behavior is demonstrated by subsequent addition of propionate and acetate, respectively.

6.3.3 Evaluation of sensor performance in spiked samples

For evaluation of the sensor performance in real samples and complex matrices, sludge samples from three different biogas plants (BP1 to BP3) were collected. Biogas production in BP1 was achieved by mono-digestion of maize silage, whereas in BP2 additionally cattle slurry was applied. The feedstock of BP3 consisted of maize silage, cattle slurry and manure. The type of feedstock used for anaerobic digestion mainly influences the viscosity of the fermentation broth. In order to test the biosensors in various media compositions, biogas plants with different feedstocks were selected. After sampling, fermentation sludges were spiked with 20 mM acetate, 5 mM propionate and each 10 mM ethanol, formate, D- and L-lactate, respectively. The concentration of VFA and OA was determined with the two biosensors and for comparative studies by gas chromatography and commercial photometric kits. Figure 6.5 provides a comparison of the results

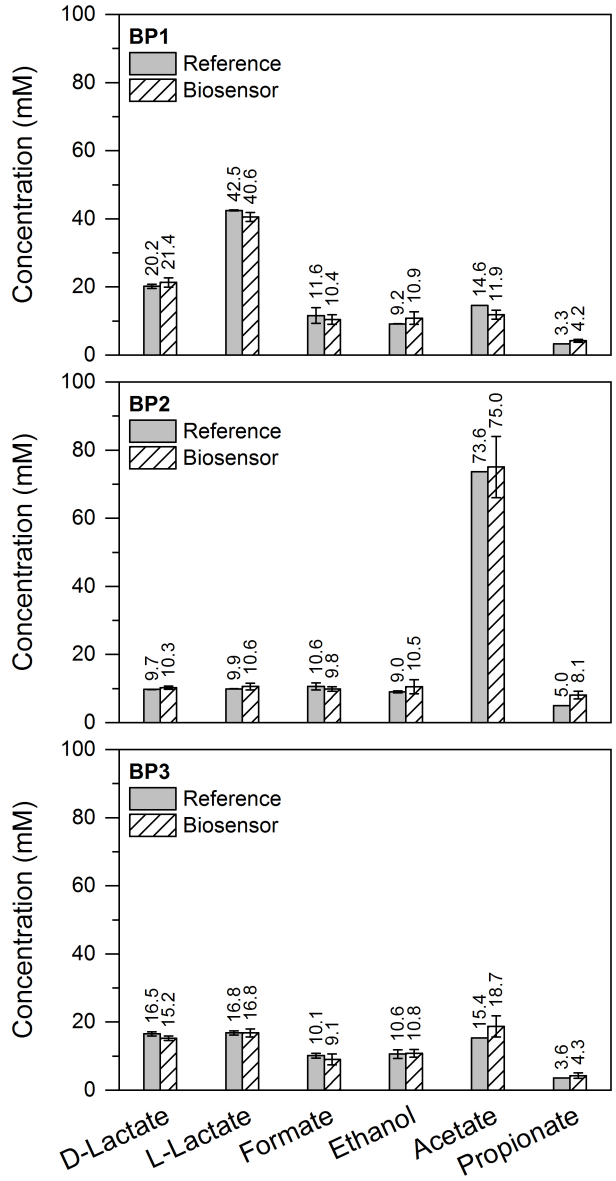

Fig. 6.5: Comparison between the results obtained by the two biosensors and the corresponding reference technique. Samples were collected from three different biogas plants (BP1, BP2, BP3) and spiked with 20 mM acetate, 5 mM propionate and 10 mM ethanol, formate, D- and L-lactate. For detection of ethanol, formate, D- and L-lactate a photometric reference technique was applied, and acetate and propionate were additionally quantified by gas chromatography.

obtained by the biosensors and reference techniques. For all three samples, the amperometrically determined concentrations correlate well with the corresponding conventional method. These findings demonstrate successfully the potential of simultaneous and rapid monitoring of several analytes in complex media by application of the electrochemical hybrid biosensor system.

6.3.4 Monitoring of a lab-scale biogas reactor

The formation of biogas from organic matter is a complex procedure carried out by a consortium of different microorganisms. It involves four phases: hydrolysis, acidogenesis, acetogenesis and methanogenesis. In the first step, complex polymers, like carbohydrates, fats and proteins are degraded into smaller molecules. Hydrolysis is followed by the acid-forming step, the acidogenesis. At this stage, the fermenting bacteria produce volatile fatty acids, alcohols as well as H_2, CO_2, and NH_4. Then, acetogenic and syntrophic bacteria metabolize fatty acids and alcohols into acetate, H_2 and CO_2. Finally, acetate and hydrogen are used by methanogenic archaea to produce CH_4 and CO_2. In an anaerobic digester, these four processes occur concurrently. In order to successfully maintain the biogas production, suitable detection systems for specific key parameters are required. Therefore, the developed hybrid biosensor system was applied for the long-term monitoring of a lab-scale biogas reactor ($0.01\,m^3$), operated at mesophilic conditions ($40\,°C$) with sugar cane silage as feedstock. Besides the concentration of OA and VFA, also several physical- and chemical parameters were investigated for a period of two months.

Figure 6.6 provides an overview of all the data obtained in this time frame. The content of CH_4 and CO_2 in the produced biogas was analyzed online. Basically, the biogas composition was stable during the first 44 days with $53.7 \pm 2.7\%$ and $39.0 \pm 7.8\%$ of CH_4 and CO_2, respectively (Fig. 6.6a). These quantities represent typical values

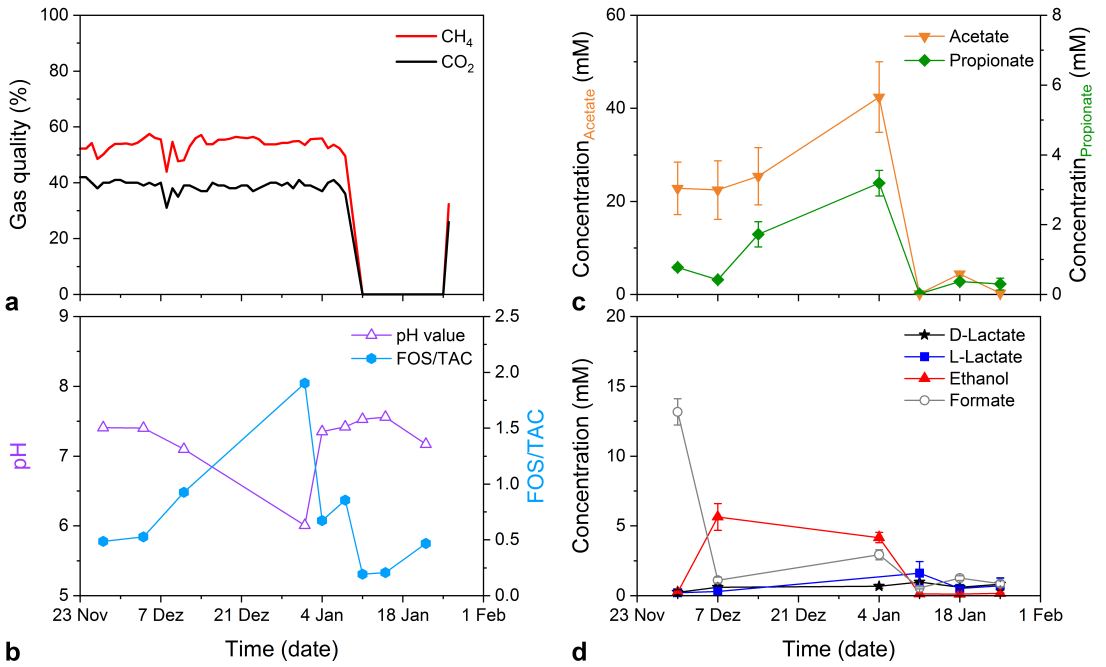

Fig. 6.6: Reactor performance of a lab-scale biogas reactor. Online monitoring of gas quality (CH_4 and CO_2) **(a)**. pH and FOS/TAC were analyzed offline **(b)**. Concentration of volatile fatty acids (acetate and propionate) **(c)** and organic acids (ethanol, formate, D- and L-lactate) **(d)** measured with the VFA and OA biosensor, respectively.

reported in literature [45]. Between day 45 and 47 the fermenter was temporarily shut down for technical reasons, which is reflected in the sudden loss of CH_4 and CO_2 release. Biogas production was resumed 5 days after restart of the digester. In addition to end-product determination, the ratio of volatile fatty acid to total alkalinity (FOS/TAC) and pH are regularly monitored process parameters and are here depicted in Fig. 6.6b. While the pH optimum is typically defined between 6.5–7.5, opinions vary regarding optimum VFA concentrations and thus FOS/TAC levels, but agree on the fact, that normal VFA levels highly depend on the individual system [36, 46]. Therefore, stable concentrations are considered more substantial than the magnitude [47]. During the observed period, FOS/TAC concentrations fluctuated between 0.5–1.0 until fermenter stoppage with one peak at day 36. This sudden increase was accompanied with a drop in pH, caused by acidification of the medium due to VFA accumulation. This change in the acid composition was detectable with the hybrid biosensor, too. As depicted in Fig. 6.6c, acetate and propionate concentrations, which have a decisive impact on FOS/TAC, showed a similar curve progress during the observed time frame. Minor changes in organic acid and alcohol content were detected by the OA sensor, too. For each measurement point, samples were also analyzed using the conventional techniques as described in Sec. 6.3.3. Again, our findings were in good agreement with the reference methods (data not shown). The results demonstrate a successful long-term application of the hybrid biosensor system for monitoring of acid composition changes. The detection of essential precursors and intermediates of the anoxic food chain, realized by the OA sensor, is a useful extension to established process parameters, as these are usually not covered by conventional monitoring systems. The combined determination of the different acids leads to an improved understanding of the events that occur during fermentation. Thus, potential bottlenecks of the process can be identified and eliminated immediately.

6.4 Conclusion

Nowadays, monitoring of organic and volatile fatty acids in anaerobic fermentation processes is only feasible by laborious techniques, such as HPLC or GC. The analysis by these methods, however, is time-consuming and results are typically provided with some delay after sampling. In this study, two different enzyme-based biosensors were demonstrated as a hybrid system for amperometric detection of several process-relevant intermediates: on the one hand, an OA biosensor for simultaneous determination of ethanol, formate, D- and L-lactate, and on the other hand, a VFA biosensor for electrochemical quantification of acetate and propionate. The effect of various potential interferents on the sensor signal of both biosensors was investigated and results revealed only limited cross-sensitivity. The acetate electrode showed 6% response to propionate and the propionate-sensing electrode was sensitive to other volatile fatty acids (28% and 1% to butyrate and valerate, respectively). The ethanol sensor displayed sensitivity to other alcohols, such as n-propanol (61%) and n-butanol (43%). Nevertheless, both biosensors showed satisfactory cross-talk behavior and the potential for practical application in complex matrices was demonstrated. These findings were also verified by evaluation of the sensor performance in spiked samples of fermentation broth from

different biogas plants. A good correlation was obtained between the biosensors and conventional reference techniques. Additionally, the electrochemical biosensor system was used for the first time for long-term monitoring of the acid composition in a lab-scale biogas reactor. Application of such a device would greatly enhance the overall understanding of complex fermentation processes. In comparison to traditional analytical procedures, the presented hybrid biosensor system offers facile, rapid and on-site determination of multiple acids, due to a portable measurement set-up.

Future work will focus on the development of a common procedure for sample preparation, which is suitable for all analytes and both biosensors. In this regard, usage of the crude extract for the electrochemical measurements is envisaged, so that sample pretreatment is not required at all. Application of such a compact monitoring device for determination of acetate, propionate, ethanol, formate, D- and L-lactate would enable early detection of imbalances in anaerobic fermentation processes. Moreover, the broad substrate spectrum of SCAOx allows a future extension of the system by substitution of PCT with other enzymes providing activated short fatty acids. Therefore, the combination of butyrate-specific enzymes with SCAOx would permit a more precise determination of the VFA content in the biogas reactor.

Acknowledgements

The authors thank H. Iken for fabrication of the sensor chips. We also acknowledge S. Jansen and G. Pohen from the Institute NOWUM-Energy for operating the lab-scale bioreactor, supplying the monitoring data (gas quality, pH and FOS/TAC) and performing gas chromatography analyses. D.L. Röhlen and J. Pilas thank FH Aachen for the Ph.D. scholarship.

References

[1] Angelidaki, I.; Ellegaard, L. (2003) Codigestion of manure and organic wastes in centralized biogas plants: Status and future trends. *Appl. Biochem. Biotechnol.* 109:95–106, doi:10.1385/ABAB:109:1-3:95.

[2] Komemoto, K.; Lim, Y. G.; Nagao, N.; Onoue, Y.; Niwa, C.; Toda, T. (2009) Effect of temperature on VFA's and biogas production in anaerobic solubilization of food waste. *Waste Manag.* 29:2950–2955., doi:10.1016/j.wasman.2009.07.011.

[3] Weiland, P. (2010) Biogas production: Current state and perspectives. *Appl. Microbiol. Biotechnol.* 85:849–860, doi:10.1007/s00253-009-2246-7.

[4] Andriani, D.; Wresta, A.; Atmaja, T. D.; Saepudin, A. (2014) A review on optimization production and upgrading biogas through CO_2 removal using various techniques. *Appl. Biochem. Biotechnol.* 172:1909–1928, doi:10.1007/s12010-013-0652-x.

[5] Achinas, S.; Achinas, V.; Euverink, G.J.W. (2017) A technological overview of biogas production from biowaste. *Engineering* 3:299–307, doi:10.1016/J.ENG.2017.03.002.

[6] Nielsen, H.; Uellendahl, H.; Ahring, B.K. (2007) Regulation and optimization of the biogas process: Propionate as a key parameter. *Biomass Bioenergy* 31:820–830, doi:10.1016/j.biombioe.2007.04.004.

[7] Boe, K.; Batstone, D.J.; Steyer, J.-P.; Angelidaki, I. (2010) State indicators for monitoring the anaerobic digestion process. *Water Res.* 44:5973–5980, doi:10.1016/j.watres.2010.07.043.

[8] Li, L.; He, Q.; Wei, Y.; He, Q.; Peng, X. (2014) Early warning indicators for monitoring the process failure of anaerobic digestion system of food waste. *Bioresour. Technol.* 171:491–494, doi:10.1016/j.biortech.2014.08.089.

[9] Montag, D.; Schink, B. (2016) Biogas process parameters – energetics and kinetics of secondary fermentations in methanogenic biomass degradation. *Appl. Microbiol. Biotechnol.* 100:1019–1026, doi:10.1007/s00253-015-7069-0.

[10] Diamantis, V.; Melidis, P.; Aivasidis, A. (2006) Continuous determination of volatile products in anaerobic fermenters by on-line capillary gas chromatography. *Anal. Chim. Acta* 573-574:189–194, doi:10.1016/j.aca.2006.05.036.

[11] Falk, H.M.; Reichling, P.; Andersen, C.; Benz, R. (2015) Online monitoring of concentration and dynamics of volatile fatty acids in anaerobic digestion processes with mid-infrared spectroscopy. *Bioprocess. Biosyst. Eng.* 38:237–249, doi:10.1007/s00449-014-1263-9.

[12] Stockl, A.; Lichti, F. (2018) Near-infrared spectroscopy (NIRS) for a real time monitoring of the biogas process. *Bioresour. Technol.* 247:1249–1252, doi:10.1016/j.biortech.2017.09.173.

[13] Zumbusch, P.v.; Meyer-Jens, T.; Brunner, G.; Märkl, H. (1994) On-line monitoring of organic substances with high-pressure liquid chromatography (HPLC) during the anaerobic fermentation of waste-water. *Appl. Microbiol. Biotechnol.* 42:140–146, doi:10.1007/BF00170237.

[14] Schiffels, J.; Baumann, M.E.M.; Selmer, T. (2011) Facile analysis of short-chain fatty acids as 4-nitrophenyl esters in complex anaerobic fermentation samples by high performance liquid chromatography. *J. Chromatogr. A* 1218:5848–5851, doi:10.1016/j.chroma.2011.06.093.

[15] Goriushkina, T.B.; Soldatkin, A.P.; Dzyadevych, S.V. (2009) Application of amperometric biosensors for analysis of ethanol, glucose, and lactate in wine. *J. Agric. Food. Chem.* 57:6528–6535, doi:10.1021/jf9009087.

[16] Rathee, K.; Dhull, V.; Dhull, R.; Singh, S. (2016) Biosensors based on electrochemical lactate detection: A comprehensive review. *Biochem. Biophys. Rep.* 5:35–54, doi:10.1016/j.bbrep.2015.11.010.

[17] Pipyn, P.; Verstraete, W. (1981) Lactate and ethanol as intermediates in two-phase anaerobic digestion. *Biotechnol. Bioeng.* 23:1145–1154, doi:10.1002/bit.260230521.

[18] Crable, B.R.; Plugge, C.M.; McInerney, M.J.; Stams, A.J.M. (2011) Formate formation and formate conversion in biological fuels production. *Enzyme Res.*

2011:1–8, doi:10.4061/2011/532536.

[19] Pilas, J.; Yazici, Y.; Selmer, T.; Keusgen, M.; Schöning, M.J. (2017) Optimization of an amperometric biosensor array for simultaneous measurement of ethanol, formate, D- and L-lactate. *Electrochim. Acta* 251:256–262, doi:10.1016/j.electacta.2017.07.119.

[20] Kaur, A.; Kim, J.R.; Michie, I.; Dinsdale, R.M.; Guwy, A. J.; Premier, G.C. (2013) Microbial fuel cell type biosensor for specific volatile fatty acids using acclimated bacterial communities. *Biosens. Bioelectron.* 47:50–55, doi:10.1016/j.bios.2013.02.033.

[21] Jin, X.; Li, X.; Zhao, N.; Angelidaki, I.; Zhang, Y. (2017) Bio-electrolytic sensor for rapid monitoring of volatile fatty acids in anaerobic digestion process. *Water Res.* 111:74–80, doi:10.1016/j.watres.2016.12.045.

[22] Sweeney, J.B.; Murphy, C.D.; McDonnell, K. (2018) Development of a bacterial propionate biosensor for anaerobic digestion. *Enzyme Microb. Technol.* 109:51–57, doi:10.1016/j.enzmictec.2017.09.011.

[23] Schievano, A.; Colombo, A.; Cossettini, A.; Goglio, V.; D'Ardes, V.; Trasatti, S.; Cristiani P. (2018) Single-chamber microbial fuel cells as on-line shock-sensors for volatile fatty acids in anaerobic digesters. *Waste Manage.* 71:785–791, doi:10.1016/j.wasman.2017.06.012.

[24] Mizutani, F.; Sawaguchi, T.; Yabuki, S.; Iljima, S. (2001) Amperometric determination of acetic acid with a trienzyme/poly(dimethylsiloxane)-bilayer-based sensor. *Anal. Chem.* 73:5738–5742, doi:10.1021/ac010622i.

[25] Mieliauskiene, R.; Nistor, M.; Laurinavicius, V.; Csöregi, E. (2006) Amperometric determination of acetate with a tri-enzyme based sensor. *Sens. Actuators B Chem.* 113:671–676, doi:10.1016/j.snb.2005.07.016.

[26] Sode, K.; Tsugawa, W.; Aoyagi, M.; Rajashekhara, E.; Watanabe, K. (2008) Propionate sensor using coenzyme-A transferase and acyl-CoA oxidase. *Protein Peptide Lett.* 15:779–781, doi:10.2174/092986608785203737.

[27] Hayashi, H.; de Bellis, L.; Ciurli, A.; Kondo, M.; Hayashi, M.; Nishimura, M. (1999) A novel acyl-CoA oxidase that can oxidize short-chain acyl-CoA in plant peroxisomes. *J. Biol. Chem.* 274:12715–12721., doi:10.1074/jbc.274.18.12715.

[28] Bijtenhoorn, P. (2005) β-Alanin-CoA-Transferase aus *Clostridium propionicum*. *Diploma thesis*, Philipps University Marburg, Marburg.

[29] Röhlen, D.L.; Pilas, J.; Schöning, M.J.; Selmer, T. (2017) Development of an amperometric biosensor platform for the combined determination of L-malic, fumaric, and L-aspartic acid. *Appl. Biochem. Biotechnol.* 183:566–581, doi:10.1007/s12010-017-2578-1.

[30] Baltazar, M.F.; Dickinson, F.M.; Ratledge, C. (1999) Oxidation of medium-chain acyl-CoA esters by extracts of *Aspergillus niger*: Enzymology and characterization of intermediates by HPLC. *Microbiol.* 145:271–278, doi:10.1099/13500872-145-1-271.

[31] Werner, W.; Rey, H.-G.; Wielinger, H. (1970) Über die Eigenschaften eines neuen

Chromogens für die Blutzuckerbestimmung nach der GOD/POD-Methode. *Z. Anal. Chem.* 252:224–228, doi:10.1007/BF00546391.

[32] Selmer, T.; Willanzheimer, A.; Hetzel, M. (2002) Propionate CoA-transferase from *Clostridium propionicum*: Cloning of the gene and identification of glutamate 324 at the active site. *Eur. J. Biochem.* 269:372–380, doi:10.1046/j.0014-2956.2001.02659.x.

[33] Pilas, J.; Yazici, Y.; Selmer, T.; Keusgen, M.; Schöning, M.J. (2018) Application of a portable multi-analyte biosensor for organic acid determination in silage. *Sensors* 18(5):1470, doi:10.3390/s18051470.

[34] Carrez, M.C. (1908) Le ferrocyanure de potassium et l'acétate de zinc comme agents de défécation des urines. *Ann. Chim. Anal.* 13(286):97–101.

[35] Rajashekhara, E.; Hosoda, A.; Sode, K.; Ikenaga, H.; Watanabe, K. (2006) Lactate and ethanol as intermediates in two-phase anaerobic digestion. *Biotechnol. Prog.* 22:334–337, doi:10. 468 1021/bp050240o.

[36] Franke-Whittle, I.H.; Walter, A.; Ebner, C.; Insam, H. (2014) Investigation into the effect of high concentrations of volatile fatty acids in anaerobic digestion on methanogenic communities. *Waste Manage.* 34:2080–2089, doi:10.1016/j.wasman.2014.07.020.

[37] Tang, X.-J.; Johansson, G. (1997) A bioelectrochemical method for the determination of acetate with immobilized acetate kinase. *Anal. Lett.* 30:2469–2483, doi:10.1080/00032719708001758.

[38] Zhou, M.; Yan, B.; Wong, J.W.C.; Zhang, Y. (2018) Enhanced volatile fatty acids production from anaerobic fermentation of food waste: A mini-review focusing on acidogenic metabolic pathways. *Bioresour. Technol.* 248:68–78, doi:10.1016/j.biortech.2017.06.121.

[39] Kim, T.S.; Jung, H.M.; Kim, S.Y.; Zhang, L.; Li, J.; Sigdel, S.; Park, J.H.; Haw, J.R.; Lee J.K. (2015) Reduction of acetate and lactate contributed to enhancement of a recombinant protein production in *E. coli* BL21. *J. Microbiol. Biotechnol.* 25(7):1093–1100, doi:10.4014/jmb.1503.03023.

[40] Yasid, N.A.; Rolfe, M.D.; Green, J.; Williamson, M.P. (2016) Homeostasis of metabolites in *Escherichia coli* on transition from anaerobic to aerobic conditions and the transient secretion of pyruvate. *R. Soc. Open Sci.* 3:1–12, doi:10.1098/rsos.160187.

[41] Sprules, S.D.; Hart, J.P.; Wring, S.A.; Pittson, R. (1995) A reagentless, disposable biosensor for lactic acid based on a screen-printed carbon electrode containing Meldola's Blue and coated with lactate dehydrogenase, NAD^+ and cellulose acetate. *Anal. Chim. Acta* 304:17–24, doi:10.1016/0003-2670(94)00565-4.

[42] Palmisano, F.; Rizzi, R.; Centonze, D.; Zambonin, P.G. (2000) Simultaneous monitoring of glucose and lactate by an interference and cross-talk free dual electrode amperometric biosensor based on electropolymerized thin films. *Biosens. Bioelectron.* 15:531–539., doi:10.1016/S0956-5663(00)00107-X.

[43] Plapp, B.V.; Green, D.W.; Sun, H.-W.; Park, D.-H.; Kim, K. (1993) Substrate

Specificity of Alcohol Dehydrogenases. In: Weiner,H.; Crabb, D.W., Flynn; T.G. (Eds.) Enzymology and Molecular Biology of Carbonyl Metabolism. 4. Advances in Experimental Medicine and Biology, Vol. 328. Boston: *Springer*, doi:10.1007/978-1-4615-2904-0_41.

[44] Azevedo, A.M.; Prazeres, D.M.F.; Cabral, J.S.; Fonseca, L.P. (2005) Ethanol biosensors based on alcohol oxidase. *Biosens. Bioelectron.* 21:235–247, doi:10.1016/j.bios.2004.09.030.

[45] Herout, M.; Malaták, J.; Kucera, L.; Dlabaja, T. (2011) Biogas composition depending on the type of plant biomass used. *Res. Agr. Eng.* 57:137–143, doi:10.17221/41/2010-RAE.

[46] Angelidaki, I.; Ellegaard, L.; Ahring, B. K. (1993) A mathematical model for dynamic simulation of anaerobic digestion of complex substrates: Focusing on ammonia inhibition. *Biotechnol. Bioeng.* 42:159–166, doi:10.1002/bit.260420203.

[47] Hamawand, I.; Baillie, C. (2015) Anaerobic digestion and biogas potential: Simulation of lab and industrial-scale processes. *Energies* 8:454–474, doi:10.3390/en8010454.

7 Screen-printed carbon electrodes modified with graphene oxide for the design of a reagent-free NAD^+-dependent biosensor array

***Analytical Chemistry* (2019), 91:15293–15299**

J. Pilas[1,2], T. Selmer[1], M. Keusgen[2] and M.J. Schöning[1,3]

[1] Institute of Nano- and Biotechnologies (INB), FH Aachen, Jülich, Germany
[2] Institute of Pharmaceutical Chemistry, Philipps-Universität Marburg, Marburg, Germany
[3] Institute of Complex Systems 8 (ICS-8), Forschungszentrum Jülich, Jülich, Germany

Submitted: 10-01-2019; Accepted: 11-01-2019; Published: 11-01-2019

https://doi.org/10.1021/acs.analchem.9b04481

Abstract

A facile approach for the construction of reagent-free electrochemical dehydrogenase-based biosensors is presented. Enzymes and cofactors (NAD^+ and $Fe(CN)_6^{3-}$) were immobilized by modification of screen-printed carbon electrodes with graphene oxide (GO) and an additional layer of cellulose acetate. The sensor system was exemplarily optimized for an L-lactate electrode in terms of GO concentration, working potential, and pH value. The biosensor exhibited best characteristics at pH 7.5 in 100 mM potassium phosphate buffer at an applied potential of +0.250 V *vs.* an internal pseudo Ag reference electrode. Thereby, sensor performance was characterized by a linear working range from 0.25 to 4 mM and a sensitivity of 0.14 µA mM^{-1}. The detection principle was additionally evaluated with three other dehydrogenases (D-lactate dehydrogenase, alcohol dehydrogenase, and formate dehydrogenase, respectively). The developed reagentless biosensor array enabled simultaneous and cross-talk free determination of L-lactate, D-lactate, ethanol, and formate.

7.1 Introduction

Nicotinamide adenine dinucleotide (NAD^+) plays an important role as an oxidizing agent in many central metabolic pathways. Thereby, the cofactor is involved in the electron transfer of dehydrogenase-catalyzed reactions [1]. Due to the great number of potentially available NAD^+-dependent dehydrogenases for a variety of analytes, this group of enzymes has been of special interest for the design of electrochemical biosensors within the last decades [2, 3]. However, application of these enzymes, as biological recognition elements, is characterized by two main restrictions [4]. On the one hand, high overpotentials are required for direct oxidation of NADH, causing interference by oxidation of other electroactive species and electrode fouling [5]. Different approaches for a mediated electron transfer are reported in literature in order to diminish this aspect by use of mediator compounds [6, 7] or enzymes, like NADH oxidase [8, 9] or diaphorase [10, 11]. On the other hand, dehydrogenase-based biosensors depend on the permanent presence of the cofactor NAD^+. This circumstance makes the design of such devices more challenging. For this reason, great efforts have been made for the construction of reagent-free systems. Efficient coimmobilization of enzymes, cofactors, and mediators has been described with, for example, functionalized carbon nanotubes [12–14], entrapment in carbon pastes [15, 16], membranes [17, 18], polypyrrol [19, 20], or chitosan films [21, 22].

Generally, research in this area focuses mainly on the development of single-analyte biosensors. For clinical, pharmaceutical, and environmental samples, however, often the simultaneous detection of more metabolites is of interest [23, 24]. In this regard, application of arrays for several analytes seems advantageous.

Screen-printing technology facilitates cost-efficient production of disposable biosensing systems with the potential of flexible array design [25, 26]. An amperometric biosensor for simultaneous determination of glucose and lactate was, for example, realized by modification of screen-printed carbon electrodes (SPCEs) with glucose oxidase and lactate oxidase, respectively [27]. Consideration of cross-talk effects is crucial for the

fabrication of multi-analyte devices. In order to minimize this aspect, two different sensing strategies have been used for dual monitoring of glucose and lactate by immobilizing glucose dehydrogenase and lactate oxidase on the working electrodes [28]. Additionally, the electrode surfaces were modified with graphene oxide (GO) for improvement of the electron transfer. Numerous studies have demonstrated the enhanced electrocatalytic activity of electrochemical biosensors functionalized with this biocompatible nanomaterial [29, 30].

Our group recently presented different multi-parameter biosensors based on platinum thin-film electrodes for detection of various analytes [31–34]. However, these systems still depend on addition of the cofactor NAD^+ to the measurement solution. The present work describes a facile approach for the development of reagentless dehydrogenase-based biosensors using SPCEs modified with GO and nafion (Fig. 7.1). The system was evaluated using the example of an L-lactate dehydrogenase for construction of an electrochemical L-lactate electrode. The sensor performance was optimized with regard to the GO concentration, applied working potential, and pH value of the buffer solution. Additionally, the proposed sensor platform was examined with other dehydrogenases. In this way, a multi-analyte biosensor array for simultaneous and cross-talk free determination of the metabolites L-lactate, D-lactate, ethanol, and formate was designed.

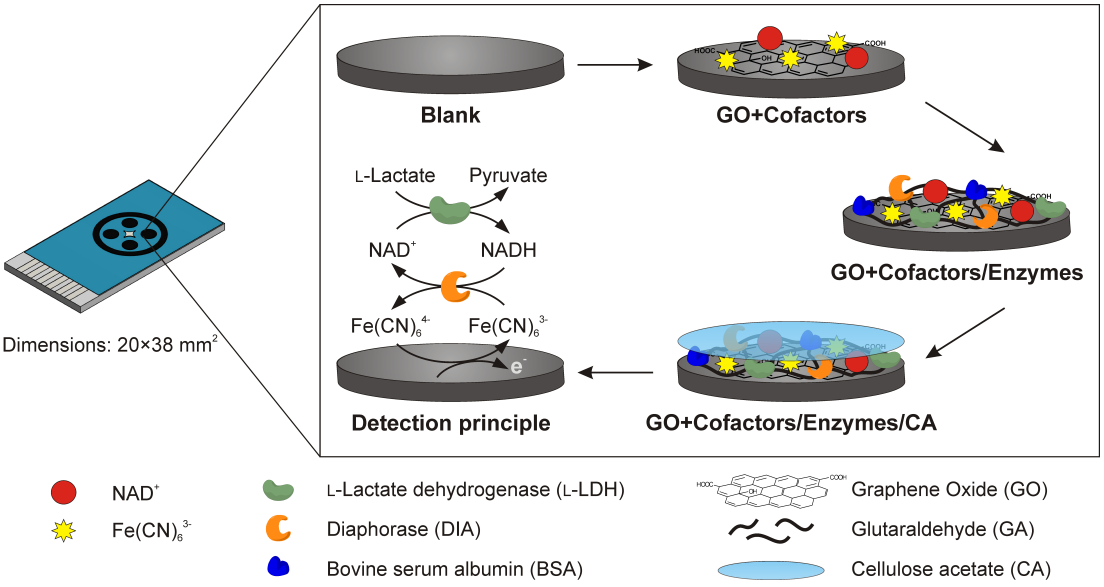

Fig. 7.1: Schematic illustration of the multi-analyte screen-printed carbon biosensor array. Extension shows exemplarily for the L-lactate sensor the different modification steps of the electrode surface and the detection principle.

7.2 Experimental

7.2.1 Chemicals and solutions

Bovine serum albumin (BSA), cellulose acetate (CA), ethanol, glutaraldehyde (GA, 25% in H_2O), glycerol, graphene oxide (GO, 4 mg mL^{-1} in H_2O), nafion, potassium ferricyanide ($K_3[Fe(CN)_6]$) and sodium D-lactate were obtained from Sigma-Aldrich. The cofactor NAD^+ and the substrates sodium formate and sodium L-lactate were purchased from AppliChem. Buffer components (K_2HPO_4, KH_2PO_4, and Tris-HCl) were from Carl Roth.

The enzymes alcohol dehydrogenase (ADH, 310 U mg^{-1} from *Saccharomyces cerevisiae*), diaphorase (DIA, 51 U mg^{-1} from *Clostridium kluyveri*), formate dehydrogenase (FDH, 0.49 U mg^{-1} from *Candida boidinii*), D-lactate dehydrogenase (D-LDH, 213 U mg^{-1} from *Lactobacillus leichmanii*) and L-lactate dehydrogenase (L-LDH, 174.5 U mg^{-1} from *Bacillus stearothermophilus*) were supplied from Sigma-Aldrich. All enzyme solutions were prepared in potassium phosphate buffer (100 mM, pH 7.5) and the enzymatic activity was determined photometrically in solution as described earlier [35]. Enzyme loadings mentioned refer to the total amount of enzyme immobilized on the electrode surface.

7.2.2 Sensor modification

Screen-printed carbon array electrodes were purchased from DropSens (ref 4W110). The sensor displayed four WEs (each Ø 2.95 mm) sharing one common carbon counter electrode (CE) and a silver pseudoreference electrode (RE). Figure 7.1 shows a schematic illustration of the sensor layout and the different steps used for construction of a reagentless dehydrogenase-based L-lactate biosensor. Prior to modification, the sensor surface was electrochemically activated at +1.4 V for 240 sec in 100 mM KCl [36]. GO (1.25 mg mL^{-1}) was dispersed in 100 mM potassium phosphate buffer (pH 7.5) by ultrasonication for 30 min and afterward, mixed with the cofactors (10 mM NAD^+, 20 mM $K_3[Fe(CN)]_6$) and 0.625% nafion. 4 µL of this solution were dropped on the electrode surface, and air-dried at room temperature. In the next step, the electrode was modified with the enzymes (1.5 U L-LDH and 6.0 U DIA). For improved enzyme immobilization within the GO matrix, the solution was enriched with 0.3% GA and 2% BSA. Finally, 3 µL of 1.2% CA (in acetone) were drop-coated on top of the enzyme membrane. The electrode was dried and kept at 4 °C when not in use.

The multi-analyte biosensor array for the simultaneous measurement of L-lactate, D-lactate, formate, and ethanol, was realized by immobilizing a different dehydrogenase on one of the four working electrodes (WEs). The enzyme loading of the D-lactate and formate electrodes was the same as described above (each 1.5 U of D-LDH and FDH, respectively). In case of the ethanol electrode, a dehydrogenase loading of 16 U ADH was used, since earlier studies revealed loss in enzyme activity after immobilization with the cross-linking agent GA [35, 37].

7.2.3 Apparatus

Electrochemical measurements were performed with a potentiostat with an integrated multiplexer (EmStatMUX16, PalmSens), which allows simultaneous analysis of up to 16 WEs. For all the experiments a conventional three-electrode arrangement was applied, consisting of the electrodes (4 WEs, CE, and RE) integrated on the SPCE array. Chronoamperometric studies were conducted at room temperature in a stirred solution of 10 mL potassium phosphate buffer (100 mM, pH 7.5) with an applied working potential of +0.250 V. For calibration of the different enzyme-modified electrodes, the increase in the current to stepwise addition of 40 mM analyte stock solution (L-lactate, D-lactate, formate, and ethanol, respectively) was recorded.

Cyclic voltammetry was carried out in the potential range between -0.4 and +0.8 V at a scan rate of 0.1 V s^{-1} in 100 mM potassium phosphate buffer (pH 7.5).

7.3 Results and discussion

7.3.1 Surface characterization

The electrode surface was characterized by scanning electron microscopy (SEM) and atomic force microscopy (AFM), in order to evaluate the alterations in the morphology after each modification step. Figure 7.2.1a-d shows SEM images taken with a Jeol JSM-7800F (JEOL GmbH, Germany). Compared to the bare SPCE (Fig. 7.2.1a), the morphology of the electrode modified with GO and the cofactors was characterized

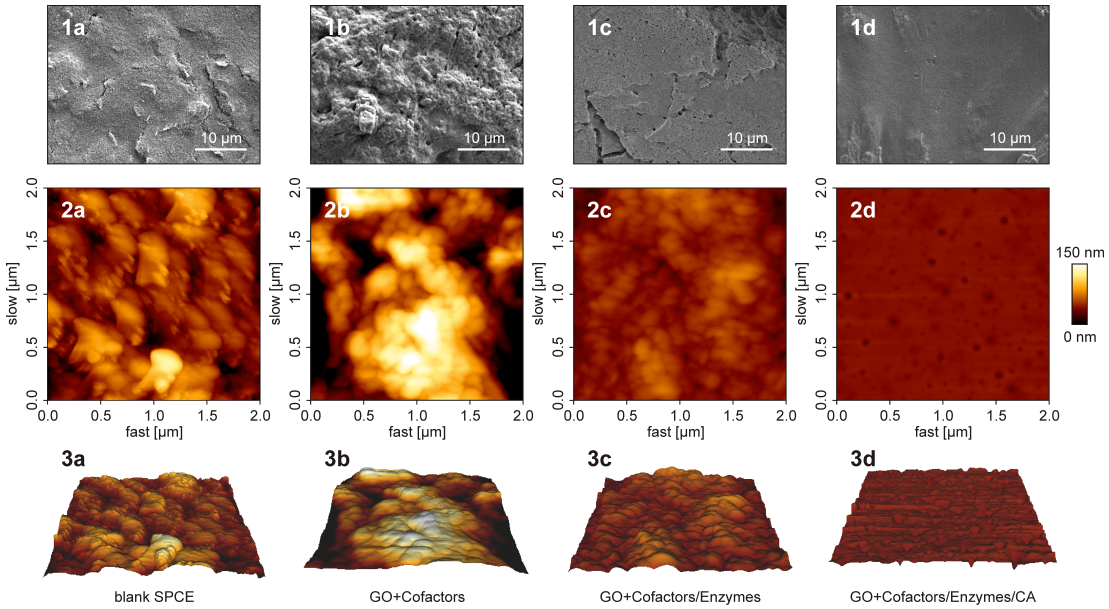

Fig. 7.2: SEM images **(1)**, AFM height **(2)**, and three-dimensional profiles **(3)** of the blank SPCE **(a)**, modified with GO and the cofactors **(b)**, an additional layer of the enzymes L-LDH and DIA **(c)** and a membrane of CA **(d)**. The scanned area of the AFM images was $2 \times 2\,\mu m^2$.

by a rougher surface with some porosity (Fig. 7.2.1b). After immobilization of the enzymes with GA within the porous GO matrix, the surface appears relatively smooth, as displayed in Fig. 7.2.1c. In comparison to the enzyme layer, the CA membrane exhibits an even smoother morphology with a denser matrix (Fig. 7.2.1d).

Figure 7.2.2a-d and Fig. 7.2.3a-d represent AFM height profiles and three-dimensional images, respectively, taken in the tapping mode with silicon cantilevers (Arrow NCR, NanoWorld AG, Switzerland) using a BioMat Workstation (JPK Instruments, Germany). The surface roughness was determined in terms of root-mean-square (RMS) roughness. The untreated SPCE exhibited a RMS of 16.5 ± 4.4 nm. After application of GO, the roughness increased to 37.8 ± 5.9 nm. Further modification steps resulted in a lower RMS of 9.2 ± 1.3 and 2.3 ± 0.7 nm of the enzyme membrane and the CA layer, respectively. These findings are consistent with the SEM images, as described above.

7.3.2 Optimization of the current response

GO concentration The protocol for the electrode modification was optimized in regard to the applied GO concentration. For this reason, the effect of the GO loading on the immobilization of the cofactors was evaluated by cyclic voltammetry. Figure 7.3 shows the cyclic voltammograms obtained with GO concentrations in the range from 0 to 1.5 mg mL^{-1}. All curves exhibited the typical cyclic voltammogram characteristic for the reversible reduction of $Fe(CN)_6^{3-}$ to $Fe(CN)_6^{4-}$ with increasing potential [38, 39]. Thereby, a higher current for the oxidation peak was observed with increasing GO loading. These results demonstrate the enhanced electrocatalytic activity of the SPCEs modified with GO. Various studies demonstrated superior electrochemical properties of different electrode materials (such as SPCEs [40, 41], glassy carbon electrodes [42, 43], and platinum electrodes [44]) by modification with GO and nafion. The electrode modified with 1.5 mg mL^{-1} GO displayed the highest current response. However, the

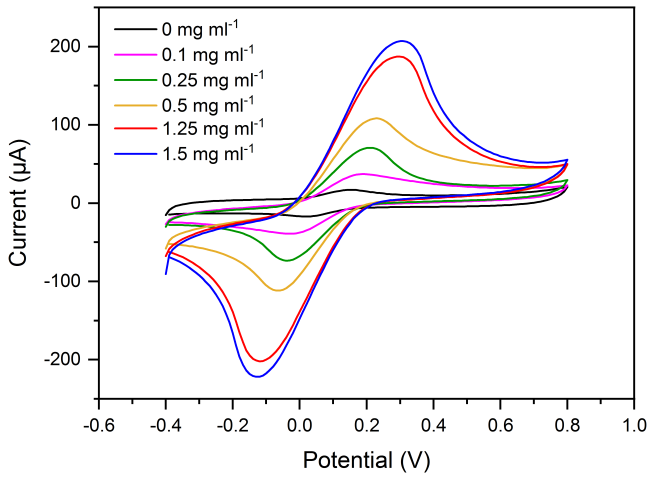

Fig. 7.3: Cyclic voltammograms of SPCEs modified with $Fe(CN)_6^{3-}$, NAD^+, and different concentrations of GO (0–1.5 mg mL^{-1}). Measurements were performed in 100 mM potassium phosphate buffer (pH 7.5).

high GO amount hindered homogeneous distribution of the solution on the electrode surface and uniform drying. So, for further experiments, a concentration of 1.25 mg mL^{-1} GO was chosen.

Working potential The optimal working conditions for amperometric detection of L-lactate were additionally examined in terms of the applied working potential and the pH value of the measurement solution. In Fig. 7.4, the relationship between the relative current response after the addition of 1 mM L-lactate and the potential applied to the WE is depicted. The signal was normalized to the maximum obtained current change. The highest signal increase was observed at a potential of +0.250 V *vs.* the internal pseudo silver reference electrode. At more positive potentials, the amperometric signal decreased to about 26.5% at +0.4 V. These results are in good agreement with the typical redox potentials of the $Fe(CN)_6^{3-}/Fe(CN)_6^{4-}$ system, as visualized by the cyclovoltamograms in Fig. 7.3. Similar optimal potentials are reported in the literature for electrochemical biosensors based on the mediated electron transfer of the redox couple $Fe(CN)_6^{3-}/Fe(CN)_6^{4-}$ [11, 45]. Thus, for further studies, a working potential of +0.250 V was selected.

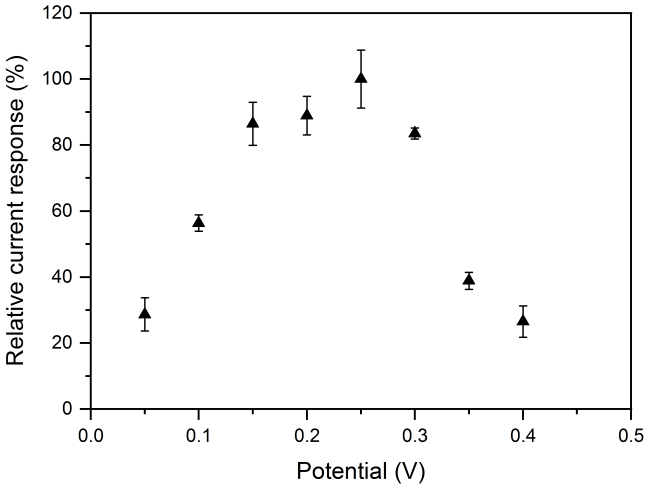

Fig. 7.4: Influence of the applied working potential on the amperometric response of the L-lactate electrode modified with 1.25 mg mL^{-1} GO to 1 mM L-lactate in 100 mM potassium phosphate buffer (pH 7.5). Relative current response represents the signal normalized to the maximum obtained current.

pH of the buffer solution The characteristics of the surrounding environment have a great impact on the catalytic activity of enzymes, which determines mainly the overall biosensor sensitivity. For this reason, the dependence of the amperometric response on the pH value of the measurement solution was studied over the range from pH 6.0 to 8.0 in potassium phosphate buffer and from pH 8.5 to 9.0 in Tris-HCl buffer. As presented in Fig. 7.5, the current increased with increasing pH value, reaching a maximum signal in phosphate buffer at pH 7.5. Measurements at higher pH values resulted in lower change in the current signal. This characteristic is consistent with other L-lactate biosensors

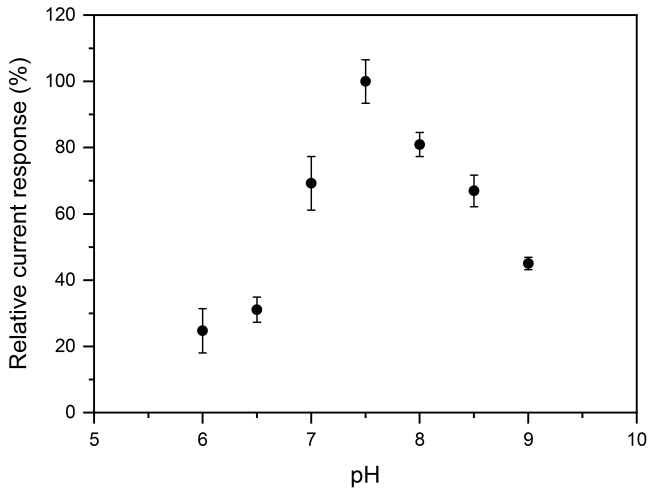

Fig. 7.5: Effect of pH on the amperometric sensor response. Experiments were carried out in 100 mM potassium phosphate buffer (pH 6.0–8.0) and Tris-HCl buffer (pH 8.5–9.0) at an applied working potential of +0.250 V. Relative current response represents the signal increase after addition of 1 mM L-lactate, normalized to the maximum obtained current.

described in literature that also utilize L-LDHs in combination with DIA [11, 35, 46] or an alternative approach for electrochemical detection of L-lactate [47, 48]. Hence, further experiments were conducted at pH 7.5 in phosphate buffer.

7.3.3 Amperometric detection of L-lactate

The effect of each component (cofactors, GO and CA, respectively) on the electrochemical electrode response was investigated by modification of the SPCE with different membrane compositions. Figure 7.6 shows the individual amperometric signal of each electrode to the successive addition of L-lactate in the concentration range from 0.25 to 6 mM. The curve in 7.6a represents an GO/Enzymes/CA electrode that has been constructed without the cosubstrates NAD^+ and $Fe(CN)_6{}^{3-}$. In this case, no change in the current occurred after stepwise increase of the L-lactate concentration. This observation proves that both cofactors are essentially required for the enzymatic reaction, as depicted in Figure 7.1, and thus, for the amperometric detection principle. In comparison, modification of the electrode surface with Cofactors/Enzymes/CA (b) resulted in a stepwise increase in the current response each time the analyte is added to the measurement solution. However, the final three concentrations steps (3, 4, and 6 mM) are accompanied by a gradual decrease of the amperometric signal, probably due to leakage of one or both of the cofactors from the sensor surface. The improved immobilization of the cofactors by modification of the electrode with GO is revealed by curve Fig. 7.6c,d. The electrode modified with GO, but without CA (see Fig. 7.6c GO+Cofactors/Enzymes), showed a continuous increase of current with increasing L-lactate concentration. This was also the case for the GO+Cofactors/Enzymes/CA electrode (d). For both electrodes a stable signal response over the whole measurement time was obtained. This might be due to an enhanced immobilization of the required cosubstances by integration of GO on the

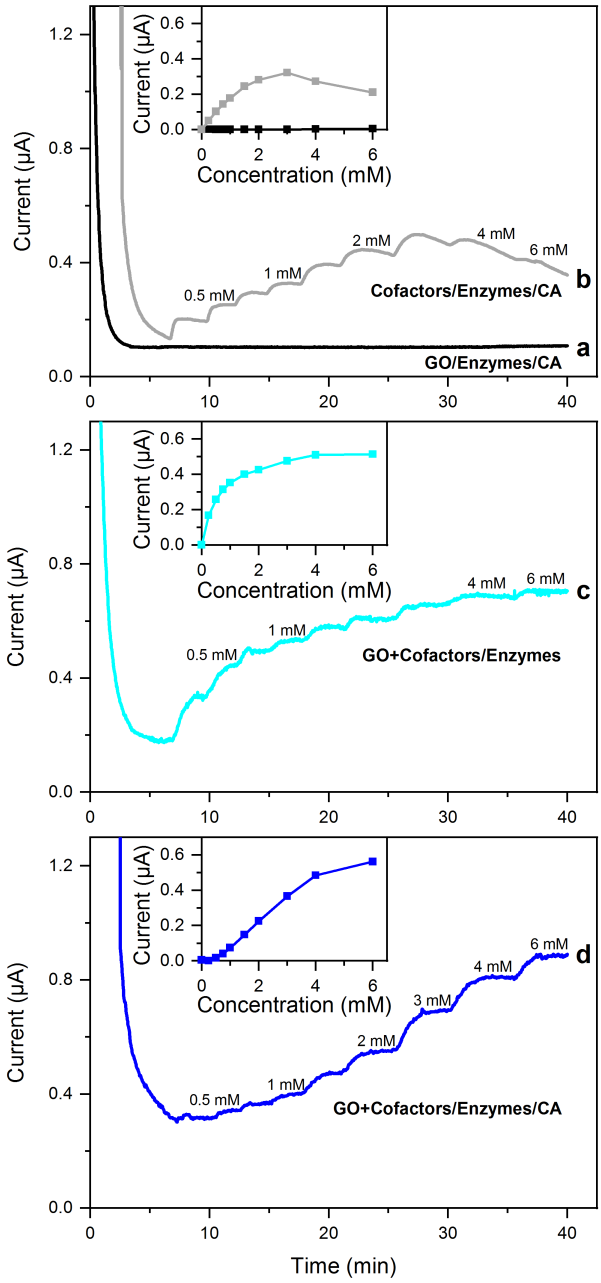

Fig. 7.6: Amperometric response of SPCEs with different electrode modifications (GO/Enzymes/CA **(a)**, Cofactors/Enzymes/CA **(b)**, GO+Cofactors/Enzymes **(c)** and GO+Cofactors/Enzymes/CA **(d)**) to the successive addition of L-lactate (0.25–6 mM). Measurements were performed in 100 mM phosphate buffer (pH 7.5) at an applied potential of +0.250 V. Insets show the corresponding calibration curves as a function of the L-lactate concentration.

sensor surface, compared to the electrode prepared without GO (Fig. 7.6a). The insets in Fig. 7.6 display the corresponding calibration curves of the different electrodes. The

sensitivities obtained for the Cofactors/Enzymes/CA, GO+Cofactors/Enzymes, and GO+Cofactors/Enzymes/ CA electrode were 0.16, 0.51, and 0.14 µA mM^{-1}, respectively. Thereby, the GO+Cosubstrates/Enzymes/CA electrode (d) exhibited the broadest linear range from 0.25 to 4.0 mM. These results demonstrated that with an additional CA layer the linear detection range can be extended, as also described by other electrochemical enzyme-based biosensors [49, 50]. The permselective membrane serves as a diffusion barrier, which hinders the transport of the analyte to the electrode surface. Consequently, the sensitivity of the SPCE is influenced. The application of such membranes is also commonly used in order to reduce the impact of other electroactive species in complex sample solutions [51].

7.3.4 Reagent-free biosensor array for simultaneous measurement

The applicability of the developed reagent-free sensor platform was evaluated with three other dehydrogenases. For construction of D-lactate-, formate-, and ethanol electrodes, D-LDH, FDH, and ADH, respectively, were used for the sensor modification, as described earlier. First, each electrode was calibrated by amperometric measurements with the corresponding analyte. Table 7.1 summarizes obtained characteristics of the different electrodes in terms of the linear working range and sensitivity. In comparison, the ethanol sensor exhibited the highest sensitivity with 1.07 µA mM^{-1}. These performances proved that the detection principle, in combination with the electrode modification, is generally applicable to different NAD^+-dependent dehydrogenases.

Tab. 7.1: Characteristics of the individual electrodes of the reagentless multi-analyte SPCE array.

Analyte	Linear range (mM)	Sensitivity (µA mM^{-1})
L-Lactate	0.25-4.0	0.14
D-Lactate	0.25-4.0	0.18
Ethanol	0.05-2.0	1.07
Formate	0.25-4.0	0.09

In order to evaluate potential cross-talk effects between electrodes modified with different dehydrogenases, a multi-analyte biosensor was constructed. Figure 7.7 illustrates an amperometric measurement of four analytes at the same applied potential of +0.250 V. The capability of cross-talk free detection is demonstrated by consecutive titration of each analyte individually (D-lactate, L-lactate, formate, and ethanol, respectively). In each case, the addition of the particular analyte results in an increase in the current signal of only the corresponding dehydrogenase electrode, while the other ones remain constant. The capability of simultaneous analysis of all four different analytes is substantiated by the last two titration steps, in which a multi-component solution was used. Hereby, all four electrodes responded with an increase in the electrochemical signal due to the increasing analyte concentration, according to the specific sensitivity for each electrode.

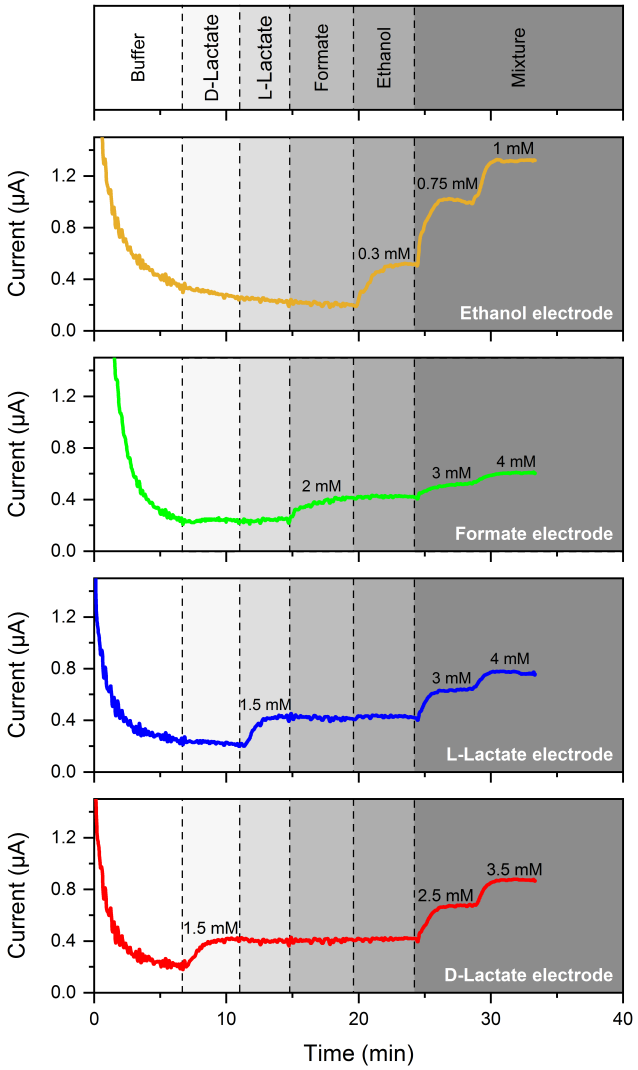

Fig. 7.7: Simultaneous amperometric responses of the reagentless multi-analyte SPCE array to successive addition of D-lactate, L-lactate, formate, ethanol and a mixture of all four analytes. Measurement was performed in 100 mM potassium phosphate buffer (pH 7.5) at an applied potential of +0.250 V.

7.4 Conclusion

The modification of SPCE with GO has provided a simple technique for construction of reagentless NAD^+-dependent biosensors. In this study, this platform has been evaluated by the development of an electrochemical enzyme-based L-lactate biosensor. The immobilization of the cofactors NAD^+ and $Fe(CN)_6^{3-}$ on the electrode surface has been achieved by functionalization with GO and an additional layer of CA. Thereby, the amperometric signal response was optimized in regard to GO concentration, working potential, and pH of the buffer solution. Experiments revealed that best results were obtained at an applied potential of +0.250 V in 100 mM potassium phosphate buffer at

pH 7.5. Furthermore, the proposed reagent-free biosensing system has been successfully tested with three other NAD^+-dependent dehydrogenases. In this way, a multi-analyte biosensor for simultaneous determination of L-lactate, D-lactate, ethanol, and formate was fabricated based on an SPCE array. This device enabled cross-talk free amperometric detection of four analytes without the requirement of adding external NAD^+ and mediator to the measurement solution. The present work demonstrates the promising potential of a disposable biosensor array characterized by facile application and rapid analysis. Such system could, for example, be used for the monitoring of fermentation processes, where knowledge about the concentration profile of different analytes is of great importance. In this regard, future work concentrates on the improvement of the sensor performance and evaluation of the stability in complex biological samples such as fermentation broth.

Acknowledgements

The authors thank J. Arreola for AFM measurements and D. Rolka for SEM images.

References

[1] Sellés Vidal, L.; Kelly, C. L.; Mordaka, P. M.; Heap, J. T. (2018) Review of NAD(P)H-dependent oxidoreductases: Properties, engineering and application. *Biochim. Biophys. Acta, Proteins Proteomics* 1866:327–347, doi:10.1016/j.bbapap.2017.11.005.

[2] Katakis, I.; Domínguez, E. (1997) Catalytic electrooxidation of NADH for dehydrogenase amperometric biosensors. *Microchim. Acta* 126:11–32, doi:10.1007/BF01242656.

[3] Lobo, M.J.; Miranda, A.J.; Tuñón, P. (1997) Amperometric biosensors based on NAD(P)-dependent dehydrogenase enzymes. *Electroanal.* 9:191–202, doi:10.1002/elan.1140090302.

[4] Radoi, A.; Compagnone, D. (2009) Recent advances in NADH electrochemical sensing design. *Bioelectrochemistry* 76(1-2):126–137, doi:10.1016/j.bioelechem.2009.06.008.

[5] Blaedel, W.J.; Jenkins, R.A. (1975) Electrochemical oxidation of reduced nicotinamide adenine dinucleotide. *Anal. Chem.* 47:1337–1343, doi:10.1021/ac60358a034.

[6] Gorton, L.; Dominguez, E. (2002) Electrocatalytic oxidation of NAD(P)/H at mediator-modified electrodes. *Rev. Mol. Biotechnol.* 82:371–392, doi:10.1016/S1389-0352(01)00053-8.

[7] Kochius, S.; Magnusson, A.O.; Hollmann, F.; Schrader, J.; Holtmann, D. (2012) Immobilized redox mediators for electrochemical $NAD(P)^+$ regeneration. *Appl. Microbiol. Biotechnol.* 93:2251–2264, doi:10.1007/s00253-012-3900-z.

[8] Leca, B.; Marty, J.-L. (1997) Reagentless ethanol sensor based on a NAD-dependent

dehydrogenase. *Biosens. Bioelectron.* 12(11):1083–1088, doi:10.1016/S0956-5663(97)00075-4.

[9] Montagné, M.; Erdmann, H.; Comtat, M.; Marty, J.-L.(1995) Comparison of the performances of two bi-enzymatic sensors for the detection of D-lactate. *Sens. Actuators B Chem.* 26-27:440–443, doi:10.1016/0925-4005(94)01636-V.

[10] Limoges, B.; Marchal, D.; Mavré, F.; Savéant, J.-M. (2006) Electrochemistry of immobilized redox enzymes: Kinetic characteristics of NADH oxidation catalysis at diaphorase monolayers affinity immobilized on electrodes. *J. Am. Chem. Soc.* 128:2084–2092, doi:10.1021/ja0569196.

[11] Antiochia, R.; Cass, A.E.G.; Palleschi, G. (1997) Purification and sensor applications of an oxygen insensitive, thermophilic diaphorase. *Anal. Chim. Acta* 345:17–28, doi:10.1016/S0003-2670(96)00618-6.

[12] Zhou, H.; Zhang, Z.; Yu, P.; Su, L.; Ohsaka, T.; Mao, L. (2010) Noncovalent attachment of NAD^+ cofactor onto carbon nanotubes for preparation of integrated dehydrogenase-based electrochemical biosensors. *Langmuir* 26(8):6028–6032, doi:10.1021/la903799n.

[13] Gallay, P.; Eguílaz, M.; Rivas, G. (2019) Multi-walled carbon nanotubes noncovalently functionalized with polyarginine: A new alternative for the construction of reagentless NAD^+/dehydrogenase-based ethanol biosensor. *Electroanal.* 31:805–812, doi:10.1002/elan.201800892.

[14] Khorsand, F.; Darziani Azizi, M.; Naeemy, A.; Larijani, B.; Omidfar, K. (2013) An electrochemical biosensor for 3-hydroxybutyrate detection based on screen-printed electrode modified by coenzyme functionalized carbon nanotubes. *Mol. Biol. Rep.* 40:2327–2334, doi:10.1007/s11033-012-2314-4.

[15] Shu, H.C.; Mattiasson, B.; Persson, B.; Nagy, G.; Gorton, L.; Sahni, S.; Geng, L.; Boguslavsky, L.; Skotheim, T. (1995) A reagentless amperometric electrode based on carbon paste, chemically modified with D-lactate dehydrogenase, NAD^+, and mediator containing polymer for D-lactic acid analysis. *Biotechnol. Bioeng.* 46:270–279, doi:10.1002/bit.260460310.

[16] Weiss, D.J.; Dorris, M.; Loh, A.; Peterson, L. (2007) Dehydrogenase based reagentless biosensor for monitoring phenylketonuria. *Biosens. Bioelectron.* 22:2436–2441, doi:10.1016/j.bios.2006.09.001.

[17] Blaedel, W.J.; Engstrom, R.C. (1980) Reagentless enzyme electrodes for ethanol, lactate, and malate. *Anal. Chem.* 52:1691–1697, doi:10.1021/ac50061a036.

[18] Maines, A.; Prodromidis, M.I.; Tzouwara-Karayanni, S.M.; Karayannis, M.I.; Ashworth, D.; Vadgama, P. (2000) Reagentless enzyme electrode for malate based on modified polymeric membranes. *Anal. Chim. Acta* 408:217–224, doi:10.1016/S0003-2670(99)00866-1.

[19] Pereira, A. (2001) Reagentless biosensor for isocitrate using one step modified Pt-Ir microelectrode. *Talanta* 53:801–806, doi:10.1016/S0039-9140(00)00566-X.

[20] Gros, P.; Comtat, M. (2004) A bioelectrochemical polypyrrole-containing $Fe(CN)_6^{3-}$ interface for the design of a NAD-dependent reagentless biosensor. *Biosens. Bioelectron.* 20:204–210, doi:10.1016/j.bios.2004.02.023.

[21] Zhang, M.; Gorski, W. (2011) Amperometric ethanol biosensors based on chitosan-NAD^+-alcohol dehydrogenase films. *Electroanal.* 23(8):1856–1862, doi:10.1002/elan.201100078.

[22] Hughes, G.; Pemberton, R.M.; Fielden, P.R.; Hart, J.P. (2015) Development of a novel reagentless, screen-printed amperometric biosensor based on glutamate dehydrogenase and NAD^+, integrated with multi-walled carbon nanotubes for the determination of glutamate in food and clinical applications. *Sens. Actuators B Chem.* 216:614–621, doi:10.1016/j.snb.2015.04.066.

[23] Justino, C.I.L.; Duarte, A.C.; Rocha-Santos, T.A.P. (2017) Recent progress in biosensors for environmental monitoring: A review. *Sensors* 17:2918, doi:10.3390/s17122918.

[24] Davis, A.N.; Travis, A.R.; Miller, D.R.; Cliffel, D.E. (2017) Multianalyte physiological microanalytical devices. *Annu. Rev. Anal. Chem.* 10:93–111, doi:10.1146/annurev-anchem-061516-045334.

[25] Couto, R.A.S.; Lima, J.L.F.C.; Quinaz, M.B. (2016) Recent developments, characteristics and potential applications of screen-printed electrodes in pharmaceutical and biological analysis. *Talanta* 146:801–814, doi:10.1016/j.talanta.2015.06.011.

[26] Hughes, G.; Westmacott, K., Honeychurch, K.C.; Crew, A.; Pemberton, R.M.; Hart, J.P. (2016) Recent advances in the fabrication and application of screen-printed electrochemical (bio)sensors based on carbon materials for biomedical, agri-food and environmental analyses. *Biosensors* 6:50, doi:10.3390/bios6040050.

[27] Sato, N.; Okuma, H. (2006) Amperometric simultaneous sensing system for D-glucose and L-lactate based on enzyme-modified bilayer electrodes. *Anal. Chim. Acta* 565:250–254, doi:10.1016/j.aca.2006.02.041.

[28] Kanso, H.; Begoña González García, M.; Ma, S.; Ludwig, R.; Fanjul Bolado, P.; Hernández Santos, D. (2017) Dual biosensor for simultaneous monitoring of lactate and glucose based on thin-layer flow cell screen-printed electrode. *Electroanal.* 29:87–92, doi:10.1002/elan.201600487.

[29] Kuila, T.; Bose, S:, Khanra, P.; Mishra, A.K.; Kim, N.H.; Lee, J.H. (2011) Recent advances in graphene-based biosensors. *Biosens. Bioelectron.* 26:4637–4648, doi:10.1016/j.bios.2011.05.039.

[30] Song, Y.; Luo, Y.; Zhu, C.; Li, H.; Du, D.; Lin, Y. (2016) Recent advances in electrochemical biosensors based on graphene two-dimensional nanomaterials. *Biosens. Bioelectron.* 76:195–212, doi:10.1016/j.bios.2015.07.002.

[31] Pilas, J.; Iken, H.; Selmer, T.; Keusgen, M.; Schöning, M.J. (2015) Development of a multi-parameter sensor chip for the simultaneous detection of organic compounds in biogas processes. *Phys. Status Sol. A* 212(6):1306–1312, doi:10.1002/pssa.201431894.

[32] Röhlen, D.L.; Pilas, J.; Schöning, M.J.; Selmer, T. (2017) Development of an amperometric biosensor platform for the combined determination of L-malic, fumaric, and L-aspartic acid. *Appl. Biochem. Biotechnol.* 183:566–581, doi:10.1007/s12010-017-2578-1.

[33] Pilas, J.; Yazici, Y.; Selmer, T.; Keusgen, M.; Schöning, M.J. (2018) Application of a portable multi-analyte biosensor for organic acid determination in silage. *Sensors* 18(5):1470, doi:10.3390/s18051470.

[34] Röhlen, D.L.; Pilas, J.; Dahmen, M.; Keusgen, M.; Selmer, T.; Schöning, M.J. (2018) Toward a hybrid biosensor system for analysis of organic and volatile fatty acids in fermentation processes. *Front. Chem.* 6:284, doi:10.3389/fchem.2018.00284.

[35] Pilas, J.; Yazici, Y.; Selmer, T.; Keusgen, M.; Schöning, M.J. (2017) Optimization of an amperometric biosensor array for simultaneous measurement of ethanol, formate, D- and L-lactate. *Electrochim. Acta* 251:256–262, doi:10.1016/j.electacta.2017.07.119.

[36] Cui, G.; Yoo, J.H.; Lee, J.S.; Yoo, J.; Uhm, J.H.; Cha, G.S.; Nam, H. (2001) Effect of pre-treatment on the surface and electrochemical properties of screen-printed carbon paste electrodes. *Analyst* 126:1399–1403, doi:10.1039/b102934g.

[37] Mateo, C.; Palomo, J.M.; van Langen, L.M.; van Rantwijk, F.; Sheldon, R.A. (2004) A new, mild cross-linking methodology to prepare cross-linked enzyme aggregates. *Biotechnol. Bioeng.* 86:273–276, doi:10.1002/bit.20033.

[38] Rock, P.A. (1966) The standard oxidation potential of the ferrocyanide-ferricyanide electrode at 25° and the entropy of ferrocyanide ion. *J. Phys. Chem.* 70(8):576–580, doi:10.1021/j100874a042.

[39] O'Reilly, J.E. (1973) Oxidation-reduction potential of the ferro-ferricyanide system in buffer solutions. *Biochim. Biophys. Acta, Bioenerg.* 292:509–515, doi:10.1016/0005-2728(73)90001-7.

[40] Brownson, D.A.C.; Banks, C.E. (2011) Graphene electrochemistry: Fabricating amperometric biosensors. *Analyst* 136:2084–2089, doi:10.1039/c0an00875c.

[41] Vasilescu, I.; Eremia, S.A.V.; Penu, R.; Albu, C.; Radoi, A.; Litescu, S.C.; Radu, G.-L. (2015) Disposable dual sensor array for simultaneous determination of chlorogenic acid and caffeine from coffee. *RSC Adv.* 5:261–268, doi:10.1039/C4RA14464C.

[42] Li, J.; Guo, S.; Zhai, Y.; Wang, E. (2009) High-sensitivity determination of lead and cadmium based on the Nafion-graphene composite film. *Anal. Chim. Acta* 649:196–201, doi:10.1016/j.aca.2009.07.030.

[43] Chen, X.; Ye, H.; Wang, W.; Qiu, B.; Lin, Z.; Chen, G. (2010) Electrochemiluminescence biosensor for glucose based on graphene/Nafion/GOD film modified glassy carbon electrode. *Electroanal.* 22(20):2347–2352, doi:10.1002/elan.201000095.

[44] Vinu Mohan, A.M.; Aswini, K.K.; Maria Starvin, A.; Biju, V.M. (2013) Amperometric detection of glucose using Prussian blue-graphene oxide modified platinum electrode. *Anal. Methods* 5:1764–1770, doi:10.1039/c3ay26310j.

[45] Zeng, K.; Tachikawa, H.; Zhu, Z.; Davidson, V.L. (2000) Amperometric detection of histamine with a methylamine dehydrogenase polypyrrole-based sensor. *Anal. Chem.* 72:2211–2215, doi:10.1021/ac9911138.

[46] Sprules, S.D.; Hart, J.P.; Wring, S.A. and Pittson, Robin(1995) A reagentless, disposable biosensor for lactic acid based on a screen-printed carbon electrode containing Meldola's Blue and coated with lactate dehydrogenase, NAD^+ and cellulose acetate. *Anal. Chim. Acta* 304:17–24, doi:10.1016/0003-2670(94)00565-4.

[47] Kwan, R.C.H.; Hon, P.Y.T.; Mak, K.K.W.; Renneberg, R. (2004) Amperometric determination of lactate with novel trienzyme/poly(carbamoyl) sulfonate hydrogel-based sensor. *Biosens. Bioelectron.* 19:1745–1752, doi:10.1016/j.bios.2004.01.008.

[48] Pérez, S.; Sánchez, S.; Fàbregas, E. (2012) Enzymatic strategies to construct L-lactate biosensors based on polysulfone/carbon nanotubes membranes. *Electroanal.* 24:967–974, doi:10.1002/elan.201100628.

[49] Maines, A.; Ashworth, D.; Vadgama, P. (1996) Diffusion restricting outer membranes for greatly extended linearity measurements with glucose oxidase enzyme electrodes. *Anal. Chim. Acta* 333:223–231, doi:10.1016/0003-2670(96)00222-X.

[50] Kanapieniene, J.J.; Dedinaite, A.A.; Laurinavicius, V.A. (1992) Miniature glucose biosensor with extended linearity. *Sens. Actuators B Chem.* 10:37–40, doi:10.1016/0925-4005(92)80008-L.

[51] Kulkarni, T.; Slaughter, G. (2016) Application of semipermeable membranes in glucose biosensing. *Membranes* 6:55, doi:10.3390/membranes6040055.

8 Concluding remarks and outlook

Enhancing the efficiency and sustainability of biogas production by anaerobic digestion requires improved process design and control as well as effective utilization of the available organic material. Currently, predominantly energetic crops, like maize or sugar cane, are used as substrate, which typically provide the advantage of high methane yields at relatively low investment costs. Waste materials have so far not been widely applied as feedstock for biogas plant operation, due to difficulties encountered by inhibited methane formation and increased risk of process instability. Independent of the applied source of organic matter, reliable process monitoring constitutes the prerequisite for successful, economic plant operation. The complexity of the anaerobic digestion process impedes facile identification of imbalanced process conditions, so that the cause of malfunction is often difficult to ascertain. Various parameters are monitored in order to prevent severe process disturbances such as biogas production rate, methane yield, temperature, pH value, buffer capacity and VFA concentration. The latter is generally known as a good indicator for unstable relation in the syntrophic process of acid consumption and methane formation. Typically, VFA concentration is determined by chromatographic techniques that depend on sampling handling, storing, transportation and analysis in external laboratories with sophisticated instruments. These requirements may lead to a significant time delay between sampling and data acquisition, which has a detrimental impact on the process performance and control.

The aim of this thesis was therefore the development of an electroanalytical device based on biosensing technology for monitoring of several process-relevant intermediates that are produced during the anaerobic digestion process. Such monitoring system should enable rapid, on-site measurement of organic acids and alcohols, in order to identify changes in the methane formation and provide additional information on the process conditions.

Within the scope of this work, four different intermediates have been selected, that so far have often been neglected as a potentially relevant parameter for the monitoring of biogas plants. Though, formation of D-lactate, L-lactate, formate and ethanol during the first three stages (hydrolysis, acidogenesis and acetogenesis) of anaerobic digestion is of central importance for the overall methane production. The regular detection of these compounds could provide a beneficial impact on the evaluation of fermentation processes. In contrast to currently employed state of the art technologies, application of a novel biosensor device could improve the basic measurement procedure. The simultaneous electrochemical determination of all four analytes with one biosensing system can be accomplished by a suitable common detection principle. In this work, NAD^+-dependent dehydrogenases were chosen for specific detection of three different organic acids and ethanol, namely D-LDH, L-LDH, FDH and ADH. These enzymes catalyze oxidation-

and reduction reactions by transfering hydrogen to the electron acceptor NAD^+/NADH. As described earlier in Sec. 2.2.3, electrochemical measurement of NADH is a quite challenging task. A bi-enzymatic detection principle with a diaphorase (DIA, EC 1.8.1.4) from *Clostridium kluyveri* was selected to meet the present requirements associated with simultaneous measurements of several analytes. The proof of concept was conducted with a platinum thin-film biosensor (see Tab. 8.1) consisting of total five WEs, which were modified with DIA in combination with D-LDH, L-LDH, FDH and ADH, respectively. However, at this stage only three analytes (D-lactate, L-lactate and formate) were measurable, whereas the electrode modified with ADH and DIA did not show a response in the current signal after addition of the analyte ethanol. The sensitivity and linear detection range of the biosensor for these three analytes was then determined and showed overall satisfactory performance, so that in the following this platform was further characterized and optimized.

The successful development of such electrochemical biosensor array for simultaneous quantification of three analytes showed a promising potential for further investigations with other NAD^+-dependent dehydrogenases. This was, for example, done in our laboratory for the construction of an amperometric sensor platform for the analysis of the substrates malate, fumarate and aspartate [1]. These compounds are key intermediates in the citric acid cycle and amino acid metabolism, as well as often applied in food industry as acidulants and artificial sweeteners. For future applications, enhancement of the biosensor array with further analyte-specific electrodes seems feasible and desirable. Custom-made biosensors for specific application in diverse fields (e.g., fermentation process control, food safety and quality) could be constructed. The integration of a glucose-, malate- and succinate electrode, for example, could greatly improve the monitoring of various fermentation processes. But also other analytes might be conceivable options.

Enzymes can be immobilized by various methods, which influence the overall catalytic activity in different manners (see Sec. 2.2.2). For the intended application of the biosensor, a simple and low-cost procedure was sought for stable fixation of the enzymes on the sensor surface. The array design required additionally some kind of treatment that was compatible with a broad range of enzymes. Immobilization with the chemical cross-linker glutaraldehyde represents such commonly used technique, which is favored for its effectiveness. The downside of relatively harsh conditions during immobilization is the potential high loss in enzyme activity. The preliminary experiments that have been performed with ADH from *Saccharomyces cerevisiae* showed exactly this damaging effect, since first attempts for construction of an ethanol-sensitive electrode failed. The applied enzyme loading of ADH (around 1.0 U per electrode) was oriented towards the other three successfully immobilized dehydrogenases, which all showed sensitivity towards their corresponding analyte at this condition. In the following, immobilization was adjusted by increasing the portion of ADH within the enzymatic membrane by a factor of almost 10. The results revealed, that harmful influence of glutaraldehye on the catalytic activity of ADH could be compensated by increasing the total protein amount. This observation showed that enzymes react differently on chemicals and operating conditions and underlined the importance of diligent selection and evaluation of applied treatments. Optimization of the ADH immobilization enabled integration of

an additional ethanol-sensing electrode to the biosensor array (see Tab. 8.1, optimized thin-film sensor array). Thereby, a multi-analyte biosensor system for simultaneous and cross-talk free analysis for four different intermediates was realized. The biosensor was additionally equipped with a blank electrode modified with the inert protein BSA, in order to detect potential interfering phenomena (e.g., oxidation of other electroactive species present in the sample) on the obtained current signal.

Sensitivity and linear detection range are two important parameters that determine biosensors performance and potential for applicability in desired real conditions. Evaluation of optimal enzyme loading and cofactor concentration is also advisable for economic reasons, as the amount of cost-intensive NAD^+ and enzymes represent the main expenses regarding the biological components required for the biosensor design. The amperometric biosensor array has been optimized in regard to enzyme loading, concentration of glutaraldehyde and cofactors (NAD^+, $Fe(CN)_6{}^{3-}$), temperature and pH of the buffer solution. Table 8.1 provides an overview of the sensor characteristics of the optimized biosensor in comparison to the previously reported biosensor, which demonstrated the proof of concept (Ch. 3). For both lactate-sensing electrodes, performance could be significantly enhanced by adjusting enzyme to glutaraldehyde ratio and environmental conditions. The sensitivity of these two was increased by the double from 13.4 to 28.4 $\mu A\,mM^{-1}\,cm^{-2}$ for D-lactate and from 17.5 to 37.2 $\mu A\,mM^{-1}\,cm^{-2}$ for L-lactate, respectively. This improvement was also accompanied by an extended linear working range with much lower detection limit, which becomes obvious by exemplarily comparing the measuring range of D-lactate prior (0.1–1.0 mM) and after optimization (0.004–2.5 mM).

Tab. 8.1: Comparison of sensor characteristics with respect to measurement conditions of platinum thin-film biosensor array (before and after optimization) and reagent-free screen-printed carbon electrode array. Measurements were performed in 100 mM potassium phosphate buffer, sensitivity was normalized to electrode area for comparability reasons.

		Thin-film array		Thick-film array
		Proof of concept (Ch. 3)	Optimized (Ch. 4–6)	Reagent-free (Ch. 7)
	pH value	7.4	7.5	7.5
	Temperature (°C)	21	21	21
	Working potential (mV)	+300	+300	+250
	NAD^+ (mM)	2.0	2.5	10
	$Fe(CN)_6{}^{3-}$ (mM)	5.0	2.0	20
D-Lactate	Linear range (mM)	0.1–1.0	0.004–2.5	0.25–4.0
	Sensitivity ($\mu A\,mM^{-1}\,cm^{-2}$)	13.4	28.4	2.6
L-Lactate	Linear range (mM)	0.1–1.0	0.002–2.0	0.25–4.0
	Sensitivity ($\mu A\,mM^{-1}\,cm^{-2}$)	17.5	37.2	2.1
Formate	Linear range (mM)	0.04–2.0	0.02–3.0	0.25–4.0
	Sensitivity ($\mu A\,mM^{-1}\,cm^{-2}$)	78.3	20.5	1.3
Ethanol	Linear range (mM)	-	0.002–1.5	0.05–2.0
	Sensitivity ($\mu A\,mM^{-1}\,cm^{-2}$)	-	35.7	15.7

Unfortunately, such distinct improvements were not achieved for all four analyte-specific electrodes, as the sensitivity towards formate decreased from 78.3 to 20.5 $\mu A\,mM^{-1}\,cm^{-2}$. In the course of the optimization, the applied FDH from *Candida boidinii* has been removed from the suppliers' range. Changes encountered are caused by application of an alternative enzyme source (from the same strain), which was characterized by a much lower specific activity. Nevertheless, the obtained measuring ranges of the biosensor array show great potential for monitoring of biogas plants. Usually, the concentration of organic acids and alcohols is in the lower millimolar range. Levels beneath the limit of detection are typically not critical for process stability. The analysis of lactate-rich samples, such as silage prepared from energy crops, might encounter measuring limits. In this case, sample dilution would be justified or alternatively integration of a membrane system to the introduced monitoring device for expansion of the linear detection region.

The optimal performance of the whole biosensor array was attained in 100 mM potassium phosphate buffer at 30 °C. For practical reasons and improved operational stability, however, ideal service temperature was set to room temperature. The biosensor array exhibited a steady working stability of more than 15 subsequent measurements at optimal conditions. Thereby, the formate electrode constituted the weakest link with only 54% of remaining signal, whereas the other three electrodes still showed a current response in the range of 72% to 80% after repeated application. These results demonstrate that to some extent further improvements are required, in order to enhance the stability of the formate electrode to the satisfactory level of the other ones. But far more mandatory it seems to integrate a pH- and temperature sensor to the biosensor array as experiments have shown the great impact of these two parameters on the sensor signal. Standard silicon technology has, for example, been used for the development of a miniaturized multi-parameter sensor for detection of three physico-chemical quantities based on different transducer principles [2]. This sensor device was equipped with a capacitively coupled four-electrode electrolyte-conductivity sensor, a capacitive field-effect pH sensor and a thin-film Pt-temperature sensor. The combination of the biosensor array with additional monitoring elements could significantly increase the reliability of the measuring system by an programmable compensation factor, which considers the actual pH value and temperature during the measurement. Furthermore, inclusion of other process-specific parameters contribute to a more comprehensive overview of the overall state of the methane formation.

An important part of this work was the development of a user-friendly and robust measurement configuration for facile application of the biosensor array in on-site measurements. In order to meet these demands, a portable prototype measurement cell housing the biosensor chip was designed and constructed by 3D-printing technology. The compact device ($60 \times 60 \times 70\,mm^3$) is equipped with a holding for a cuvette (2 mL filling volume) and electrical connection to a potentiostat, including the user interface. Precise positioning of the electrodes is guaranteed by exact contacting of the biosensor and the external miniaturized Ag/AgCl RE. For improved usability, the sensor chip was redesigned by integration of the CE on the sensor chip, too. In Tab. 8.2, the specifications of the different biosensor arrays and the electrode configurations are listed. The novel sensor design, in combination with the constructed measurement chamber,

Tab. 8.2: Overview of sensor chips, incorporated in printed circuit boards (PCB), used in this work for development of an electrochemical multi-analyte biosensor.

	Platinum thin-film electrode array		Screen-printed carbon electrode array
	Ch. 3–4	Ch. 5–6	Ch. 7
	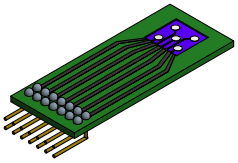	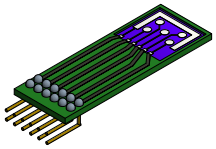	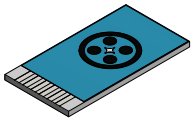
Sensor chip (mm^2)	10×10	14×14	15×15
PCB (mm^2)	20×50	16×45	20×38
WE (mm)	Ø 2.0 (n=5)	Ø 2.0 (n=5)	Ø 2.95 (n=4)
CE (mm^2)	44.2*	40.5	43.9
RE	Ag/AgCl*	mini. Ag/AgCl*	pseudo Ag

* not part of sensor chip

was employed in a mobile hand-held device, which could be used within minutes for field measurements after brief introduction to the basic measuring principle. Thereby, a substantial advantage is provided in comparison to conventional state of the art methods for the analysis of organic acids and alcohols, because analysis could be performed on-site without the requirement of storing and transporting samples to external measurement stations. The long-term stability of the biosensor was investigated over a period of 140 days at different storing conditions. After repeated regular application, individual electrodes of the biosensor array exhibited highest stability when stored at −21 °C. The biosensor could be used under this condition for more than 14 days. For future applications, the stability could be further improved to provide more economic utilization of the biosensing system.

Preliminary studies were carried out in samples of maize- and sugar silage, which were pretreated by chemical Carrez clarification. The applied procedure, known from literature and commercial reagent kits, was firstly modified by adjusting the reagent concentrations and volumes in order to minimize sample dilution. Afterwards, the revised clarification method was evaluated by determination of recovery rates from spiking experiments, which demonstrated the required reliability for sample preparation. It should be noted that extensive mixing of viscous samples with a high solid content is essential. The analysis of the intermediates D-lactate, L-lactate, formate and ethanol with the biosensor array showed excellent correlation to measurements performed with commercial photometric reference kits. Quantification of the analyte concentration with such ready-to-use assays requires for each compound a different single-analyte specific kit, each constituted with several reagents. This circumstance results in more handling steps, increased measurement time (reported are approximately 5 to 12 min for each analyte) and higher experimental costs than simultaneous measurement of all four analytes with the developed biosensor array (less than 3 min). For improved usability of the biosensing system, measurements ideally should be performed directly in the

sample solution without any prior pretreatment. This could be accomplished in future experiments by a filter system, which separates the analytes of interest from disturbing, interfering substances in the sample solution.

Obtaining accurate data from on-site/off-line monitoring relies in particular on representative samples collected from the biogas plant, careful sample handling and accurate measurements. Variability in sampling, sample storage and transportation can have a detrimental effect on data reliability, thus standard sampling guidelines have been stated for accurate sampling from biogas plants, for example by the VDI-Gesellschaft Energie und Umwelt [3]. Many drawbacks associated with sampling could be avoided with an automatic sampling unit, which can perform sampling from the biogas plant, filtration and optional dilution of the sample, as well as injection to the integrated biosensing system for monitoring the organic acids and ethanol. Initial steps towards development of such an automated sampling and monitoring system were conducted by combination of the biosensor array with a temperature-sensitive hydrogel-based actuator system [4, 5]. Thereby, analyte solution was automatically pumped into the cuvette of the hand-held device. The analyte supply was controlled within microfluidic channels with light-addressable valves based on responsive hydrogels with incorporated graphene oxide (GO). The further improvement of such technology for the development of a LoC system could establish a simple device for the monitoring of fermentation processes.

After successful optimization of the biosensing unit and development of a practical and mobile hand-held device, the applicability of the biosensor array under real conditions was tested in sludge samples from three industrial biogas plants to evaluate the influence of various matrices on the sensor signal. The biogas plants were all fed with different substrates, which resulted in differing viscosity, solid content, pH and ammonia concentration. Samples were spiked prior to analysis, so that the obtained results could be compared more efficiently with standard reference techniques. These measuring series were enhanced by application of an acetate and propionate biosensor, which has been developed by D.L. Röhlen [6]. Measurements proved the reliability of both biosensors for accurate and reproducible acid determination in such complex samples. Furthermore, both biosensors have been utilized for long-term monitoring of a lab-scale biogas reactor on weekly basis supplementary to other off-line determined parameters (pH and FOS/TAC). Results were again in good agreement in comparison to conventional analytical methods applied for quantification of VFAs (GC), organic acids and ethanol (photometry). Both of these techniques have the drawback that generally elaborate sample pre-treatment is mandatory for preparation of clear and particle-free samples. Preliminary experiments have shown, however, that reliable amperometric measuring with the biosensor array is also possible in untreated fermentation sludges. The developed biosensing system offers additionally the advantage of on-site application due to the compact and mobile design of the measurement equipment. Photometry, GC and HPLC typically require expensive and sophisticated instruments, which are less suitable for on-site application.

So far, amperometric measurements with the developed biosensor array required addition of both cofactors (NAD^+ and $Fe(CN)_6^{3-}$) to the buffer solution. This circum-

stance is on the one hand to some extent inconvenient and otherwise the measurements become more error-prone. In accordance to the definition stated by IUPAC, a biosensor should be a reagentless self-contained analytical device with all parts being packaged together in the same unit. These aspects motivated the development of a reagent-free NAD^+-dependent biosensor array, constructed as ready-to-use sensor device. The basis for this system were commercial screen-printed carbon electrode arrays as depicted in Tab. 8.2. Fabricated by thick-film technology and equipped with CE and pseudo RE, these sensors are ideal for disposable utilization. The electrode surface was modified with GO to enhance enzyme fixation and coimmobilization of cofactors. First of all, the system was evaluated for reagentless detection of L-lactate with immobilized L-LDH and DIA in the presence of NAD^+ and $Fe(CN)_6{}^{3-}$ within the electrode membrane. Working conditions were optimized with respect to pH and working potential, showing optimal influence on sensor performance at pH 7.5 at 300 mV. In the following, a multi-analyte biosensor was realized for D-lactate, L-lactate, formate and ethanol to perform simultaneous analysis of these analytes. Table 8.1 presents sensitivity and linear detection ranges obtained with this device compared to previously described thin-film electrode arrays. Direct comparison shows much lower sensitivity towards the different analytes and similar upper linear detection limits. For the first time, such reagent-free biosensing device has been established, however, several strategic optimization steps are required to improve the overall performance. The electrode modification could, for example, be simplified by integration of GO and cofactors within the screen-printed carbon material. In this way, an automated immobilization process might be conceivable for enhanced reproducibility. The sensitivity of the different electrodes could also be increased by application of a more gentle immobilization procedure than cross-linking with glutaraldehyde.

These overall findings of this thesis showed the promising potential of the developed biosensors for rapid and facile monitoring of biogas plants with a user-friendly measurement device. Further improvements are required prior such a system could be applied in industrial or agricultural biogas plants at reasonable investment costs. In this regard, it is of special interest to examine how the different acid concentrations change in response to specific disturbances. Fermentation processes could, for example, be disturbed actively by increasing the organic load, decreasing the retention time or malfunction in the stirring unit. Imbalances in the process could also be provoked by addition of known inhibiting compounds (such as antibiotics or heavy metal ions), which directly interfere the microbial metabolism. In this context, monitoring of the microbial activity is another attractive approach for improved understanding of the methane formation. The metabolic activity of *Corynebacterium glutamicum* after glucose uptake has, for example, been studied with a light-addressable potentiometric sensor (LAPS) system [7]. This technology (LAPS) monitors extracellular pH changes on the sensor surface induced by the metabolic activity of the involved microorganisms. Knowledge about the metabolic state of the microorganisms in the biogas plant, together with specific information about the acid composition in the fermentation medium, could help to operate the anaerobic digestion process with higher stability and economy. The electrochemical enzyme-based biosensor array developed in this work could thereby, significantly contribute to this much needed changes required in the energy sector.

References

[1] Röhlen, D.L.; Pilas, J.; Schöning, M.J.; Selmer, T. (2017) Development of an amperometric biosensor platform for the combined determination of L-malic, fumaric, and L-aspartic acid. *Appl. Biochem. Biotechnol.* 183:566–581, doi:10.1007/s12010-017-2578-1.

[2] Huck, C. (2014) Multi-parameter physico-chemical sensing principles for biogas-process monitoring. *Ph.D. thesis*, Hasselt University.

[3] VDI-Gesellschaft Energie und Umwelt (2016) VDI-Richtlinien: Vergärung organischer Stoffe – Substratcharakterisierung, Probenahme, Stoffdatenerhebung, Gärversuche (VDI 4630). Berlin: *Beuth Verlag GmbH.*

[4] Breuer, L.; Pilas, J.; Guthmann, E.; Schöning, M.J.; Thoelen, R.; Wagner, T. (2019) Towards light-addressable flow control: Responsive hydrogels with incorporated graphene oxide as laser-driven actuator structures within microfluidic channels. *Sens. Actuators B Chem.* 288:579–585, doi:10.1016/j.snb.2019.02.086.

[5] Breuer, L. (2019) Light-addressable valves based on responsive hydrogels for lab-on-chip applications. *Ph.D. thesis*, Hasselt University.

[6] Röhlen, D.L.; Pilas, J.; Dahmen, M.; Keusgen, M.; Selmer, T.; Schöning, M.J. (2018) Toward a hybrid biosensor system for analysis of organic and volatile fatty acids in fermentation processes. *Front. Chem.* 6:284, doi:10.3389/fchem.2018.00284.

[7] Dantism, S.; Röhlen, D.; Selmer, T.; Wagner, T.; Wagner, P.; Schöning, M.J. (2019) Quantitative differential monitoring of the metabolic activity of *Corynebacterium glutamicum* cultures utilizing a light-addressable potentiometric sensor system. *Biosens. Bioelectron.* 139: 111332, doi:10.1016/j.bios.2019.111332.

9 Zusammenfassung

Angesichts des stetig steigenden Energiebedarfs und der unvermeidbaren Erschöpfung fossiler Brennstoffe, gewinnt der weitere Ausbau an erneuerbaren Energien immer mehr an Bedeutung. Biomasse kann dabei in vielfältiger Weise einen entscheidenden Beitrag zur nachhaltigen Energieversorgung leisten. Für eine effiziente Gewinnung von Biogas durch anaerobe Vergärung organischer Stoffe sind jedoch einige Verbesserungen innerhalb der Wertschöpfungskette erforderlich. Insbesondere eine zuverlässige Prozessüberwachung ist unerlässlich, um stabile Prozessbedingungen und damit einen wirtschaftlichen Betrieb von Biogasanlagen zu gewährleisten. Ein Indikator für Prozessstörungen stellt dabei unter anderem die Konzentration von verschiedenen Zwischenprodukten dar, die während des anaeroben Fermentationsprozesses gebildet werden. Bislang werden dabei vor allem die Konzentrationen an flüchtigen organischen Fettsäuren (z.B. Acetat und Propionat) als wichtige Prozessgrößen erachtet, während anderen organischen Säuren und Alkoholen in der Regel weniger Bedeutung zugesprochen wird. Da diese Intermediate jedoch zentrale Bausteine in der Methanogenese darstellen, könnte eine schnelle sensorbasierte Erfassung dieser Metabolite die Prozesssteuerung von Biogasanlagen positiv beeinflussen.

In Rahmen dieser Arbeit wurde ein enzymbasiertes elektrochemisches Biosensorarray zum simultanen Nachweis von D-Lactat, L-Lactat, Formiat und Ethanol entwickelt. Das amperometrische Detektionsprinzip basiert auf jeweils zwei Enzymen: einer analytspezifischen NAD^+-abhängigen Dehydrogenase und einer Diaphorase aus *Clostridium kluyveri*. Letztere wandelt das Substrat $Fe(CN)_6^{3-}$ in $Fe(CN)_6^{4-}$ um, welches durch Oxidation an einer polarisierten Elektrode einen analytabhängigen Strom erzeugt. Die entsprechenden Enzyme wurden mittels chemischer Quervernetzung mit Glutaraldehyd auf Dünnschichtelektroden aus Platin immobilisiert. Das Signal des Biosensors wurde hinsichtlich Enzymbeladung, Konzentration an Glutaraldehyd und Cofaktoren (NAD^+ und $Fe(CN)_6^{3-}$), pH-Wert und Temperatur optimiert. Untersuchungen der Arbeits- und Lagerstabilität zeigten, dass eine mehrfache und langfristige Anwendung möglich ist. Die spezifische Nachweis eines Analyten wird bei Biosensoren durch das biologische Erkennungselement gewährleistet. Messungen in realen Proben sind jedoch anfällig für Interferenzen durch andere elektroaktive Substanzen in der Probenlösung. Aus diesem Grund wurde zunächst der Einfluss von verschiedenen potenziell störenden Verbindungen auf das Sensorsignal untersucht; dabei konnte gezeigt werden, dass eine simultane Detektion von vier verschiedenen Analyten durchgeführt werden kann. Im weiteren Verlauf wurde die Funktionalität des Biosensorsystems unter realen Bedingungen getestet. Zu diesem Zweck erfolgte die Quantifizierung von D-Lactat, L-Lactat, Formiat und Ethanol in verschiedenen Fütterungssubstraten (Mais-, und Zuckerrohrsilage) und gespikten Fermentationsproben, die aus drei industriellen Biogasanlagen entnommen wurden. Die dabei bestimmten Konzentrationen zeigten eine gute Übereinstimmung

zur konventionellen Referenzanalytik mittels Photometrie und Gaschromatographie. Im Gegensatz zum Biosensorarray, ist für die zuverlässige Anwendung dieser Methoden in der Regel eine aufwendige Probenvorbereitung notwendig, da diese Messsysteme klare und partikelfreie Proben erfordern. Weitere Nachteile dieser Form der Prozesskontrolle sind der Zeitverzug zwischen Probennahmen und Analytik in externen Laboren und die hohen Analysekosten. Für einen Zeitraum von zwei Montaten erfolgte erstmalig die Langzeitüberwachung eines Biogasreaktors im Labormaßstab ($0.01\,m^3$) mit dem Biosensorarray. Das Monitoring umfasste standardmäßige Parameter wie die Biogasproduktion, Methanausbeute, pH-Wert und Temperatur, sowie die Detektion der organischen Säuren und Ethanol durch das entwickelte Biosensorsystem. Im Verlauf dieser Untersuchung konnte gezeigt werden, dass diese zusätzlichen Messdaten dazu beitragen können, Veränderungen im Fermentationsprozess zu erkennen und so potentiell auch frühzeitig Prozessstörungen detektiert werden können.

Um eine bessere praktische Anwendung des Biosensorarrays zu ermöglichen, wurden die beiden erforderlichen Cofaktoren zusammen mit den Enzymen auf der Sensoroberfläche von Dickfilmelektroden aus Kohlenstoff immobilisiert. Durch die Modifikation mit Graphenoxid konnte ein reagenzfreies Biosensorsystem etabliert werden, das mittels Dickschichttechnik kostengünstig hergestellt werden kann. Solche Einweg-Teststreifen könnten zukünftig für das Monitoring von Biogasanlagen genutzt werden, um vor Ort auf schnelle und unkomplizierte Weise die Konzentration an mehreren wichtigen Zwischenprodukten zu bestimmen.

Publications

Peer-reviewed publications

[1] **Pilas, J.**; Iken, H.; Selmer, T.; Keusgen, M.; Schöning, M.J. (2015) Development of a multi-parameter sensor chip for the simultaneous detection of organic compounds in biogas processes. *Phys. Status Sol. A* 212(6):1306–1312, doi:10.1002/pssa.201431894.

[2] **Pilas, J.**; Yazici, Y.; Selmer, T.; Keusgen, M.; Schöning, M.J. (2017) Optimization of an amperometric biosensor array for simultaneous measurement of ethanol, formate, D- and L-lactate. *Electrochim. Acta* 251:256–262, doi:10.1016/j.electacta.2017.07.119.

[3] Röhlen, D.L.; **Pilas, J.**; Schöning, M.J.; Selmer, T. (2017) Development of an amperometric biosensor platform for the combined determination of L-malic, fumaric, and L-aspartic acid. *Appl. Biochem. Biotechnol.* 183(2):566–581, doi:10.1007/s12010-017-2578-1.

[4] **Pilas, J.**; Yazici, Y.; Selmer, T.; Keusgen, M.; Schöning, M.J. (2018) Application of a portable multi-analyte biosensor for organic acid determination in silage. *Sensors* 18(5):1470, doi:10.3390/s18051470.

[5] Röhlen, D.L.; **Pilas, J.**; Dahmen, M.; Keusgen, M.; Selmer, T.; Schöning, M.J. (2018) Toward a hybrid biosensor system for analysis of organic and volatile fatty acids in fermentation processes. *Front. Chem.* 6:284, doi:10.3389/fchem.2018.00284.

[6] Breuer, L.; **Pilas, J.**; Guthmann, E.; Schöning, M.J.; Thoelen, R.; Wagner, T. (2019) Towards light-addressable flow control: Responsive hydrogels with incorporated graphene oxide as laser-driven actuator structures within microfluidic channels. *Sens. Actuators B Chem.* 288:579–585, doi:10.1016/j.snb.2019.02.086.

[7] **Pilas, J.**; Selmer, T.; Keusgen, M.; Schöning, M.J. (2019) Screen-printed carbon electrodes modified with graphene oxide for the design of a reagent-free NAD^+-dependent biosensor array. *Anal. Chem.* 91:15293–15299, doi:10.1021/acs.analchem.9b04481.

Proceedings

[1] **Pilas, J.**; Selmer, T.; Keusgen, M.; Schöning, M.J. (2015) Optimization of an enzyme-based multi-parameter biosensor for monitoring biogas processes. *Procedia Eng.* 120:532-535, doi:10.1016/j.proeng.2015.08.702.

[2] **Pilas, J.**; Selmer, T.; Keusgen, M.; Schöning, M.J. (2017) Portable multi-analyte sensor system for on-site monitoring of fermentation processes. *Proceedings* 1(8):796, doi:10.3390/proceedings1080796.

[3] **Pilas, J.**; Röhlen, D.L.; Selmer, T.; Keusgen, M.; Schöning, M.J. (2018) Multi-analyte biosensor chip for determination of organic acids in biogas processes. *17th International Meeting on Chemical Sensors - IMCS 2018.* Biosensors 3:143–144, doi:10.5162/IMCS2018/BS3.5.

Oral and poster presentations

[1] **Pilas, J.**; Röhlen, D.L.; Dantism, S.; Selmer, T.; Schöning, M.J. Enzyme-based amperometric biosensors for monitoring key parameters in the biogas process. *Engineering of Functional Interfaces* in Jülich, Germany (14-15 July 2014).

[2] **Pilas, J.**; Röhlen, D.L.; Dantism, S.; Selmer, T.; Keusgen, K.; Schöning, M.J. Enzymbasierte amperometrische Biosensoren für die Überwachung von Biogas-Prozessen. *Deutsches BioSensor Symposium* in Munich, Germany (11-13 March 2015).

[3] **Pilas, J.**; Keusgen, K.; Selmer, T.; Schöning, M.J. Application of a bienzyme sensor setup for the amperometric detection of alcohols in biogas processes. *Engineering of Functional Interfaces* in Hannover, Germany (05-07 July 2015).

[4] **Pilas, J.**; Mariano, K.; Keusgen, K.; Selmer, T.; Schöning, M.J. Optimization of an enzyme-based multi-parameter biosensor for monitoring biogas processes. *Eurosensors* in Freiburg, Germany (06-09 September 2015).

[5] **Pilas, J.**; Mariano, K.; Keusgen, K.; Selmer, T.; Schöning, M.J. Enzyme immobilization through avidin-biotin interaction on self-assembled monolayers. *Engineering of Functional Interfaces* in Wildau, Germany (04-05 July 2016).

[6] **Pilas, J.**; Selmer, T.; Keusgen, K.; Schöning, M.J. Enzyme immobilization through avidin-biotin interaction on self-assembled monolayers. *Electrochemical Micro and Nanosystem Technologies* in Brussels, Belgium (17-19 August 2016).

[7] **Pilas, J.**; Dantism, S.; Röhlen, D.L.; Selmer, T.; Keusgen, K.; Wagner, T.; Schöning, M.J. Development of a mobile monitoring system for evaluation of biogas processes. *Kurt-Schwabe-Symposium* in Mittweida, Germany (04-07 September 2016).

[8] **Pilas, J.**; Hamacher, T.; Selmer, T.; Keusgen, K.; Schöning, M.J. Monitoring of fermentation processes by application of an electrochemical biosensor set-up. *Engineering of Functional Interfaces* in Marburg, Germany (27-29 August 2017).

[9] **Pilas, J.**; Selmer, T.; Keusgen, K.; Schöning, M.J. Portable multianalyte sensor system for on-site monitoring of fermentation processes. *International Symposium on Sensor Science* in Barcelona, Spain (27-29 September 2017).

[10] **Pilas, J.**; Röhlen, D.L.; Selmer, T.; Keusgen, K.; Schöning, M.J. Development of a portable multi-parameter biosensor set-up for monitoring of biogas processes. *BioProScale* in Berlin, Germany (20-22 March 2018).

[11] **Pilas, J.**; Selmer, T.; Keusgen, K.; Schöning, M.J. Evaluation of the storage stability of an enzyme-based biosensor system for multi-analyte detection. *Engineering of Functional Interfaces* in Wittenberg, Germany (01-03 July 2018).

[12] **Pilas, J.**; Röhlen, D.L.; Selmer, T.; Keusgen, K.; Schöning, M.J. Multi-analyte biosensor for determination of organic acids in biogas processes. *International Meeting on Chemical Sensors* in Vienna, Austria (15-19 July 2018).

[13] **Pilas, J.**; Röhlen, D.L.; Selmer, T.; Keusgen, K.; Schöning, M.J. Monitoring of fermentation processes using an enzyme-based biosensor array. *European Biosensor Symposium* in Florence, Italy (18-21 February 2019).

[14] **Pilas, J.**; Selmer, T.; Keusgen, K.; Schöning, M.J. Comparative study between screen-printed carbon- and platinum thin-film electrodes for construction of enzyme-based multi-analyte biosensors. *Engineering of Functional Interfaces* in Leuven, Belgium (08-09 August 2019).

Acknowledgements

At this point I would like to acknowledge and thank all the people who supported and inspired me scientifically as well as on a personal level in so many different ways throughout the last years.

First of all, I would like to express my sincere gratitude to my supervisor Prof. Dr. Michael J. Schöning for the opportunity to conduct my doctoral research at the Institute of Nano- and Biotechnologies. Thank you for your support, patient guidance, the trust in my work and the encouragement to put my own skepticism aside. Furthermore, I would like to thank for all the corrections and proofreading of numerous abstracts, posters, presentations and manuscripts and for providing the chance to present my research at so many national and international conferences.

In the same way, I would like to thank Prof. Dr. Michael Keusgen for the supervision of my research project and the great collaboration of the Philipps-Universität Marburg with the Institute of Nano- and Biotechnologies. I have always benefited from your helpful comments, suggestions and constructive advice.

I would also like to thank the other members of the examination committee, Prof. Dr. Marcus Baumann and Prof. Dr. Shu-Ming Li for their valuable time and interest.

Special acknowledgment belongs to Prof. Dr. Thorsten Selmer for his interest in the biogas project, fruitful discussions, ambitious plans and helpful tips and skills in the daily lab routine.

I also like to appreciate the PhD scholarships received from the FH Aachen, hereby, special acknowledgment goes to Prof. Dr. Doris Samm and Judith Kürten for their support in the grant process.

I am very grateful to the most helpful colleagues at the Institute of Nano- and Biotechnologies. My special thanks belong to Heiko Iken for fabrication of so many wafers throughout the last years, David Rolka and Stefan Beging for their help in all kinds of situations, Benno Schneider for the support in 3D-printing and Melanie Gellissen for the pleasant assistance in the laboratory.

I am further thankful to all present and former PhD students. Thank you Dr. Matthias Bäcker and Dr. Christina Huck for being wonderful office mates and so helpful especially at the beginning of my work. I was very lucky to work on the project together with Leila Röhlen, thanks for making it possible to always find something to laugh about in times of true frustration. Thank you Shahriar Dantism for being such a haven of tranquility in our office. Also big thanks to Dr. Lars Breuer for your willingness to organize all the Pub nights, Julio Arreola for the AFM measurements, Thomas Bronder for reminding me about the importance of the sunny side of life, Alex Kremers for the help in all kind of technical questions, Dr. Farnoosh Vahidpour, Melanie Jablonski and René Welden for the cheerful lunch breaks. It was a great experience and pleasure to work with all of you and I want to highlight the great teamwork which I experienced

during this time.

All the experiments and measurements would not have been possible without the great contribution of eager and motivated students. It was a pleasure to supervise the internships and bachelor theses of Niklas Warmbold, Krichelle Mariano, Thorben Hamacher and Yasemen Yazici. Thank you for asking questions, performing experiments over and over again and spurring my own inquisitiveness. I also like to thank Markus Dahmen, Sveja Paulsen and Gino Pohen from the Institute NOWUM-Energy for the supply with real fermentation samples and the expertise in operation and monitoring of biogas plants.

Finally, special thanks go to my family and friends for their constant support, words of encouragement and all the refreshing moments of distraction.

Thank you!

Curriculum vitae

The curriculum vitae is not part of the online version.